

การประเมินศักยภาพของตะกอนไหลถล่มและน้ำปนตะกอนป่า ในปี 2544  
บริเวณพื้นที่น้ำก้อ อำเภอหล่มสัก จังหวัดเพชรบูรณ์ ภาคกลางของประเทศไทย

นายสมบัติ อยู่เมือง

วิทยานิพนธ์นี้เป็นส่วนหนึ่งของการศึกษาตามหลักสูตรปริญญาวิทยาศาสตรดุษฎีบัณฑิต

สาขาวิชาธรณีวิทยา ภาควิชาธรณีวิทยา

คณะวิทยาศาสตร์ จุฬาลงกรณ์มหาวิทยาลัย

ปีการศึกษา 2548

ISBN 974-14-2174-5

ลิขสิทธิ์ของจุฬาลงกรณ์มหาวิทยาลัย

EVALUATION OF POTENTIAL FOR 2001 DEBRIS FLOW AND DEBRIS FLOOD  
IN THE VICINITY OF NAM KO AREA, AMPHOE LOM SAK,  
CHANGWAT PHETCHABUN, CENTRAL THAILAND

Mr. Sombat Yumuang

A Dissertation Submitted in Partial Fulfillment of the Requirements  
for the Degree of Doctor of Philosophy Program in Geology

Department of Geology

Faculty of Science

Chulalongkorn University

Academic year 2005

ISBN 974-14-2174-5

Thesis Title Evaluation of potential for 2001 debris flow and debris flood  
in the vicinity of Nam Ko area, Amphoe Lom Sak, Changwat  
Phetchabun, Central Thailand

By Sombat Yumuang

Filed of study Geology

Thesis Advisor Assistant Professor Nopadon Muangnoicharoen, Ph.D.

Thesis Co-advisor Associate Professor Kittitep Fuenkajorn, Ph.D.

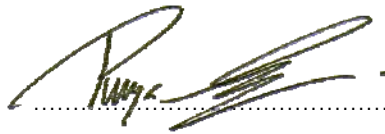
---

Accepted by the Faculty of Science, Chulalongkorn University in Partial Fulfillment of the Requirements  
for the Doctor's Degree



..... Dean of the Faculty of Science  
(Professor Piamsak Menasveta, Ph.D.)

THESIS COMMITTEE



..... Chairman  
(Associate Professor Punya Charusiri, Ph.D.)



..... Thesis Advisor  
(Assistant Professor Nopadon Muangnoicharoen, Ph.D.)



..... Thesis Co-advisor  
(Associate Professor Kittitep Fuenkajorn, Ph.D.)



..... Member  
(Associate Professor Warakorn Mairaing, Ph.D.)



..... Member  
(Assistant Professor Somchai Nakapadungrat, Ph.D.)



..... Member  
(Sunya Sarapirome, Ph.D.)

สมบัติ อยู่เมือง : ชื่อวิทยานิพนธ์. EVALUATION OF POTENTIAL FOR 2001 DEBRIS FLOW AND DEBRIS FLOOD IN THE VICINITY OF NAMKO AREA, AMPHOE LOM SAK, CHANGWAT PHETCHABUN, CENTRAL THAILAND อ. ที่ปรึกษา : ผศ.ดร. นกมล ม่วงน้อยเจริญ, อ.ที่ปรึกษาร่วม : รศ.ดร. กิตติเทพ เพ็ญขจร 297 หน้า. ISBN 974-14-2174-5.

การศึกษาระดับปริญญาตรีที่มีอิทธิพลต่อการเกิดตะกอนไหลถล่มและน้ำปนตะกอนป่า ที่เกิดขึ้นเมื่อวันที่ 11 สิงหาคม 2544 บริเวณพื้นที่น้ำก้อ อำเภอหล่มสัก จังหวัดเพชรบูรณ์ กระทำโดยใช้ข้อมูลที่จัดทำและแปลความหมายด้วยระบบสารสนเทศภูมิศาสตร์และข้อมูลจากการสำรวจระยะไกล ข้อมูลจากการสำรวจภาคสนาม และข้อมูลจากการวิเคราะห์ในท้องปฏิบัติ การข้อมูลดังกล่าวยังใช้เพื่อพิสูจน์หลักฐานพื้นที่ที่มีศักยภาพเป็นแหล่งกำเนิดตะกอน บริเวณที่มีการเคลื่อนตัวของตะกอน และบริเวณที่มีการสะสมตัวของตะกอน รวมทั้งกำหนดเกณฑ์ที่สามารถแสดงศักยภาพของพิบัติภัยจากการเกิดตะกอนไหลถล่มและน้ำปนตะกอนป่า ในบริเวณลุ่มน้ำก้อใหญ่และเนินตะกอนรูปพัด การศึกษาระดับปริญญาตรียังกระทำเพื่อหาความสัมพันธ์ระหว่างลำดับชั้นของตะกอนและการเกิดตะกอนไหลถล่มและน้ำปนตะกอนป่าในบริเวณพื้นที่เนินตะกอนรูปพัด อีกด้วย

การวิเคราะห์เพื่อประเมินความสัมพันธ์ของปัจจัยที่มีอิทธิพลต่อการเกิดตะกอนไหลถล่มและน้ำปนตะกอนป่า ได้ใช้ข้อมูลร่องรอยการเกิดตะกอนถล่มและน้ำปนตะกอนท่วมและข้อมูลที่เกี่ยวข้อง มาทำการวิเคราะห์ด้วยวิธีของความน่าจะเป็นแบบตัวแปรเดียว และการคำนวณค่าความสัมพันธ์ของปัจจัยที่มีอิทธิพลต่อการเกิดพิบัติภัยจากตะกอนไหลถล่มและน้ำปนตะกอนป่า ผลการวิเคราะห์ได้จัดทำเป็นแผนที่แสดงความสัมพันธ์ของปัจจัยที่มีอิทธิพลต่อการเกิดพิบัติภัยตะกอนไหลถล่มและน้ำปนตะกอนป่าขึ้นในพื้นที่

สำหรับการอธิบายถึงเหตุการณ์ของการเกิดและศักยภาพของตะกอนไหลถล่มและน้ำปนตะกอนป่านั้นสามารถสรุปได้ว่าเหตุการณ์พิบัติภัยดังกล่าวนี้ไม่ได้มีสาเหตุมาจากการทำงานของฝนตกหนักผิดปกติแต่เพียงอย่างเดียวตามที่คาดกันไว้ แต่เป็นการทำงานร่วมกันของปัจจัยที่มีอิทธิพลหลายประการจากลักษณะภูมิประเทศที่มีสิ่งปกคลุมดินเป็นลักษณะเฉพาะ คุณสมบัติทางธรณีเทคนิคของวัสดุรองรับในพื้นที่ และการหน่วงเพื่อการสะสมตัวของซากต้นไม้และตะกอน การประสมประสานของปัจจัยที่มีอิทธิพลดังกล่าวเหล่านี้ได้ทำให้เกิดตะกอนไหลถล่มและน้ำปนตะกอนป่าได้ กระบวนการดังกล่าวนี้ยังทำให้เกิดความรุนแรงมากขึ้นอีกเนื่องจากการเกิดแนวชั่วคราวกั้นการไหลตามธรรมชาติที่ต่อมาได้พังทลายลงจากน้ำหนักของน้ำที่กักเอาไว้

หลังจากการเกิดเหตุการณ์พิบัติภัยครั้งนี้แล้ว สามารถประเมินได้ว่าต้องใช้เวลาก่อนที่จะเกิดเหตุการณ์ตะกอนไหลถล่มและน้ำปนตะกอนป่าครั้งต่อไปขึ้นอีก เนื่องจากต้องการเวลาสำหรับสะสมซากต้นไม้และตะกอนในลุ่มน้ำให้มีปริมาณมากพอเสียก่อน

ภาควิชา.....ธรณีวิทยา..... ลายมือชื่อนิติ.....  
สาขาวิชา.....ธรณีวิทยา..... ลายมือชื่ออาจารย์ที่ปรึกษา.....  
ปีการศึกษา 2548 ลายมือชื่ออาจารย์ที่ปรึกษาร่วม.....

## 4373862023 : MAJOR GEOLOGY

KEY WORD: POTENTIAL / DEBRIS FLOW AND DEBRIS FLOOD / GIS AND REMOTE SENSING / NAM KO / PHETCHABUN / THAILAND

SOMBAT YUMUANG : EVALUATION OF POTENTIAL FOR 2001 DEBRIS FLOOD IN THE VINICITY OF NAMKO AREA, AMPHOE LOM SAK, CHANGWAT PHETCHABUN, CENTRAL THAILAND. THESIS ADVISOR : ASST. PROF. DR. NOPADON MUANGNOICHAROEN, THESIS COADVISOR : ASSOC.PROF. DR. KITTITEP FUENKAJORN, 297 pp. ISBN 974-14-2174-5.

Thematic (GIS and remote sensing) data interpretation, field investigation, and laboratory analysis were carried out to investigate the parameters influencing the debris flow and debris flood (flow-flood) occurrence on 11<sup>th</sup> August 2001 (8/11) in Nam Ko area, Changwat Phetchabun, central Thailand. The purpose of study was to identify the potential source area, run-out zone, and depositional area, and to determine the evidences of the potential for hazards in Nam Ko Yai sub-catchment and its alluvial fan. The relationship between the sedimentary sequences and debris flow-flood occurrence in the alluvial fan was also defined.

The relationship between debris flow-flood and relevant parameters was analyzed for debris flow-flood susceptibility assessment. In Nam Ko Yai sub-catchment, scar-scouring locations detected from remote sensing interpretation and field surveys were compiled into a GIS database. Various maps were constructed from the flow-flood relevant parameters derived from the database. The parameters, univariant probability method, and calculation of debris flow-flood susceptibility were applied to analyze and produce the susceptibility map of debris flow-flood hazard in the sub-catchment.

From the debris flow-flood event reconstruction and its potential, it was concluded that the disastrous event was not the work of the unusually heavy rainfall alone as previously concluded, but it was the work of combined parameters including the terrain characteristics with specific land cover, underlain-material geotechnical properties, and time-delay for accumulation of plant debris and sediments. Combination of parameters could lead to a debris flow-flood. The process could be worse with a natural temporary landslide dam formed and then the dam was destroyed under the weight of impounded water. After this disastrous event, it should take time for the next debris flow-flood to recur as accumulation of more plant debris and sediments in the sub-catchment would be needed.

Department.....Geology.....Student's signature.....

Field of study.....Geology.....Advisor's signature.....

Academic year 2005 Co-advisor's signature.....

## ACKNOWLEDGEMENTS

The Graduate School of Chulalongkorn University and the Ministry of Interior provided a partial funding for this study.

I sincerely thank my Advisor, Asst. Prof. Dr. Nopadon Muangnoicharoen of Chulalongkorn University and Co-advisor, Assoc. Prof. Dr. Kittitep Fuenkajorn of Suranaree University of Technology for their supports, encouragements, critically advises and reviews of this thesis. Appreciation is also done to thank Asst. Prof. Dr. Somchai Nakapadungrat, Asst. Prof. Virote Daorerk, and Assoc. Prof. Dr. Punya Charusiri, the successive chairmen of Department of Geology, Chulalongkorn University for supporting and allowing me to use facilities at the department during the study, and Assoc. Prof. Dr. Chaiyudh Khantaprab and Assoc. Prof. Dr. Wasant Pongsapich especially for their valuable ideas and moral support. I would also like to thank Dr. Supichai Tangjaitrong for technical support.

I would like to thank Prof. Dr. Philip E. LaMoreaux, former State Geologist of Alabama and retired professor of the University of Alabama, USA for encouraging my publication.

I sincerely gratify the Land Development Department of the Ministry of Agriculture and Cooperation, Geo-Informatics and Space Technology Development Agency (Public Organization), Royal Thai Survey Department, Thai Meteorology Department, and Environment System Research Institute (Thailand) Co. Ltd. for their permission to use essential data for this research.

The technical supports were provided by the staff of Geo-Informatics Center for Thailand (GISTHAI) of Chulalongkorn University and the staff of Geomechanics Research Unit of Suranaree University of Technology.

Finally, I thank my wife, Vorasa, my daughter, Thitikant, and my son, Sirawit, for their support and encouragement throughout this time of hardship.

## TABLE OF CONTENT

	page
Abstract in Thai .....	iv
Abstract in English .....	v
Acknowledgements .....	vi
List of Tables .....	xiii
List of Figures .....	xv
Chapter 1 Introduction .....	1
1.1 Rationale .....	1
1.2 Objectives .....	5
1.3 Hypothesis .....	6
1.4 Scope and limitation .....	6
1.5 Location of the study area .....	7
1.6 Expected outputs .....	10
1.7 Research methodology .....	10
1.7.1 Preparation .....	10
1.7.2 Field investigation .....	11
1.7.3 Laboratorial studies .....	12
1.7.4 Synthesis, discussion and conclusion .....	13
1.8 Components of the thesis .....	15
Chapter 2 Literature review .....	17
2.1 Introduction .....	17
2.2 Definition and Terminology .....	17

	page
2.3	Landslide classification systems ..... 18
2.4	Landslide hazard..... 21
	2.4.1 Scale factor in analysis ..... 24
	2.4.2 Knowledge types used in prediction of landslide hazard ..... 26
2.5	Disaster management ..... 27
	2.5.1 Geo-spatial requirements ..... 29
	2.5.2 Risk assessment as central theme..... 31
2.6	Use of remote sensing in landslide hazard assessment ..... 33
2.7	Geographical Information Systems (GIS) and landslide hazard assessment.....36
2.8	Basic concepts on evaluation of the potential for debris-flows and related sediment-flows ..... 41
2.9	Previous investigations on evaluation of the potential for debris-flows and related sediment-flows ..... 51
Chapter 3	Thematic data preparation ..... 60
	3.1 Phases of natural hazard analysis in GIS-based landslide hazard zoning techniques ..... 60
	3.2 Thematic data preparation from GIS and remote sensing techniques..... 62
	3.3 Elevation ..... 65
	3.3.1 Data entry ..... 65
	3.3.2 Input map generation..... 65

3.4	Geology .....	72
	3.4.1 Data entry .....	72
	3.4.2 Input map generation.....	72
3.5	Soil property .....	74
	3.5.1 Data entry .....	74
	3.5.2 Input map generation.....	74
3.6	Land cover .....	76
	3.6.1 Data sources.....	78
	3.6.2 Data processing.....	78
	3.6.2.1 Image rectification and restoration .....	78
	3.6.2.2 Reduction of noise and image enhancement .....	80
	3.6.2.3 Image classification .....	81
	3.6.2.4 Post-processing.....	82
	3.6.2.5 Accuracy assessment.....	82
	3.6.2.6 Classification result.....	83
3.7	Infrastructure and human settlement.....	85
3.8	Flow-flood inventory: scar-scouring and depositional locations.....	86
	3.8.1 Data entry .....	86
	3.8.2 Data processing.....	86
	3.8.3 Accuracy assessment of scar-scouring delineation .....	95

	page
3.9	Rainfall intensity..... 100
3.9.1	Data entry ..... 100
3.9.2	Input map generation..... 104
Chapter 4	Debris flow-flood hazard analysis in Nam Ko Yai sub-catchment..... 105
4.1	Trends in landslide hazard zonation..... 105
4.2	Debris flow-flood susceptibility analysis ..... 106
4.2.1	Susceptibility analysis using univariant probability method..... 108
4.2.1.1	Relationship between scar-scouring and slope..... 109
4.2.1.2	Relationship between scar-scouring and landform topography ..... 112
4.2.1.3	Relationship between scar-scouring and aspect..... 112
4.2.1.4	Relationship between scar-scouring and geology..... 116
4.2.1.5	Relationship between scar-scouring and soil group unit. .... 120
4.2.1.6	Relationship between scar-scouring and soil thickness ..... 124
4.2.1.7	Relationship between scar-scouring and land cover..... 127
4.2.1.8	Relationship between scar-scouring and buffering distance to drainage-line ..... 129
4.2.2	Calculation of debris flow-flood susceptibility..... 133

Chapter 5	Evidences and parameters affecting debris flow-flood processes in Nam Ko Yai sub-catchment .....	136
5.1	Evidences of geotechnical properties of rocks and soils in Nam Ko Yai sub-catchment.....	136
5.1.1	Geotechnical study of point load testing .....	137
5.1.1.1	Point load testing overview.....	137
5.1.1.2	Rock specimen sampling .....	140
5.1.1.3	Point load testing results.....	140
5.1.2	Geotechnical study of soil properties .....	140
5.1.2.1	Soil sampling preparation .....	140
5.1.2.2	Laboratorial study of soil properties.....	141
5.1.2.3	Study results of soil geotechnical properties .....	141
5.2	Evidences of a suspected temporary landslide dam location and channel configurations in the central part of Nam Ko Yai sub-catchment .....	144
5.2.1	Evidences of a temporary landslide dam location.....	144
5.2.2	Evidences of channel configurations .....	148
Chapter 6	Evidences of debris flow-flood activities in the alluvial fan.....	157
6.1	Recognition and characterization of the alluvial fan.....	157
6.1.1	Defining activeness of the alluvial fan.....	157
6.1.2	Defining geomorphology, local subsurface geology, and stratigraphic recognition of the alluvial fan.....	166

	page
6.1.2.1 Geomorphology of the alluvial fan .....	166
6.1.2.2 Local subsurface geology of the previous alluvial fan deposits .....	167
6.1.2.3 Stratigraphic recognition of the previous alluvial fan deposits .....	168
Chapter 7 Discussion.....	179
7.1 Debris flow-flood susceptibility results .....	179
7.2 Debris flow-flood event reconstruction and its potential.....	182
7.3 FLO-2D simulation results for validation of the suspected temporary landslide dam occurrence .....	185
Chapter 8 Conclusion .....	191
8.1 Evaluation of potential for the 2001 debris flow and debris flood.....	191
8.2 Recommendation for more accurate evaluation of potential for debris flow and debris flood.....	193
References.....	195
Appendices .....	211
Appendix A.....	212
Appendix B .....	216
Appendix C.....	225
Appendix D.....	229
Curriculum Vitae .....	271

## LIST OF TABLES

Table		page
2-1	Landslide classification system by Sharpe (1938) .....	19
2-2	Landslide classification according to Hutchinson (1988).....	20
2-3	Landslide classification system by Varnes (1978).....	21
2-4	Key elements of disaster management (Van Westen, 1994).....	29
3-1	Overview of the important input data themes that were pre-processed and invented in this thesis .....	64
3-2	Multi-temporal aerial photographs and satellite images that are used as primary data sources of this thesis .....	79
3-3	Land cover classification of the study area (on 21 <sup>st</sup> November, 2001) .....	84
3-4	Error matrix resulting from classifying training set pixels .....	99
4-1	Trends in landslide hazard zonation (Van Westen, 1993) .....	106
4-2	Relation of flow-flood with slope in Nam Ko Yai sub-catchment.....	111
4-3	Relation of flow-flood and landform topography in Nam Ko Yai sub-catchment .....	114
4-4	Relation of flow-flood and aspect in Nam Ko Yai sub-catchment.....	118
4-5	Relation of flow-flood and geology in Nam Ko Yai sub-catchment.....	120
4-6	Relation of flow-flood and soil group unit in Nam Ko Yai sub-catchment .....	123
4-7	Relation of flow-flood and soil thickness unit in Nam Ko Yai sub-catchment .....	126
4-8	Relation of flow-flood and land cover in Nam Ko Yai sub-catchment.....	128

Table		page
4-9	Relation of flow-flood and buffering distance to drainage-line in Nam Ko Yai sub-catchment.....	131
5-1	The referenced data of sample numbers, sample locations, type of samples, rock unit of rock samples, rock grade testing values, and type of laboratorial analysis for each sample in the study area.....	138
5-2	Analytical results of soil engineering properties of the soil samples .....	143

## LIST OF FIGURES

Figure		page
1-1	Geographic setting of the study area.....	8
1-2	a) Location of the study area with important reference locations, and b) three-dimensional drape of Nam Ko Yai sub-catchment and alluvial fan boundary (black color line) of the study area and surrounding terrains.....	9
1-3	Schematic diagrams illustrating the research methodology system .....	14
2-1	Graphical representation of hazard, vulnerability and risk (Varnes, 1984).....	22
2-2	Overview of landslide hazard zonation activities (Varnes, 1984).....	23
2-3	Scales of analysis and minor details (Sgzen, 2002) .....	25
2-4	Process of Remote Sensing (Van Westen, 1994) .....	34
2-5	GIS and its related software systems as components of GIS (Sgzen, 2002).....	38
2-6	Phases of a GIS (Sgzen, 2002) .....	39
2-7	Questions which a well-built GIS should answer (Sgzen, 2002).....	39
3-1	Flow chart of a GIS-based landslide hazard zonation (Van Westen, 1994) .....	62
3-2	Color-coded contour map of the study area .....	66
3-3	Color-coded DEM of the study area .....	66
3-4	Color-draped relief model of the study area (illumination 45°, vertical exaggeration x 3) .....	67
3-5	Drainage system of the study area, including micro-catchments and drainage-lines (in blue colored lines) .....	68
3-6	Buffering distance to drainage-line in the study area.....	69
3-7	Aspect map of the study area .....	69
3-8	Slope map of the study area .....	70

Figure	page
3-9	Landform topography of the study area ..... 71
3-10	Previous geologic map of the study area (modified after Yooyen, 1985, etc.) ..... 73
3-11	Compiled geologic map of the study area ..... 74
3-12	Soil group unit map of the study area (modified after Land Development Department, 2002) ..... 76
3-13	Soil thickness map of the study area (modified after Land Development Department, 2002) ..... 77
3-14	Survey tracks (pink colored dots) for field data collection and land cover classification accuracy assessment in the study area..... 83
3-15	Land cover map of the study area (classified from Landsat 7 ETM+ acquired on 21 <sup>st</sup> November 2001) ..... 84
3-16	Infrastructure and human settlement map of the study area ..... 85
3-17	False color composite of Landsat 7 ETM+ (R=5, G=4, B=3) acquired on 5 <sup>th</sup> January 2001 (before 8/11) in the study area..... 89
3-18	False color composite of Landsat 7 ETM+ (R=5, G=4, B=3) acquired on 21 <sup>st</sup> November 2001 (after 8/11) in the study area ..... 89
3-19	Normalized different vegetation index (NDVI) of Landsat 7 ETM+ (R=5, G=4, B=3) acquired on 5 <sup>th</sup> January 2001 (before 8/11) in the study area ..... 90
3-20	Normalized different vegetation index (NDVI) of Landsat 7 ETM+ (R=5, G=4, B=3) acquired on 21 <sup>st</sup> November 2001 (after 8/11) in the study area ..... 90
3-21	Resulted significant change detection of NDVI that used to detect the scar-scouring and depositional locations in the study area that are caused from the 8/11 flow-flood occurrence ..... 92

Figure	page
3-22	a) Significant change of NDVI (referred to Fig. 3-21) overlain on the orthophotograph image acquired on 9 <sup>th</sup> January 2002 (after 8/11); and b) photographs of four locations (number referred to the location in the map) taken a few days after the 8/11 event showing the ground truth evidences ..... 93
3-23	Examples of high resolution remote sensing imageries (acquired after the 8/11 event) used for classifying accuracy and validating NDVI results that related to detect the scar-scouring and depositional locations in the study area ..... 94
3-24	Accuracy assessment verification in training area (red box) located in Landsat 7 ETM+ (R=5, G=4, B=3) acquired on 21st November 2001 in Nam Ko Yai sub-catchment ..... 96
3-25	Scar-scouring locations interpreted from NDVI change in training area ..... 97
3-26	Scar-scouring delineation digitized from orthophotograph acquired on 14 th January 2003 (1:20,000 scale) in training area ..... 98
3-27	Location of seven rainfall-measurement stations of Thai Meteorological Department (TMD) near the study area ..... 100
3-28	Graph showing the pattern distribution of rainfall measurements in August 2001 recorded from the seven locations near the study area ..... 102
3-29	Average rainfall value (mm.) of each station near the study area during 1-10 <sup>th</sup> August 2001 (before the 8/11 event) ..... 102
3-30	Graph showing the pattern distribution of rainfall measurements in August 2002 recorded from the eight locations near the study area..... 103

Figure	page
3-31	Graph showing the average rainfall value (mm.) of each station near the study area during 1-10 <sup>th</sup> August 2002 (one year after the 8/11 event) ..... 103
3-32	Isohyte map of rainfall intensity during 1-10 <sup>th</sup> August 2001 in the study area ..... 104
4-1	Slope map overlain with scars-scouring locations (grouped in red color) in Nam Ko Yai sub-catchment..... 110
4-2	Map illustrating b/a ratio as probability of flow-flood susceptibility on slope in Nam Ko Yai sub-catchment ..... 110
4-3	Histogram distribution of a) scar-scoring number of cells on slope, and b) b/a ratio on slope in Nam Ko Yai sub-catchment..... 111
4-4	Landform topography overlain with scar-scouring locations (grouped in red color) in Nam Ko Yai sub-catchment..... 113
4-5	Map illustrating b/a ratio as probability of flow-flood susceptibility on landform topography in Nam Ko Yai sub-catchment..... 113
4-6	Histogram distribution of a) scar-scoring number of cells on landform topography, and b) b/a ratio on landform topography in Nam Ko Yai sub-catchment ..... 115
4-7	Aspect overlain with scar-scouring locations (grouped in red color) in Nam Ko Yai sub-catchment..... 117
4-8	Map illustrating b/a ratio as probability of flow-flood susceptibility on aspect in Nam Ko Yai sub-catchment..... 117
4-9	Histogram distribution of a) scar-scoring number of cells on aspect. and b) b/a ratio on aspect in Nam Ko Yai sub-catchment ..... 118
4-10	Geologic map overlain with scar-scouring locations (grouped in red color) in Nam Ko Yai sub-catchment..... 119

Figure	page
4-11	Map illustrating b/a ratio as probability of flow-flood susceptibility on geology in Nam Ko Yai sub-catchment ..... 119
4-12	Histogram distribution of a) scar-scoring number of cells on geology, and b) b/a ratio on geology in Nam Ko Yai sub-catchment ..... 121
4-13	Soil group unit map overlain with scar-scouring locations (grouped in red color) in Nam Ko Yai sub-catchment..... 122
4-14	Map illustrating b/a ratio as probability of flow-flood susceptibility on soil group unit in Nam Ko Yai sub-catchment ..... 122
4-15	Histogram distribution of a) scar-scoring number of cells on soil group unit, and b) b/a ratio on soil group unit in Nam Ko Yai sub-catchment ..... 123
4-16	Soil thickness map overlain with scar-scouring and depositional locations (grouped in red color) in the study area..... 125
4-17	Map illustrating b/a ratio as probability of flow-flood susceptibility on soil thickness in Nam Ko Yai sub-catchment ..... 125
4-18	Histogram distribution of a) scar-scoring number of cells on soil thickness, and b) b/a ratio on soil thickness in Nam Ko Yai sub-catchment ..... 126
4-19	Land cover map overlain with scar-scouring locations (grouped in red color) in Nam Ko Yai sub-catchment..... 127
4-20	Map illustrating b/a ratio as probability of flow-flood susceptibility on land cover in Nam Ko Yai sub-catchment ..... 128
4-21	Histogram distribution of a) scar-scoring number of cells on land cover, and b) b/a ratio on land cover in Nam Ko Yai sub-catchment ..... 129
4-22	Buffering distance to drainage-line map overlain with scar-scouring locations (grouped in red color) in Nam Ko Yai sub-catchment..... 130

Figure	page
4-23	Map illustrating b/a ratio as probability of flow-flood susceptibility on buffering distance to drainage-line in Nam Ko Yai sub-catchment ..... 131
4-24	Histogram distribution of a) scar-scoring number of cells on buffering distance to drainage-line, and b) b/a ratio on buffering distance to drainage-line in Nam Ko Yai sub-catchment..... 132
4-25	Flow-flood susceptibility index (FFSI) of Nam Ko Yai sub-catchment ..... 134
4-26	Flow-flood susceptibility map illustrating five classes of very high, high, moderate, low, and very low susceptibility in Nam Ko Yai sub-catchment ..... 134
5-1	Field traverses and sample locations in Nam Ko Yai sub-catchment. .... 137
5-2	Orthophotograph (1:25,000 scale, 9 <sup>th</sup> January 2002 after the 8/11 event) illustrating the specific configuration of Nam Ko Yai stream in the central part of the study area ..... 145
5-3	Closed-up orthophotograph in figure 5-2 illustrating the local geography of Nam Ko Yai stream that is suspected to be a natural temporary landslide dam location (ND) in front of the location of Tad Fa waterfall ..... 145
5-4	Photographs (looking eastward direction) illustrating the configuration of Nam Ko Yai stream channel at location ND (referred to figure 5-3) that is suitable for accumulated sediments for blockage a torrent stream and formed a natural temporary landslide dam ..... 146
5-5	Photographs (looking eastward direction) showing the different relief of about 20 m between Tad Fa waterfall (location referred to figure 5-3) and the downstream V-shape channel that is suitable for increasing water turbulent to form flow-flood occurrence ..... 147

Figure	page
5-6	Slope map of the upstream and downstream area above and below the suspected natural landslide dam location (ND) in Nam Ko Yai stream channel ..... 149
5-7	Elevation map of the upstream and downstream area above and below the suspected natural landslide dam location (ND) in Nam Ko Yai stream channel ..... 149
5-8	Topographic shape of upstream and downstream area away from the suspected natural landslide dam location (ND) in Nam Ko Yai stream channel ..... 150
5-9	Photograph showing the soft and non-resistant volcanic rocks of Lom Sak Formation in the upstream from the suspected natural temporary dam location..... 150
5-10	Three cross-sections (line A-B, C-D and E-F) across Nam Ko Yai stream channel and its valley at the upstream area, the suspected natural landslide dam location, and Tad Fa waterfall, respectively..... 151
5-11	Three cross-sections (line G-H, I-J and K-L) across Nam Ko Yai stream channel and its valley at the downstream areas from the suspected natural landslide dam location (ND) ..... 152
5-12	Photographs illustrating a) the traces of erosional feature in the out curving-bank and b) huge logs or intertwined bamboo clumps after the 8/11 flow- flood event in Nam Ko Yai stream channel at location X in Figure 5-11 ..... 153

Figure	page
5-13	Photograph showing general characteristics of the high-resistant volcanic rocks of Lom Sak Formation (Ls) in the downstream from the suspected natural temporary dam location..... 154
5-14	Photographs of the flat valley area with gentle slope in Nam Ko Yai stream channel at location Y in Figure 5-10 illustrating the rock boulder deposits along the bottom channel, as well as the erosional bank that prevailed the previous debris flow deposits with floating texture, unsorted, and unstratified characteristics of about 1.2 m thick..... 155
5-15	Oblique aerial photographs along Nam Ko Yai stream channel. The photograph, at location Z in Figure 5-11, illustrates the flow-flood track along plant debris and soils had been strongly eroded and transported from its banks before reaching the outlet of the Nam Ko Yai sub-catchment ..... 156
6-1	Aerial photograph (1:15,000 scale) acquired on 24 <sup>th</sup> December 1974 showing characteristics of the alluvial fan at the canyon mouth of Nam Ko Yai stream with contour intervals (in the solid red-line block)..... 159
6-2	Orthophotograph (1:50,000 scale) acquired on 6 <sup>th</sup> January 1996 showing characteristics of the alluvial fan at the canyon mouth of Nam Ko Yai stream without significant change in land cover..... 160
6-3	Orthophotograph (1:25,000 scale) acquired on 9 <sup>th</sup> January 2002 (after the 8/11 flow-flood occurrence) showing the distinctive active alluvial fan deposit. The main area on the northern bank of Nam Ko Yai stream with populated settlement of Ban Nam Ko Yai (brown color zone surrounding the D location) was strongly damaged..... 161

Figure	page
6-4	Expanded features of orthophotograph (1:25,000 scale) acquired on 9 <sup>th</sup> January 2002 (after the 8/11 flow-flood occurrence) showing the clear traces and tracks of flow-flood from the evidence of the distinctively active alluvial fan deposit (in brown color area) that mainly covered and severely damaged houses and orchards in the northern bank of Nam Ko Yai stream ..... 162
6-5	Two oblique aerial photographs perceivably illustrating the characteristic and extension of a large volume of deposited sediments as evidences of 8/11 incidence. .... 163
6-6	Four photographs showing some examples of seriously structural damage of houses and other infrastructures in Ban Nam Ko Yai (in the area between A and B in figure 6-5) battered and caused by the fast-moving 8/11 flow-flood..... 164
6-7	Detection change of NDVI value in the depositional location of the alluvial fan (expanded from figure 3-21) overlain on the orthophotograph (1:25,000 scale) acquired on 9 <sup>th</sup> January 2002 (as shown in figure 6-3)..... 164
6-8	Height map of the flow-flood levels detected from the mud traces on the trees and house walls (as illustrating in the attached photographs below the map) in the severely damaged area of Ban Nam Ko Yai after the fast-moving 8/11 flow-flood. .... 165
6-9	Location map of the seven measured stratigraphic profiles and a line of five resistivity survey points used for investigating the stratigraphic recognition and local subsurface geology of the previous alluvial fan deposits ..... 167

Figure	page
6-10	Cross-section of the resistivity survey interpreted from the five survey points (NK 01 – NK 05 as shown in figure 5-9) that revealed four sedimentary units lying less than 100 m below ground surface.....169
6-11	Photographs illustrating the actual location of the seven measured stratigraphic profiles (zones Pink, Green, Blue1, Blue2, Blue3, Yellow1 and Yellow2 ) along the eroded-bank of Nam Ko Yai stream..... 171
6-12	Photographs illustrating lateral and vertical stratigraphic characteristics of three sedimentary units (debris flow unit, coarse-grained fluvial unit, and fine-grained fluvial and debris flow unit) of the previous alluvial fan that well exposed along the eroded-bank of Nam Ko Yai stream ..... 172
6-13	Photographs illustrating detailed sedimentary and stratigraphic characteristics in vertical and lateral succession of three sedimentary units (debris flow unit, coarse-grained fluvial unit, and fine-grained fluvial and debris flow unit) of the previous alluvial fan deposits at the zone Green .....173
6-14	Photographs illustrating detailed sedimentary and stratigraphic characteristics in vertical succession of two sedimentary units (coarse-grained fluvial unit, and fine-grained fluvial and debris flow unit) of the previous alluvial fan deposits at the zones Yellow1 and Yellow2..... 174
6-15	Photographs illustrating detailed sedimentary and stratigraphic characteristics in vertical succession of the fine-grained fluvial and debris flood unit that overlay with the sharp contact manner on top of the coarse-grained fluvial unit at the zones Blue1, Blue2 and Blue3..... 175

Figure	page
6-16	Photographs illustrating the general characteristics in the uppermost fine-grained fluvial and debris flood unit at the zone Pink (referred to figure 6-9 and 6-11) and the preserved large wood debris at the lower part (PLW) and at the upper part (PUW) locations ..... 177
6-17	Closed-up photographs of the collected wood debris samples from the preserved locations at PLW and PUW (as shown in figure 6-16) illustrating their general characteristics of charcoal characteristic with fibrous texture and pale brown wood with rather complete wooden texture, respectively..... 178
7-1	Three-dimensional drape of the interpreted scar-scouring locations (grouped in red color) through a 1:20,000 base-scale DEM in Nam Ko Yai sub-catchment..... 181
7-2	Three-dimensional drape of five classes of very high, high, moderate, low, and very low susceptibility, respectively, through a 1:20,000 base-scale DEM in Nam Ko Yai sub-catchment ..... 181
7-3	Three-dimensional drape of false color composite of Landsat 7 ETM+ (R=5, G=4, B=3) acquired on 5 <sup>th</sup> January 2001 through a 1:20,000 base-scale DEM illustrating the general characteristics before the 8/11 flow-flood occurrence in Nam Ko Yai sub-catchment and its alluvial fan..... 183
7-4	Three-dimensional drape of false color composite of Landsat 7 ETM+ (R=5, G=4, B=3) acquired on 21 <sup>st</sup> November 2001 through a 1:20,000 base-scale DEM showing distinguish characteristics after 8/11 flow-flood occurrence in Nam Ko Yai sub-catchment, and the depositional area of alluvial fan ..... 183

Figure	page
7-5	FLO-2D simulation results of the channel flow conditions of water height from the condition without dam while the rainfall accumulation was more than 100 mm at 8 p.m. on 9 <sup>th</sup> August 2001 (about 31 hours before the 8/11 event)..... 188
7-6	FLO-2D simulation results of the channel flow conditions of water height from the condition without dam while the rainfall accumulation was 120 mm at 3 a.m. on 10 <sup>th</sup> August 2001 (about 24 hours before the 8/11 event)..... 188
7-7	FLO-2D simulation results of the channel flow conditions of water height from the condition without dam while the rainfall accumulation was more than 140 mm at 3 a.m. on 11 <sup>th</sup> August 2001 (0.5 hour before the 8/11 event) ..... 189
7-8	FLO-2D simulation results of the channel flow conditions of water height from the condition with dam while the rainfall accumulation was 120 mm at 3 a.m. on 10 <sup>th</sup> August 2001 (about 24 hours before the 8/11 event). ..... 189
7-9	FLO-2D simulation results of the channel flow conditions of water height from the condition with dam while the rainfall accumulation was more than 140 mm at 3 a.m. on 11 <sup>th</sup> August 2001 (0.5 hour before the 8/11 event). ..... 190

# CHAPTER 1

## INTRODUCTION

Every year, natural disasters have claimed several thousand lives all over the world. This is quite costly to the world economy both in human affairs and in economical aspects as natural disasters have major direct and indirect economic and socio-economic effects as well as physical destruction. Unfortunately, the impact of these disasters is more severe in many developing countries as the developed countries have already created disaster mitigation and disaster preparedness programs while the developing countries normally only give in to such vulnerability.

The natural hazard events are the disasters of a natural phenomenon or combination of phenomena, such as landslides, floods, earthquakes, volcanic eruptions, tsunamis, etc., which can cause some loss of lives and property damage. Literally, no where on earth is safe from the impact of the natural hazards. Due to an increasing population density and non-existing or inadequate development plan, especially in Thailand, more and more people are prone to such disasters.

### 1.1 Rationale

On 11<sup>th</sup> August 2001 (here after referred to as 8/11) at 3:30 a.m., a disastrous debris flow and associated debris flood had severely damaged Ban Nam Ko Yai situated on the alluvial fan just below the canyon mouth of the same-named Nam Ko Yai stream, a tributary of Pa Sak river in Amphoe Lom Sak, Changwat Phetchabun, central Thailand. The muddy flood water, full of debris of fallen trees, had destroyed several houses along the stream banks and claimed 136 lives with an estimation of over 200 million Bath of the property damage (Secretariat Office of Government, 2002). This is one of the so many severe tragedies caused by the debris flows and debris floods in Thailand in the past few decades.

A complete understanding of the processes and relevant parameters that influence this 8/11 incident in Nam Ko Yai sub-catchment and the alluvial fan below in terms of action, source areas and run-out zones, as well as the evaluation of the potential for debris-flow and debris-flood hazards in this event has never been accomplished. Besides, the repetition of such debris flow and debris flood in this area is yet to be evaluated. A case study analysis of this event should also provide essential basic information to mitigate any future debris flows and debris floods in this area and the areas of similar geographical conditions.

In general, debris flows and related sediment flows are fast-moving flow-type landslides composed of slurry of rock, mud, organic matter, and water that move down drainage-basin channels to the alluvial fan. Debris flows and related sediment flows may be initiated on the adjacent steep slopes or within channels by one of the two processes, by landsliding or by sediment bulking of surface water flows during periods of rapid addition of water to the terrain, either by intense rainfall or rapid snowmelt. Flows typically incorporate additional sediment and vegetation as they travel down channel (Cannon, 1997). When flows reach an alluvial fan formed by such previous flows, they lose channel confinement. Then the flows spread laterally and deposit more entrained sediment overbanks. These alluvial fans are normally the favorable living sites so the settlements are merely vulnerable to such flows and floods. Thus a debris-flow-hazard evaluation is essential when development is planned on alluvial fans (U.S. National Research Council, 1996).

Variations in sediment-water concentrations produce a continuum of sediment-water flow types that build alluvial fans. Beverage and Culbertson (1964), Pierson and Costa (1984), and Costa (1988) describe the following flow types based on generalized sediment-water concentrations and resulting flow behavior: stream flow (less than 20% sediment by volume), hyperconcentrated flow (20 to 60% sediment by volume), and debris flow (greater than 60% sediment by volume). These categories are only approximations because the exact sediment-water concentration and flow type depend on the grain-size distribution and physical-chemical composition of the flows. Also, field observations and

video recordings of poorly sorted, water-saturated sediment provide evidence that no unique flow type adequately describes the range of mechanical behaviors exhibited by these sediment flows (Iverson, 2003). Also, all three flow types can occur together during a single event. The U.S. National Research Council (1996) considers stream, hyperconcentrated, and debris-flow types of alluvial-fan flooding in the report on Alluvial-Fan Flooding. The term debris flood had been used in Utah to describe hyperconcentrated flows (Wieczorek and others, 1983). Debris floods were also referred to in many other terms in the technical literatures, including waterflood with large sediment load (Costa and Jarrett, 1981), sediment flow (Ikeya, 1981) and mud flood (U.S. National Research Council, 1982).

In the last two decades the "state-of-the-art" of evaluation of debris-flow hazard continues to evolve as our knowledge of sediment-flow processes advances. As new techniques become available and are generally accepted, they should be used in future hazard evaluations. Wieczorek and others (1983) proposed the techniques to evaluate potentials for a debris flow-flood that should answer the following questions; relationship between rainfall (or snowmelt) and landslide movement, stability of the partly-detached landslides, process of transformation from landslide to debris flow, incorporation of channel materials by debris flow, transition from debris flow to debris flood, factors that control debris flow run-out, and recurrence of debris floods-flows at canyon mouths.

According to U.S. National Research Council (1996), an alluvial fan flooding hazard is indicated by three related criteria, namely, flow path uncertainty below the hydrographic apex, abrupt deposition and ensuing erosion of sediment when a stream or debris flow loses its competence to carry eroded material from a steeper upstream source area, and an environment where the combination of sediment availability, slope, and topography creates an ultrahazardous condition for which elevation on fill will not reliably mitigate the risk.

The guidelines for the geologic evaluation of debris-flow hazard on alluvial fans were also proposed by Giraud (2005) to be necessarily for safe and appropriate land use that could prevent loss of life and property damage. In general, the purpose of a

geologic evaluation is to determine whether or not a debris-flow hazard exists in the area of interests, to describe the hazard if exist, and if needed, to provide geologic parameters necessarily for hydrologists and engineers to design risk-reduction measures. Determination of active depositional areas, frequency, and magnitude (volume) of previous flows, and likely impacts of future sedimentation events are the expected outputs from such geological evaluation. Dynamic analysis of debris flows-floods using hydrologic, hydraulic, and other engineering methods to design site-specific risk-reduction measures should also be addressed by these guidelines.

However, a geologic evaluation of potential for debris-flow- and related-sediment-flow hazard requires a large spatial variability of the required input data, while the techniques of analysis may be very costly and time-consuming. Over the past three decades, the increasing availability of remote sensing technology and geographic information systems (GIS) has created opportunities for a more detailed and rapid analysis of landslide hazard in large areas (Van Westen, 1994). Because landslides directly affect the ground surface to give scar records, remote sensing techniques are hence suitable to slope instability studies. The term remote sensing being used here is in the widest sense, including aerial photography and imagery obtained by satellites and any other remote-sensing techniques. Remote sensing is particular useful when stereo images are used because they depict in the stereo model the typical morphologic features of landslides, which often provide diagnostic information concerning the type of movement. Also, the overall terrain conditions, which are critical in determining the susceptibility of a site to slope instability, can profitably be interpreted from remote sensing data. GIS can be used to update, manipulate, integrate and analyze the spatially distributed data, and to prepare the final maps related to the purpose of a geologic evaluation of debris-flow- and related-sediment-flow-hazard. It is essential that the potential source areas and run-out zones of debris flows are correctly assessed and mitigation measures adopted using modern mapping and monitoring techniques (Corominas and others, 1996). Detailed specification of the above mentioned literatures will be explained in the following chapter.

Therefore, a debris flow-hazard evaluation is necessarily for safe and appropriate land use determination to prevent loss of life and property damage. Understanding the processes that govern a debris-flow initiation, debris-transport and water-transport action in the drainage basin, sediment bulking, and deposition on the alluvial fan is vital to a hazard evaluation. Debris-flow hazards may be managed differently in terms of land-use planning and protective measures, but because debris-flow and stream-flow hazards are closely associated, concurrent evaluation of both debris-flow and stream-flow components of alluvial-fan flooding is often beneficial.

This thesis addresses only a hazard evaluation associated with debris-flow and debris flood (or hyperconcentrated-flow), sediment-water concentrations, and not stream-flow flooding on alluvial fans. The term *flow-flood* will be conveniently used here in a general way to include all flows within the debris-flow and debris flood (or hyperconcentrated-flow) sediment-water concentration range that are difficult to distinguish from each other based on their deposits.

## 1.2 Objectives

The purposes of this present study are

- To investigate the parameters influencing the case-study 8/11 flow-flood occurrence in Nam Ko Yai sub-catchment,
- To identify the potential source area, run-out zone, and depositional area of the 8/11 flow-flood occurrence in Nam Ko Yai sub-catchment and the alluvial fan,
- To determine the evidences of the potential for hazards from the flow-flood occurrence in Nam Ko Yai sub-catchment and the alluvial fan, and
- To define the relationship between the sedimentary sequences and the flow-flood occurrence in the alluvial fan.

### 1.3 Hypothesis

As the "state-of-the-art" of debris-flow- hazard evaluation continues to evolve as our knowledge of sediment-flow processes advances in the last two decades. The techniques of landslide hazard assessment especially for debris flow-hazard evaluation proposed by Wieczorek and others (1983), Van Westen (1994), Corominas and others (1996), U.S. National Research Council (1996), Giraud (2005) become available and are generally referred to. Besides, flow-flood susceptibility analysis by using univariant probability analysis (Lee and Min, 2001) is a simplest technique which can attempt to assess the probabilistic relationship between relevant environmental parameters and the occurrence of landslides in a given region. Those techniques should possibly be applicable for evaluating the potential of flow-flood in the Nam Ko area as the first case study in Thailand.

Theoretically, the major parameters being suspected to affect this 8/11 event should be the landforms, slope gradient, underlying materials, land cover and land use, and heavy rainfalls. Whereas the tropical storm "Usa-ngi" that passed through here with the unusual high amount of rainfalls during the first two weeks of August 2001, the inappropriate land use in the strongly deforested of Nam Ko Yai sub-catchment are primarily blamed to be the major causes of this tragedy by the publics and academics. Thus this research attempts to apply those "state-of-the-art" techniques of evaluation for flow-flood hazard to identify the flow-flood hazard, to determine parameters necessary for the initiation of the flow-flood process, and to determine whether or not a flow-flood hazard can occur again.

### 1.4 Scope and limitation

This thesis is limited to identify the parameters influencing the 8/11 flow-flood occurrence by the field-knowledge base integrated with the application of the remote sensing and geographic information system (GIS) techniques. Detailed field investigation was conducted only in the main target areas that were analyzed as the potential source areas, run-out zones, and depositional areas of the flow/flood in Nam Ko Yai sub-

catchment. In addition, detailed investigating of sedimentary sequences to define the relationship between the sedimentary sequences and the flow-flood occurrence were done only in the active alluvial fan.

Dynamic analysis of flow-flood using hydrologic, hydraulic, and other engineering methods to design site-specific risk-reduction measures was not addressed in detail in this research. Ranges for debris-flow bulking rates, flow volumes, runout distances, deposit areas, and deposit thicknesses were neither studied, thus further research is necessary to quantify the physical characteristics of debris flows all over the sub-catchment. The methods outlined in this thesis are considered to be practical and reasonable for obtaining planning, design, and risk-reduction information, but these methods may not be applicable in all cases.

### 1.5 Location of the study area

The study area (Figure 1-1) is located in the northwestern corner of the main upper Pa Sak catchment at the foot of Khao Ko and Phu Hin Rong Kla mountains of Phitsanulok-Phetchabun range, central Thailand. The area comprising approximately 75 square kilometers, geographically defined as Nam Ko Yai sub-catchment and its alluvial fan, is in Amphoe Lom Sak, Changwat Phetchabun (Figure 1-2). Ban Nam Ko Yai is situated on the alluvial fan. The extents of the coordinates of the study area are approximately defined as 1868500 N, 719600 E in the northwestern edge and 1856000 N, 735500 E in the southeastern edge in Universal Transverse Mercator projection with 47 North zone in Indian 1975 ellipsoid. The sub-catchment configuration is north-southerly trending upstream, then southeasterly. The sub-catchment area is 14 km long and 5 km wide. The upstream rims are bounded by the steep slopes to a maximum altitude of 1,746 m in the northwestern part, down to the gentler slopes then flat rolling sub-catchment terrain and the alluvial fan at an altitude of 160 m.

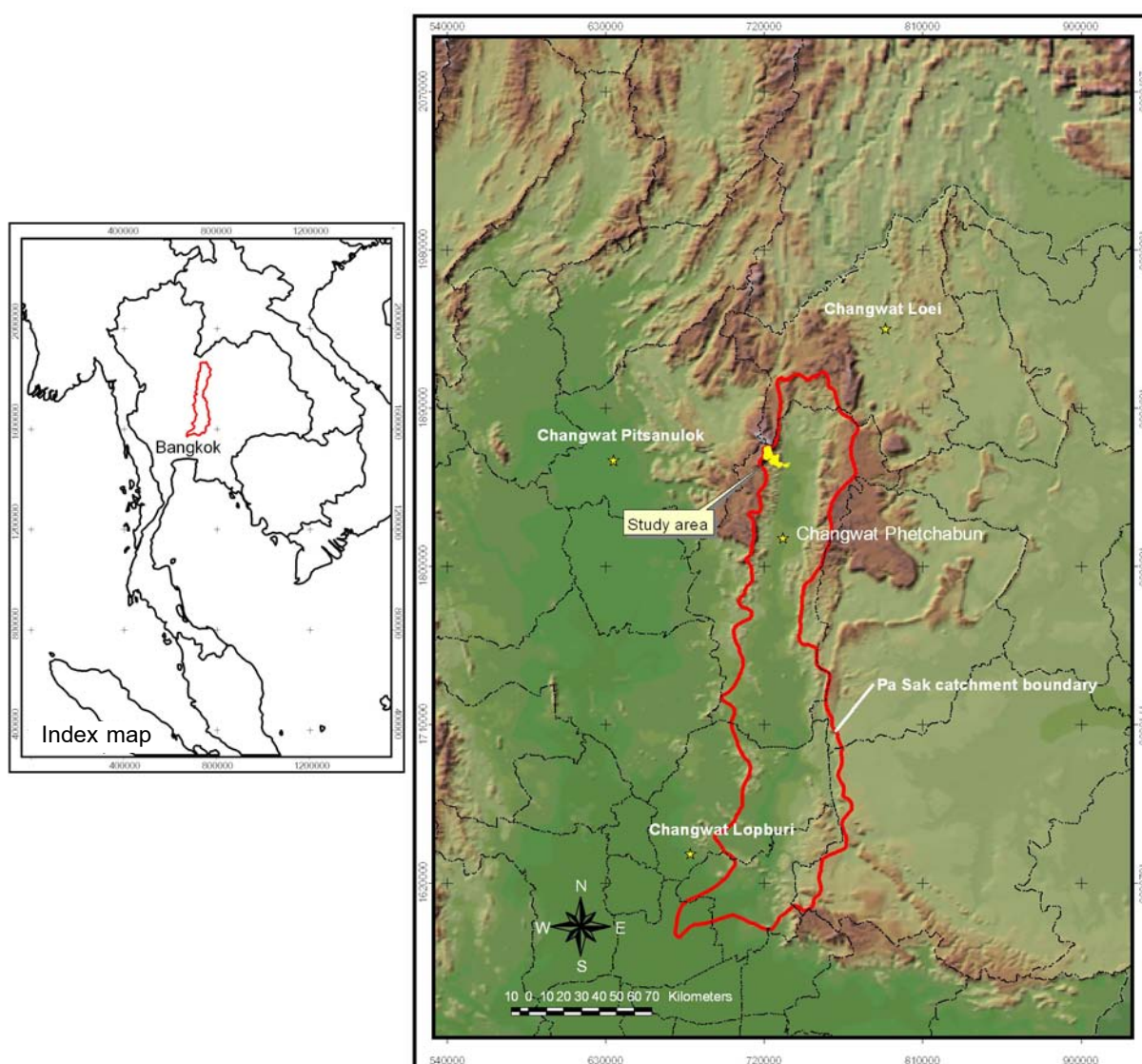
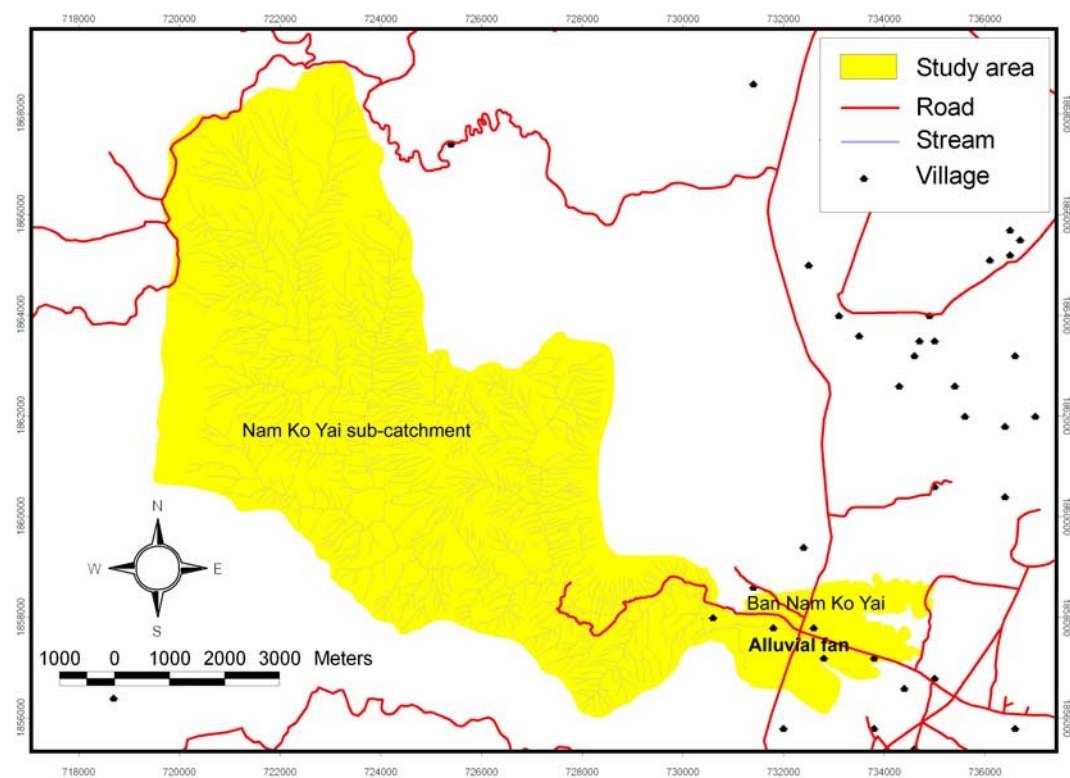
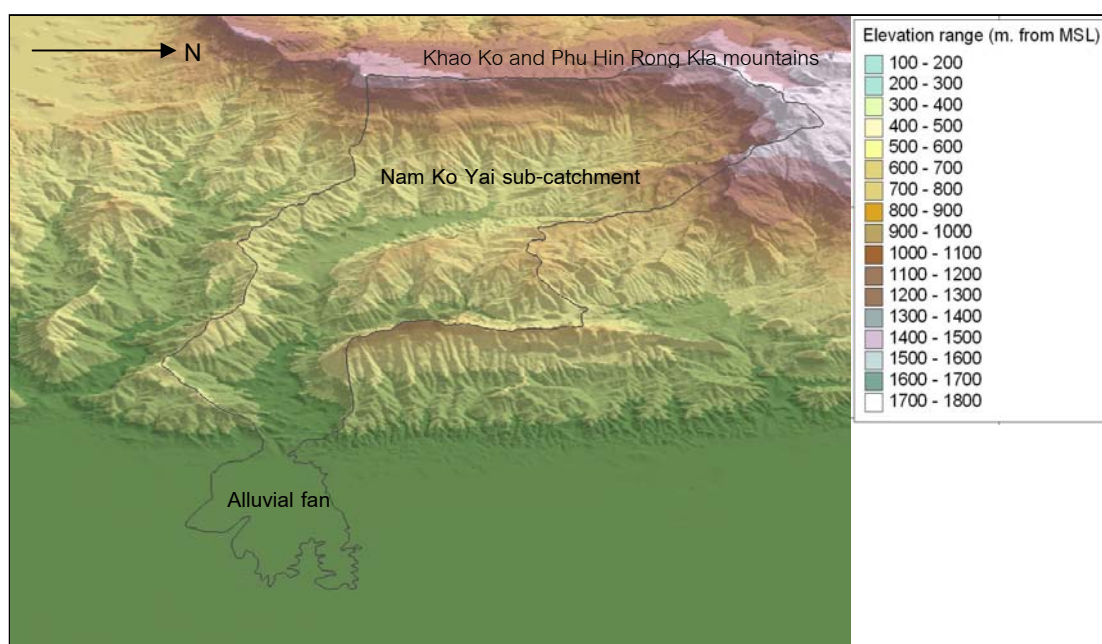


Figure 1-1 Geographic setting of the study area.



a)



b)

Figure 1-2 a) Location of the study area with important reference locations, and  
 b) Three-dimensional drape of Nam Ko Yai sub-catchment and its alluvial fan boundary (black color line) of the study area and surrounding terrains.

## 1.6 Expected outputs

The expected outputs of this thesis consist of:

- Debris flow-flood susceptibility in Nam Ko Yai sub-catchment.
- Three dimension models and maps representing the potential source areas, run-out zones, and depositional areas of the 8/11 flow-flood in the study area.
- Evidence and relationship between the sedimentary sequences and the flow-flood occurrence in the alluvial fan.
- Criteria to determine the potential for the future disastrous events in the study area.

These results should supply planners and decision-makers with adequate and understandable information for a more effective planning with appropriate strategies for reducing and mitigating the debris-flow hazards and related phenomena in a long term risk that may be repeatedly occurred in the study area as well as in other areas of similar geographical conditions, especially, along the western flank of Phitsanulok-Phetchabun mountain range.

## 1.7 Research methodology

To accomplish the aims of this thesis, the research involves four sequential steps are designed. Each of which is described as follows:

### 1.7.1 Preparation

This step includes:

- Literature review of the related researches in the study area, southern Thailand, and other countries.
- Acquisition and study of the previous basic data acquisition, i.e. aerial photographs (1:25,000 and 1:50,000 scale), satellite images of medium resolution (Landsat), topographic map, geologic map, and land use map

to understand the topography, geology, and land use pattern of the study area as general background information.

- Intensive comprehension on the conceptual framework of landslide and especially the criteria to evaluate potential of flow-flood occurrence.

### 1.7.2 Field investigation

The field investigation and direct observation were carried out as follows:

- Reconnaissance to understand and recognize the limitation in the study area for preparing the data and related plan that would be used in further steps of the field investigation
- Intermediate field investigation to investigate and define the physical conditions, geologic characteristics and soil characteristics that may affect the occurrence of flow-flood, and to conduct ground-truth to inspect the correctness of the analyzed results from the remote sensing image analysis and interpretation
- Detailed survey to collect the elevation data of the scar-scouring from 8/11 flow-flood along the both sides of Nam Ko Yai stream, to interview local people who witnessed in the 8/11 event, and to collect samples of weathered products of the rock formations that were sensitive to the flow-flood occurrence especially in the major potential source areas and run-out zones of Nam Ko Yai sub-catchment. The results from the detailed survey are used as evidences of the potential source areas, run-out zones, and depositional areas of the 8/11 flow-flood.
- Investigation the sedimentary sequences to define the relationship between the sedimentary sequences and the flow-flood occurrence in the alluvial fan.
- Performing a resistivity survey in the alluvial fan area to estimate the subsurface characteristics of the sedimentary sequences

### 1.7.3 Laboratorial studies

The laboratorial analysis is conducted as follows:

- Thematic (GIS and remote sensing) data preparation. These inventory data consist of topography, geology, geomorphology, terrain unit, morphometry (digital elevation model (DEM), slope, aspect), land use and land cover, hydrology (drainage network, river and basin configurations), meteorology of rainfall intensity. Softwares of geographic information system (GIS) and remote sensing (ArcInfo, ArcView 3.3, ArcView 3D Analysis, ArcView Image Analysis, and ERDAS IMAGINE 8.5) are applied in developing, manipulating, and analyzing the digital data. The digital elevation data is converted from a 1:20,000 scale digital topographic map (10 m contour interval) derived from Land Development Department (LDD).
- Interpretation of aerial photographs (1:25,000 and 1:50,000 scale), orthophotograph rectified images (1:25,000 scale), and satellite images of medium and high resolution (Landsat TM and IKONOS) that were acquired before and after the 8/11 flow- flood event. This sub-step was conducted to develop the new data (e.g. scars-scourings from the 8/11 flow-flood event), and update or improve the secondary data from the above data pre-processing sub-step. These inventory data were also checked from ground-truth information from brief field traverses to inspect the accuracy in the intermediate field investigation.
- Debris flow-flood hazard analysis in Nam Ko Yai sub-catchment in terms of debris flow-flood susceptibility analysis and calculation of debris flow-flood susceptibility is conducted. This is preliminary debris flow-flood hazard analysis by univariant probability method to present the spatial relationship between the scar-scouring locations and each of available flow-flood influencing parameters (as theoretically mentioned) in Nam Ko Yai sub-catchment, namely, slope, landform topography, geology, soil group unit, soil thickness, land cover, and stream proximity, respectively.

The GIS was used to compile a vast amount of data efficiently, and a statistical program was used to maintain specificity and accuracy.

- Laboratory geotechnical testing of the weathered products of the rock formation collected from the detailed survey of field investigation step. This defines some engineering properties of sedimentary properties and basic geotechnical properties (e.g. the grain size analysis, determination of Atterberg limits and indices, natural moisture content, and shear strength) that were used to identify the sensitivity from the 8/11 flow-flood occurrence.

#### 1.7.4 Synthesis, discussion and conclusions

This step includes:

- Synthesizing, discussing and concluding debris flow-flood susceptibility in Nam Ko Yai sub-catchment.
- Synthesizing, discussing and concluding the potential source areas, run-out zones, and depositional areas of the 8/11 flow- flood occurrence in Nam Ko Yai sub-catchment and the alluvial fan.
- Synthesizing, discussing and concluding the criteria of the potential for hazards from the flow-flood occurrence in the study area.
- Synthesizing, discussing and concluding the relationship between the sedimentary sequences and the flow-flood occurrence in the alluvial fan.

In order to accomplish the objectives of this research, the schematic diagram illustrating the present methodology system was designed as shown in Figure 1-3.

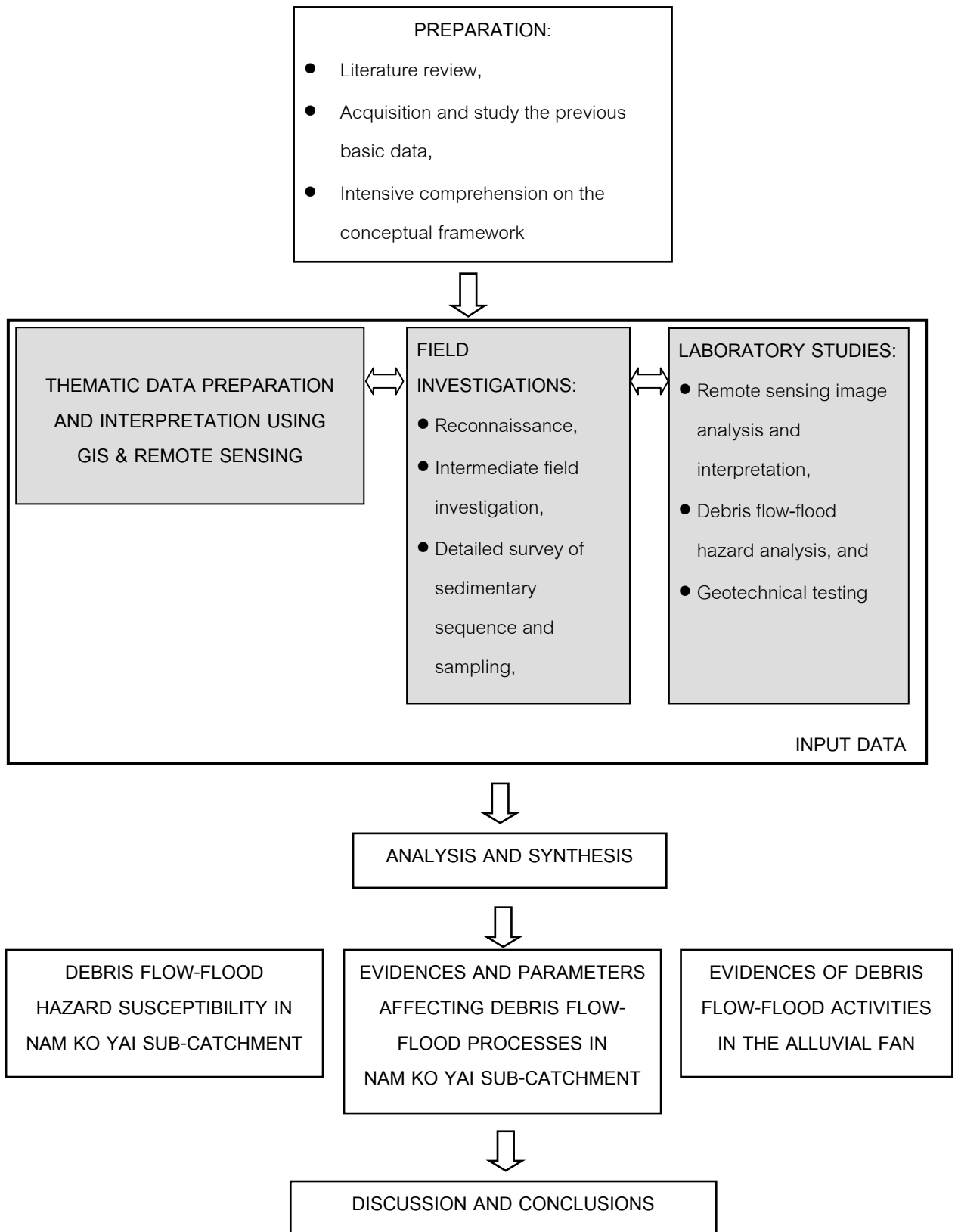


Figure 1-3 Schematic diagrams illustrating the research methodology system.

## 1.8 Components of the thesis

This thesis comprises eight chapters including this introductory Chapter 1. Chapter 2 is initiated with an intensive comprehension on basic concepts on evaluation of the potential for debris-flows and related sediment-flows as well as the previous investigations from the related technical literatures are presented. The applications of the remote sensing and geographic information system (GIS) in landslide hazard assessment are briefly reviewed.

Since the possibilities and limitations of the proposed methodology can only be evaluated critically when field data are available. Data preparation and interpretation in terms of types of input data and data production stage is given in Chapter 3. In this chapter, data input from thematic data pre-processed with the application of geographic information system (GIS) and remote sensing techniques are produced and interpreted. Following the data preparation and interpretation stages, debris flow-flood hazard analysis of Nam Ko Yai sub-catchment by the statistic approach is proposed in Chapter 4. Debris flow-flood susceptibility is preliminary analyzed using the influencing parameters by univariant probability method to present the spatial relationship between the detected scar-scouring locations and each of the influencing parameters in the sub-catchment. Besides, calculation of debris flow-flood susceptibility in the sub-catchment is also proposed in this chapter.

The core of this thesis is presented in the Chapters 5 and 6. The investigation of the available and new evidences and parameters affecting debris flow-flood processes, namely, evidences of geotechnical properties of soil and rock samplings, as well as evidences of suspected temporary landslide dam location and the channel configuration in Nam Ko Yai sub-catchment are presented in Chapter 5. Recognition and characterization of the alluvial fan, by defining its activeness as well as the geomorphology and the stratigraphic recognition of the previous alluvial fan deposits are the subjects in Chapter 6.

In Chapter 7 the attention is focused on discussion of the debris flow-flood susceptibility results, the flow-flood event reconstruction and its potential, and FLO-2D

simulation results for validation of the suspected temporary landslide dam occurrence in the central part of Nam Ko Yai sub-catchment, respectively. Finally, the evaluation of potential for the 2001 flow-flood in Nam Ko Yai sub-catchment and its alluvial fan are summarized and concluded with further recommendation in Chapter 8.

## CHAPTER 2

### LITERATURE REVIEW

#### 2.1 Introduction

In this chapter, the definition and terminology given for landslide classification system, landslide hazard, knowledge types used in prediction of landslide hazard, and basic concepts and previous investigations on evaluation of the potential for debris-flows and related sediment-flows, are reviewed. Besides, use of the remote sensing and geographic information system (GIS) techniques in landslide hazard assessment are also briefly mentioned.

#### 2.2 Definition and Terminology

A wide variety of terms have been used for the denudational process whereby soil or rock is displaced along the slope by mainly gravitational forces. The frequently used terms are slope movement, mass movement, mass wasting, and landslide.

Mass movement is defined as "the outward and downward gravitational movement of earth material without the aid of running water as a transporting agent" (Crozier, 1986), or "the movement of a mass of rock, debris or earth down a slope" (Cruden, 1991). These are the most widely used definitions of the phenomenon. Although they are slightly different from each other when considering beyond the scope of inclusion of water, both definitions point to a mass transportation down slope in which a hazardous activity for humans may occur.

In the last few decades, landslide is a term being the most used, though in the narrow sense of the word (*sensu strictu*), it only indicates a specific type of slope movement with the specific composition, form and speed.

### 2.3 Landslide classification systems

The following factors can be used and have been used to classify landslides:

- Material (rock, soil, lithology, structure, geotechnical properties);
- Geomorphic attributes (weathering, slope form);
- Geometry of landslide body (depth, length, height etc.);
- Type of movement (fall, slide, flow etc.);
- Climate (tropical, temperate, periglacial etc.);
- Water (dry, wet, saturated);
- Speed of movement (very slow, slow etc.);
- Triggering mechanism (earthquake, rainfall etc.).

Therefore, numerous approaches to classification of slope movements have been made, those concerning the type of movement, material, velocity, morphometric parameters, amount of water involved, velocity, climate, etc. The most common classifications are discussed briefly below.

Sharpe (1938) gave a classification based on the type of movement (slip and flow), kind of material (earth or rock) and the role of water/ice as main factors, while the speed of the movement is a secondary parameter (Table 2-1).

The continuum of slope movements to the transportation of solids mainly by water (fluvial transportation) or by ice (glacial transportation) is clearly shown in the setup of the classification. Hutchinson (1988) used type of movement and morphology, which enables for a classification based only on field observation or the evaluation of landslides by means of on aerial photography. A practical classification also was that of Crozier's (1986). He used the threshold values of morphometric criteria (width, depth, length, dilatation, etc.) to define the different types of landslides (Table 2-2).

Table 2-1 Landslide classification system by Sharpe (1938).

		MOVEMENT		ICE					EARTH OR ROCK			WATER	
		KIND	RATE										
				CHIEFLY ICE	EARTH OR ROCK PLUS ICE	EARTH OR ROCK DRY OR WITH MINOR AMOUNTS OF ICE OR WATER	EARTH OR ROCK PLUS WATER			CHIEFLY WATER			
WITH FREE SIDE	FLOW	USUALLY IMPERCEPTIBLE	SLOW TO RAPID	GLACIAL TRANSPORTATION	ROCK GLACIER CAP	ROCK --- CREEP	SOLIFLUCTION		TALUS CREEP		FLUVIAL TRANSPORTATION		
					DEBRIS --- AVALANCHE	SOIL CREEP	EARTHFLOW		MUDFLOW SEMARID, ALPINE VOLCANIC				
NO FREE SIDE	SLIP OR FLOW	PERCEPTIBLE	SLOW TO RAPID	GLACIAL TRANSPORTATION	DEBRIS --- AVALANCHE	SLUMP		DEBRIS --- AVALANCHE					
					DEBRIS --- SLIDE	DEBRIS --- FALL							
		VERY RAPID				ROCKSLIDE		ROCKFALL					
		FAST OR SLOW				SUBSIDENCE							

Varnes (1978) proposed a classification based on the type of movement and material type as shown in Table 2-3. This classification nominated primarily types of movement and types of material (as bed rock and engineering soils) as main factors.

Rather than dealing with the types, activities and definitions, as they are defined by the I AEG Commission on Landslides in the 1990's, a more relational approach was given by Soeters and Van Westen (1996) as "Slope instability processes are the product of local geomorphic, hydrologic and geologic conditions; the modification of these by geodynamic processes, vegetation, land use practices and human activities; and the frequency and intensity of precipitation and seismicity".

Table 2-2 Landslide classification according to Hutchinson (1988).

Rebound	When ground is unloaded, either artificially by excavation or naturally by erosion, the unloaded area responds, initially elastically and subsequently by slow swelling
Creep	Any extremely slow movements which are imperceptible except through long-period measurement
Sagging of mountain slopes	A general term for these deep-seated deformations of mountain slopes, which, in their present state of development, do not justify classification as landslides.
Landslide	Relatively rapid downslope movements of soil and rock, which take place characteristically on one or more discrete bounding slip surfaces which divide the moving mass.
Debris movement of flow like form	Term covering five types of movement of flow-like form, which differ markedly in mechanism: non-periglacial mudslides, periglacial mudslides, flow slides, debris flows and sturzstroms.
Topple	A movement that occurs when the vector of resultant applied forces falls through, or outside a pivot point in the base of the affected block.
Fall	The more or less free and extremely rapid descent of masses of soil or rock of any size from steep slopes or cliffs.
Complex slope movement	The combination of two or more of the types of movements described above.

Table 2-3 Landslide classification system by Varnes (1978).

<i>Type of Movement</i>			<i>Type of Material</i>		
			Bedrock	Engineering Soils	
				Predominantly Coarse	Predominantly Fine
Falls			Rock Fall	Debris Fall	Earth Fall
Topples			Rock Topple	Debris Topple	Earth Topple
Slides	Rotational	Few Units	Rock Slump	Debris Slump	Earth Slump
	Translational		Rock Block Slide	Debris Block Slide	Earth Block Slide
			Many Units	Rock Slide	Debris Slide
Lateral Spreads			Rock Spread	Debris Spread	Earth Spread
Flows			Rock Flow (Deep Creep)	Debris Flow (Soil Creep)	Earth Flow
Complex – Combination of Two or More Principal Types of Movement					

## 2.4 Landslide hazard

Mass movement, or slope instability or landsliding are the same natural denudational and degradational processes, unless they threaten human life. Their interference with ongoing human activities in the terrain marks a landslide hazard. The general accepted terminology explained below is that's of Varnes's (1984) and is illustrated in a form of formula:

$$R_s = H * V$$

Where

Natural hazard (H): The probability of occurrence of a potentially damaging phenomenon within a specified period of time and within a given area (Figure 2-1).

**Vulnerability (V):** The degree of loss of a given element or set of elements at risk resulting from the occurrence of a natural phenomenon of a given magnitude. Scale is 0 (no change) to 1 (total loss).

**Specific risk (Rs):** The expected degree of loss due to a particular natural phenomenon. It may be expressed by the product of H and V.

The total risk could also be expressed in another formula:

$$R_t = E * R_s$$

Where

**Elements at Risk (E):** The population, properties, economic activities, including public services, etc., at risk in a given area.

**Total Risk (Rt):** The expected number of lives lost, persons injured, damage to property or disruption of economic activity due to a particular natural phenomenon.

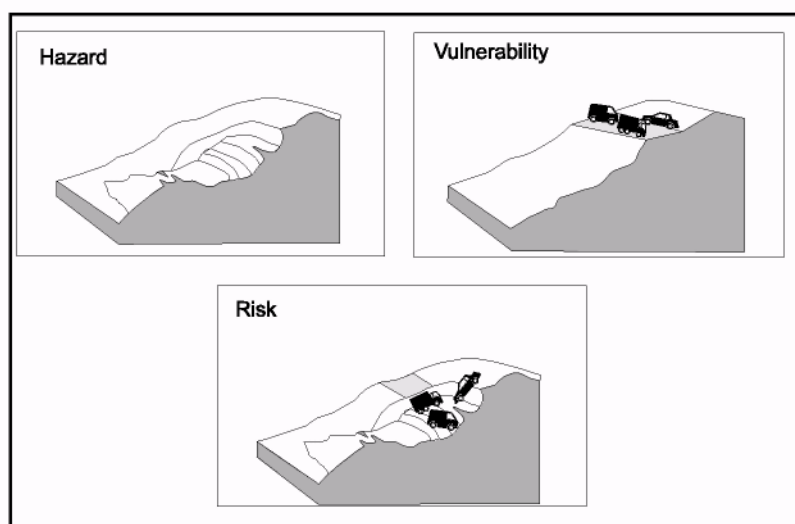


Figure 2-1 Graphical representation of hazard, vulnerability and risk (Varnes, 1984).

Based on the above definitions, hazard and risk information are generally represented as discrete maps. The discrete classes represent equal probability classes, which are in turn equal hazard or risk classes. The differentiation of hazard classes and

their groupings are called "zonation". The formal definition given by Varnes (1984) is "The term zonation refers to the division of land into homogenous areas or user defined domains and the ranking of these areas according to their degrees of actual or potential natural hazards".

The natural hazard zoning/mapping constitutes the first and major task of the earth scientists in natural hazard analysis. The zoning of a natural hazard is the vital part of the study strategy in which the whole strategy will be based on. The zonation activities are mutually dependent on some factors as shown in Figure 2-2.

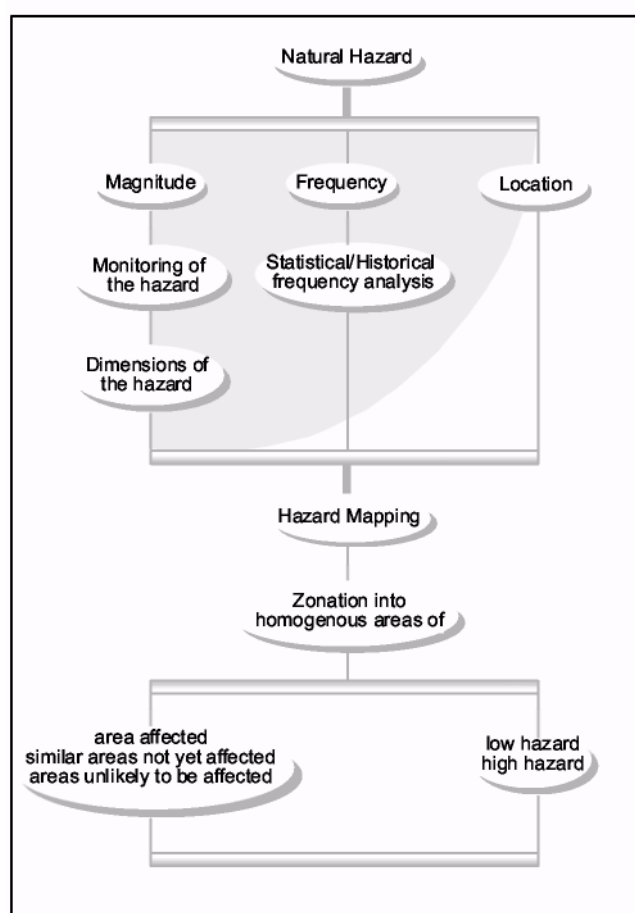


Figure 2-2 Overview of landslide hazard zonation activities (Varnes, 1984).

These factors can be grouped into magnitude properties of the hazard, frequency of the hazard and the spatial location of the hazard. The next step in hazard mapping is to show the mapped hazard and to classify the hazard map into some homogenous areas regarding the equal attributes of the hazard map.

The natural hazard zoning is controlled mainly by two factors, such as: the scale of the zoning or mapping and the knowledge type used in the hazard zoning.

#### 2.4.1 Scale factor in analysis

Before starting any data collection, an earth scientist working on a hazard analysis project should have to answer a number of interrelated questions below.

- What is the aim of the study?
- What scale and with what degree of precision must the result be presented?
- What are the available resources in the form of money, data and manpower?

As the aim of the study would be previously defined, the scale and the precision are the first parameters to be defined prior to the start of the project. Hence, the scale factor must be determined at the first glance as it controls the type of the input data, nature of the analysis, and the output data of the study. The outcome precision also depends on the scale chosen; however is independent parameter regarding the nature of the project. The necessary adjustments should be made with the scale until the output precision and the desired precision fulfills the project conditions. The resource analysis will be conducted after the aim and scale is fixed.

The following scales of analysis, which were presented in the International Association of Engineering Geologists (IAEG) Monograph on engineering geological mapping (IAEG, 1976) can also be distinguished in general natural hazard zonation (Figure 2-3).

##### a. National Scale (<1/1,000,000)

The national scale analysis is used only to outline the problem, give an idea about the hazard types and affected hazard prone areas. They are prepared generally for the entire country and the required map detail is very low, even in the best case giving only data based on records in the form of an inventory. The degree of the hazard is assumed to be uniform. These kinds of maps are generally prepared for agencies

dealing with regional (agricultural, urban or infrastructure) planning or national disaster prevention / hazard assessment agencies.

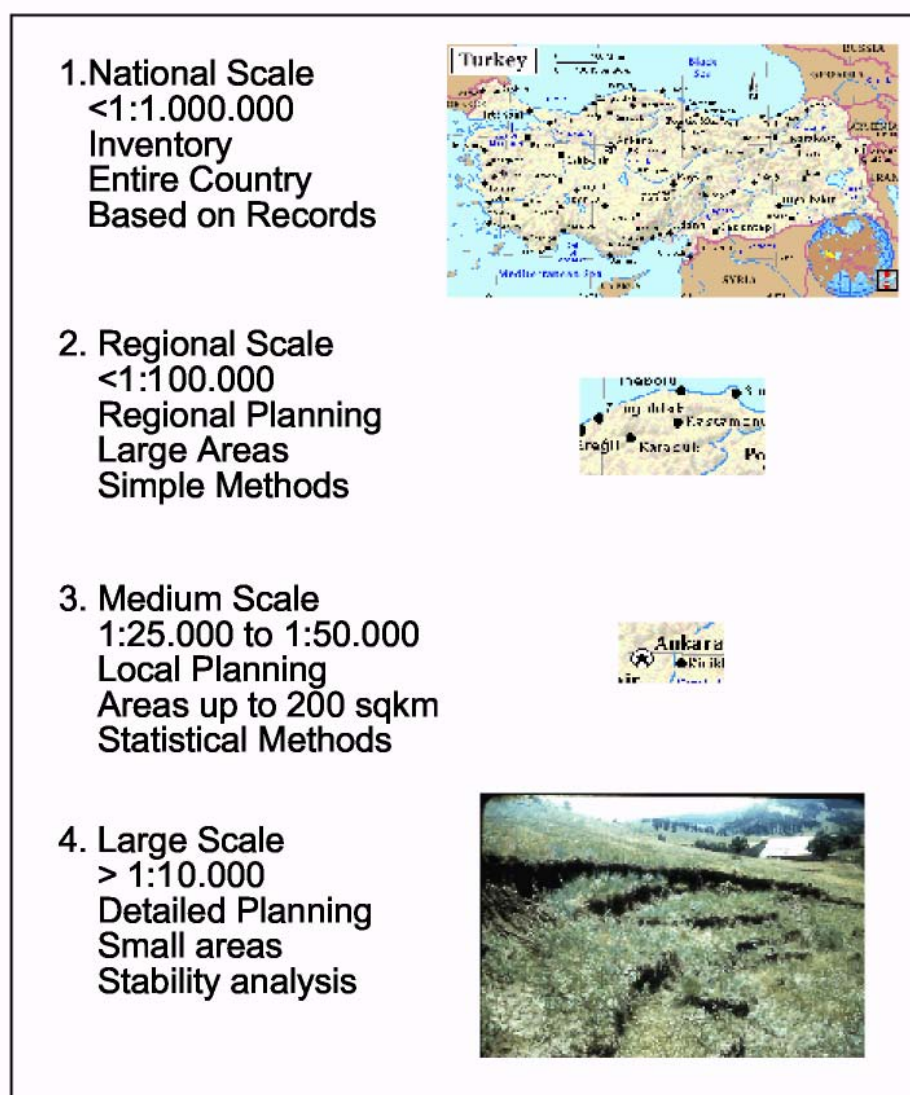


Figure 2-3 Scales of analysis and minor details (Sgzen, 2002).

#### b. Regional/Synoptic Scale (< 1/100,000)

The scale is still so small to be used in any quantitative method, but these maps are for regional planning and in early stages of appropriate region planning activities. The areas to be investigated are still too large, in an order of thousands of square kilometers, and the map detail is also low. Only simple methods are used with qualitative data combination and the zoning is primarily based on regional geomorphological Terrain Mapping Units / Complexes (TMU) or dependent on regional geological units.

#### **c. Medium Scale (1/25,000 -1/50,000)**

These hazard maps are made mainly for agencies dealing with inter municipal planning or companies dealing with feasibility studies for large engineering works. The areas to be investigated will be of several hundreds square kilometers. At this map scale, considerably more detail is required than at the regional scale. These maps do serve especially the choice of corridors for infrastructure construction or zones for urban development. Statistical techniques are dominantly used in this scale.

#### **d. Large Scale (> 1/10,000)**

These hazard maps are produced generally for authorities dealing with detailed planning of infrastructure, housing or industrial projects or with evaluation of risk within a city or within a specified project area. They cover very small areas hence the deterministic hazard analyses become available to be used. The detail level of the maps is set into a maximum. They are based on physical numerical models that require extensive data collection in the field and laboratory surveys.

### **2.4.2 Knowledge types used in prediction of landslide hazard**

Prediction of landslide hazard for areas not currently subject to landslide hazard is based on the assumption that hazardous phenomena that have occurred in the past can provide useful information for prediction of future occurrences. Unlike general educational geological phrases in this case, "Present is not a key to the past but present and past are the keys to future", of which the real value of engineering and its futuristic approaches are represented. Therefore, mapping these phenomena and the factors thought to be of influence is very important in hazard zonation. In relation to the analysis of the terrain conditions leading to slope instability, two basic methodologies can be recognized (Van Westen, 1993) as below.

The first mapping methodology is an experience-driven applied-geomorphic approach, by which the earth scientist evaluates direct relationships between landslides and their geomorphic and geologic settings by employing direct observations during a

survey of as many existing landslide sites as possible. This is also known as direct mapping technology.

Contrarily to this experience based- or heuristic approach is the indirect mapping methodology, which consists of mapping of a large number of parameters considered to potentially affect landsliding and subsequently analyzing (statistically) all these possible contributing factors with respect to the occurrence of slope instability phenomena. In this way the relationships between the terrain conditions and the occurrence of the landslides may be identified. On the basis of the result of this analysis, statements are made regarding the conditions under which slope failures occur.

Another division of techniques for assessment of slope instability hazard was given by Hartlen and Viberg (1988), who differentiated between relative and absolute hazard assessment techniques. Relative hazard assessment techniques differentiate the likelihood of occurrence of mass movements for different areas on the map without giving exact values. While absolute hazard maps display an absolute value for the hazard such as a factor of safety or a probability of occurrence.

Furthermore the hazard assessment techniques can also be divided into three broad classes based on use of statistical methods (Carrara, 1983; Hartlen and Viberg, 1988; Soeters and Van Westen, 1996) as follow.

- White box models: based on physical models (slope stability and hydrologic models), also referred to as deterministic models;
- Black box models: not based on physical models but strictly on statistical analysis; and
- Gray box models: partly based on physical models and factual data and partly on statistics.

## 2.5 Disaster management

A way of dealing with natural hazards is to ignore them. In many parts of the world, neither the population nor the authorities choose to take the danger of natural hazards

seriously, for various reasons namely socio-economic, political, cultural, religious, etc. To effectively mitigate disasters, a complete strategy for disaster management is required, which is also referred to as the disaster management cycle.

Disaster management consists of two phases that take place before a disaster occurs, disaster prevention and disaster preparedness (both phases together are also referred to as disaster mitigation), and three phases after the occurrence of a disaster: disaster relief, rehabilitation and reconstruction.

Unfortunately, the emphasis in most countries has always been on the phase of disaster relief, and most disaster management organizations in developing countries have been established only for this purpose. Recently, the emphasis is being changed to disaster mitigation, and especially to vulnerability reduction.

Investment companies, (international) donor agencies, banks, and governments are increasingly requiring precise data on the risk due to hazards that may hamper the investment or reduce the return of their investment. Insurance and reinsurance companies similarly are demanding the more detailed risk evaluations to be able to set the insurance premiums for projects. Standard procedure will also be (or going to be) the development of risk scenarios that minimize the adverse consequences for the project and financial losses. Projects can be: civil engineering works, housing projects, mining, agricultural and forest developments, etc. (Van Westen, 1994).

Table 2-4 Key elements of disaster management (Van Westen, 1994).

Pre-disaster phases				Post-disaster phases	
Risk Identification	Mitigation	Risk Transfer	Preparedness	Emergency response	Rehabilitation and Reconstruction
Hazard Assessment	Physical structural mitigation works	Insurance/reinsurance of public infrastructure and private assets	Early warning systems. Communication systems	Humanitarian assistance / rescue	Rehabilitation/reconstruction of damaged critical infrastructure
Vulnerability assessment	Land-use planning and building codes	Financial market instruments	Monitoring and forecasting	Clean-up, temporary repairs and restoration of services	Macroeconomic and budget management
Risk Assessment	Economic incentives	Privatization of public services with safety regulations	Shelter facilities Emergency planning	Damage assessment	Revitalization of affected sectors
GIS mapping and scenario building	Education, training and awareness	Calamity funds (national or local level)	Contingency planning (utility companies / public services)	Mobilization of recovery resources	Incorporation of disaster mitigation components in reconstruction

(Note: The green colored blocks indicate those activities for which remote sensing and GIS are most useful)

### 2.5.1 Geo-spatial requirements

Mitigation of natural disasters will be successful only when detailed knowledge is obtained, including the expected frequency, characteristics, and magnitude of hazardous events in an area, as well as the vulnerability of the people, buildings, infrastructure and economic activities in the potentially dangerous area. Many types of information that are needed in natural disaster management have both an important spatial as well as temporal component.

Remote sensing and GIS provide a historical database, from which hazard maps may be prepared, to indicate which areas are potentially dangerous. Remote sensing data should be linked with other types of data, derived from mapping, measurement networks or sampling points, to derive parameters useful in the study of disasters. GIS may give models for various hazard and risk scenarios of an area to be developed in the future.

The spatial modeling of hazards is a complex task, in which many factors play a role, and which only experts can execute. It also involves a large number of uncertainties, which have to be taken into account. The zonation of hazard must be the basis for any disaster management project and should supply planners and decision-makers with adequate and understandable information.

Remote sensing data derived from satellites are excellent tools in the mapping of the spatial distribution of disaster related data within a short period of time. Many different satellite based systems exist nowadays, with different characteristics related to their spatial-, temporal- and spectral resolution. As many types of disasters, such as floods, drought, cyclones, volcanic eruptions, etc., will have certain precursors. Real time and near-real time satellite remote sensing may detect the early stages of these events as anomalies in a time series.

When a disaster is about to occur, the speed of information collection from air- and space borne platforms and the possibility of information dissemination with a corresponding swiftness make it possible to monitor the chance of disaster. Simultaneously, GIS analysis may be used to plan evacuation routes, design centers for emergency operations, and integration satellite data with other relevant data.

In the disaster relief phase, GIS is extremely useful in combination with Global Positioning Systems (GPS) for search and rescue operations. Remote sensing and GIS can assist in damage assessment and aftermath monitoring, providing a quantitative base for relief operations.

In the disaster rehabilitation phase, GIS can organize the damage information and the post-disaster census information, as well as sites for reconstruction. Remote sensing updates databases used for the reconstruction of an area.

Disaster management is a multidisciplinary activity requiring spatial and temporal information and expertise from many different specialization fields (Van Westen, 1994), such as:

- Expertise on techniques for the collection of geo-information, generation of data bases, and design of disaster management information systems.
- Expertise on the analysis of disastrous phenomena, their location, frequency, magnitude, etc.
- Expertise on hazard zonation and mapping the environment in which the disastrous events might take place: namely topography, geology, geomorphology, soils, hydrology, land use, vegetation, etc.
- Expertise on the inventory of elements that might be destroyed if the event takes place: infrastructure, settlements, population, socio-economic data, emergency relief resources, such as hospitals, fire brigades, police stations, warehouses, etc.
- Expertise on cost-benefit analysis, spatial decision support systems, conflict management, and the implementation of disaster management in organizations in developing countries.

### 2.5.2 Risk assessment as central theme

Much of the effort in disaster management is on the policy and social side. However, the decision-makers must be supplied with reliable, up-to-date, and well-interpreted information on the nature and geographical distribution of hazard and risk, and the possible risk scenarios. Risk assessment is considered as the central and most important aspect within disaster management. Risk is defined as "the expected number of lives lost, people injured, or economic losses due to potentially damaging phenomena within a given period of time " by Van Westen (1994).

In order to obtain quantitative risk maps, the first essential requirement is to carry out a quantitative hazard assessment. Most hazard maps still are of a qualitative nature and do not express the probability of occurrence of potentially damaging phenomena with a certain magnitude within a given period of time. In many developing countries, qualitative hazard maps are the only possibility, due to the scarcity of input data for quantitative analysis. There is an important role for data collection using remote sensing and the design of data bases for hazard assessment, as well as the use of various types of modeling techniques depending on the available data and the scale of analysis. Emphasis should be given to the development of quantitative hazard maps, derived by earth scientists, based on probabilistic or deterministic modeling. In data-scarce situation qualitative techniques should be applied, based on terrain analysis.

Another aspect which needs to be worked out in more detail is the quantification of vulnerability, which is achieved by making an inventory of the elements at risk (population, building stock, essential facilities, transportation and lifeline utilities, high potential loss facilities, economic activities) and an assessment of the degree of damage that may result from the occurrence of a potentially damaging phenomena. Emphasis should be given to techniques for rapid inventory of elements at risk in densely populated areas (urban and rural), using high resolution images., and the generation of elements at risk databases, which should be designed for multi-purposes, on the basis of cadastral databases. Furthermore, an aspect for modeling of vulnerability, using vulnerability curves in GIS is as well essential. Also input from partners is needed in order to include the economic aspects, in order to come to quantitative loss estimation.

The combined information of hazard and vulnerability is used to derive at quantitative risk analysis, including the total losses due to different hazards with different return periods and magnitudes. Methodology for data handling and quantification of risks in a large area is yet to be developed.

One of the large challenges is the implementation of these risk maps into risk scenarios, and the development of spatial decision support systems for disaster management, to be used in:

- Anticipating the possible nature and scope of the emergency response needed to cope with disaster,
- Developing plans for recovery and reconstruction following a disaster, and
- Mitigating the possible consequences of disasters

(Van Westen, 1994).

## 2.6 Use of remote sensing in landslide hazard assessment

Remote Sensing can be defined as the instrumentation, techniques and methods to observe the Earth's surface at a distance and to interpret the images or numerical values obtained in order to acquire meaningful information of particular objects on earth.

Three definitions of remote sensing are given below:

- Remote sensing is the science of acquiring, processing and interpreting images that record the interaction between electromagnetic energy and matter.(Sabins, 1997)
- Remote sensing is the science and art of obtaining information about an object, area, or phenomenon through the analysis of data acquired by a device that is not in contact with the object, area, or phenomenon under investigation. (Lillesand and Kiefer, 1994)
- The term remote sensing means the sensing of the Earth's surface from space by making use of the properties of electromagnetic waves emitted, reflected or diffracted by the sensed objects, for the purpose of improving natural resources management, land use and the protection of the environment. (Van Westen, 1994)

The process of Remote Sensing is schematically shown in Figure 2-4.

The phenomenon, landslide, is affecting the earth's surface, hence it also falls in to the research and application areas of both aerial and space born remote sensing. The nature of this phenomenon as it is occurring at the surface of earth allows the earth scientists to exploit this fact using remotely sensed data. On the other hand, the nature of this phenomenon again limits the applications, as being dynamic and sometimes being quite small in terms of conservative remote sensing language. Furthermore they reveal very small information when they are observed in planar two-dimension, however, they contain large amounts of data when explored in three-dimension. Basing on this fact the use of stereo-remote sensing products seems to be indispensable, which reveals the true morphodynamical features of the landslides. These information are providing the diagnostic information regarding the type of the movement (Crozier, 1973). The general application fields of remote sensing in landslide business are monitoring the change of landslide activities through time (change detection) and mapping out where the hazard occurs.

Plenty of researchers have tested the usage of remote sensing products during the last 30 years. Two major groupings could be made upon the investigation of this research. These are aerial photography and space-born sensor images.

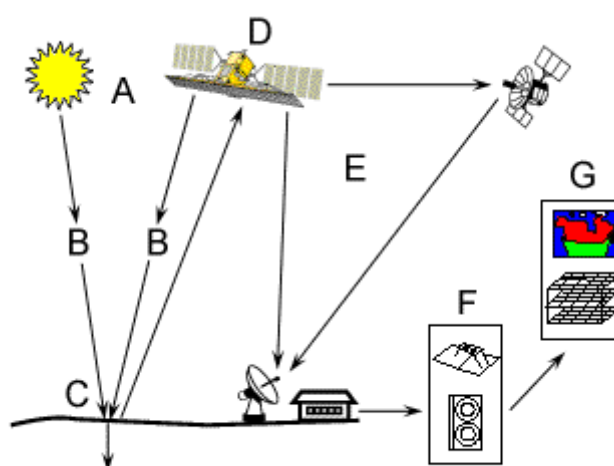


Figure 2-4 Process of Remote Sensing (Van Westen, 1994).

Note: A) Energy source to illuminate the target; B) Interaction of the radiation with the earth's atmosphere; C) Radiation-target interactions; D) Data reception; E) Data transmission; F) Data processing; G) Data application)

Numerous applications have been carried out which generally define the landslide areas. Chandler and Moore (1989), Chandler and Brunsten (1995) and Fookes and others (1991) gave excellent applications for photogrammetry. For single landslide within a smaller area, a monitoring scheme is best applicable with this technique with good accuracy. However, the application of this technique in a larger area of interest is limited as such larger areas could be easily accomplished by classical aerial photographic studies.

The landslide information extracted in the remotely sensing studies normally shows a relationship with the morphology, vegetation and the hydrological conditions of the slope. The slope morphology can be examined with stereographical coverages. Generally the identification of the slope instabilities is an indirect method. The failures are identified by associated elements with slope instability process. The advantages of aerial photographs can be listed as follows:

- They provide quite older coverages before digital world starts.
- The flight coverages are adjustable for new missions.
- The spatial and temporal resolutions are very high.
- Stereoscopic coverage provides access to slope identification.
- Most of the geoscientist are familiar to them.
- Every country have at least one full coverage of their land due to military reasons.

The disadvantages are as follows:

- Low spectral resolution
- The nature of photograph as hardcopy, hence not very handy
- Presence of distortions in parts of the images
- Orthorectification is needed to remove distortion and add coordinate information

- Absence of coordinate information
- The resultant map is dependent to the experience of interpreter

The applications with space born images are quite new compared to the others. Furthermore, they are generally defining the landslides indirectly by mapping out other parameters such as land cover. Gagon (1975); Mc Donalds and Grubbs (1975); Sauchyn and Trench (1978); Stephens (1988); Huang and Chen (1991); and many more workers could give discussion on this topic.

In comparison to the aerial photographs, the advantages of satellite images are as follow:

- Bigger coverage picture
- Larger spectral range
- Easily accessible
- No significant distortion
- Only georeference is needed to mark the geographic coordinates

The disadvantages are as follow:

- Low spatial resolution
- More expensive than aerial photographs of the same resolution
- Limited stereo graphic capability
- Limited number of geoscientists who are familiar with them

## **2.7 Geographical Information Systems (GIS) and landslide hazard assessment**

Geographic data have previously been presented in the form of hard-copy maps. But the recent rapid development of computer hard- and software help introducing them in a digital form which is more applicable. Many organizations now spend so much money on establishing Geographic Information Systems (GIS) and the geographic data bases. The demand for the storage, analysis and display of complex and voluminous environmental data has led, in recent years, to the use of computer for data handling and the creation of sophisticated information systems. Effective use of

large spatial volumes depends on the existence of efficient systems that can transform these data into usable information. Geographic Information Systems (GIS) becomes an essential tool for analyzing and graphically transferring knowledge.

GIS is a "powerful set of tools for collecting, storing, retrieving at will, transforming, and displaying spatial data from the real world for particular set of purposes" (Burrough, 1986). A more specific definition is given by Bonham-Carter (1996) as

"A geographic information system, or simply GIS, is a computer system for managing spatial data. The word geographic implies that the locations of the data items are known, or can be calculated, in terms of geographical coordinates. The word information implies that the data in GIS are organized to yield useful knowledge, often as colored maps and images, but as also statistical graphics, tables and various on-screen responses to interactive queries. The word system implies that a GIS is made up from several interrelated and linked components with different functions. Thus, GIS has functional capabilities for data capture, input, manipulation, transformation, visualization, combination, query, analysis, modeling and output."

These internationally valid definitions of GIS are certainly contradicted to the belief that GIS is only a Computer Aided Drawing (CAD) software or only a drawing tool. Generally, CAD can only constitute a small portion of the whole integrated system, whereas an ideal GIS and its possible integrated components are as shown in Figure 2-5 and 2-6. GIS, if based on the right components should answer several questions as shown in Figure 2-7.

More over the products of mapping and inventory are being stored in data banks for their ultimate retrieval or combination with data from other sources. Often they are incorporated GIS or LIS (Land Information Systems) which serves as a base for programmable data manipulation and selective information extraction for planning and project assessment.

The development of GIS and LIS is of considerable interest in the context of satellite surveying, change detection, and monitoring. The flexibility of digital data processing, combined with quick input of new data (possible from updating on the basis of satellite remote sensing records) offers new possibilities to the surveyor, cartographer and planner.

It is clear that in a rapidly developing society, change detection is of great importance. In modern society, mapping suffers from high rate of change, such as, change in land use in rural and urban areas, change in requirements for maps and inventories, change in concepts in the various disciplines of earth and social sciences, leading to different interpretations of the same data, and change in the economical and technical factors on which mapping methods were based.

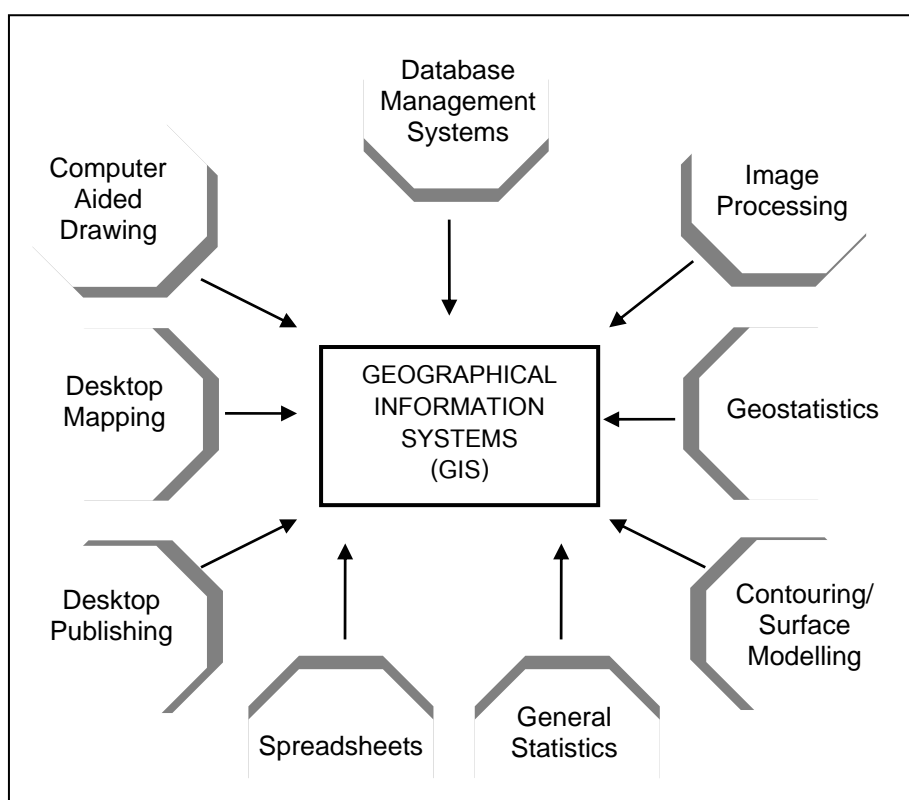


Figure 2-5 GIS and its related software systems as components of GIS (Sgzen, 2002).

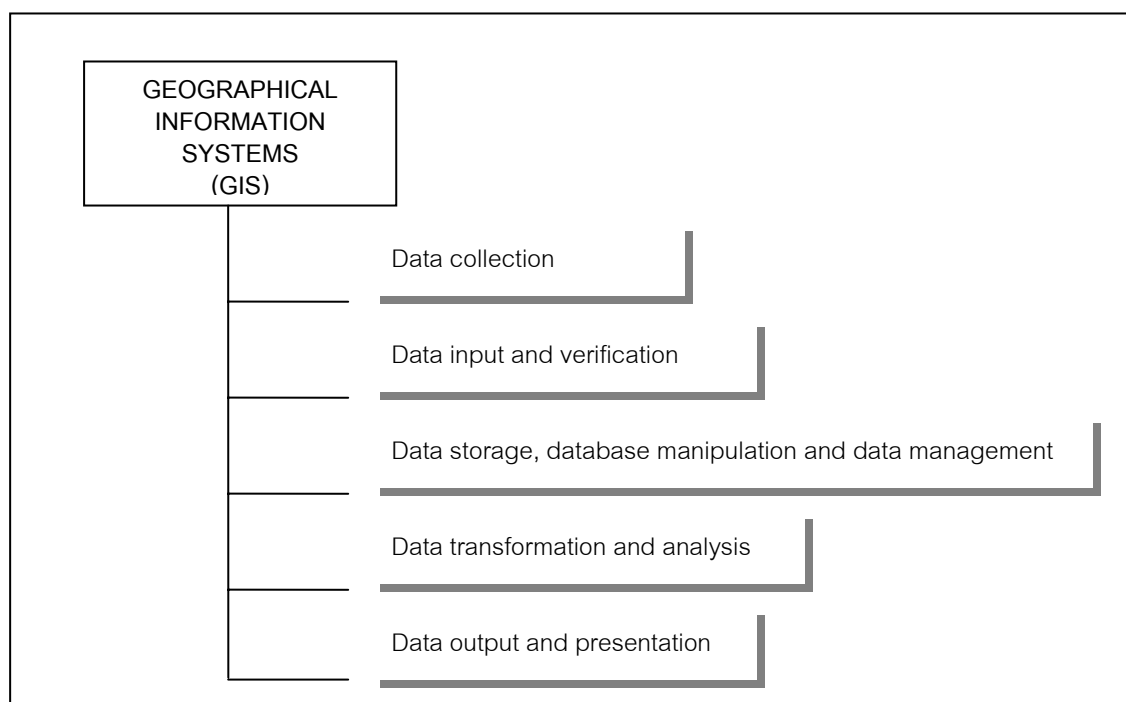


Figure 2-6 Phases of a GIS (Sgzen, 2002).

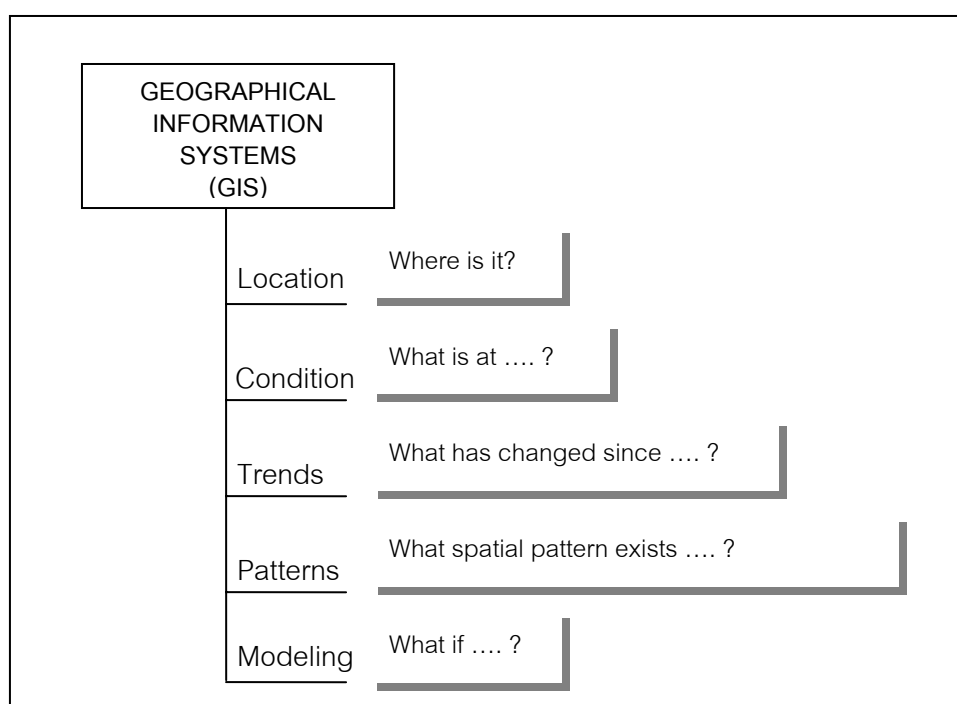


Figure 2-7 Questions which a well-built GIS should answer (Sgzen, 2002).

In order to refine the discussion around landslide hazard, one can say that the occurrence of slope failure depends generally on the complex interactions among a large number of partially interrelated factors. Analysis of landslide hazard requires evaluation of the relationships between various terrain conditions and landslide occurrence. An experienced earth scientist has the capability of mind to assess the overall slope conditions and to extract the critical parameters. However, an objective procedure is often desired to quantitatively support the slope instability assessment. This procedure requires the evaluation of the spatially varying terrain conditions as well as the spatial representation of landslides. GIS is allowed for the storage and manipulation of information concerning the different terrain factors as distinct data layers, and thus provides an excellent tool for slope stability hazard zonation.

The advantages of the use of GIS for assessing landslide hazard as compared to conventional techniques are treated extensively by several previous workers including Burrough (1986) and Aronoff (1989). The advantages of GIS for assessing landslide hazard include the follow.

1. The much larger variety of hazard analysis techniques that becomes attainable. Due to the speed of calculation, complex techniques requiring a large number of map overlaying and table calculations become feasible.
2. The possibility to improve models, by evaluating their results and adjusting the input variables. The users can achieve the best results in a process of trial and error, by running the models several times, whereas it is difficult to use these models even once in a conventional manner. Therefore more accurate results can be expected.
3. In the course of a landslide hazard assessment project, the input maps derived from field observations can be updated rapidly when new data are added. Also after the completion of the project the data can be used by the others in any other effective manner.

The disadvantages of GIS for assessing landslide hazard include the follow.

1. The large amount of time needed for data entry. Digitizing is very time-consuming.
2. The danger of placing too much emphasis on the data analysis as such, at the expense of data collection and manipulation based on professional experience. It is possible to use many different techniques of analysis, but often the necessary data are missing. In other words, the tools are available but cannot be used due to the lack, or uncertainty, of input data.

## **2.8 Basic concepts on evaluation of the potential for debris-flows and related sediment-flows**

Basic concepts on evaluation of the potential for debris-flows and related sediment-flows are briefly reviewed from the related literatures below.

The term landslide includes a wide variety of processes that result in the downward and outward movement of slope-forming materials. The mass may move by any types of five principle types of motion: falling, toppling, sliding, spreading, or flowing, or combinations of these (Varnes, 1978). As both the kind of involved material and the movements are of importance in all phases of landslide investigation--from recognition to mitigation—these two factors, namely, type of movement and type of material, are generally used to identify types of landslide. Each region has its distinctive suite of problems that are determined by the characteristics of geology, topography, climate, and other aerial factors. Moreover, each kind of landslide process required its own kind of response directed toward recognition, avoidance, or mitigation.

With these basic ideas in mind, the goals of the landslide process and prediction segment can be summarized as follow:

- To determine the inherent geologic, topographic, and hydrologic conditions that set the stage for slope failures,

- To determine the factures, either natural, such as storms and earthquakes, or man-induced that lead to change slope stability,
- To analyze the time, physical setting, mechanism, rate, and extent of past failures in order to develop capacity to predict future failures,
- To acquire new knowledge of slope failure processes that is applicable to method for avoiding, preventing, or mitigation damage, and
- To present conclusions regarding hazardous slope processes in forms suitable to devise methods to map and assess the degree of hazard in large or small areas.

The several steps that are necessary to reach these goals are as follow:

- 1) Identify those slope processes that are hazardous,
- 2) Determine the relative degree of hazard and risk presented by the various processes of slope failure,
- 3) Identify gaps in knowledge regarding below topics
  - a) Methods for recognition of unstable areas,
  - b) Prediction of place, extent, time, and potential damage of failures, and
  - c) Devise techniques to avoid, prevent, or mitigate landslide hazards and damage.

U.S. Geological Survey (1982) explained that the relation of debris flows to weather-related triggering events presents problems in predicting time and place that involves not only the geologic and topographic setting but also regional and local meteorological conditions. To improve their predictive capability a coordinated combination of field, laboratory, analytical, and statistic studies should be undertaken by the following specific tasks:

- Construct analytical, numerical, and laboratory physical models to help understand the generation and mechanical behavior of debris flows,
- Undertake geotechnical investigations to characterize hillside soils in potential debris-flow source areas to determine which soil types are most

susceptible to oversaturation and mobilization under heavy precipitation, snow-melt, or thawing of frozen ground,

- Provide instrumentation at field locations to monitor precipitation, groundwater levels, and movements in potential debris flow source areas,
- Augment existing data bases and construct statistical models relating debris flow to mapable parameters such as bedrock lithology, soil type, slope, vegetation, and precipitation,
- Determine the effect of denudation of vegetation (due to forest fires, timber clear-cutting, and so forth) on subsequent erosion and downstream sedimentation patterns as related to debris flow,
- Reconstruct a history of climatic variation in the recent geological record of a climate area,
- Devise and improve techniques to find date of the recent geologic features for determining the timing and frequency of debris flows,
- Conduct statistic studies of recent rainfall histories of selected mapping areas to investigate effects of rainfall variations during drought-wet cycles, and
- Organize teams of scientists and engineers to investigate major debris-flow events during and immediately after they occur.

Ikeya (1974) proposed three main causes for debris flows as follow: (1) sediments produced by breaking up hill slopes mix with water and flow down, (2) collapsed sediments dam up a river and dam outbursts, and (3) riverbed deposit experiences strong scouring action.

Takei (1980) provided a more detailed list of causes for debris flows as follow:

- High rainfall intensity in a short period of time after a period of continuous rainfall.
- High rainfall intensity in a short period of time in an area with new volcanic sediments.

- Unstable sediments on steep torrent beds ( $>20^\circ$ ) become saturated; liquefaction occurs as a result of the impact of surface runoff.
- Collapsed materials flow down carrying water and sediment from the torrent bed.
- Collapsed sediments block a torrent stream to form natural dam then break allowing the collapsed sediments and water to form a debris flow
- Landslide materials turn into a debris flow as a result of liquefaction.
- Earthquakes or vibrations from volcanic eruptions cause parts of slopes to break off and the flowing torrent bed sediment liquefies.
- Other causes e.g. pyroclastic flow (volcanic eruption), and rapid melting snow.

Wieczorek and others (1983) summarized that abundant coarse-grained sediment can be transported and deposited by two processes, debris flow and debris flood. Both processes commonly occur during periods of rapid accumulation of water to the landscape, either by rainfall or snowmelt. In debris flow, water and soil materials including rocks combine to form muddy slurry much like very wet concrete, considerably more viscous than flowing water that moves down-canyon with a front armored of coarse-grained materials such as boulders. Debris flows may leave levees along the edges of the flow that indicate lateral and vertical dimensions of the flow front. In debris flood, soil materials with a greater relative proportion of water are transported by fast-moving flood waters. Deposits formed by debris flood can be distinguished from those of debris flow by greater degree of sorting those general characterized water-borne deposits. Debris flow deposits, in contrast, are characteristically poorly sorted, showing that rock fragments suspended randomly in poorly sorted matrix typically consisting of silty sand with a small but significant content of clay. Debris flow and debris flood may well form a continuum. As water content of a debris flow is increased, its plastic strength decreased abruptly and its viscosity approaches that of flowing water with entrained sediment.

The careful evaluation of potential for debris flows and debris floods should address the following questions (Wieczorek and others, 1983):

- 1) Relations between rainfall ( or snowmelt), ground-water levels, and landslide movement,
- 2) Stability of the partly-detached landslides,
- 3) Process of transformation from landslide to debris flow,
- 4) Incorporation of channel materials by debris flow,
- 5) Transition from debris flow to debris flood,
- 6) Factors that control debris flow run-out, and
- 7) Recurrence of debris floods and debris flows at canyon mouths.

Varnes (1984) proposed that landslides are inherent parts of the environment that require control and management strategy. Hazards themselves are not disaster but rather a factor in causing a disaster. Hazards are natural agents that transform a vulnerable condition into a disaster. Terminology related to hazards and disasters has numerous definitions depending on the particular nature or special interest of the person or organization concerned. It should therefore be a great value if a more general and internationally accepted definition could be applied to these terms.

Varnes (1984) also specified that the parameters consider for assessment of the landslide hazard, vulnerability and risks included a landslide map (both of recent and old landslides), major land use/cover categories, topographic factors, etc. Synthesizing from the assessment of the landslide hazard, vulnerability and risks mentioned above, the landslide hazard management tool would be conducted to aid in the identification of the occurrence of landslides, of the degree of loss as a factor of vulnerability, and would ultimately allow the assessment of risk from landslides. Therefore, risk assessments are a combination of hazard and vulnerability measurements that will assist with predicting locations where landslide events might cause damage in each study area.

Hansen (1984) presented that mass movements in mountainous terrain were of the natural degradational processes. Most of the terrain in mountainous areas has been subjected to slope failure at least once, under the influence of a variety of casual factors, and triggered by events such as earthquakes or extreme rainfall. Mass movements become problem when they interfere human activity. The frequency and the magnitude

of slope failures may increase due to some human activities, such as deforestation or urban expansion. In developing countries, this problem is especially great due to rapid non-sustainable development of natural resources. Losses due to mass movements are estimated to be one quarter of the total losses caused by natural hazards.

Innes (1985) reported that the frequency of debris flow events from individual source areas was controlled by the rate of accumulation in hollows or channels, and by the recurrence of climatic triggering events. Because the rate of accumulated debris was limited, there must be an upper limit to the magnitude-frequency of debris flows.

Crozier (1986) proposed that mitigation of landslide disasters could be successful only when detailed knowledge was obtained about the expected frequency, character, and magnitude of mass movement in an area. The zonation of landslide hazard must be the basis for any landslide mitigation project and should supply planners and decision-makers with adequate and understandable information. Analysis of landslide hazard was a complex task, as many factors could play a role in the occurrence of mass movements.

Osterkamp and Hupp (1987) reported that radiocarbon dating, lichenometry and dendrochronology had proved to be very useful techniques in estimating debris flow recurrence.

Hutchinson (1988) concluded that some landslides moved slowly and cause damage gradually, whereas others moved so rapidly that they could destroy property and took lives suddenly and unexpectedly. Debris flows were common types of fast-moving landslides or flows. They were potentially a very destructive form of mass movement in mountainous areas, where sudden access of water, usually from heavy rainfall or melting snow, could mobilize debris mantling the slopes and incorporate it into a debris flow. Debris flows from many different sources could combine in channels where their destructive power might be greatly increased. They continued flowing down hills and through channels, growing in volume with the addition of water, sand, mud, boulders, trees, and other materials.

Van Westen (1993) summarized that a wide variety of names had been used for the denudational process whereby soil or rock was displaced along the slope by mainly gravitational forces. The names most frequently used are slope movement, mass movement, mass wasting, and landslide. In the last decades landslide was the term most used, though in the narrow sense of the word (*sensu strictu*) it only indicates a specific type of slope movement with a specific composition, form and speed.

Van Westen (1994) also proposed that landslide disasters could have been prevented or mitigated if there were proper precautions. The precautions could be either to stabilize the slide-prone slopes or to avoid the slide-prone areas. In either approach, landslide-related information of the area must be known. He also concluded that the information required for analyzing landslide hazards should include that in the following categories.

- geomorphology: terrain mapping units, geomorphologic units, geomorphologic subunits, landslide (recent), landslide (older period)
- topography: digital terrain model (DTM), slope map, slope direction map, breaks of slope, concavities/convexities
- engineering geology: lithology, material sequences, sample points, fault & lineaments, seismic events
- land use: (recent) infrastructure, (older) infrastructure, (recent) land use, (older) land use, cadastral blocks; and
- hydrological data: drainage, catchment areas, meteorological data, water table.

According to the increasing availability of remote sensing technology and geographic information systems (GIS) during the last decades has created opportunities for a more detailed and rapid analysis of landslide hazard in large areas. Westen (1994) also applied these technologies in the analysis of landslide hazard that requires a large number of input parameters. The techniques of analysis might be very costly and time-consuming, however.

Corominas and others (1996) defined a debris flow as a rapid mass movement of a mixture of fine and coarse material, with a variable quantity of water, that formed muddy slurry which moved downslope, usually in surges induced by gravity and the sudden collapse of river bank material. Three distinctive elements involved in a debris flow were the source area, the main tract, and the depositional toe. The flows commonly followed pre-existing drainage ways. The tracts had a V-shape or rectangular cross-section. Some of the coarse debris might be heaped up along the sides of the track forming lateral ridges. Debris flow deposits were left where the channel gradient decreased or at the toe of mountain fronts. Successive surges might build up into a debris fan. Some debris flows had high energy, their deposits could travel long distances beyond the source area. The deposits of these low viscosity debris flows spreaded out in areas of decreased confinement to form alluvial fans. Corominas and others (1996) also described that the socio-economic impact and the loss of life, property and agriculture could be catastrophic in the case of large debris flows through populated areas. However, smaller debris flows might also cause serious damage, especially in upland watersheds of mountainous regions (e.g. destroying houses, roads, railways and bridges). The deposits were also responsible for severe indirect damage and hazards such as damming of rivers or sudden debris supply to river systems. It was essential that the potential source areas and run-out zones were correctly assessed and mitigation measures adopted using modern mapping and monitoring techniques.

U.S. National Research Council (1996) reported that debris flows could result from the existence of a large percentage (up to 70-90% of flow by weight) of fine sediment such as silt and clay in steeply-flowing floodwaters. This enabled the muddy flow to transport sand, gravel, boulders, and dislodged timber and brush from the mountain watershed onto a fan surface. Conditions favoring the formation of debris flows are: available unconsolidated silt, clay and larger rock in the basin watershed (due to minimal vegetation), heavy or sustained rainfall in the basin, and the presence of steep basin and fan slopes. Fans which had been formed from repeated debris flow activity were called debris fans, and were composed of deposits of rock, soil and vegetation from the upstream watershed. Alluvial fans, and flooding on alluvial fans,

showed a great diversity because of variations in climate, fan history, rates and styles of tectonism, source area lithology, vegetation, and land use. Acknowledging this diversity, the U.S. National Research Council's document provided an approach that considered site-specific conditions in the identification and mapping of flood hazards on alluvial fans. Investigation and analysis of the site-specific conditions might require knowledge in various disciplines such as geomorphology, soil science, hydrology, and hydraulic engineering. Although the scope of study might constrain the degree of site-specific consideration undertaken, it was essential that field inspections of the alluvial fan should be conducted.

U.S. National Research Council (1996) further provided guidance for the identification and mapping of flood hazards occurring on alluvial fans, irrespective of the level of fan forming activity. The term alluvial fan flooding encompasses what would later be described as active alluvial fan flooding and inactive alluvial fan flooding. In general, the criteria used to assess whether or not an area was subject to alluvial fan flooding, and defining the spatial extent of such flooding, could be divided into three stages: namely

- 1) Recognizing and characterizing alluvial fan landforms,
- 2) Defining the alluvial fan environment and identifying active and inactive components of the fans; and
- 3) Defining and characterizing areas of the fan affected by the 100-year flood.

Miyajima (2001) defined debris flows as a mixture of loose soil, rocks, organic material, and water that moved rapidly downhill destroying everything in its path. In order to mitigate the damages caused by the flows, it was necessary to have a good understanding of their mechanisms. He concluded that data collection is an important first step in study of debris flow. He also summarized some characteristics (velocity and unit weight, causes, and types) of debris flows and outlined the type of data that needed to be collected in survey.

Giraud (2002) also revealed that the character of past debris-flow deposits provided a basis for determining the nature of future debris-flow deposition and the

associated hazards due to impact, inundation, and burial. The findings of this study revealed that the drainage basin slopes and channels supplied sediment to alluvial fans, and the sediment-supply conditions governed the volume and frequency of future debris flows. Historical records indicated that 80 to 90 percent of debris-flow volume was bulked from drainage-basin channels. Therefore, evaluation of the drainage basin focused on determining the volume of channel sediment available for sediment bulking. The inventory of sediment supply provided information on the character, size, gradation, and volume of sediment available for incorporation into future flows. The flow volume determined from sediment-bulking estimates provided an independent check for flow volumes determined in the fan evaluation.

Giraud (2005) further proposed the guidelines for the geologic evaluation of debris-flow hazards on alluvial fans by the evaluation of debris-flow hazards on alluvial fans that was necessarily for safe and appropriate land use to prevent loss of life and property damage. These guidelines outline techniques to address debris-flow hazards by evaluating: the past flows on alluvial fans, and the drainage basin and channel sediment-supply conditions. Understanding the processes that governed debris-flow initiation, transport in the drainage basin, sediment bulking, and deposition on the alluvial fan were vital to hazard evaluation. The geologic evaluation of past flows on alluvial fans followed a two-step procedure consisting of an initial delineation of the active (generally Holocene) depositional area, and a subsequent detailed, site-specific analysis of the hazard within the active depositional area. In the detailed fan evaluation, flow-type, frequency, volume, and run-out data were collected to characterize the hazard based on the past debris-flow deposits. Surficial geologic mapping, dating methods, and subsurface exploration were used to investigate and describe the geomorphology, sedimentology, and stratigraphy of alluvial-fan deposits. Dynamic analysis of debris flows-floods using hydrologic, hydraulic, and other engineering methods to design site-specific risk-reduction measures should also be addressed in these guidelines.

## 2.9 Previous investigations on evaluation of the potential for debris-flows and related sediment-flows

The previous investigations on evaluation of the potential for debris-flows and related sediment-flows have been studied in many parts of the world. Some important literatures have been briefly reviewed below in chronological order to be the background information.

Owen and others (1995) conducted the study of mass movement induced both by shaking during 20 October 1991 Grahwal earthquake and by heavy rainfalls during the 1992 monsoon season in the Bhagirathi and Jumna catchment areas, Garhwal Himalaya to assess their role as natural hazards. Avalanching was the major mass movement process that occurred during the earthquake and during the heavy monsoonal rains, and was the greatest in the lower reaches of the valleys where the rivers were actively eroded steep rocks and debris slopes and where road construction had cut into slopes. Inventories of both the earthquake and rainfall-induced mass movements were used to characterize the different types and distribution of mass movements. The extent and type of damage, ground conditions, geology and geomorphology were mapped in order to produce hazard map for the region and to identify areas of the greatest risk.

Cannon (1997) investigated the potential of significant debris- and hyperconcentrated-flow activity in Capulin Canyon that was evaluated through 1) a systematic consideration of geologic and geomorphic factors that characterized the condition of the hillslope materials and channels following the fire, 2) examination of sedimentary evidence for past debris-flow activity in the canyon, and 3) evaluation of the response of the watershed through the 1996 summer monsoon season. His findings revealed that the factors, namely lack of accumulations of dry-ravel material on the hillslopes or in channels, absence of a continuous hydrophobic layer, relatively intact condition of the riparian vegetation and of the fibrous root mat on the hillslopes, and lack of evidence of widespread past debris- and hyperconcentrated-flow activity, even with evidence of past fires, indicated a low potential for debris-flow activity in Capulin

Canyon. In addition, thunderstorms during the summer monsoon of 1996 had resulted in abundant surface overland flow on the hillslopes which transported low-density pumice, charcoal, ash and some mineral soils downslope as small-scale and non-erosive debris flows. In some places cobble- and boulder-sized material was moved short distances. A moderate potential for debris- and hyperconcentrated-flow activity was identified for the two major tributary canyons to Capulin Canyon based on evidence of both summer of 1996 and possible historic significant debris-flow activity.

Morgan and others (1997) reported an analysis of areas susceptible to debris flows including an examination of source areas, channels and areas of deposition. The analysis was used to develop a methodology for identifying areas subject to debris flow hazards in Madison County, Virginia, United States. The preliminary carbon-14 dated from the older deposits of fossil soils, grey horizons with abundant organic remains in the deposits of prehistoric debris flows was used to interpret the recurrence interval for the debris flow events. The stratigraphy was also studied to compare with those recurrent interval interpreted from carbon-14 dating of the prehistoric debris flows. The report concluded with a discussion of strategies for reducing debris-flow hazards and the long term risk of these hazards in the study area as well as for similar areas along the eastern flank of the Blue Ridge mountain.

Singhroy (1998) reported on the use of Interferometric SAR, RADARSAT, and airborne SAR combined with Landsat TM images to identify diagnostic features of landslides and their slope characteristics in Canada that the landslide types were found in different physiographic regions and associated with certain kinds of soil and rock materials, geological structures and topographic settings. He concluded that Interferometric SAR images provided information on detail slope profiles of the large rock slides on steep slopes and along faults in the Canadian Cordillera. From this image, faults, rock slumps, block slides, slide scars, and debris slopes were identified. RADARSAT images with incident angles varied from 40-59 degrees, particular the fine mode images, were the most useful to identify landslide features in mountainous areas. An interpretation of retrogressive slope failures on the shale banks of the Saskatchewan

river was conducted using a combined Landsat TM and SAR images. Flow slides on sensitive marine clays were identified on airborne SAR images in the Ottawa valley.

Taylor (1999) conducted a study of the production, transport, and storage of sediments in drainage basins by comparative geomorphic analysis of surficial deposits at three central Appalachian watersheds that was essential for understanding their evolution and geomorphic behaviors. The mechanisms for routing and storage of sediments in the Appalachian region were poorly understood. This study involved a comparative geomorphic analysis of three watersheds underlain by interbedded sandstones and shales of the Acadian clastic wedge. GIS-based analyses of surficial map units allowed first-order approximation of valley-bottom storage volumes. Volume estimates were examined in tandem with clast-size analysis and bedrock-channel distribution to make inferences regarding controls on sediment-transport efficiency in the central Appalachians.

Jishan and Tianchi (2001) reported the study in China, described the types, characteristics, dynamics, and fundamental mechanics of debris flows, as well as the type of damage they caused to roads and other structures, settlements, and farmland. Five different ways of classifying debris flows were done based on the viscosity, composition, triggering factors, origin, and scale. The differences between debris flows and other similar phenomena such as landslides and floods were also summarized.

In Thailand, the literatures on the landslide investigations and similar phenomena are also reviewed in chronological order as below.

Perhaps the first brief investigation on landslide in Thailand was made by Ruenkairergsa and Chinpongsonond (1980) for the Department of Highways. They reported the incident in northern Thailand. Causes of landslides were due to geological factors especially lineament, water infiltration, and microseismic activities.

Later, Brand (1984) gave a short historical review on the landslide situation from published literatures in Thailand during 1976-1980.

Wannakao and others (1985) studied the engineering properties of rocks causing of slope failures along the Lorn Sak-Chum Phae highway between Kms. 18 to 24 where the failures were most intensified. Slope failures at this site could be classified into planar, circular, wedge, and block falls.

Tingsanchali (1989) conducted a study on a huge 1988 landslide in southern Thailand and proposed that the two principal methods for controlling debris flows were structural control measures and non-structural control measures. The suitability of these two methods or their combinations depended on the size and characteristics of the area considered the socio-economic condition and the financial and political factors.

The event had been studied by many other workers as well. According to Aung (1991) most failures took place on slope with gradient between 10 to 30 degrees and extended from the ground surface to the depth of 1 to 3 meters into the residual soil layer. These evidences indicated that those failures were mostly surface erosion or earth flow types. He also constructed the landslide susceptibility map in the area west of Amphoe Phi Pun, Changwat Nakhon Si Thammarat.

Zhibin (1991) investigated the characteristics of weathered granites exposed along the flanks and bottom of numerous landslide scars beside the Krathun stream and its tributaries. The study also embraced the effect of typical climatic condition (microclimate), the destruction of natural forest and changing to para-rubber plantation, the importance of subtle landform (depressions) on the landslides. Typical weathering profile of granite terrain was summarized and correlated to the landslides. Landslide types observed, based on field evidences, was mainly erosion, gully, earth flow, soil slump, debris flow, and rock slide.

Nutalaya (1991) concluded that the followings were the factors of landslides and sheet flooding during the rainstorm event of 20<sup>th</sup>-23<sup>rd</sup> November 1988, Khao Luang Mountain Range. They included (1) deforestation of areas which significant by caused the erosion of steep slopes; (2) steep gradient over 35 per cent and sharp change in gradient which occurred when the mountain streams met the flat valley floor resulted in

the deposition of alluvial fans, and (3) deeply saturated residual sand on the granitic rocks.

Tantiwanit (1992) investigated the characteristics of landslides activities from the November 1988 storm event. The study revealed that the significant factors controlling landslides could be summarized as follows: (1) residual soil from weathered granitic rocks was most susceptibility to landslide; (2) steep gradient over 30 per cent; (3) the change of vegetation cover to para-rubber plantations, and (4) the triggering factor was highly rainfall intensity.

Khantaprab (1993) conducted a study on the same November 1988 landslides in southern Thailand and proposed the following factors that influencing the landslides: (1) slope gradient greater than 12 degrees; (2) deforestation and changing pattern of land use and land cover to para-rubber plantations; (3) the areas underlain by granitic terrain with residual soils of weathered granite, and (4) high cumulative rainfall intensity the triggering factor.

Nilaweera (1994) studied the effects of root strength properties and root morphological of para-rubber plantations compared with other kinds of forest tree that produced hard deep penetrating root systems in the area of Khao Luang Mountain Range. The replacement of forest trees could cause instability to soil slopes. From the event, the slope, between 10 to 40 degrees in gradient was where the most of landslides occurred.

Pantanahiran (1994) summarized the primary factors that controlled landslides in the Khao Luang Mountain Range during November 1988 storm as follows: (1) fractured limestone and granitic bedrock; (2) shallow sandy soil from the weathering of granitic rock; (3) steep slope of more than 30 per cent; (4) high rainfall in earlier November as well as particular storm in November; (5) the pathway of storm; (6) reduction in natural forest cover; (7) planting of shallow root trees and crops, and (8) recentness of clearing and replanting. He also used GIS and statistical technique to develop a landslide prediction model for Khao Luang Mountain Range. The model included eight

parameters namely, elevation, aspect of slope, TM 4 (Thematic Mapping Band-4), flow accumulation, brightness, wetness, slope and flow direction. This model was capable of classifying 82 per cent of landslides in the Tha Di stream basin at a 0.4 cutoff probability.

Tangjaitrong (1994) developed a framework for integrating the techniques of geographic information system (GIS), remote sensing, and knowledge based system to predict landslide hazard zones in the study area comprising approximately 200 square kilometers that lying on a part of Khao Luang Range in Amphoe Phipun, Changwat Nakhon Si Thammarat. The intention of the designed framework was to ensure that the prediction could be done under limited information conditions. The study established an image-based GIS through process of research design, data collection, and software development. It also developed a knowledge-based system through similar processes (designing, knowledge acquisition, and software developing). The study had engineered those two systems so they could be integrated perfectly. Four methods of landslide hazard prediction were investigated in the study: (1) the method using experts' knowledge, (2) the method using infinite slope analysis, (3) the method using a logistic model, and (4) the method using knowledge elicited from the GIS. Results of the investigation showed that the integration of an image-based geographic information system and a knowledge-based system was a useful approach for predicting landslide hazard zones.

Jworchan (1995) investigated the characteristics of residual soils of November 1988 debris flows in the Khao Luang Mountain Range. The study revealed that the degree of weathering of residual soils were Grade IV to VI for the soil thickness of 1 to 2 meters, with the slope greater than 26 degrees. Moreover, sandy and cohesion less of clayey soil was susceptible to surface erosion once saturated.

Harper (1996) determined of the importance of topographic, geologic and geomorphic factors to debris flows susceptibility. The study used both the number of debris flows per square kilometer and the percentage of total land area in each basin, sub-basin, and the Tapi plain foothills as indicators of debris flows susceptibility. He

found that hillslope areas in tropical regions underlain by granite were more susceptible to debris flows than those underlain by clastic sedimentary or metamorphic rocks. The most frequent mode of land use in which debris flows occurred was rubber tree plantation.

Elsewhere, the National Economic and Social Development Board (1997) conducted the study of natural hazard management in southern region of Thailand. The study consisted of 6 sub-topics as follows: (1) types of natural hazards and the effected areas, (2) flood hazard and risk assessment, (3) landslide hazard and risk assessment, (4) soil erosion hazard and risk assessment, and (5) recommendation for natural hazard management in the southern region of Thailand. Geographic information system was also applied to manipulate, analyze and present in the study.

Thassanapak (2001) investigated the landslide assessment of Changwat Phuket using the influencing parameters of geology, landform, surface drainage zone, land use and land cover, soil characteristics, and rainfall intensity. The relationship between these parameters and the spatial data were evaluated using the proposed weight-rating technique. The findings of this study revealed that most of the potential areas to be affected by very high and high susceptibility to landslide included the famous tourist resorts.

Petchprayoon (2002) developed the prediction models of flash floods caused by dam failure and overflow through a spillway case study at Tha Dan Dam, Changwat Nakhon Nayok. The study used the technique on the integration of software MIKE 11, remote sensing and geographic information system for conducting this prediction. The study consisted of 5 main steps: (1) studying general characteristics of dam-location and of watercourse in downstream area with remote sensing technique, (2) modeling dam-failure with mathematic model, (3) estimating of damaged areas using geographic information system, (4) mapping the flooding in various degrees of severity , and (5) testing the assumption.

In the present study area, there are many preliminary studies that had been done. Pattanakanok (2001) proposed the landslide hazard monitoring in Nam Ko area using (1) analysis of Landsat TM (4R 5G 3B) to classify land use by Maximum Likelihood Classification, (2) creating 3D digital terrain model from 20 meter contour intervals, (3) creating slope in 5 degree interval, (4) analysis the levels of the landslide hazard zonation by using 3 major groups: land use, soil and geological properties, as well as slope and 3D digital terrain model. It was noted that the factors related to the landslide occurrence used in this analysis were only those 3 major groups.

The Secretariat Office of Government (2002) had formed a technical committee from the personnels of many disaster-related government organizations preliminary concluded and proposed the technical draft-report from the 2001 Nam Ko disaster in the following topics: (1) background of the area (geography, land use, geology and soil, and climate), (2) occurrence characteristics (rainfall and river-water quantity, areas that were damaged from the flood and landslide), and (3) causes of the disaster and mitigation concept. However, this draft-report had been done in very short time for the preliminary mitigation management in the Nam Ko and other similar areas in Thailand so the primary and actual data collected and related to the disaster in the area had not been systematically investigated in details.

Local Government Office (2002) reported the general information of the existing risk areas from flooding and associated disasters in 11 Amphoes in Changwat Phetchabun. It noted that if there were continuing and heavily rainfall occurrence, the risk areas in Amphoe Lom Sak could be identified into two types: (1) the overbank flooded areas in the lower flood plain of Pa Sak River and Nam Pung, and (2) the flash flood areas in the areas of that lied on the canyon mouths of Nam Ko Yai stream, Nam Chun stream, Thanthip stream, and Nam Duk stream that originating from Khao Kao and Nam Nauw mountain ranges. The report also concluded that the major factors influencing flooding were as follows: a lot of sediments in the main rivers and canals, heavily rainfall, lack of enough water retentions and reservoirs, and the obstacle from the transportation routes, etc.

Research and Development Center of Soil Engineering and Foundation (2002) conducted a proposal report on sustainable solution for slope stabilization to mitigate the debris flow and flash flood at Nam Ko area, Amphoe Lom Sak, Changwat Phetchabun. The investigation had been examined to identify preliminary geotechnical engineering characteristics of landslide areas as follows: water and mud flow, land use, topography of river channels, landslide areas, river deposits, general geology, types of hazard in river channels, soil strength-test in the field, soil profiles, and permeability testing. The review of this event from local people was also conducted to receive the eye-witness evidences. In addition, the damage from this event was informally summarized as two categories: the severe damage in the community and agricultural areas, and the damage in Nam Ko Yai sub-catchment.

Environmental Geological Division (2003) conducted a project of hazard zonation mapping from landslide in the whole Thailand in a scale 1:250,000 for identify the specific target areas to mitigate, monitor, and improve. The areas of Nam Ko and Nam Chun in Amphoe Lom Sak, Changwat Phetchabun were selected for this practical approach that had been applied landslide mathematical predictive model of Pantanahiran (1994) to analyze the landslide hazard zonation. It was noted that the parameters that used in the model consisted of elevation, adjusted aspect, slope, water flow direction, water flow accumulation, vegetation index from Landsat TM, soil characteristic (brightness), and wetness. Landslide hazard zonation had been divided into 4 probability level levels as very high, high, medium and low. The proposed landslide hazard maps from the study will be investigated the accuracy and reliability in the field survey to further improve this prototype model.

## CHAPTER 3

### THEMATIC DATA PREPARATION

The sources of input data and the steps in input data production to be comprehensively explained hereafter indicate that data entry and production are the most cumbersome and time consuming steps of any kinds of GIS and remote sensing techniques. The thematic data used in this thesis are to be prepared and processed below. Meanwhile, phases of natural hazard analysis in GIS-based landslide hazard zoning techniques are reviewed. However, the detailed statistic hazard analysis of the flow-flood database and the parameter maps are to be explained in the following chapter.

#### 3.1 Phases of natural hazard analysis in GIS-based landslide hazard zoning techniques

The following phases can be distinguished in the process of a hazard analysis using GIS (Van Westen, 1993 and 1994). They are listed in logical order or sequence though sometimes they may be overlapping (Figure 3-1) as follows:

- Preliminary phase:

- Phase 1: Defining the objective of study, the working scale and the methods of analysis to be applied

- Data collection phases:

- Phase 2: Collection of existing data (collection of existing maps and reports with relevant data)

- Phase 3: Image interpretation (interpretation of images and creation of new input maps)

- Phase 4: Data base design (design of the database and definition of the way in which the data will be collected and stored)

Phase 5: Fieldwork (to verify the photo-interpretation and to collect relevant quantitative data)

Phase 6: Laboratory analysis

■ GIS work:

Phase 7: Data entry (digitizing of maps and attribute data)

Phase 8: Data validation (validation of the entered data)

Phase 9: Data manipulation (manipulation and transformation of the raw data in a form which can be used in the analysis)

Phase 10: Data analysis and modeling (analysis of data for preparation of hazard maps)

Phase 11: Presentation of output maps (final production of hazard maps and adjoining report)

Phase 12: Error evaluation and reporting (evaluation of the reliability of the input maps and inventory of the errors which may have occurred during the previous phases)

The phases of a GIS-supported landslide hazard assessment project are in part different from those in a conventional project. An ideal GIS for landslide hazard zonation combines conventional GIS procedures with image processing capabilities and a relational data base. Map overlaying, modeling, and integration with remote sensing images (scanned aerial photos and satellite images) are required, thus a raster system is preferred. The program should be able to perform spatial analysis on multiple-input maps and connected attribute data tables for map overlay, reclassification, and various other spatial functions, incorporating logical, arithmetical, conditional, and neighborhood operations, including iteration. The system should provide the use of batch files and macros for those models that require similar analysis using different parameters. Since most data sets for landslide hazard zonation project are still relatively small (mostly less than 100 Megabyte), the use of less expensive, PC-based systems is possible.

### 3.2 Thematic data preparation from GIS and remote sensing techniques

Remote sensing data can be readily merged with other sources of geo-coded information as a GIS. This allows the overlapping of several layers of information with the remotely sensed data, and the application of a virtually unlimited number of forms of data analysis.

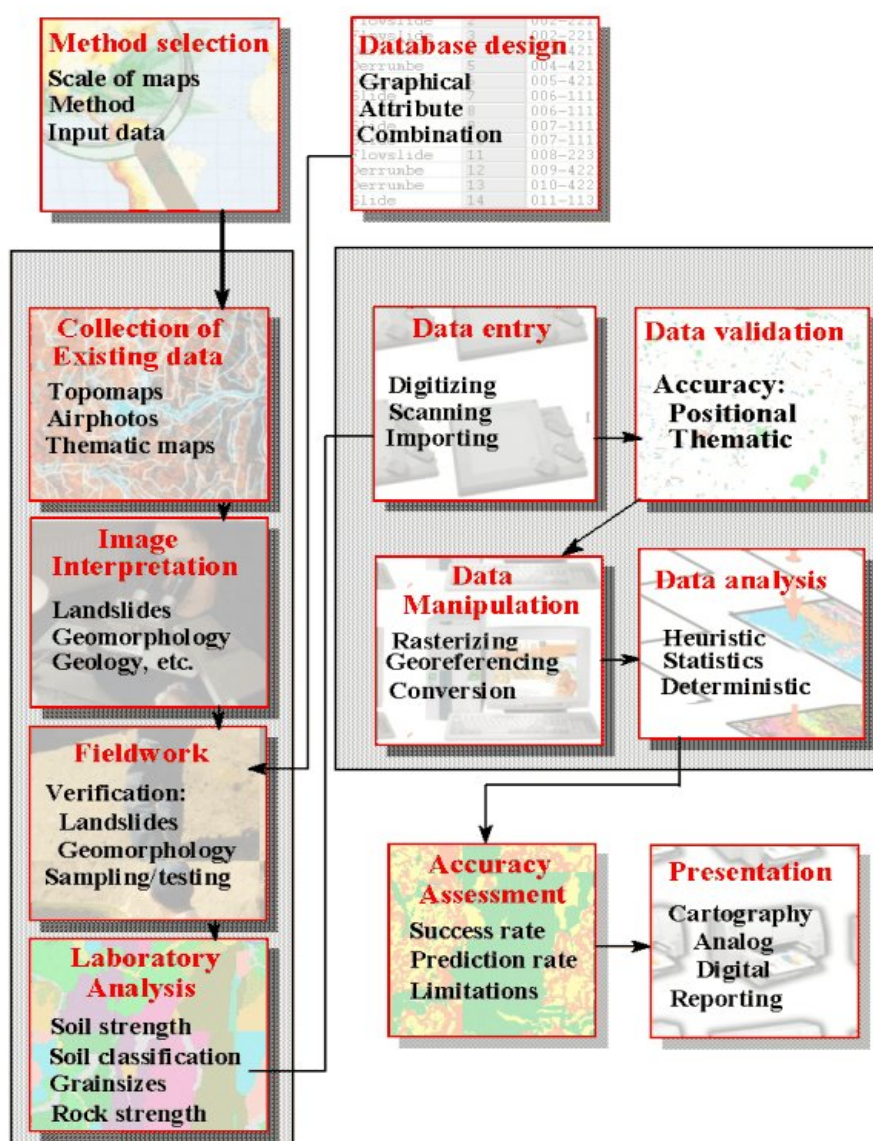


Figure 3-1 Flow chart of a GIS-based landslide hazard zonation (Van Westen, 1994).

As the use of geographic information systems increases, the availability of timely and up-to-date spatial data in digital format is required; this is expected to be easily fulfilled. Satellite imageries combined with the increased processing capability to generate meaningful data sets which represent new knowledge now available in various technologies.

GIS is suitable to meet the requirements of synthesizing the available information. The strength of a GIS lies in this capability of storing interpreted and available information as maps and linked attributes. For developing a GIS application as a landslide hazard management tool, a three-tiered GIS approach is adopted as follows; hazard assessment, vulnerability assessment and risk assessment. The parameters to be considered for assessment of the landslide hazard are vulnerability and risks being included in a landslide map, major land use/ land cover categories and topographic factors. The resulting landslide hazard management tool will help identifying the occurrence of landslides, the degree of loss as a factor of vulnerability, and will ultimately allow the assessment of risk from landslides. Therefore, risk assessments are a combination of hazard and vulnerability measurements that will assist with predicting locations where landslide events may cause damages.

The input data used for flow-flood hazard assessment in this thesis consists of several spatial data categories from the available resources (as shown in Table 3-1), being digitized from available maps and prepared from image interpretation, and from field investigation data. These input data will be further used to analyze the debris flow-flood hazard by the statistic analysis in the next chapter.

The brief techniques and thematic maps of the input data produced in this thesis, namely, elevation (digital elevation data , Digital Elevation Model-DEM, aspect, slope, landform topography), hydrology (drainage pattern, sub-catchments characteristics), geology (rock unit), soil properties (soil group unit, soil thickness), land cover, infrastructure and human settlement, flow-flood inventory of scar-scouring and

depositional locations, and meteorology of rainfall intensity are consequently presented as below.

Table 3-1 Overview of the important input data themes that were pre-processed and invented in this thesis.

Main themes	Sub-themes	Data preparation methodology
Elevation	Digital elevation data	converted from a 1:20,000 scale digital topographic map of Land Development Department (LDD)
	Digital Elevation Model (DEM)	Derived from digital elevation data with GIS
	Aspect	Derived from DEM with GIS
	Slope	Derived from DEM with GIS
	landform topography (Topographic shape)	Derived from DEM With GIS, image interpretation, field investigation
Hydrology	Drainage system	Digitized from Topographic maps, extracted from DEM with GIS
	Buffering distance to drainage-line	Digitized from topographic maps, extracted from DEM with GIS
Geology	Rock unit	Digitized from a 1:50,000 scale geological map of Department of Mineral Resources (DMR), adjusted with remote sensing imageries and field investigation
Soil properties	Soil group unit	Derived from a 1:20,000 scale soil property map of LDD and field investigation
	Soil thickness	Digitized from a 1:20,000 scale soil property map of LDD and field investigation
Land cover	Land cover	Derived from interpretation of remote sensing imageries and field investigation
Infrastructure and human settlement	Roads and villages	Digitized from geological map, adjusted with remote sensing imageries
Flow-flood inventory	Scar-scouring and depositional locations	Derived from interpretation of multi-temporal remote sensing imageries and field investigation
Meteorology	Rainfall intensity	Interpolated from existing rainfall information of the observation stations of Thai Meteorological Department (TMD)

### 3.3 Elevation

#### 3.3.1 Data entry

The digital elevation data of the study area was converted from a 1:20,000 scale digital topographic map (10 m contour interval) derived from the Land Development Department (LDD). This data is composed of contour lines and points with elevation information conducted in ARC/INFO format. This map is called the color-coded contour map (Figure 3-2).

#### 3.3.2 Input map generation

Instead of using a discrete elevation map such as contour lines, it is more advantageous to work with a continuous map. Regarding this advantage, the contour data was converted into a color-coded continuous map (Digital Elevation Model-DEM) as shown in Figure 3-2 at 10 m spatial grid resolution. DEM is used to create a slope, aspect and landform topographic shape. In order to increase visual interception of DEM, it had been chosen to convert into a color-coded DEM (Figure 3-3) and a color-draped relief model (Figure 3-4). The produced DEM would be used as the elevation input data for the elevation attributes of flow-flood.

For an accurate modeling of the topography in the study area, a watershed analysis was carried out to extract the micro-catchments, the ridge point and the drainage-lines (Figure 3-5). The process began by evaluating of elevation raster for depressions and constructs watershed polygons based on the depression recognized. This procedure identified watersheds from a raster surface image either automatically for the entire study area or for a user-defined "seed" feature image. With the automatic method, micro-catchment delineation determines the enclosed watersheds of a given raster image according to the given a real threshold.

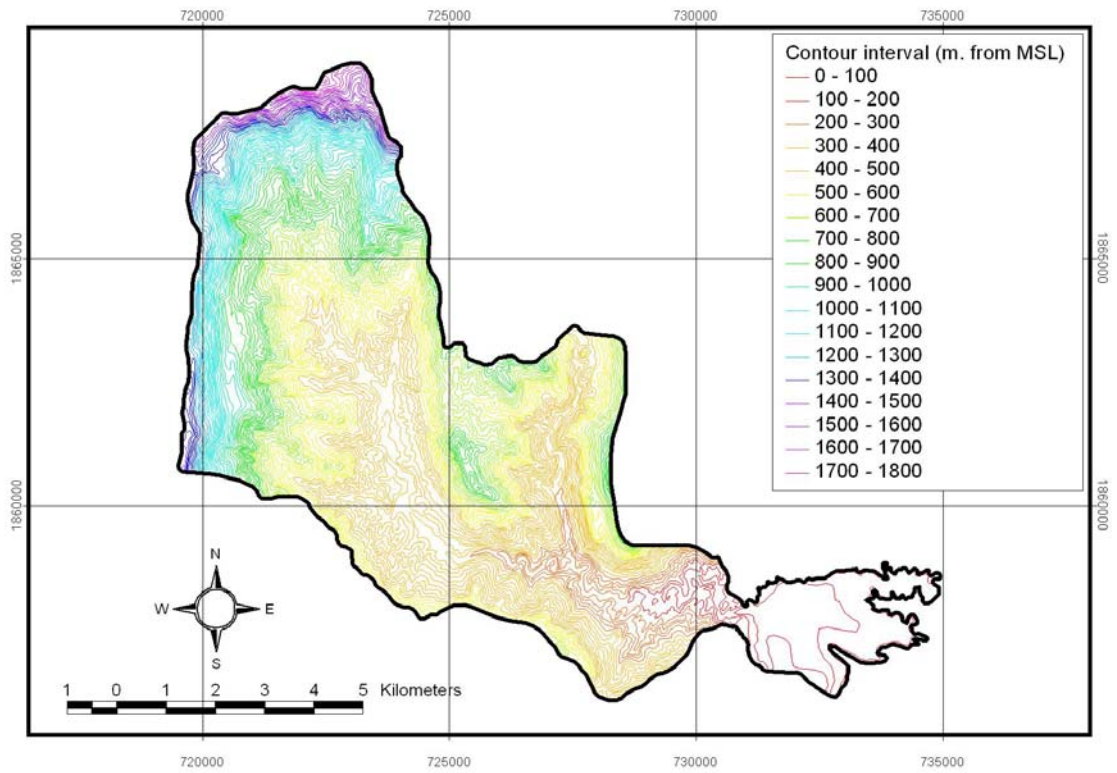


Figure 3-2 Color-coded contour map of the study area.

(Data Source: Land development Department).

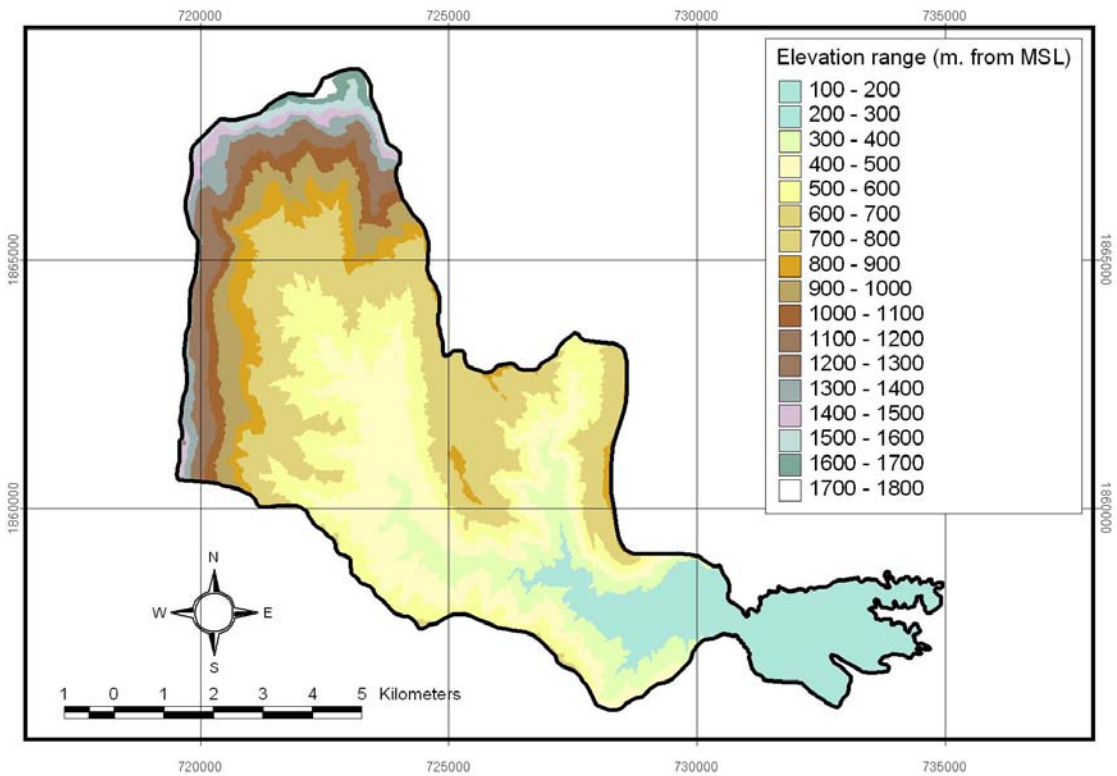


Figure 3-3 Color-coded DEM of the study area.

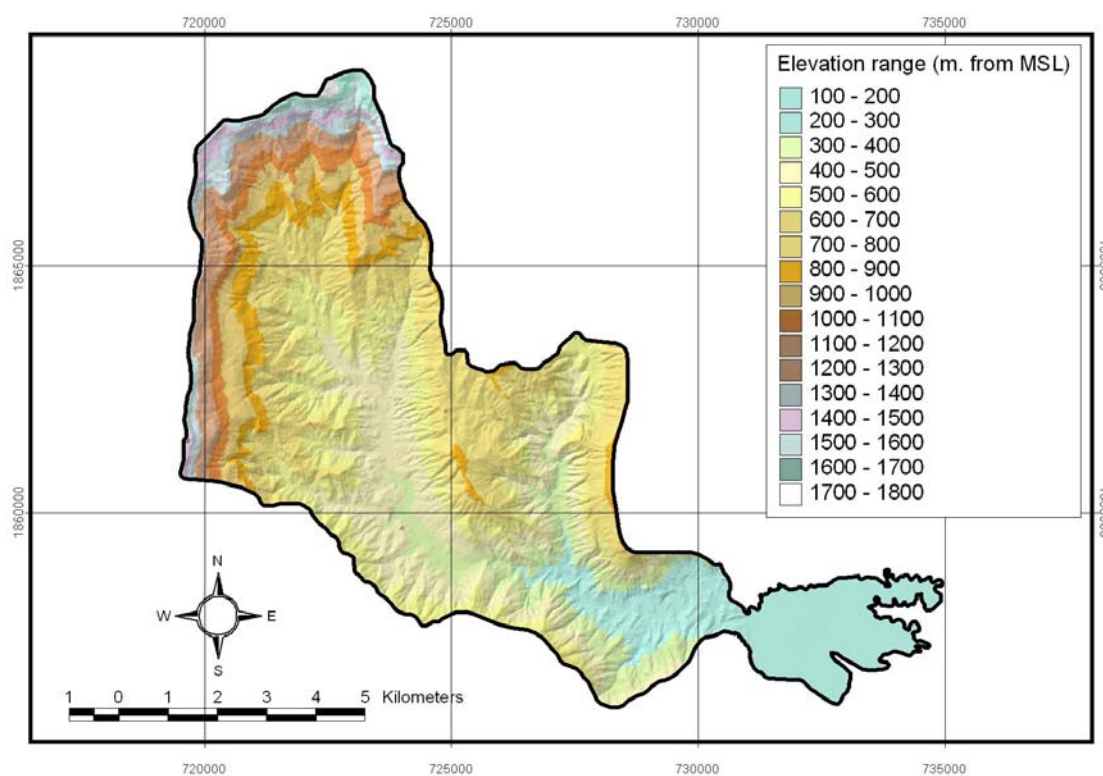


Figure 3-4 Color-draped relief model of the study area (illumination  $45^\circ$ , vertical exaggeration  $\times 3$ ).

The threshold is the minimum number of cells in a watershed. Watersheds are identified if they meet or exceed this threshold number of cells and if their outlets are within the image. In the output image, each watershed was given a unique sequential identifier, starting with 1. Any pixel that was not a part of watershed as defined above was given the value 0.

The distances of every pixel regarding the drainage-lines were calculated and presented in Figure 3-6. The minimum distance of pixels was 1 meter and the maximum, 2,320.39 meters. The buffering distance to drainage-line had average value of 41.55 with standard deviation of 141.76 which means that more than 68.2 percent of Nam Ko Yai sub-catchments has distance from drainage line of basin less than 183.31 meters.

The topographical modeling of the study area also serves as an input to calculate the topographic derivatives such as aspect and slope maps of the sub-

catchment. These topographic derivatives are very crucial and contain vital information for the flow-flood development in the area.

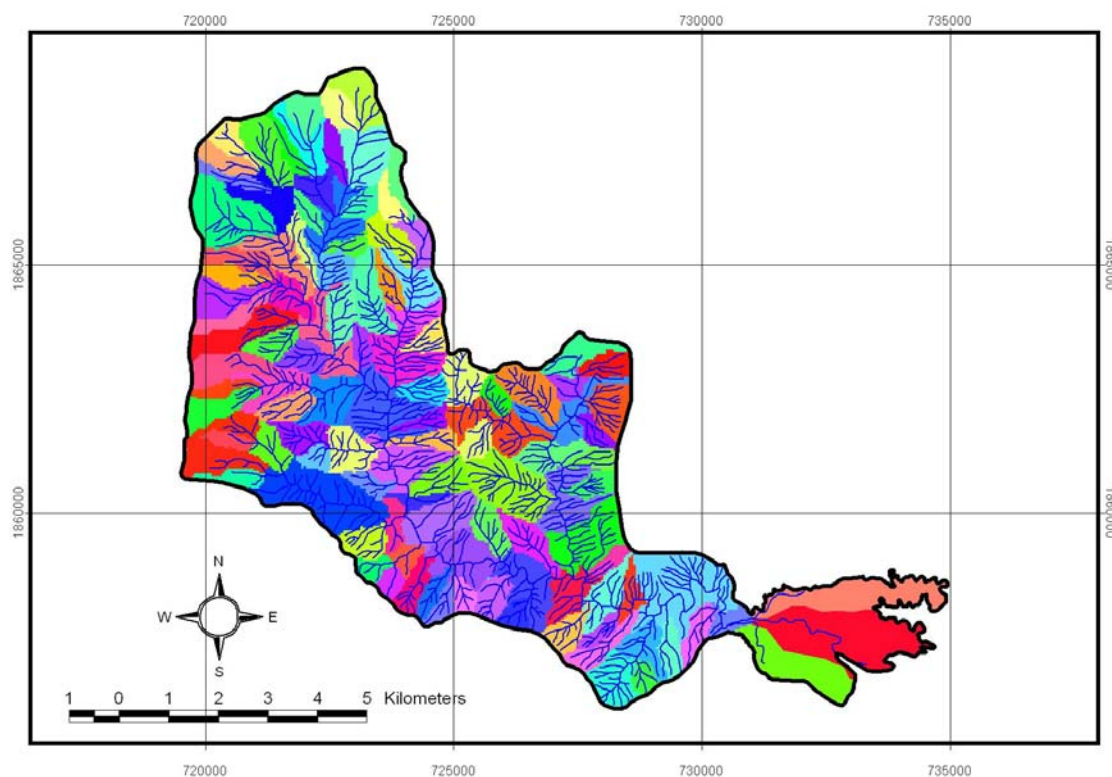


Figure 3-5 Drainage system of the study area, including micro-catchments and drainage-lines (in blue colored lines).

(Note: Color coding of micro-catchments is arbitrary)

The aspect is a measure of slope orientation and is calculated in geographic directions as the azimuthal degree from the North. Due to raster data format and the computational limits the aspect distribution has sensitivities in principle directions and in every 22.5 degrees, which is a drawback of the algorithm used. The produced and color-coded aspect map and its frequency distribution are presented in Figure 3-7. The aspect map reveals a range between -1 and 359, -1 representing the flat lying areas (no direction) and 0 as the North, and other values are the azimuth measurement from North. The minimum value is -1 and the maximum 359 degrees. The distribution has a mean value of 182.45 with standard deviation of 110 which means that most of Nam Ko Yai sub-catchments (more than 68.2 percent) has the faces to East direction (aspect faces to 65.7-112.5 degrees).

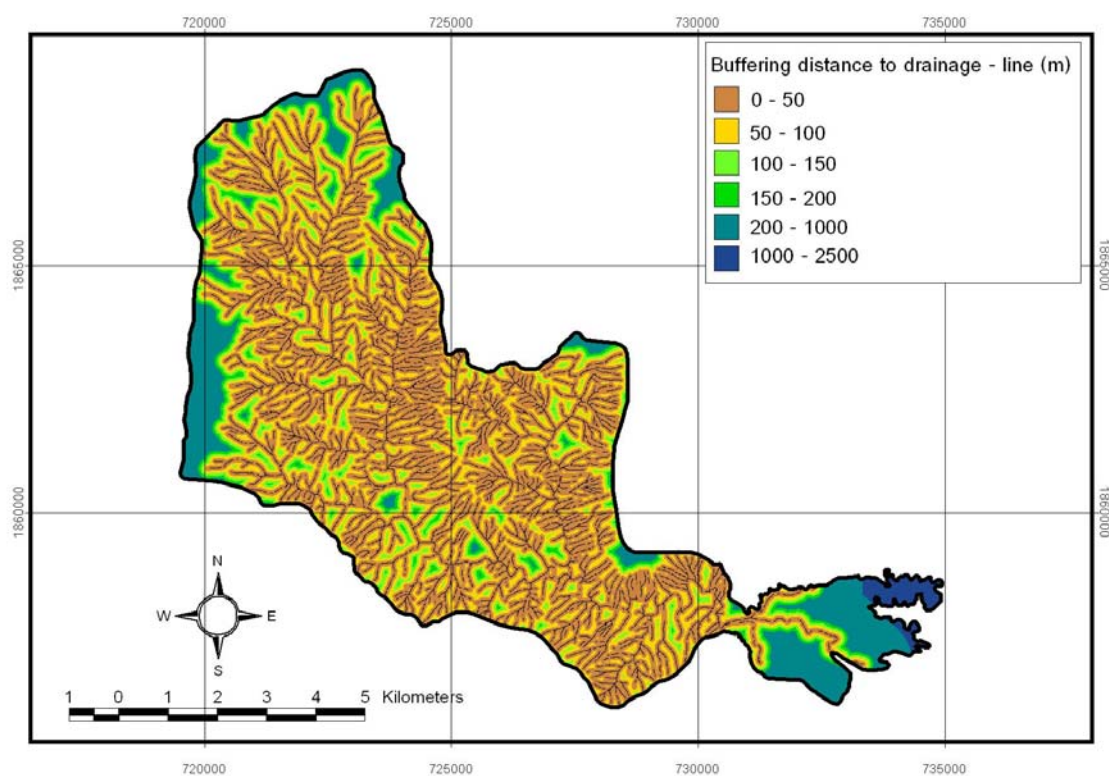


Figure 3-6 Buffering distance to drainage-line in the study area.

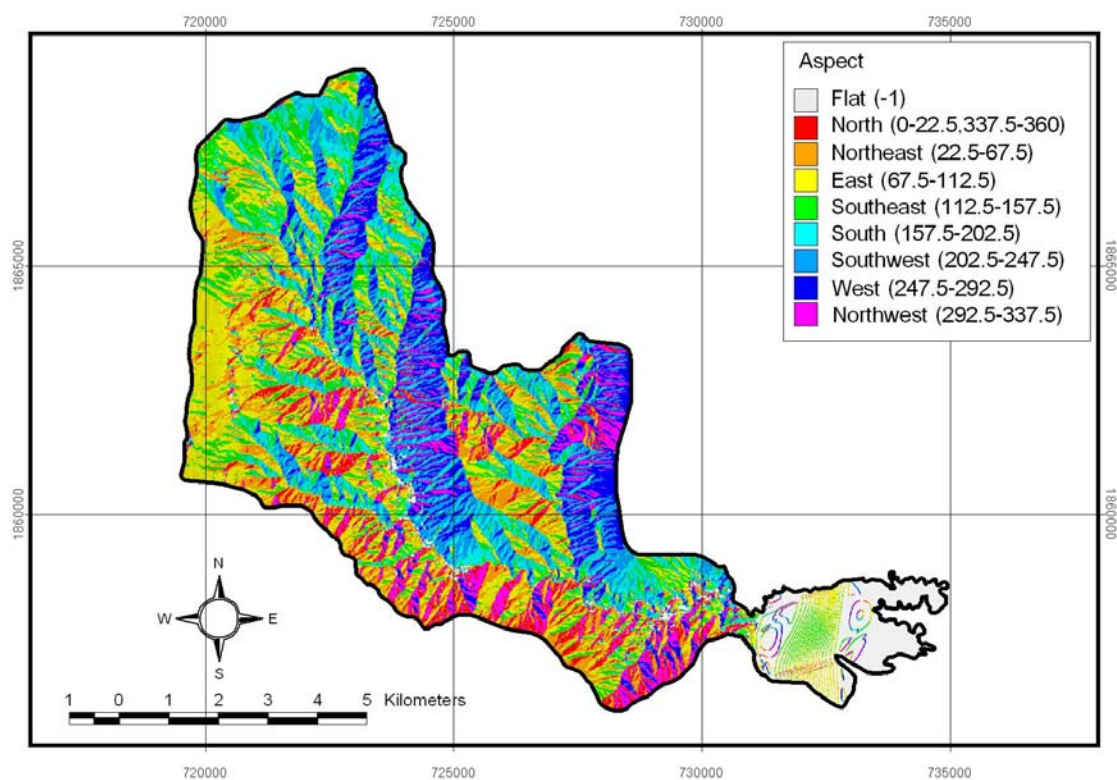


Figure 3-7 Aspect map of the study area.

The slope is a measurement of surface steepness and is calculated in degrees of inclination. The produced and color-coded slope map and its frequency distribution are presented in Figure 3-8. The slope has a range between 0 degree and 90 degrees, 0 degree representing the flat lying areas and 90 degrees as the vertical ones. Any other value indicates the inclined areas.

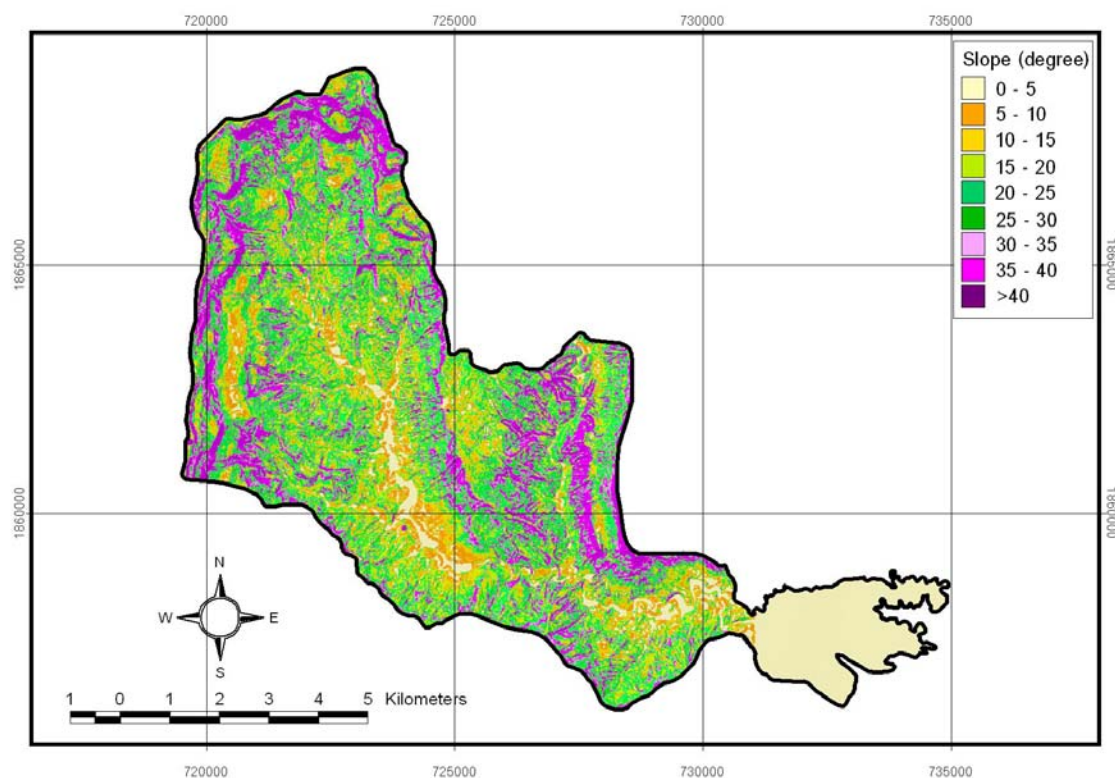


Figure 3-8 Slope map of the study area.

Hence the minimum value is 0 degree and the maximum 85.95 degrees. The distribution has a mean value of 13.28 degrees with standard deviation of 11.92 which means that most of Nam Ko Yai sub-catchments (more than 68.2 percent) has slope below 25 degrees.

From DEM data, landform topography (topographic shape) of sub-catchments was classified into 11 possible topographic features: peak, ridge, saddle, flat, ravine, pit, convex hillside, saddle hillside, slope hillside, concave hillside, and inflection hillside (Figure 3-9) by Idrisi32 software. Landform topography created by TOPOSHAPE module in Idrisi32, perform a Fourier analysis on the DEM for TOPOSHAPE results. The Fourier transform produces results that are more meaningful with better continuity of

topographic features. The procedure is performed on either a regular DEM, or on a DEM that has been transformed, filtered, and back-transformed with FOURIER and its companion modules.

The "TOPOSHAPE" module classifies each cell of an input digital elevation grid according to its topographic appearance: ridge, valley, convex slope, and eight other categories. The output is another grid of cells, each of which contains a numerical code for the topographic category.

Surface shape classification is based on polynomial surface fitting of each 3 x 3 pixel area. Eigenvalues are solved from the second directional derivative of the partial quadratic equation for a central pixel of a 3 x 3 neighborhood. The eigenvalues hold the information for the magnitude of rate of change of a tangent line along the mathematically described curve in the aspect direction of the pixel and in the direction orthogonal to aspect.

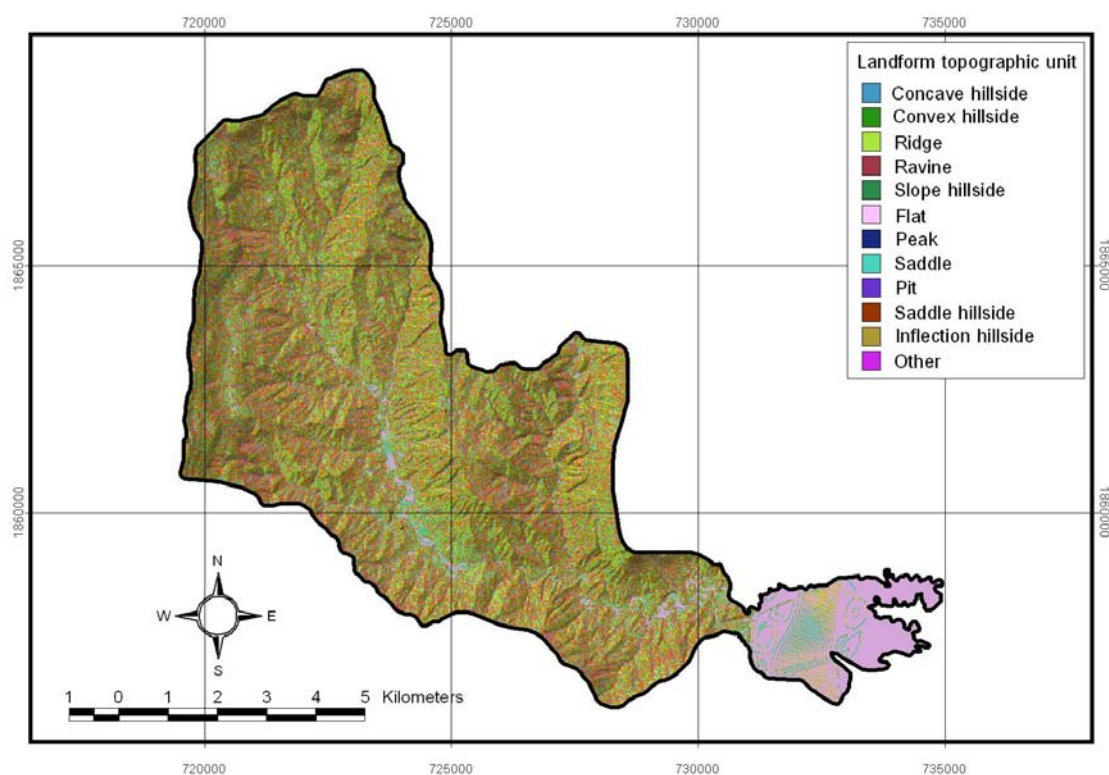


Figure 3-9 Landform topography of the study area.

## 3.4 Geology

### 3.4.1 Data entry

The previous geological map of the study area preliminary compiled from the available reports, publications, and analogue maps was prepared. The compiled analogue maps were transformed into digital image, via digitizing and edit using Arc/Info GIS software (as shown in Figure 3-10).

### 3.4.2 Input map generation

In the compiled geological map in this thesis, the elevation data from the previous section (e.g. slope, aspect, topographic shape, etc.), the combination of Landsat ETM+ imageries and normalized different vegetation index or NDVI (to be mentioned later) were used as additional input information for geological revision. Besides, field data from ground-truth survey was also combined to revise the previous geologic map (Figure 3-10). Finally, the compiled geologic map of the study area is proposed in Figure 3-11.

In general, various rock units ranging from the uppermost Paleozoic and Mesozoic sedimentary and volcanic rocks to the younger unconsolidated sediments were noted in the study area from the previous study by Yooyen (1985). Stratigraphically, the lowest rock unit, generally exposed in the eastern part of the study area, is Permian Lom Kao (Lk) Formation that consists of folded limestone, massive shale and slaty shale.

Unconformably above that, Triassic Lom Sak (Ls) Formation that comprises volcanic complex, siltstone, shale and slate covers the most part of the study area, especially adjacent to the central stream channel. This Ls Formation is subsequently angular- unconformably overlaid by the gently westerly-dipping Khorat Group that mainly exposed on the steepest and highest western and northern rims, to the tops of a flat highland away from the study area. This Khorat Group consists of Phu Kradung (Pk) Formation (red siltstone, conglomeratic sandstone, tuffaceous sandstone and siltstone)

and Phra Wihan (Pw) Formation (gray sandstone, tuffaceous siltstone, and red shale), both Jurassic in age, and Phu Phan (Pp) Formation (pebbly sandstone) of Cretaceous period.

The younger unconsolidated sediments of fluvial deposits (Qa1) of Quaternary age are those of mainly stream deposits, composing of river sands and gravels, silts, clays and gray soils along the drainage system here. The sediments of Quaternary age also form in the alluvial fan as alluvial fan deposits (Qa2) at the canyon mouth to the southeastern limit of the study area. It is noted that the younger unconsolidated sediments of fluvial deposits (Qa1) and alluvial fan deposits (Qa2) of Quaternary age are the new rock units that are compiled and proposed in this thesis.

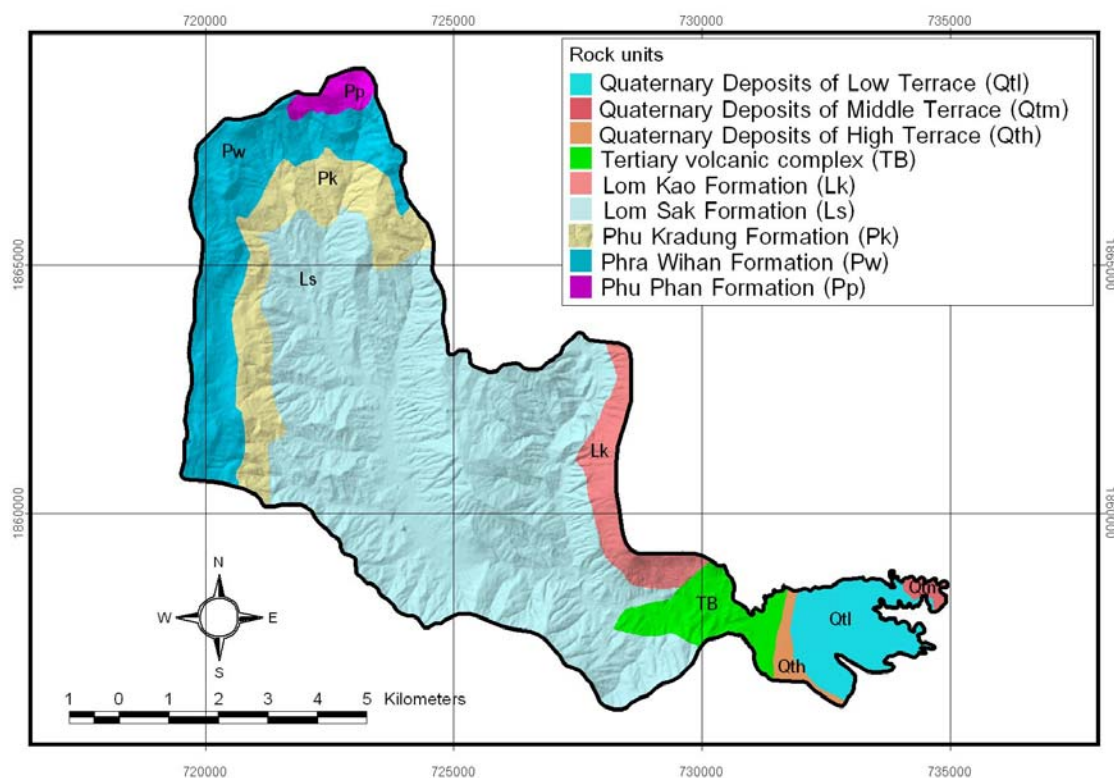


Figure 3-10 Previous geologic map of the study area (modified after Yooyen, 1985, etc.)

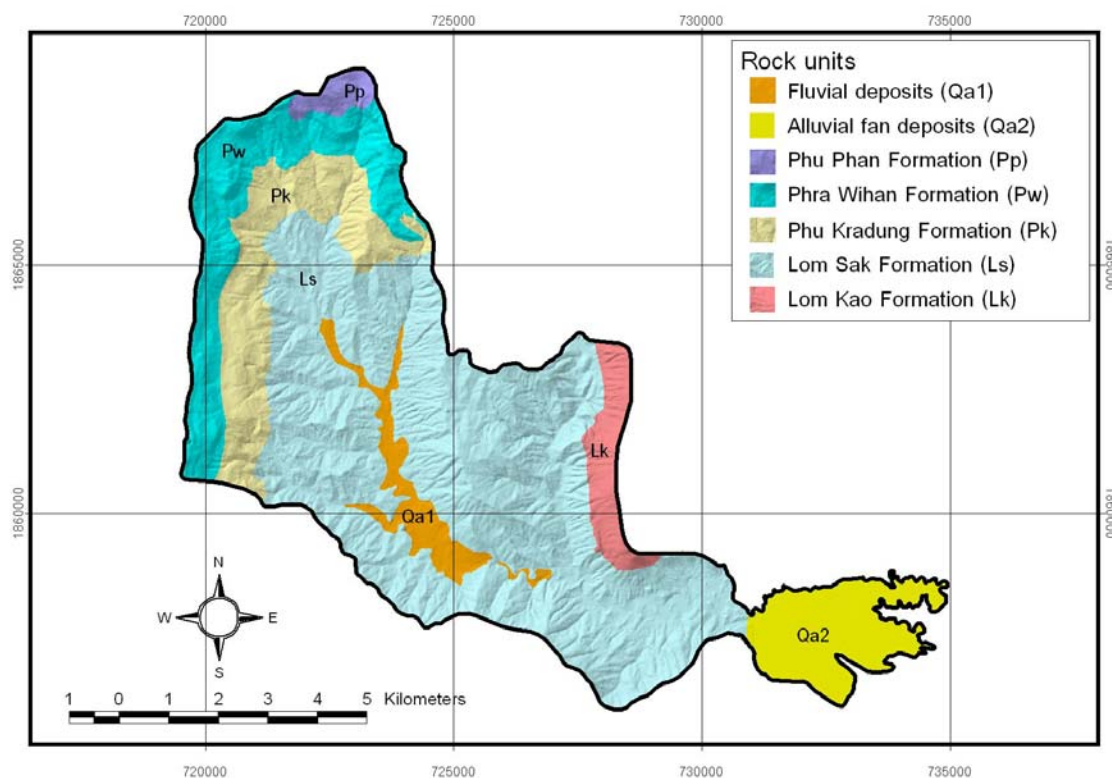


Figure 3-11 Compiled geologic map of the study area.

### 3.5 Soil property

#### 3.5.1 Data entry

The soil property collected in a form of soil group unit map and soil thickness map of the study area was prepared by compiling data from the available reports, publications, and analogue map of Land Development Department (2002). The compiled analogue maps were transformed into digital image, via digitizing and edit using Arc/Info GIS software. (as shown in Figure 3-12)

#### 3.5.2 Input map generation

The soil group unit map of the study area is further explained below.

In the study area, soils on dissected erosional surfaces are wide different according to the parent materials. Soils that derived from limestones and from basic to intermediate igneous rocks are grouped in Soil Group Unit 47 (Li, Muak Lek, Nakon

Sawan, Tali, Sob Prab and Phai Sali units). This group of soil covers 84.47 percent of total area, located on 2-20 percent (inclination) slope. Soil thickness is shallow (50-80 cm.). Soil fertility is very low with highly erosion rate. Soil pH of this group unit varied from 5.0-7.5.

As referred to Land Development Department (2002), soils that derived from sedimentary or metamorphic rocks were classified as red-yellow podzolic soils, reddish brown lateritic soils, and non-calcic brown soils and were group in Soil Group Unit 48: Ta Yang, Mae Rin, Na Cha Liaeng, Pa Yao and Nam Kun). This group of soils covers 0.189 percent of total area, located on 3-25 percent (inclination) slope. Soil thickness is very shallow (below 50 cm.), soil fertility is very low and soil fertility is very low. Soils on the high terraces were grouped in red-yellow podzolic soils, reddish brown lateritic soils, and grumusols (Soil Group Unit 55: Wang Sapung, Tab Kwang and Cha Turas). Most of these soils are well to moderately well suited for upland crops. This group of soils covers 2.30 percent of total area. Soils on the low terraces are considered to be fairly- to poorly suitable for rice growing as they are somewhat poorly drained, with coarser texture and relatively low fertility. These soils are grouped in low humic gley soils, hydromorphic and non-calcic brown soils (Soil Group Unit 28: Chai Badan, Lopburi, Wang Chompu and Samor Thod). This group of soils covers 2.76 percent of total area.

Soils on semi-recent terrace are mainly the lowland soils. The lowland soils are grouped in low humic gley soils, hydromorphic non-calcic brown soils, and grumusols (Soil Group Unit 4: Chai Nat, Ratchaburi, Tha Phon and Saraburi) and are well suitable for transplanted rice growing. The upland soils in this area are usually well suitable for upland crops. This group of soils covered 2.01 percent of total area. Soils on levees (Soil Group Unit 29: Ban Chong, Nong Mod, Mae Taeng, Pak Chong, Hang Chat, Khao Yai and Chok Chai) are well suitable for upland crops. Soils on flood plain are grouped as alluvial soils (Soil Group Unit 18: Khao Yoi, Chon Buri and Khok Samrong). They are somewhat poorly drained, with fine texture and relatively high nutrient status so they are well suitable for rice growing.

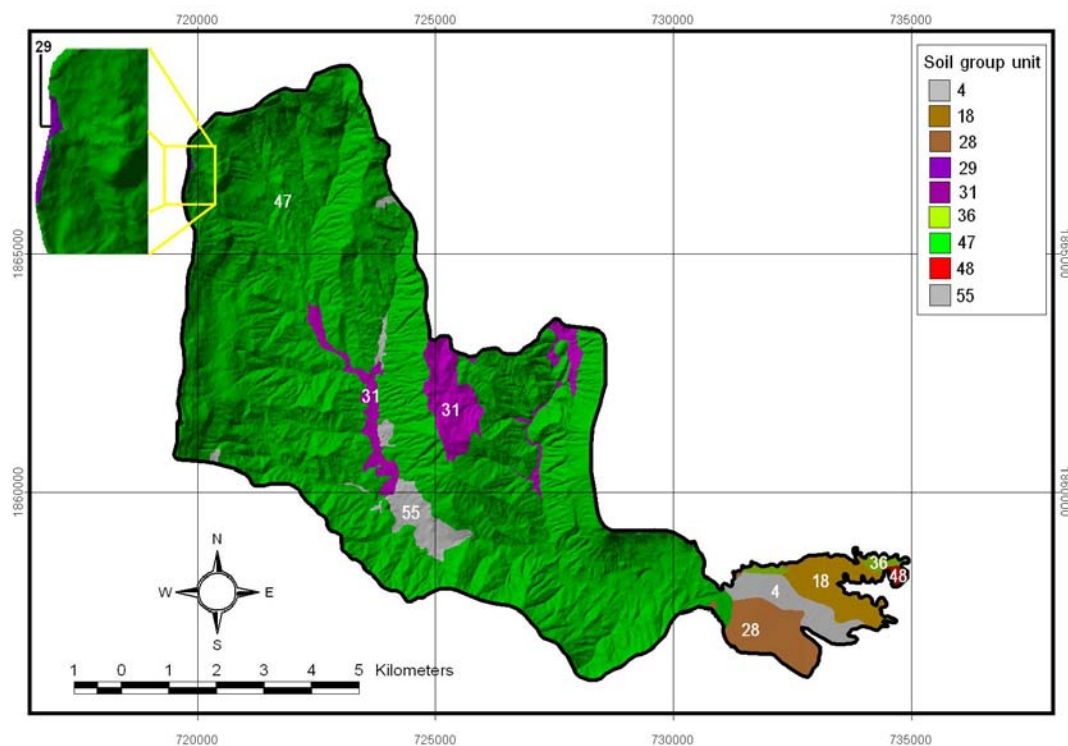


Figure 3-12 Soil group unit map of the study area (modified after Land Development Department, 2002).

Besides, soil thickness map of the study area compiled from the available reports, publications, and analogue map of Land Development Department (2002) was also prepared. The compiled analogue maps were transformed into digital image, via digitizing and edit using Arc/Info GIS software (as shown in Figure 3-13).

### 3.6 Land cover

About the land cover, Nam Ko Yai sub-catchment is covered by dense forests only on the western and northern high steep-slope area. Along the undulating valley floor of the stream in the central part of the sub-catchment, the deforestation is so vast to make land for agricultural usage. Erosional phenomena of many different types, ranging from sheet and rill erosion to mass movement, forming gullies and badlands, are widespread across the whole sub-catchment area. In the eastern extreme of the sub-catchment and on the alluvial fan, irrigated orchards and densely populated settlements are noted. It was noticed that the inappropriate land use in the highly deforested areas

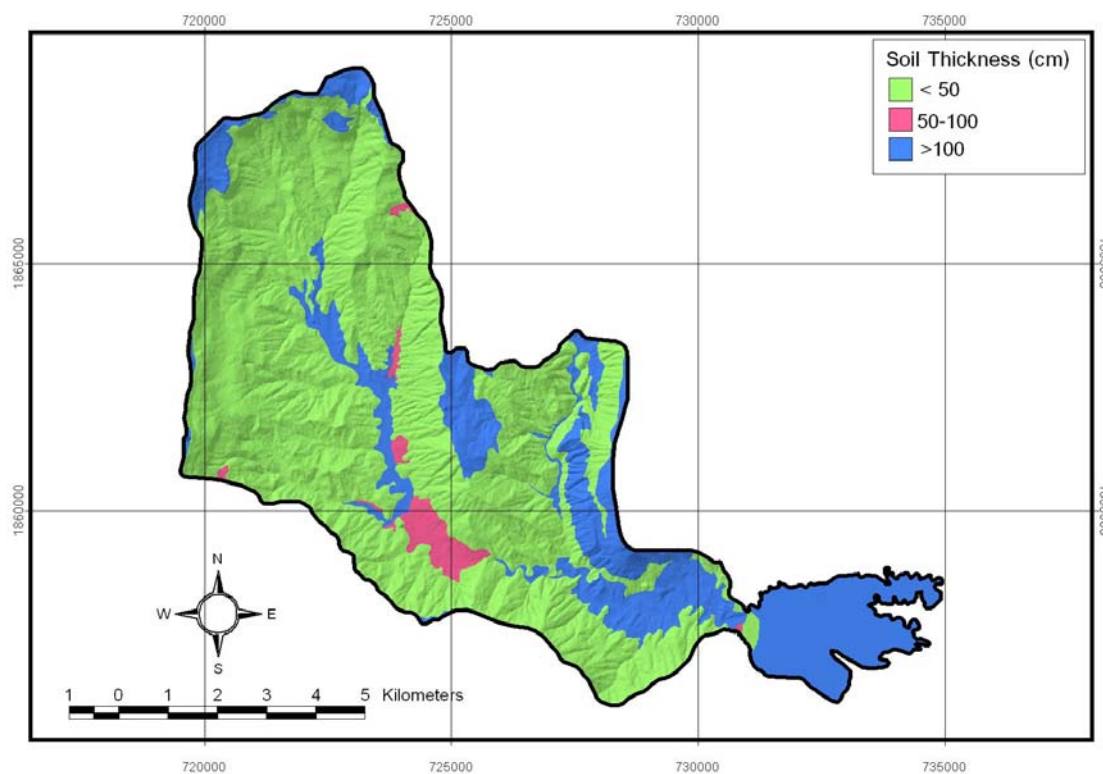


Figure 3-13 Soil thickness map of the study area (modified after Land Development Department, 2002).

of the sub-catchment was first blamed to be the major cause of this 8/11 tragedy by the publics and academics.

As a landslide hazard assessment should not only depend on the production of landslide inventory map and its analysis, a complete hazard assessment system will require also the assessment of external factors leading to instability rather than the topography and material derived properties. The land cover distribution is one of the external factors that can easily be mapped and monitored in time if needed with the aid of satellite images (Soeters and Van Westen, 1996). In landslide hazard assessment projects and in environmental and engineering studies, accurate and up to date information about land cover on a regional scale often resembles vital information to help for decision rule generation.

Basically a land cover map is obtained by classifying remotely sensed images. Typically this is performed by the spectral analysis of individual pixels and their

association with other neighboring pixels. The results of classification depend largely on the type of area, land-cover type, and image acquisition date. However, the results of the classification are directly affected by spectral confusion of land-cover types and mixed pixels. The vegetation and soil moisture conditions produce distinctive spectral responses in the electromagnetic spectrum that give the opportunity to the classifier to classify them easily.

### **3.6.1 Data sources**

Classification of land cover in the study area was carried out using many sources of remotely sensed data. Sources of data using for this study are summarized in Table 3-2. Landsat 7 ETM+ acquired on 21<sup>st</sup> November 2001, the date close to the 8/11 event, was selected as primary remotely sensed data used for classifying the land cover in the study area in the following data processing steps.

### **3.6.2 Data Processing**

Satellite imagery was analyzed using the program PCI Easi+ version 9.1, Erdas Imagine version 8.7 to obtain the results for land-use classification and grid interpolation and results plot. This study use ArcView GIS version 3.2a for analyzing previous secondary data and classifying results. Digital data analysis techniques employed in this study involved the following steps.

#### **3.6.2.1 Image rectification and restoration**

Since a large amount of data sets were involved, preprocessing of the data in the most efficient way is the prime concern. It is necessary to geometrically correct LANDSAT images to remove image distortion caused by variations of orbital parameters of the satellite and by imperfections of the sensor. The precise geometric correction could be applied by using the known ground control points (GCPs) from maps with a standard cartographic projection such as the Universal Transverse Mercator Projection

Table 3-2 Multi-temporal aerial photographs and satellite images that are used as primary data sources of this thesis

Image type	Acquisition date	Original		
		Format	Scale and Resolution	Source
Landsat TM5	December 12, 1995	LGSOWG	30 m.	GISTDA
Landsat 7 ETM+	March 7, 2000	LGSOWG	30 m.	GISTDA
	January 1, 2001	LGSOWG	30 m.	GISTDA
	November 21, 2001	LGSOWG	30 m.	GISTDA
IKONOS	October 31, 2002	GeoTiff	1 m.	GISTDA
Aerial Photograph	November 30, 1974	B&W	1:15,000	RTSD
	December 10, 1974	B&W	1:15,000	RTSD
	December 11, 1974	B&W	1:15,000	RTSD
	December 21, 1974	B&W	1:15,000	RTSD
	December 24, 1974	B&W	1:15,000	RTSD
	January 27, 1975	B&W	1:15,000	RTSD
	January 29, 1975	B&W	1:15,000	RTSD
	January 6, 1996	B&W	1:15,000	LDD
Orthophotographs	January 9, 2002	Color	1:25,000	MOAC
	December 18, 2002	Color	1:25,000	MOAC
	January 14, 2003	Color	1:25,000	MOAC
	January 15, 2003	Color	1:25,000	MOAC

Remarks:           GISTDA           Geo-Informatics and Space Technology Development Agency (Public Organization)

                          RTSD            Royal Thai Survey Department

                          LDD            Land Development Department

                          TMD            Thai Meteorology Department

                          MOAC          Ministry of Agriculture and Cooperation

                          ESRI          Environment System Research Institute (Thailand) Co. Ltd.

(UTM). After taking known GCPs from the topographic map (scale 1:50,000), the LANDSAT satellite imageries were geo-rectified by using the first order nearest neighbor methods. The pixel size of the rectified image is 25 m x 25 m.

Transformation matrices containing the coefficients for converting coordinates were calculated from the GCPs by the least square regression methods. The best GCPs were selected and adjust until the total RMS (Root Means Square) error was less than the tolerance level (0.5 of pixel size). The first-order transformation was applied which yields adequate result because of flat terrain of the study area. Nearest neighbor interpolation was followed during re-sampling.

The formulae (Equations 3-1 and 3-2) were used to rectify the satellite image so that its geographical reference was the same as the other layers in the GIS.

$$X = X_0 + a_1 (x - x_0) + a_2 (y - y_0) \dots\dots\dots \text{(Equation 3-1)}$$

$$Y = Y_0 + b_1 (x - x_0) + b_2 (y - y_0) \dots\dots\dots \text{(Equation 3-2)}$$

Where

$X, Y$  = satellite image coordinates

$x, y$  = map coordinates

$X_0, Y_0$  = coordinates of the center (arithmetic mean) of the GCPs from satellite image

$x_0, y_0$  = coordinates of the center (arithmetic mean) of the GCPs from map

$a_t, b_t$  = model constants

The values of  $x_0, y_0, X_0, Y_0$  are dependent of the subset image and the positions of the ground control points. The model constants ( $a_t$  and  $b_t$ ) are dependent of the relative orientation between the two coordinate systems.

### 3.6.2.2 Reduction of noise and image enhancement

Noise is a digital image that can manifest itself as either inaccurate gray level readings or missing data altogether. Noise is the result of sensor malfunctions during the recording or transmittal of information. Unlike geometric distortions and other radiometric

degradation, noise is readily identifiable, even to those unfamiliar with the scene of the image. Noise can be removed by using Fourier method; the image is then enhanced to encompass a variety of operation design to improve the visual interpretability of an image, by increasing the apparent distinction between features in a scene.

In the present study, all spectral bands excluding Thermal Infrared Channel of TM (band 6) and ETM+ (band 6L and 6H), were used. To minimize the effect of illumination difference, spectral band were normalized by an equation of total intensity below.

$$NB_i = 255 (OB_i / \sum OB_i) \quad i = 1 \text{ to } n \quad \dots\dots\dots \text{(Equation 3-3)}$$

Where

$NB_i$  = band normalized by total intensity

$OB_i$  = original spectral band

The constant 255 is to fit the data in a byte range of 0-255. The resulting bands have the property that the sum of some pixel values is 255 due to normalization. After normalization, the locations of these objects are projected onto a diagonal line of uniform intensity, indicating that the objects are free from intensity variation.

### 3.6.2.3 Image classification

The intention of classification process is to categorize all pixels in a digital image into one of several land cover classes or themes. This categorized data set will then be used to produce thematic maps of land cover presented in an image. Thematic maps provide an easily interpretable summary with which the eventual end user can make the well-informed decisions.

In conventional classification of multi spectral data, the maximum likelihood classifier is considered to provide the best results since it takes into account the shape, size and orientation of a cluster. Based on the class mean and the variance-covariance matrix, an unknown pixel is assigned to the most likely class.

Maximum likelihood classification (MLC) technique was employed to perform the classification of an unknown pixel. This technique had been found to be the most accurate procedure in quantitatively evaluate both the variance and correlation of the category spectral reflectance patterns. In this study land cover was classified into seven categories based on vegetation characteristics and field investigations.

This technique calculates the distance from each feature vector (pixel to be classified) to class means. The within-class variability is taken care of by adding a factor, which was a function of the variance-covariance matrix of that class. The formula used (Mather, 1987) is below:

$$D_i(x) = \ln |V_i| + (X-M_i)^T V_i^{-1} (X-M_i) \dots\dots\dots \text{(Equation 3-4)}$$

In which;  $D_i(x)$  = distance between pixel vector  $X$  and a class means based on probabilities;  $X$  = mean pixel vector  $X$ ;  $M_i$  = mean vector of the class considered;  $V_i$  = variance-covariance matrix of the class considered;  $V_i^{-1}$  = inverse of  $V_i$ ;  $|V_i|$  = determinant of  $V_i$ ;  $(X- M_i)$  = distance towards a class means' and  $(X-M_i)$  = transportation of  $(X-M_i)$

#### 3.6.2.4 Post-processing

During the classification process, the "island themes" may appear. These are single pixel themes that are most likely classification errors. These island themes can be assigned the same gray level as their phenomenon-surrounding theme using a mode filter. The mode filter is a filter algorithm that replaces a pixel gray value with the mode of the gray levels within the filter windows surrounding that pixel. This research applied mode filter with 5x5 windows size to reduce the island themes.

#### 3.6.2.5 Accuracy assessment

A complete accuracy test of a classification map would be a verification of the class of every pixel. Obviously this is impossible and indeed defeats the purpose of the image classification. Therefore, representative test areas must be used instead to estimate the map accuracy with as little error as possible. Classified image accuracy consists of two accuracy

types. Firstly, overall accuracy which represents the accuracy of the entire product and secondly, user's accuracy (or map accuracy) which a map user is interested in the reliability of the map in how well the map represents what be really on the ground. Figure 3-14 illustrated the survey tracks for field data collection and land cover classification accuracy assessment.

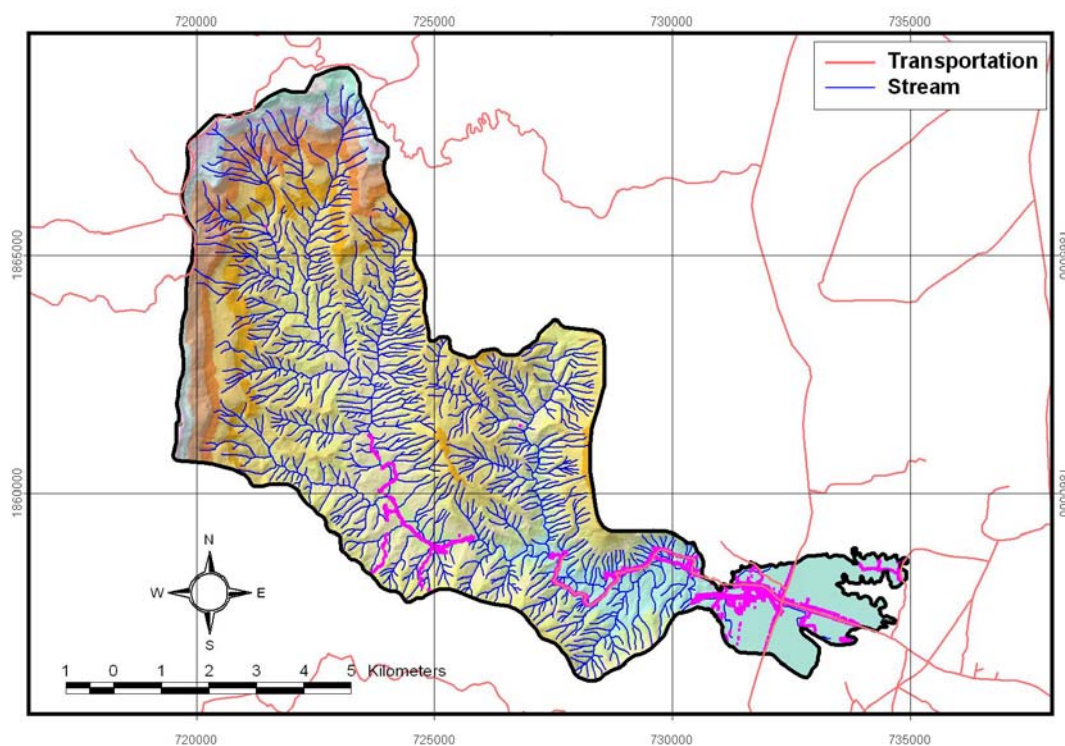


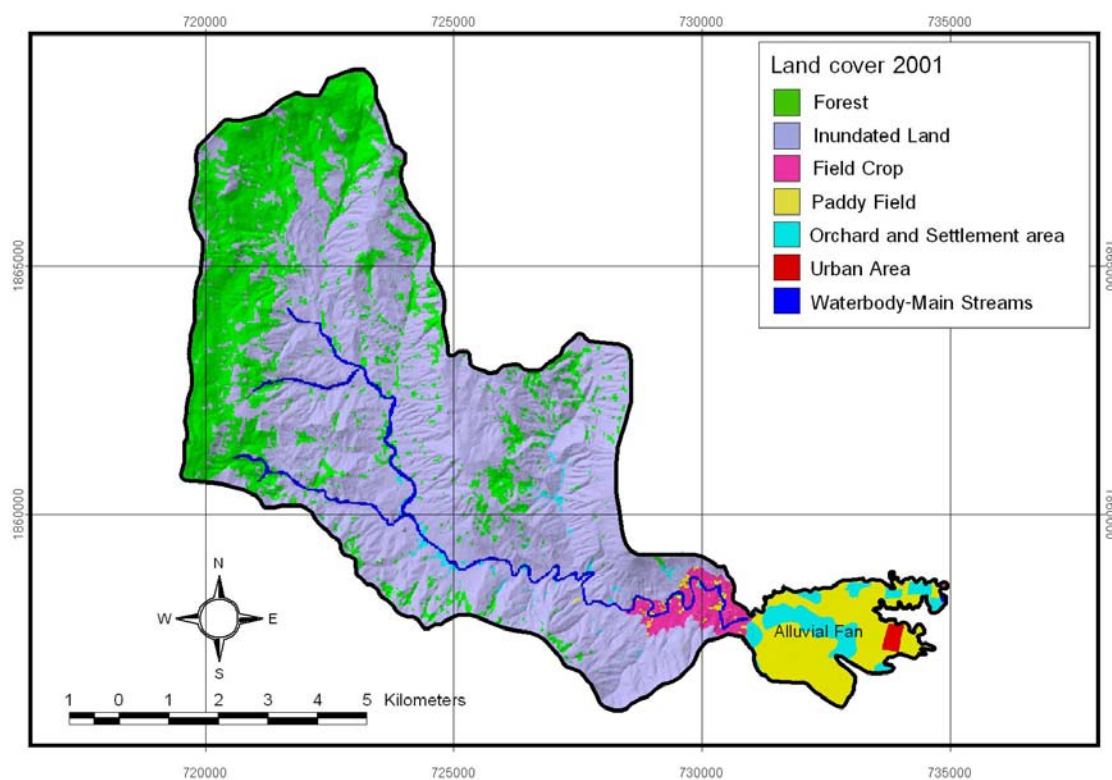
Figure 3-14 Survey tracks (pink colored dots) for field data collection and land cover classification accuracy assessment in the study area.

### 3.6.2.6 Classification result

The land cover classification of the study area was presented in Table 3-3 and Figure 3-15. Land cover pattern can be classified into 7 categories, namely, forest, paddy field, field crop, inundated land, urban area, water body, and orchard and settlement area.

Table 3-3 Land cover classification of the study area (on 21<sup>st</sup> November, 2001).

Land cover type	Area (pixel.)	Area (sq.km.)
Forest	183,087	18.3087
Paddy Field	46,269	4.6269
Field Crop	15,187	1.5187
Inundated Land	471,853	47.1853
Urban Area	1,832	0.1832
Waterbody (Main Streams)	15,442	1.5442
Orchard and Settlement Area	19,753	1.9753
Total	753,423	75.3423

Figure 3-15 Land cover map of the study area (classified from Landsat 7 ETM+ acquired on 21<sup>st</sup> November 2001).

### 3.7 Infrastructure and human settlement

The presence of several infrastructure elements such as houses, power lines and road network might contribute to the evolution of landslide in the area. The infrastructure has a mutual relationship with the flow-flood hazard as it either causes the slide or is affected from the hazard.

For the construction of infrastructure and human settlement map, the necessary features were digitized from 1:50,000 scale topographic maps of Royal Thai Survey Department (RTSD). Infrastructure (roads) and human settlement (villages) in the study area (Figure 3-16) were also mapped in addition from multi-temporal aerial photographs and satellite images as mentioned in Table 3-2.

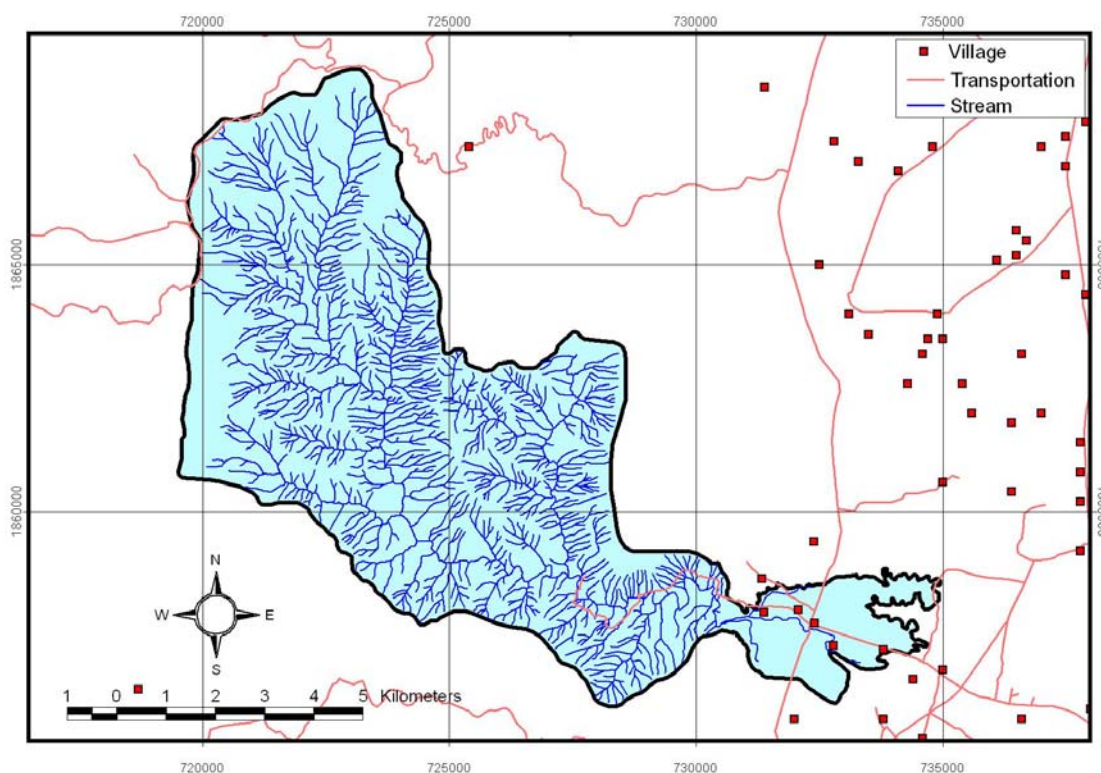


Figure 3-16 Infrastructure and human settlement map of the study area.

### 3.8 Flow-flood inventory: scar-scouring and depositional locations

#### 3.8.1 Data entry

For landslide susceptibility analysis, accurate detection of scar-scouring and depositional locations is very important, by which a field survey being the most exact method. However, finding all the landslides in a large area is very difficult and is expensive in time and money. This is especially true in mountainous areas where there is no access, and visiting to the flow-flood location is difficult or even impossible. As it would be very difficult to obtain sufficient data in this way for an accurate statistical analysis, a field survey can be used to verify the results of an orthophotograph interpretation and satellite-image analysis. Fortunately, many high-resolution aerial photos and satellite images that can be used to detect the flow-flood locations are available. In this study, 1 meter-resolution IKONOS image and 0.5 meter-resolution orthophotographs were used to detect the flow-flood locations for ground truth flow-flood phenomena field check for adjusting the classification of Landsat 7 ETM+ land cover classification.

The following process describes the combination of Landsat 7 ETM+ imageries and elevation data derived from a Digital Elevation Model-DEM (e.g. slope, aspect, topographic shape, etc.) to detect and classify fresh distinctive scar-scouring and depositional locations in the sub-catchment and its alluvial fan within the study area.

#### 3.8.2 Data Processing

The combination of Landsat 7 ETM+ imageries data and elevation data shows the characteristics of fresh scar-scouring and depositional locations clearly observable in the Landsat imageries, aerial photographs and orthophotographs. Brief field traverses were then performed at some localities as a field check to gather the ground-truth information needed to adjust the accuracy of Landsat imagery classification as well as aerial photograph and orthophotograph interpretation.

Two sets of multi-spectral Landsat imageries of different periods, one on 5 January 2001 (before 8/11) and the other on 21 November 2001 (after 8/11), were classified (as shown on Figure 3-20 and 3-21). Preprocessing of the six spectral bands (not included thermal infrared band) of these Landsat imageries involve an atmospheric correction based on the standard atmospheric-model approach. Orthorectification is accomplished using GIS vectors of road- and stream data, as well as a DEM interpolated from contour vectors (1:20,000 scales). In this data process, normalized difference vegetation index (NDVI) was used to establish a threshold of vegetated and un-vegetated pixels in the Landsat imageries for the change detection of the scar-scouring and depositional locations.

A vegetative index is a value that is calculated (or derived) from sets of remotely-sensed data that is used to quantify the vegetative cover on the Earth's surface. Though many vegetative indices exist, the most widely used index is the Normalized Difference Vegetative Index (NDVI). NDVI, like most other vegetative indices, is calculated as a ratio between measured reflectivity in the red- and near infrared portions of the electromagnetic spectrum. These two spectral bands are chosen because they are most affected by the absorption of chlorophyll in leafy green vegetation and by the density of green vegetation on the surface. Also, in the red- and near-infrared bands, the contrast between vegetation and soil is at a maximum.

NDVI is a type of product known as a transformation, which is created by transforming raw image data into an entirely new image using mathematical formulas (or algorithms) to calculate the color value of each pixel. This type of product is especially useful in multi-spectral remote sensing since transformation can be created to highlight the relationships and differences in spectral intensity across multiple bands of the electromagnetic spectrum. NDVI transformation is computed as the ratio of the measured intensities in the red (R) and near infrared (NIR) spectral bands using the following formula.

$$\text{NDVI} = (\text{NIR} - \text{red}) / (\text{NIR} + \text{red}) \quad \dots\dots\dots \text{(Equation 3-5)}$$

The resulting index value is sensitive to the presence of vegetation on the land surface and can be used to address issues of vegetation type, amount, and condition. Many satellites have sensors that measure the red- and near-infrared spectral bands, and many variations on NDVI exist. The Thematic Mapper (TM and Enhanced Thematic Mapper Plus (ETM+) in bands 3 and 4) provide RED and NIR measurements and therefore can be used to generate NDVI data sets with the following formula.

$$\text{(TM or ETM+) NDVI} = (\text{Band 4} - \text{Band 3}) / (\text{Band 4} + \text{Band 3}) \quad \text{..... (Equation 3-6)}$$

The Red and NIR images are used to calculate an NDVI value for each pixel. The NDVI equation produces values in the range of -1.0 to 1.0, where vegetated areas typically have values greater than zero, while the negative values indicate the non-vegetated surface features such as water, barren, ice, snow, or clouds. In order to maximize the range of values and provide numbers that are appropriate to display in an 8 bit image, NDVI value must be scaled. This scaling converts a number between -1.0 and 1.0 into a pixel value that is appropriate on a dark-and-white display. One example of scaling an NDVI value for display is the following equation.

$$\text{Scaled NDVI} = 100(\text{NDVI} + 1) \quad \text{..... (Equation 3-7)}$$

Thus, using this equation, a pixel with an NDVI value of 0.43 would be scaled into a gray scale value of 143. Using this technique, the NDVI computed value is scaled to the range of 0 to 200, where computed -1.0 equals 0, computed 0 equals 100, and computed 1.0 equals 200. As a result, NDVI values less than 150 represent clouds, snow, water, and other non-vegetative surfaces, and NDVI values which equal or greater than 150 represent vegetative surfaces. The resulting scaled values can be displayed on a gray tone display or even converted to a color image.

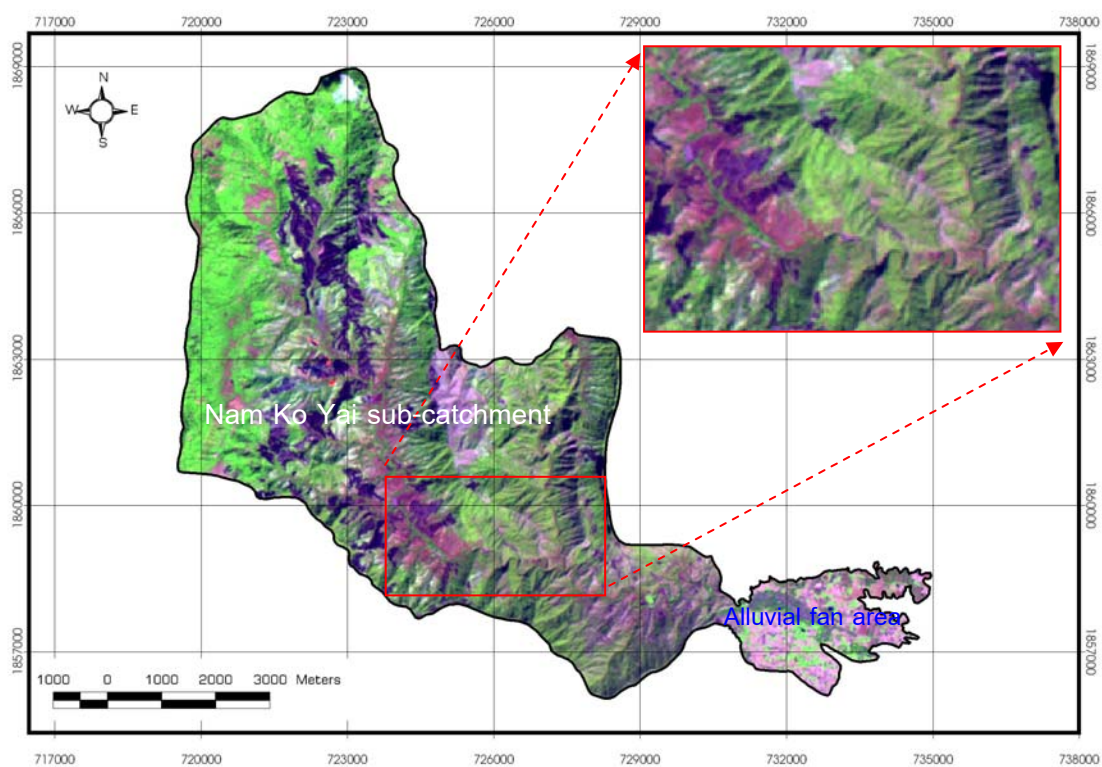


Figure 3-17 False color composite of Landsat 7 ETM+ (R=5, G=4, B=3) acquired on 5<sup>th</sup> January 2001 (before 8/11) in the study area.

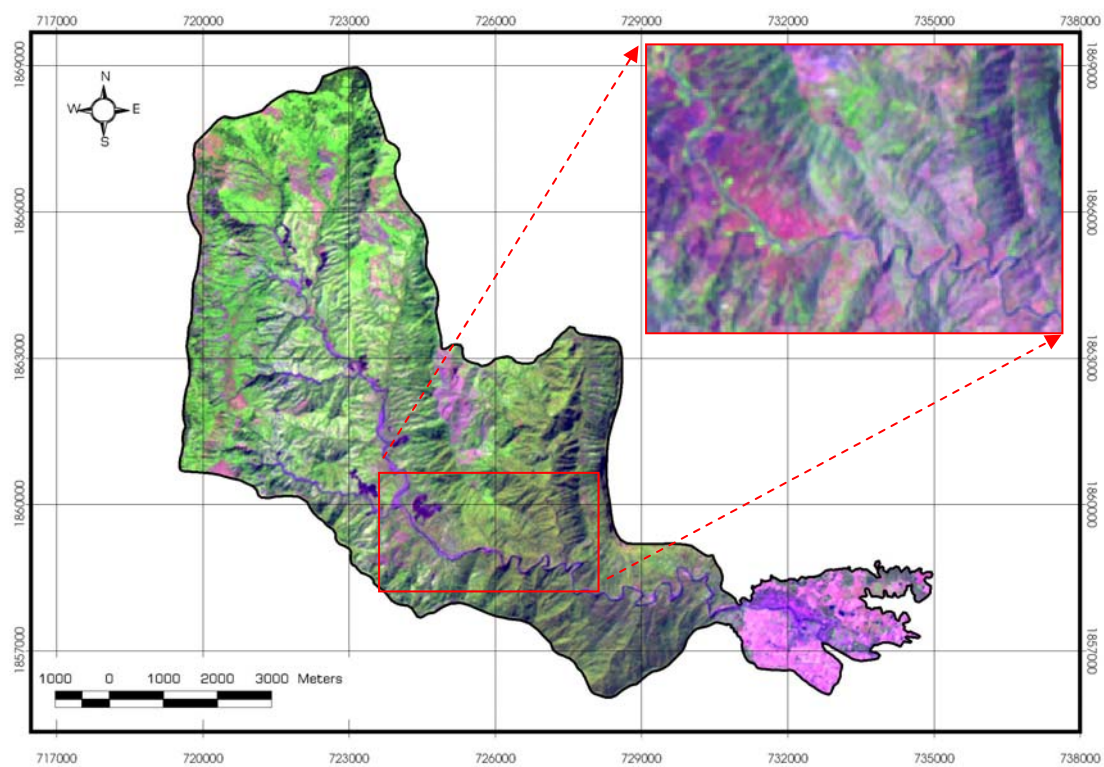


Figure 3-18 False color composite of Landsat 7 ETM+ (R=5, G=4, B=3) acquired on 21<sup>st</sup> November 2001 (after 8/11) in the study area.

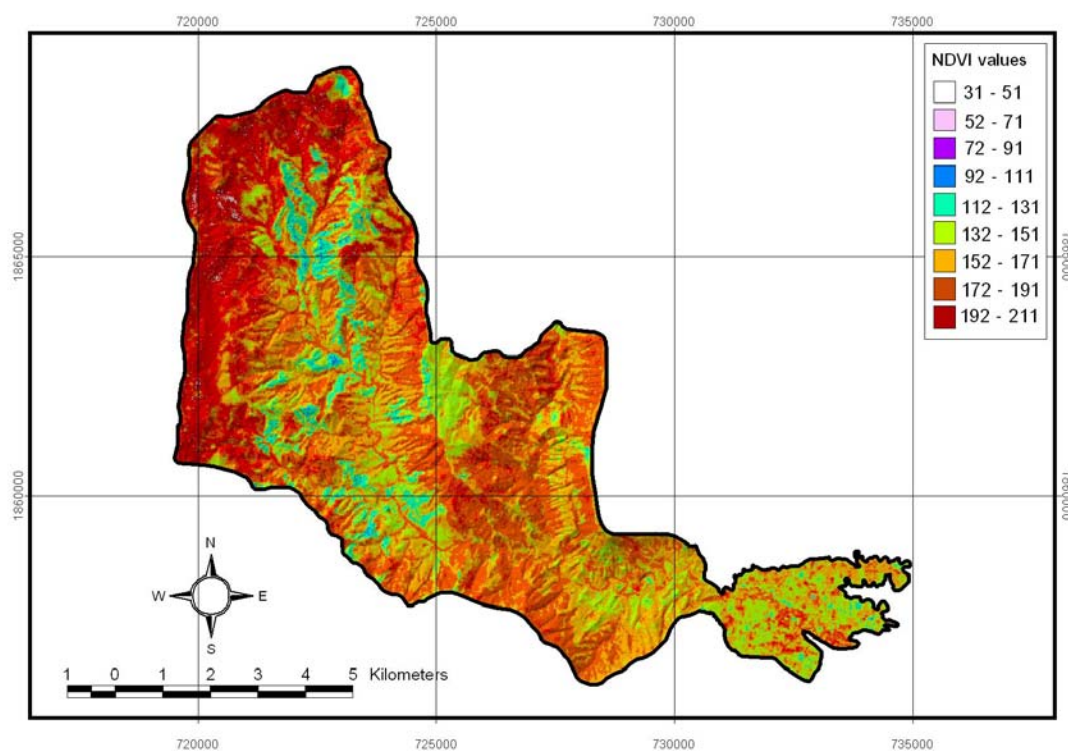


Figure 3-19 Normalized different vegetation index (NDVI) of Landsat 7 ETM+ (R=5, G=4, B=3) acquired on 5<sup>th</sup> January 2001 (before 8/11) in the study area.

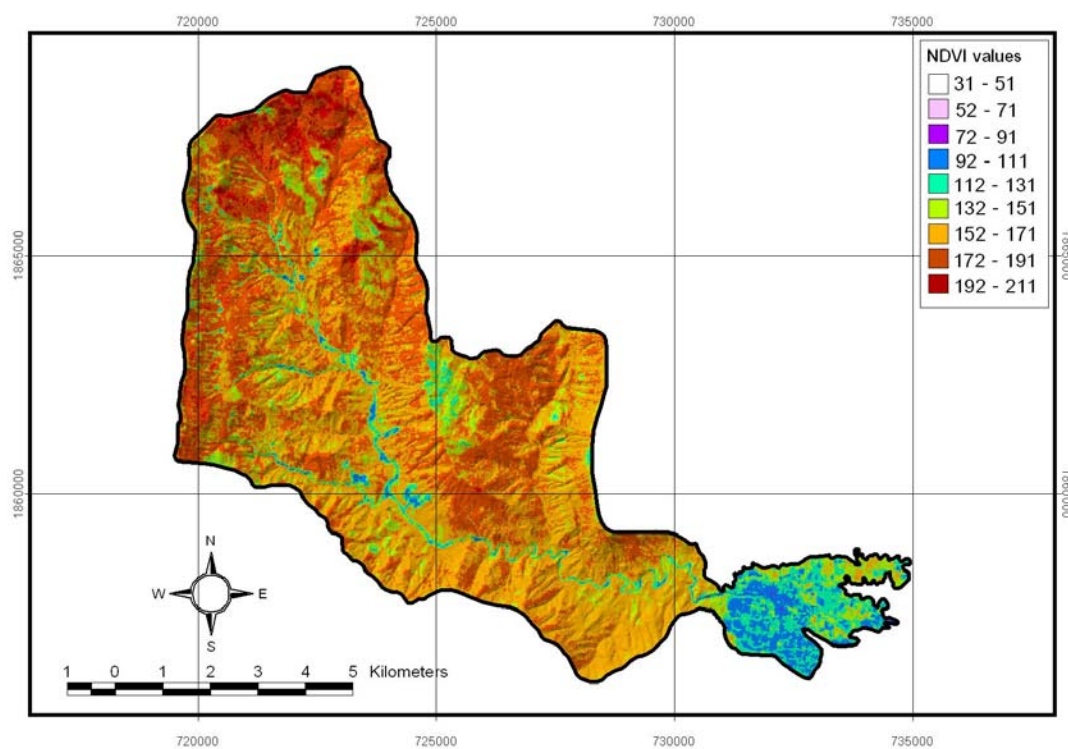


Figure 3-20 Normalized different vegetation index (NDVI) of Landsat 7 ETM+ (R=5, G=4, B=3) acquired on 21<sup>st</sup> November 2001 (after 8/11) in the study area.

The results of NDVI analyzed from the red- and infrared spectral bands of multi-spectral Landsat imageries (as shown in Figure 3-17 and Figure 3-18) are presented in Figure 3-19 and Figure 3-20. Finally, the NDVI imageries are used to establish a threshold of vegetated and un-vegetated pixels in the images for the change detection as the scar-scouring and depositional locations in the study area as shown in Figure 3-21.

The classification scheme used to detect the scar-scouring and depositional locations depended on a user-specified hierarchical structure to eliminate image objects that were not of interest. The first level was a division of the image between the vegetated and un-vegetated objects based on their NDVI value. The choice of 150.00 was empirically based on an inspection of the image objects from the ground-truth information. Those objects with NDVI value below 150.00 were considered as un-vegetated objects, and those above 150.00 as vegetated ones.

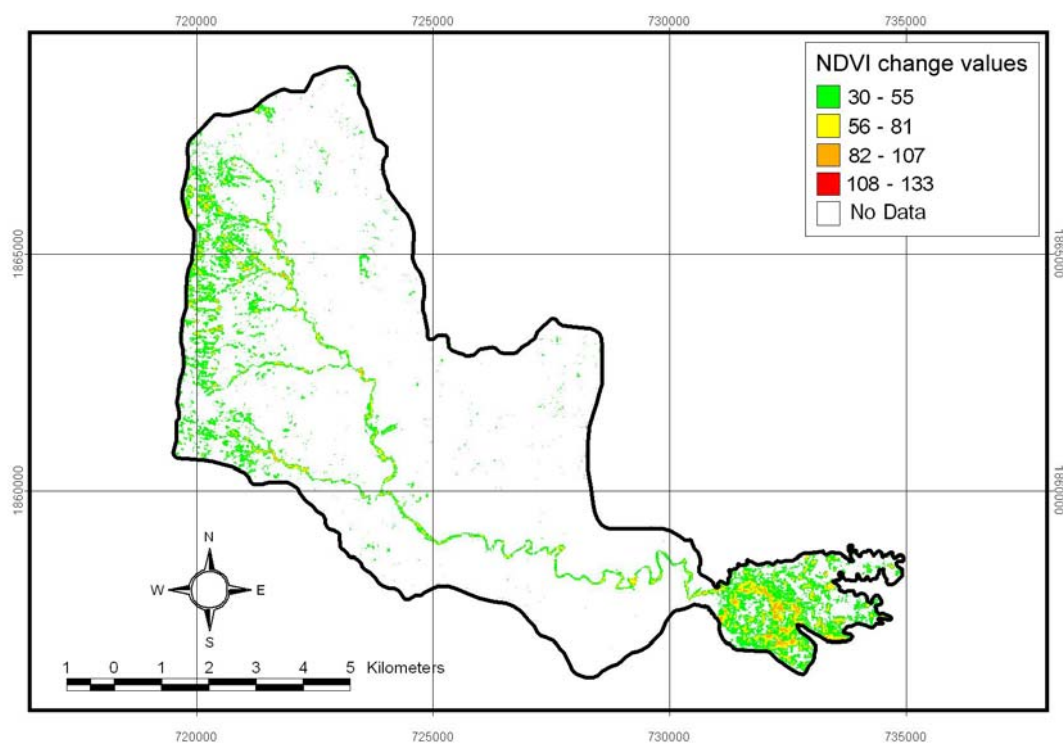


Figure 3-21 Resulted significant change detection of NDVI that used to detect the scar-scouring and depositional locations in the study area that are caused from the 8/11 flow-flood occurrence.

The scar-scouring and depositional locations were also detected and validated by an accuracy assessment. Classification accuracy was determined by comparing a sample of classified pixels with ground-truth information derived from the orthophotographs, IKONOS imagery (acquired after the 8/11 event) and the field observation (Figure 3-22 and Figure 3-23). The validity of the classified results was tested through the identified ground-truth information of the scar-scouring and depositional locations.

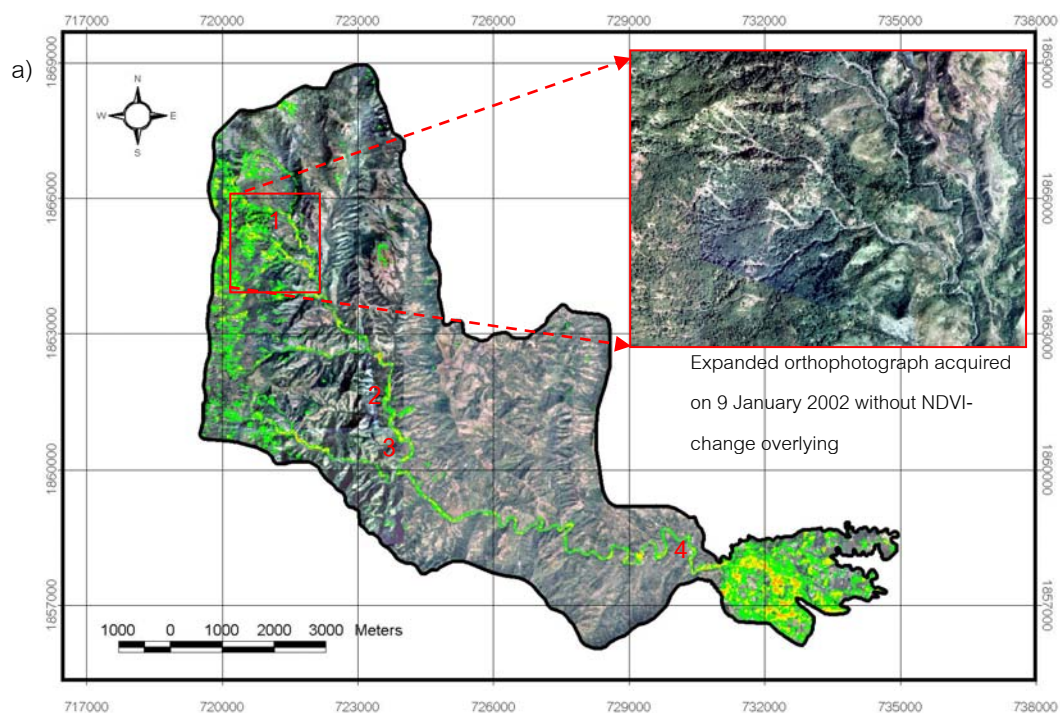


Figure 3-22 a) Significant change of NDVI (referred to Figure 3-21) overlain on the orthophotograph image acquired on 9<sup>th</sup> January 2002 (after 8/11); and b) photographs of four locations (number referred to the location in the map) taken a few days after the 8/11 event showing the ground truth evidences.



a) Orthophotographs acquired on 9<sup>th</sup> January 2002



b) Orthophotographs acquired on 29<sup>th</sup> March 2002



c) IKONOS imagery acquired on 31<sup>st</sup> October 2002

Figure 3-23 Examples of high resolution remote sensing imageries (acquired after the 8/11 event) used for classifying accuracy and validating NDVI results that related to detect the scar-scouring and depositional locations in the study area.

### 3.8.3 Accuracy assessment of scar-scouring delineation

This step applied the confusion matrix method to determine the accuracy of scar-scouring delineation from training area of Landsat imagery acquired on 21<sup>st</sup> November 2001 in Nam Ko Yai sub-catchment (Figure 3-24). The confusion matrix was used to compare the evaluating classification of scar-scouring locations interpreted from NDVI change (Figure 3-25) and ground truth data of scar-scouring delineation manually digitized from 1:20,000 orthophotograph acquired on January 14, 2003 (Figure 3-26). These two set data of the scar-scouring boundaries were used for calculating the accuracy assessment in 10 meter-resolution.

An error matrix was presented in Table 3-4 to determine how well a classification has categorized a representative subset of pixels used in the training process of classification. This matrix was stemmed from classifying the sampled training set pixels and listed the known ground cover types used for training (columns) versus the pixels actually classified into each classification category (rows).

Several other descriptive measures can be obtained from the error matrix. For example, the overall accuracy is computed by dividing the total number of correctly classified pixels (i.e., the sum of the elements along major diagonal) by the total number of reference pixels. Likewise, the accuracies of individual categories can be calculated by dividing the number of correctly classified pixels in each category by either the total number of pixels in the corresponding row or column. What are often termed producer's accuracies results from dividing the number of correctly classified pixels in each category (on the major diagonal) by the number of training set pixels used for that category (the column total). This number indicates how well training set pixels of the given cover type are classified.

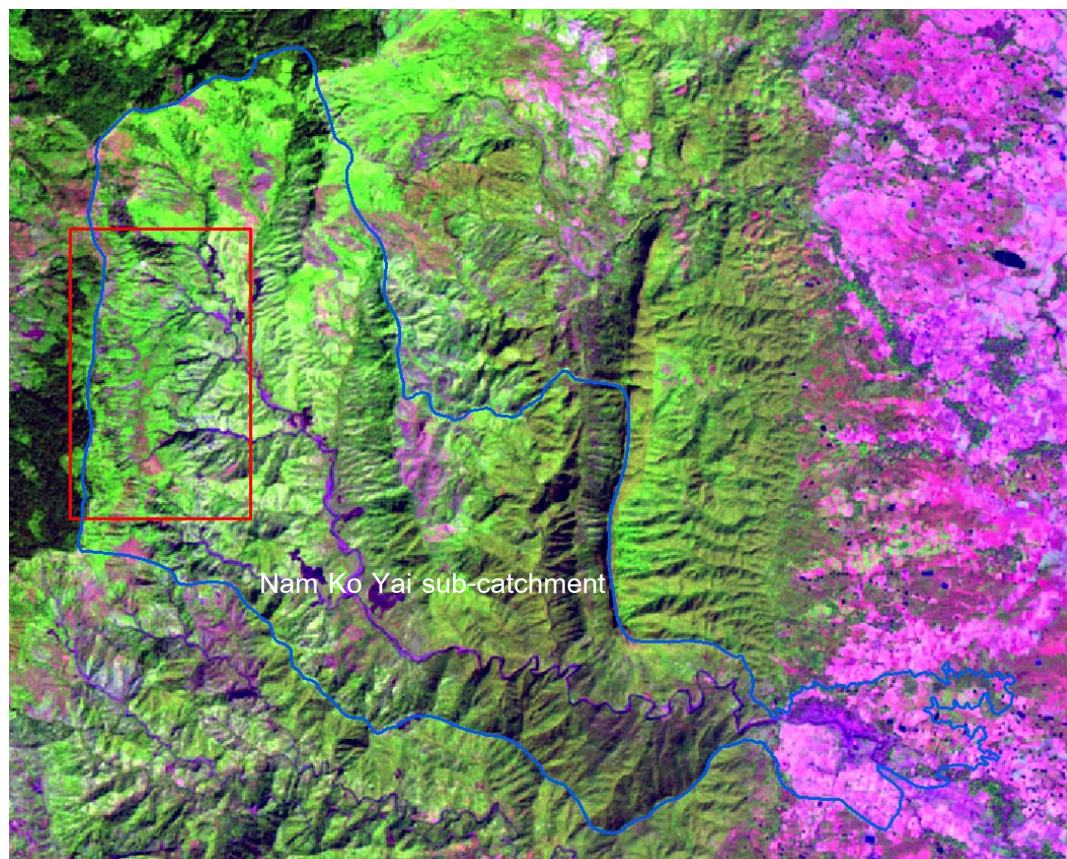
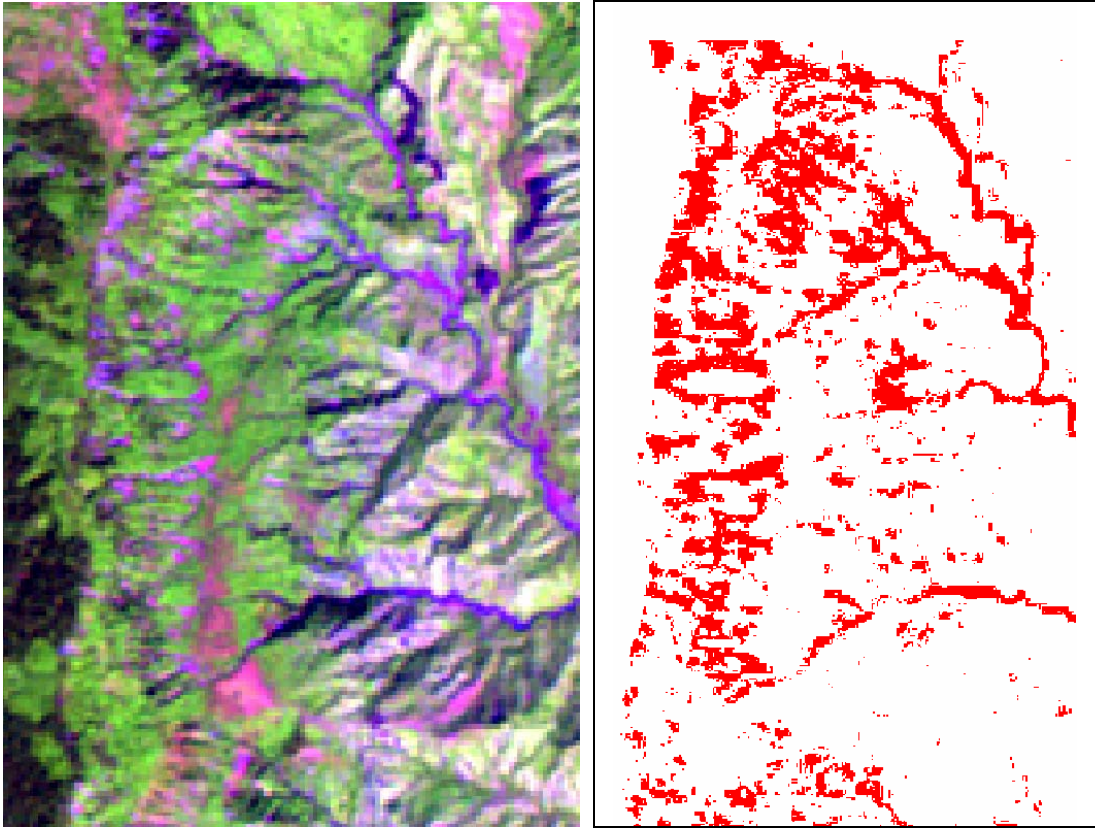


Figure 3-24 Accuracy assessment verification in training area (red box) located in Landsat 7 ETM+ (R=5, G=4, B=3) acquired on 21<sup>st</sup> November 2001 in Nam Ko Yai sub-catchment.



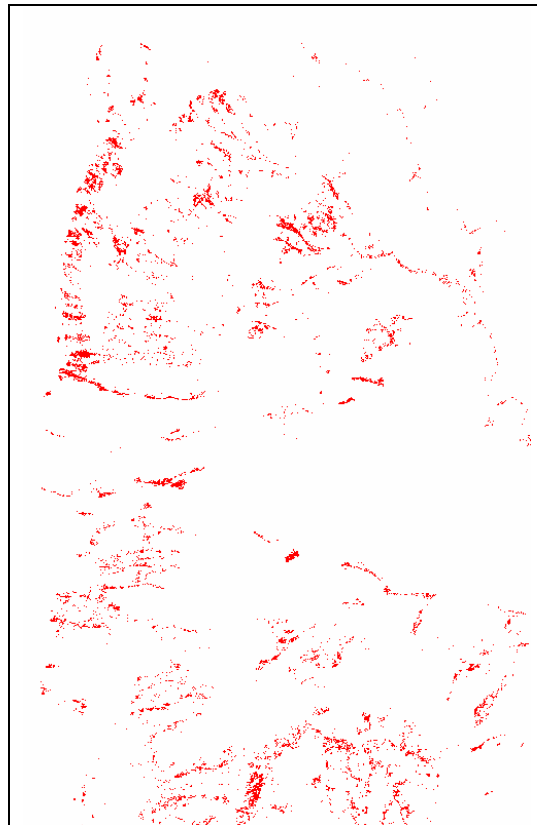
Training area (red box) referred to Figure 3-24

Scar-scouring locations (grouped in red)  
interpreted from NDVI change (referred to  
Figure 3-21)

Figure 3-25 Scar-scouring locations interpreted from NDVI change in training area.



Orthophotograph acquired on 14<sup>th</sup> January 2003  
(1:20,000 scale) in training area of Figure 3-24



Digitized scar-scoring delineation from the  
orthophotograph in training area

Figure 3-26 Scar-scouring delineation digitized from orthophotograph acquired on 14<sup>th</sup> January 2003 (1:20,000 scale) in training area.

Table 3-4 Error matrix resulting from classifying training set pixels

Categories	Ground truth verification data (from orthophotograph interpretation)		
	correctly classified pixels as scar- scourings	correctly classified pixels as no scar- scourings	Row Total
Classification data			
correctly classified pixels as scar-scourings	3,207	90,583	93,790
correctly classified pixels as no scar-scourings	11,156	458,638	469,794
Column total	14,363	549,221	563,581

According to the error matrix resulting from classifying training set pixels as presented in Table 3-4, producer's accuracy, user's accuracy and overall accuracy of scar-scouring delineation were evaluated as follows:

Producer's accuracy

$$\text{Scar-scourings} = 3,207/14,363 = 22.33 \%$$

$$\text{No scar-scourings} = 90,583/549,221 = 16.49 \%$$

User's accuracy

$$\text{Scar-scourings} = 3,207/93,793 = 3.42 \%$$

$$\text{No scar-scourings} = 11,156/469,794 = 2.37 \%$$

$$\text{Overall accuracy} = (3,207+458,638) / 563,581$$

$$= 81.95\%$$

### 3.9 Rainfall intensity

#### 3.9.1 Data entry

In this upper Pa Sak region, the average annual rainfall normally exceeds 1,000 mm. The climate is a tropical kind, occasionally with tropical storms in the early and middle periods of rainy season (June-October). The tropical storm “Usa-ngi” that passed through here during the first two weeks of August 2001 was blamed to cause this tragedy.

In this study, rainfall data were received from observation stations of Thai Meteorology Department during 1<sup>st</sup>-31<sup>st</sup> August 2001 being put into database around Nam Ko Yai sub-catchment (as show in Figure 3-27).

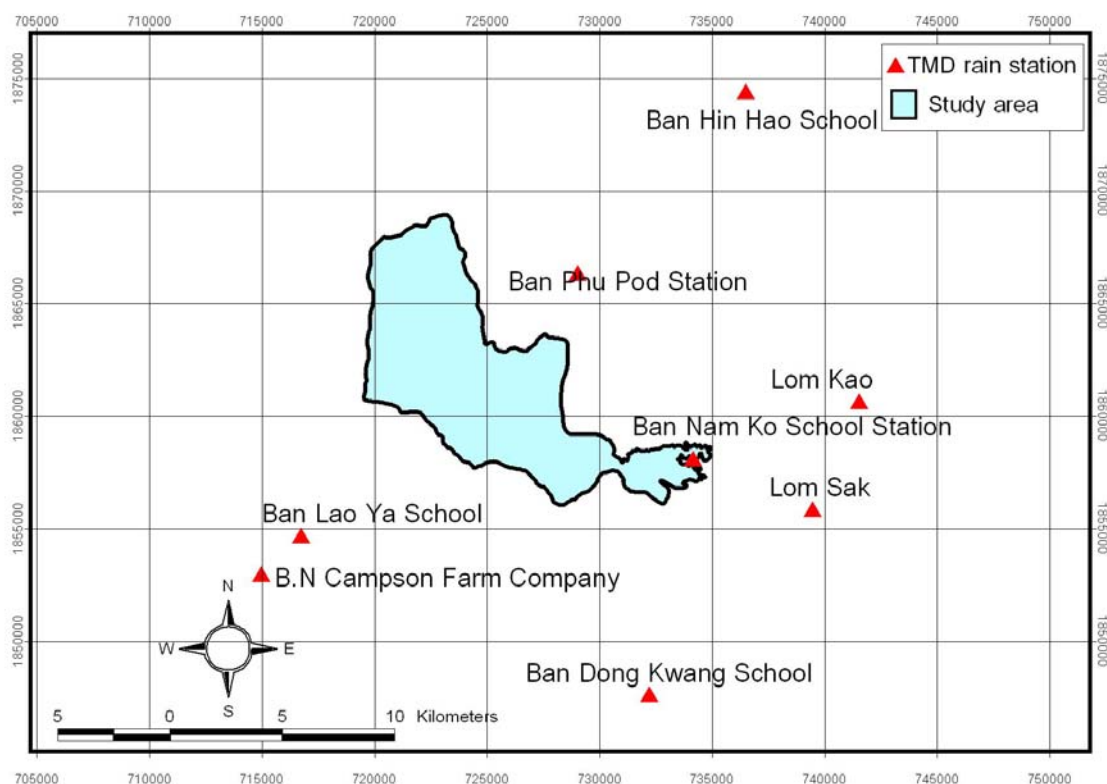


Figure 3-27 Location of seven rainfall-measurement stations of Thai Meteorological Department (TMD) near the study area.

The analysis of rainfall data (derived and interpolated from the observation stations of Thai Meteorology Department) during 1<sup>st</sup>-10<sup>th</sup> August 2001 (before 8/11 event) in relation to the configuration of sub-catchment and channel characteristics had been conducted and used as one of the most critical factors to identify the potential for the event in the study area. The graph of rainfall measurements in August 2001 from seven locations surrounding the study area (as shown in Figure 3-27) is summarized in Figure 3-28.

The pattern of rainfall during 1<sup>st</sup>-31<sup>st</sup> August 2001 recorded in most of the stations reveals the same manner that there was continuous rainfall during 2<sup>nd</sup>-14<sup>th</sup> August 2001 with the most intense raining of about 60 and 100 mm was recorded on 10<sup>th</sup> August 2001 at the Ban Lao Ya station (southwest of the study area) and Ban Hin Hao station (northeast of the study area), respectively. The average rainfall value during 1<sup>st</sup>-10<sup>th</sup> August 2001 recorded from these seven locations in Figure 3-28 is 12.98 mm whereas the average rainfall value of each station is illustrated in Figure 3-29.

For the following year 2002, the graph of rainfall measurements from eight locations surrounding the study area (seven previous locations plus a newly installed station at Ban Nam Ko Yai) is summarized in Figure 3-30. The average rainfall value during 1<sup>st</sup>-10<sup>th</sup> August 2002 recorded from the seven locations is 11.4102 mm as shown in Figure 3-31.

According to the Figure 3-29 and Figure 3-31, the average rainfall value (mm) of each station surrounding the study area during 1<sup>st</sup>-10<sup>th</sup> August 2001 (before 8/11 event) and the average rainfall value (mm) of each station surrounding the study area during 1-10<sup>th</sup> August 2002 (one year after the 8/11 event) are calculated as 12.9806 mm and 11.4102 mm, respectively. The rainfall intensity of 10 August 2001 (one day before the 8/11 event) was the highest value of this 1<sup>st</sup>-10<sup>th</sup> August 2001 duration.

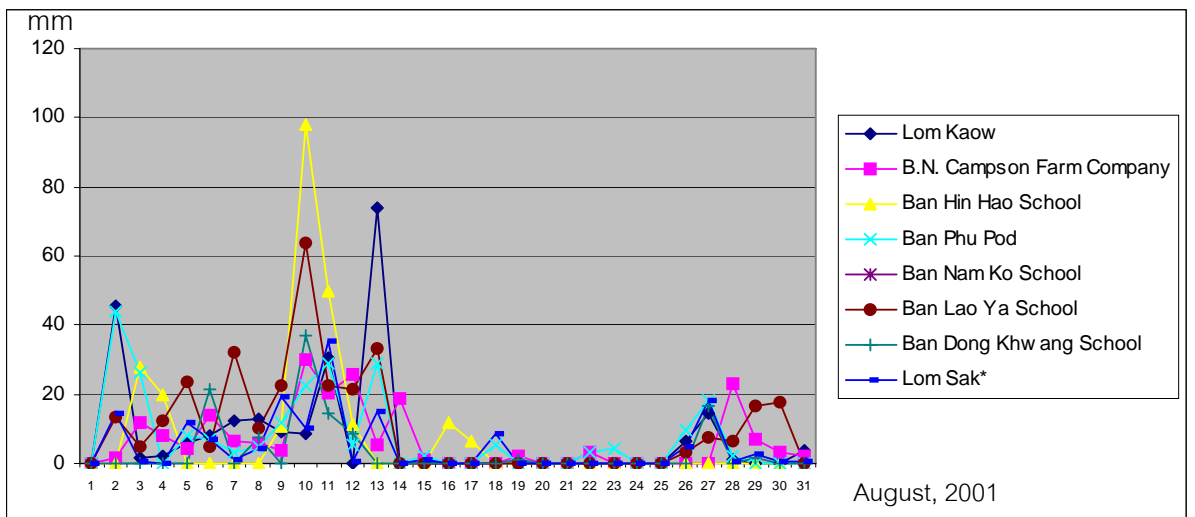


Figure 3-28 Graph showing the pattern distribution of rainfall measurements in August 2001 recorded from the seven locations near the study area.

(Note: the data of Ban Nam Ko School, the newest station in 2002, was not available during those period)

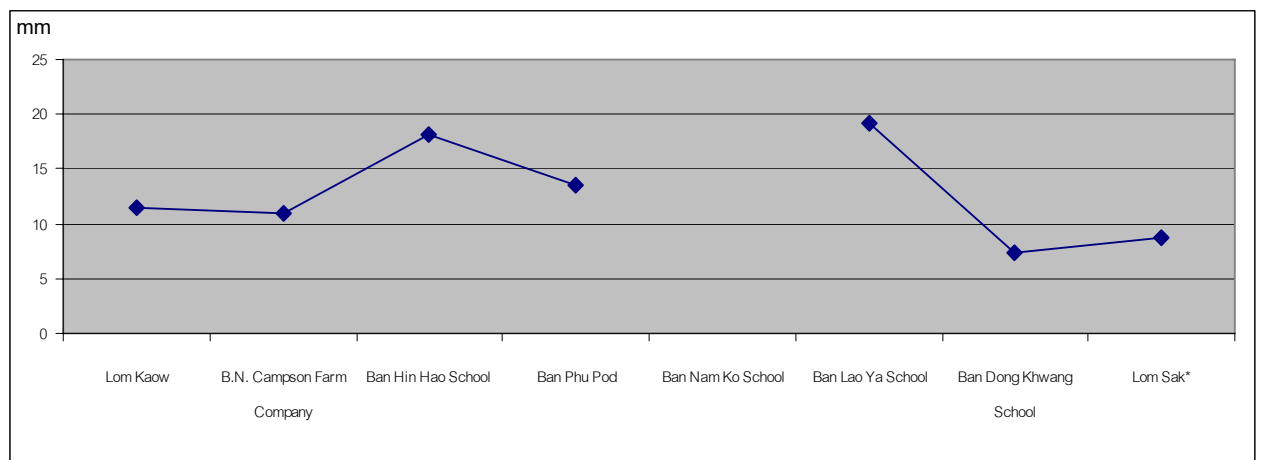


Figure 3-29 Average rainfall value (mm) of each station near the study area during 1<sup>st</sup>-10<sup>th</sup> August 2001 (before the 8/11 event).

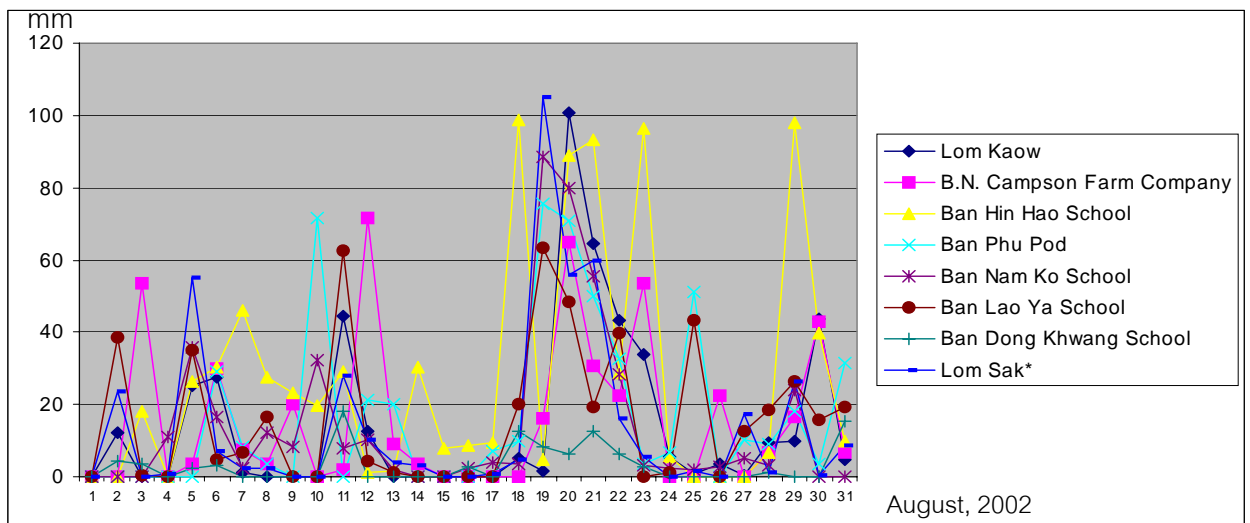


Figure 3-30 Graph showing the pattern distribution of rainfall measurements in August 2002 recorded from the eight locations near the study area.

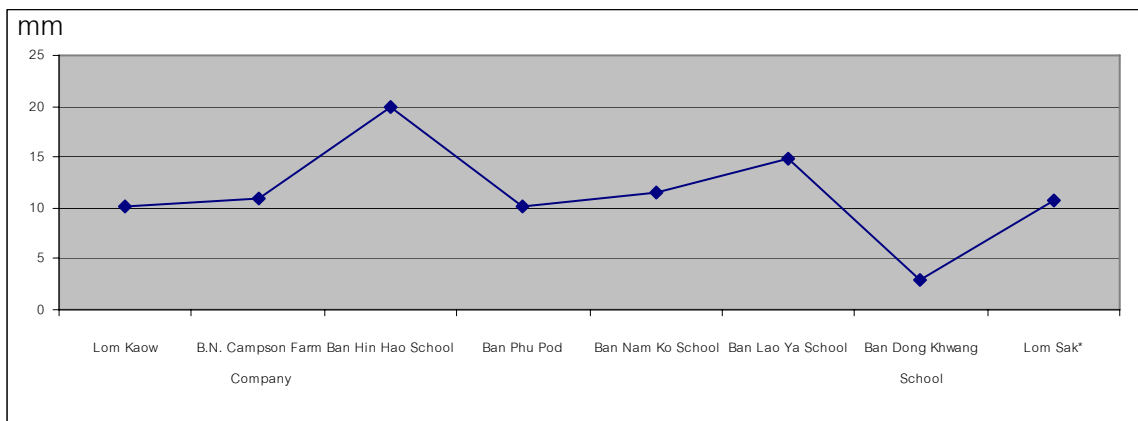


Figure 3-31 Graph showing the average rainfall value (mm) of each station near the study area during 1<sup>st</sup>-10<sup>th</sup> August 2002 (one year after the 8/11 event).

It is noted that the intensity and duration of rainfall in August 2002 as shown in the graph of rainfall measurements (Figure 3-30) were much stronger and longer than those of the year 2001 (Figure 3-28). However, there was no disastrous event of debris flow and debris flood in the study area during this time. Only a mild flash overbank-flood had occurred here throughout the whole month.

### 3.9.2 Input map generation

From the rainfall database mentioned above, the rainfall intensity grid during 1<sup>st</sup>-10<sup>th</sup> August 2001 (that was the strongest period of rainfall before the 8/11 event) is generated by interpolated rainfall station by Krigging procedure. The isohyte of the rainfall intensity during 1<sup>st</sup>-10<sup>th</sup> August 2001 is presented in Figure 3-31. It is remarked that the most intense raining of about 150 and 160 mm was illustrated in the western and northern steep-cliff of Nam Ko Yai sub-catchment of the study area in that duration of ten days before the 8/11 event.

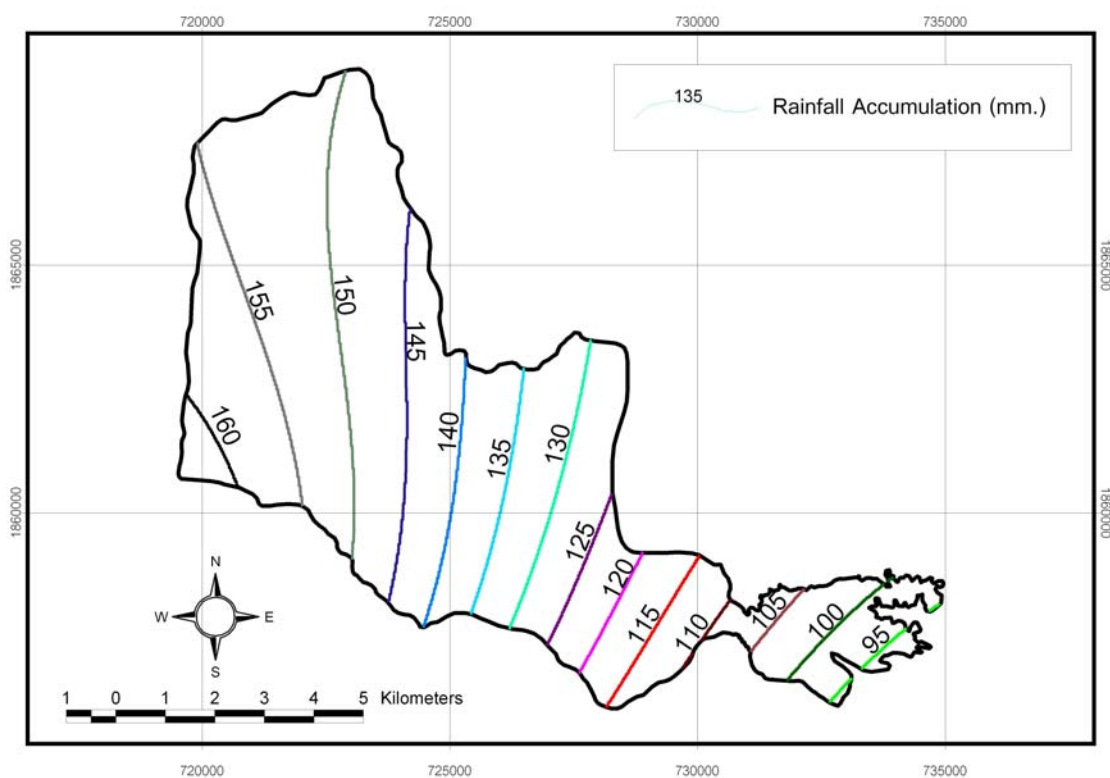


Figure 3-32 Isohyte map of rainfall intensity during 1<sup>st</sup>-10<sup>th</sup> August 2001 in the study area.

## CHAPTER 4

### DEBRIS FLOW-FLOOD HAZARD ANALYSIS IN NAM KO YAI SUB-CATCHMENT

In this chapter, debris flow-flood hazard analysis in Nam Ko Yai sub-catchment is conducted from the significant and cost-effective information on flow-flood as previously mentioned in Chapter 3. Trends in landslide hazard analysis are briefly presented and the detailed statistical analysis of flow-flood susceptibility in Nam Ko Yai sub-catchment are proposed in detail as follows.

#### 4.1 Trends in landslide hazard zonation

A large amount of researches on hazard zonation has been done in the last three decades through the world as a consequence of an urgent demand for slope instability hazard mapping. Overviews of the various slope instability hazard zonation techniques can be found in the works of, for examples, Hansen (1984), Varnes (1984), Hartlen and Viberg (1988). The general trends in landslide hazard zonation are given in Table 4-1. The distribution analyses and qualitative analyses are generally used for the very large areas with very low detail such as national hazard maps. The deterministic and frequency analyses are used generally for very small areas, such as areas of specific large engineering projects like dams, nuclear power plants, highway strips, open-pit mine slopes and spoils. Monitoring and laboratory analyses are indispensable for these analyses. There are many studies involving landslide hazard evaluation (Gokceoglu and Aksoy 1996; Larsen and Torres-Sanchez 1998; Turrini and Visintainer 1998; Guzzetti and others 1999; Lee 2000, Lee and Min, 2001). In particular, Guzzetti and others (1999) summarized many cases of landslide hazard evaluation studies.

## 4.2 Debris flow-flood susceptibility analysis

According to the landslide analysis method, there are three steps (Einstein, 1988) in landslide risk analysis, i.e. susceptibility, possibility, and risk, as specified in formulas 1, 2 and 3 below.

$$\text{Susceptibility} = f(\text{landslide, landslide-related parameters}) \dots\dots\dots (1)$$

$$\text{Possibility} = f(\text{susceptibility, impact parameters}) \dots\dots\dots (2)$$

$$\text{Risk} = f(\text{possibility, damageable objects}) \dots\dots\dots (3)$$

Table 4-1 Trends in landslide hazard zonation (Van Westen, 1993).

Type of landslide hazard analysis	Main characteristics
A. Distribution analysis	Direct mapping of mass movement features resulting in a map, which gives information only for those sites where landslides have occurred in the past.
B. Qualitative analysis	Direct, or semi-direct, methods in which the geomorphological map is re-numbered to a hazard map, or in which several maps are combined into one using subjective decision rules, based on the experience of the earth scientist.
C. Statistical analysis	Indirect methods in which statistical analyses are used to obtain predictions of the mass movement hazard from a number of parameter maps.
D. Deterministic analysis	Indirect methods in which parameter maps are combined in slope stability calculations.
E. Landslide frequency analysis	Indirect methods in which earthquake and/or rainfall records or hydrological models are used for correlation with known landslide dates, to obtain threshold values with a certain frequency.

The susceptibility is a function of the probability of potential landslide occurrence and landslide-related factors. It does not depend on impact factors such as rainfall, earthquake, or human activity. The possibility depends on the impact

parameters and the susceptibility. The risk depends on vulnerable objects such as people and property, and on the possibility. Of these three, only the first is further considered in details, and only flow-flood's that occurred as a result of heavy rain are discussed here.

For the flow-flood susceptibility analysis only in Nam Ko Yai sub-catchment of the study area was selected according to the scar-scouring locations (hereafter referred to as scar-scouring) from flow-flood occurrence were clearly detected whereas the alluvial fan of resulting depositional locations was not included in the analysis. Accurate detection of the scar-scouring that mainly occurred in Nam Ko Yai sub-catchment was very important. According to significant and cost-effective information on the flow-flood hazard assessment as discussed in Chapter 3, the medium scale (1:25,000-1:50,000) was chosen. Theoretically, statistical techniques were dominantly used in this scale.

In general, statistical techniques are the indirect methods in which statistical analyses are used to obtain predictions of the mass movement hazard from a number of parameter maps. The statistical or probabilistic approach is based on the observed relationship between each parameter and the past and present landslide distribution. The strong point of this functional approach is also directly dependent on the quality and quantity of the data collected. Drawbacks are derived from the fact that few parameters are relevant for landslide assessment and are mappable at a reasonable cost. The statistical approach, in turn, can be applied following different techniques which essentially differ on the statistical procedure used (univariate or multivariate), and on the type of mapping-unit selected. The conceptually (but not operationally) simplest technique is a conditional analysis which attempts to assess the probabilistic relationship between relevant environmental parameters and the occurrence of landslides in a given region.

In this part, the flow-flood susceptibility analysis was preliminary analyzed by using univariate probability analysis (Lee and Min, 2001) which is further explained below.

#### 4.2.1 Susceptibility analysis using univariant probability method

Flow-flood susceptibility in this thesis was preliminary analyzed by univariant probability method to present the spatial relationship between the scar-scouring locations and each of available flow-flood influencing parameters (as theoretically mentioned by Van Westen (1994) in Chapter 2 and conducted in Chapter 3) in Nam Ko Yai sub-catchment, namely, slope, landform topography, geology, soil group unit, soil thickness, land cover, and stream proximity, respectively. The GIS was used to compile a vast amount of data efficiently, and a statistical program was used to maintain specificity and accuracy. A key assumption using this approach is that the potential (occurrence possibility) of flow-flood processes would be comparable to the actual frequency of flow-flood processes and relationships between each parameter are independent. The results of the statistic analysis were later verified in detail by using the field and laboratory evidence data in the Chapters 5 and 6.

For the univariant probability method to present the spatial relationship between the detected scar-scouring locations and each of the mentioned flow-flood influencing parameters in Nam Ko Yai sub-catchment, the spatial data were converted to a 10 x 10 m grid or cell (ARC/INFO GRID type), then further converted to ASCII data for a use with a general statistical program. For Nam Ko Yai sub-catchment, the total number of cells are 690,509 while the detected scar-scouring number of cells are 47,774. The correlation ratios were performed on the relationship between the detected scar-scouring locations and each parameter's range. The ratio between the number of the detected scar-scouring cell numbers (hereafter to be called b, for convenience) and the number of the non-detected scar-scouring cell numbers (hereafter to be called a, for convenience) was calculated as probability of flow-flood susceptibility in each parameter's range. The  $b/a$  ratio equal 1 defines an average value, greater than 1 means a high correlation, and less than 1 means a low correlation. A high correlation indicates a high probability of the flow-flood susceptibility in each flow-flood influencing parameter. Such relationships in Nam Ko Yai sub-catchment were briefly concluded in below.

#### 4.2.1.1 Relationship between scar-scouring and slope

Theoretically, the slope angle is an essential component in slope stability analysis. As the slope angle critically increases, shear stress in soils or other unattached materials along a potential failure plane tend to increase as well. Gentler slope is expected to have a low frequency of scar-scouring locations because of generally lower shear stress associated with low gradient.

For slope as a parameter, the frequencies of recent scar-scouring number of cells for a given interval of slope angle were noted as shown in Figures 4-1, 4-2 and 4-3 and Table 4-4. The frequencies were determined by counting the scar-scouring number of cells for each 5 degree interval of slope angle, then ratios of pixel which scar-scouring were detected and pixel which scar-scoring are not detected (hereafter to be called b/a ratio, for convenience) were calculated. The b/a ratio indicated the susceptibility or probability of each interval of slope angle to flow-flood.

For area in slope below  $5^\circ$ , the b/a ratio was 2.76, indicating a very high probability. From  $5$  to  $10^\circ$ , the b/a ratio was 1.08, indicating a moderately probability also. From  $10$  to  $30^\circ$ , the b/a ratio was in the range of 0.68-0.84, indicating a low probability. From  $30$  to  $35^\circ$ , the b/a ratio was 1.06, indicating a moderate probability. From  $35$  to  $40^\circ$  and above  $40^\circ$ , the b/a ratios were 1.43 and 1.54, respectively, indicating a high probability. It means that scar-scouring probability increases according to slope angle. If the slope angle is higher than  $30^\circ$ , scar-scouring may occur.

It was generally noted in Nam Ko Yai sub-catchment that the steeper slope, the greater the flow-flood probability. But it was also noted that the flow-flood probability is commonly a high correlation in a gentle terrain with the slope below  $5^\circ$ . This was especially in the clear and opened area along Nam Ko Yai stream channel and its banks. So, this could be an effect of other parameters beyond the slope inclination alone.

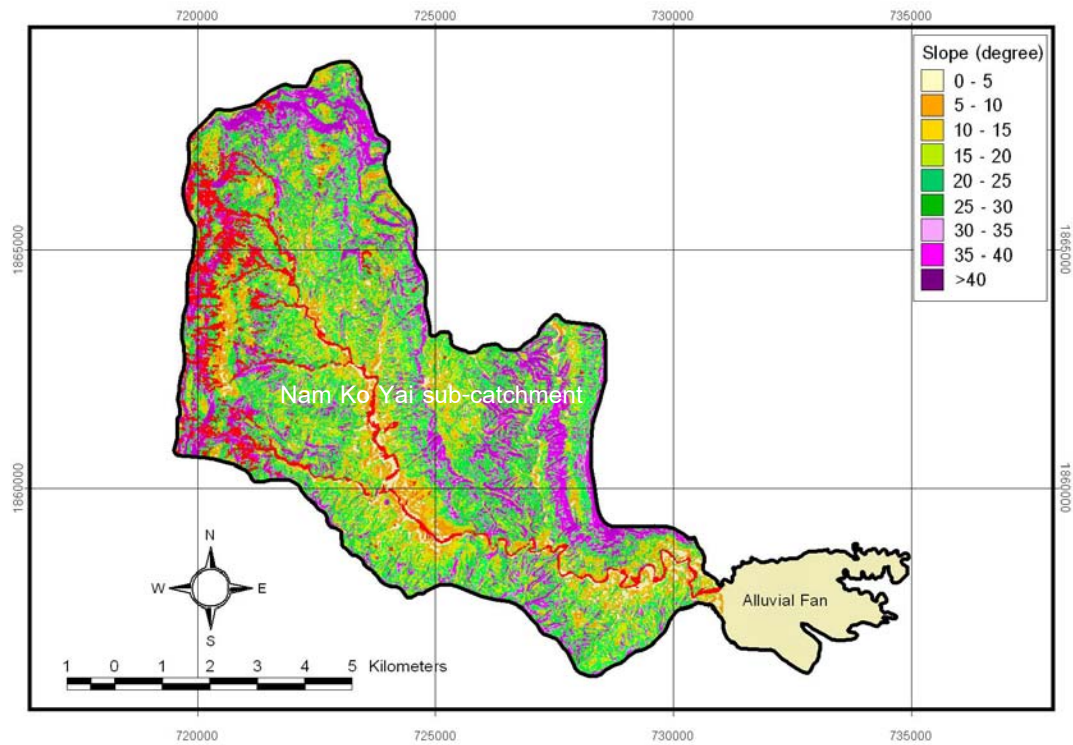


Figure 4-1 Slope map overlain with scars-scouring locations (grouped in red color) in Nam Ko Yai sub-catchment.

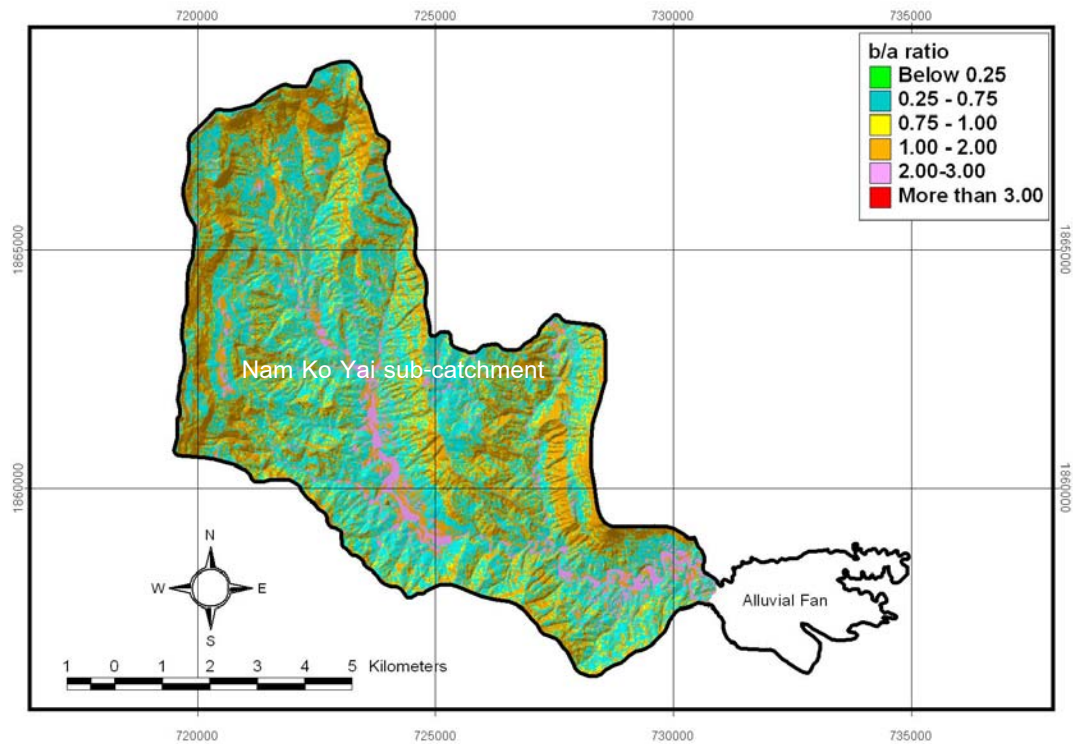
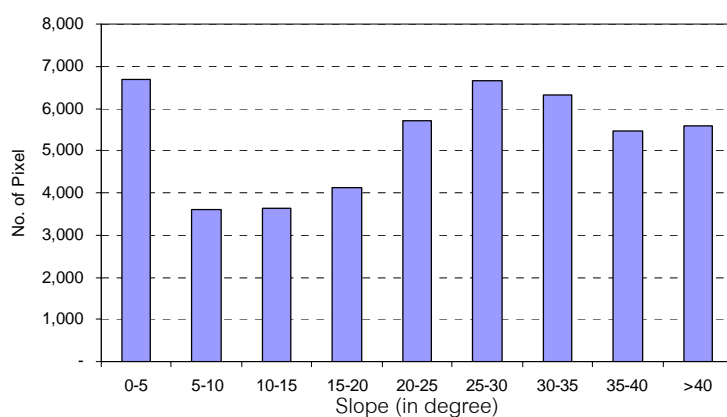


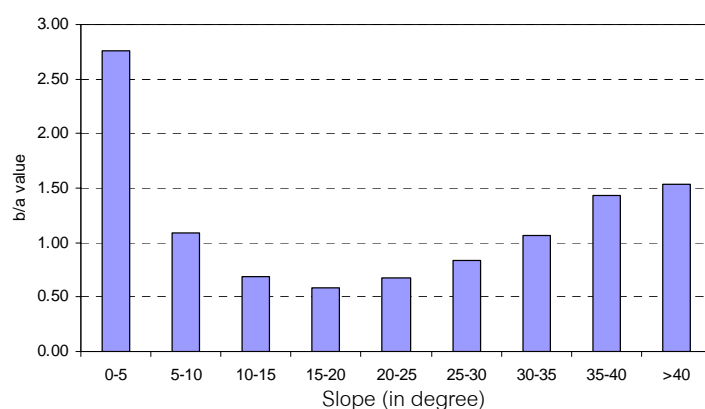
Figure 4-2 Map illustrating b/a ratio as probability of flow-flood susceptibility on slope in Nam Ko Yai sub-catchment.

Table 4-2 Relation of flow-flood and slope in Nam Ko Yai sub-catchment.

Slope range	Scar-scouring did not occur		Scar-scouring occurred		b/a
	Count	Ratio (%) a	Count	Ratio (%) b	
0-5 °	32,671	5.08	6,701	14.03	2.76
5-10 °	44,684	6.95	3,596	7.53	1.08
10-15 °	71,342	11.10	3,629	7.60	0.68
15-20 °	94,386	14.69	4,133	8.65	0.59
20-25 °	112,870	17.56	5,706	11.94	0.68
25-30 °	106,687	16.60	6,666	13.95	0.84
30-35 °	79,874	12.43	6,309	13.21	1.06
35-40 °	51,394	8.00	5,452	11.41	1.43
More than 40 °	48,827	7.60	5,582	11.68	1.54
Total	642,735	100.00	47,774	100.00	



a) Distribution of scar-scoring cell numbers on slope.



b) b/a ratio on slope.

Figure 4-3 Histogram distribution of a) scar-scoring number of cells on slope, and b) b/a ratio on slope in Nam Ko Yai sub-catchment.

#### 4.2.1.2 Relationship between scar-scouring and landform topography

In the case of landform topography, the frequencies were determined by counting the scar-scoring number of cells for a given topographic shape unit (namely, peak, ridge, saddle, flat, ravine, pit, convex hillside, concave hillside, slope hillside, inflection hillside and saddle hillside) and presented in Figures 4-4, 4-5 and 4-6 and Table 4-3.

It was noted that a very high probability was observed in flat landform that the b/a ratio was 5.05. A high probability was observed in saddle and pit landforms that the b/a ratios were 2.37 and 2.30, respectively. A moderate probability was generally observed in concave hillside, inflection hillside, slope hillside, ridge and ravine landforms that b/a ratios were in the range of 1.08-1.26. Whereas a low probability was only observed in convex hillside landform that the b/a ratio was 0.96.

It is concluded that the flow-flood probability was commonly a high correlation with the specific type of flat landform that especially was in the clear and opened area along Nam Ko Yai stream channel and its banks of the flat landform.

In the case of slope and landform topography as mentioned above, it is generally concluded that the flow-flood probability is commonly a high correlation with the area in slope below  $5^{\circ}$  and flat landform in Nam Ko Yai sub-catchment. The slope and landform topography are summarized to be ones of the significant relevant parameters to the flow-flood occurrence that will be later used to calculate the debris flow-flood susceptibility.

#### 4.2.1.3 Relationship between scar-scouring and aspect

In case of aspect or direction that a slope facet, the frequencies were determined by counting the scar-scouring cell number for a given slope aspect and presented in Figures 4-7, 4-8 and 4-9 and Table 4-4. Theoretically, the aspect is an essential component in slope stability analysis because some directions of slope facets

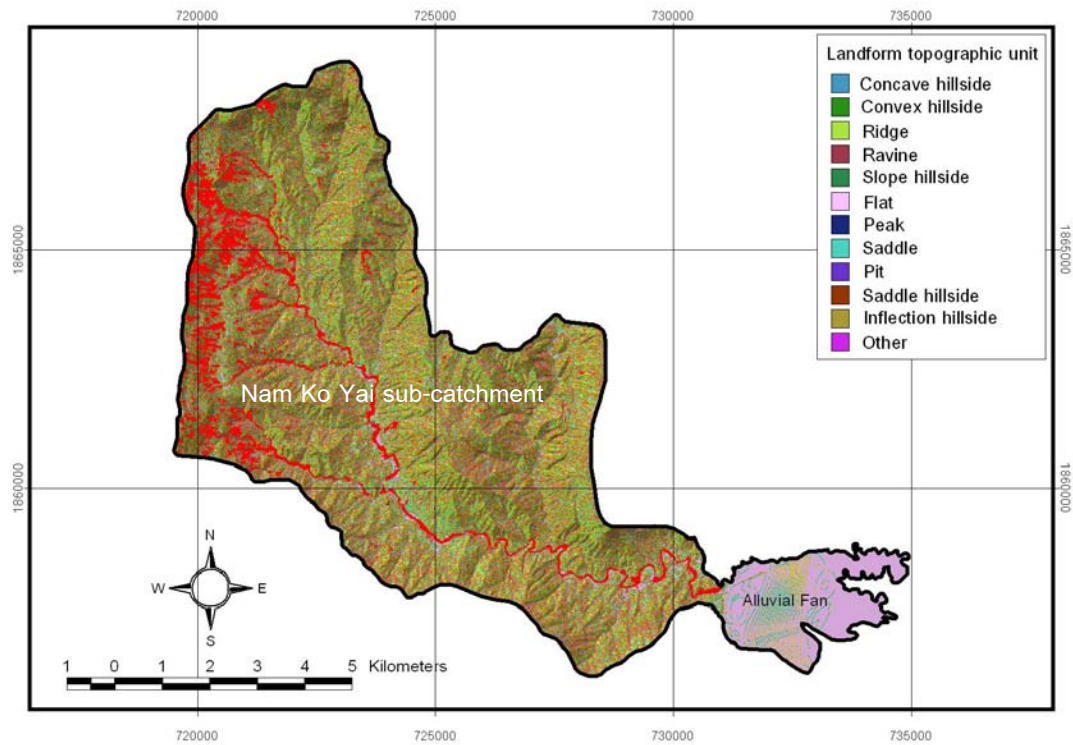


Figure 4-4 Landform topography overlain with scar-scouring locations (grouped in red color) in Nam Ko Yai sub-catchment.

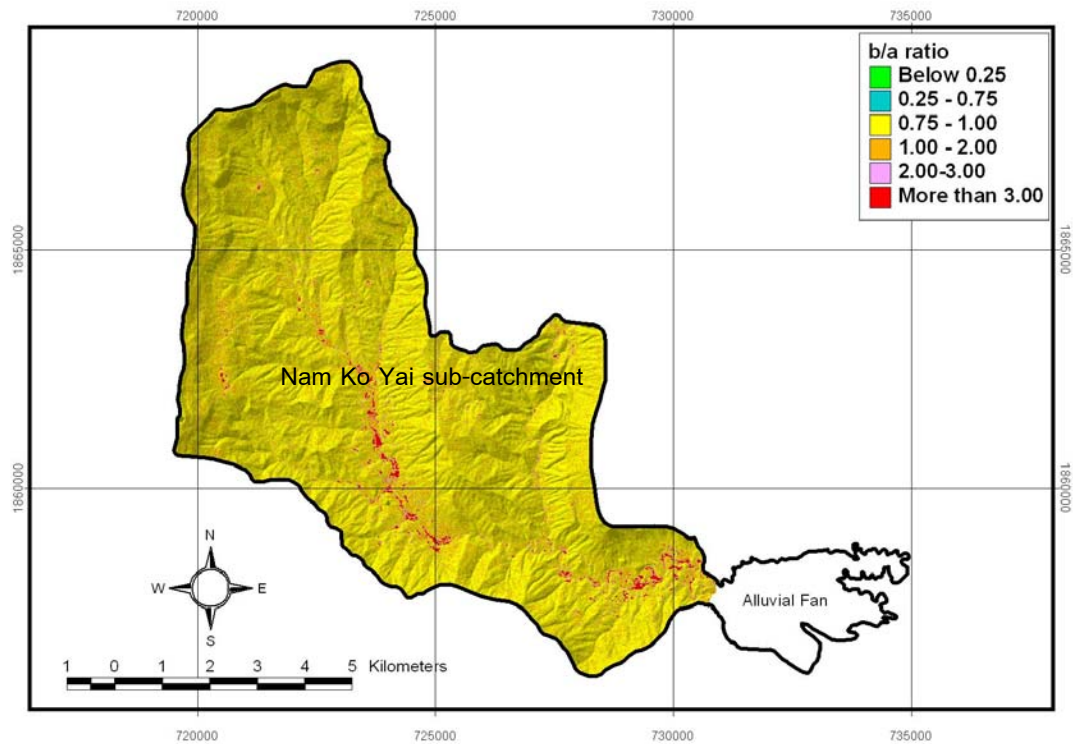


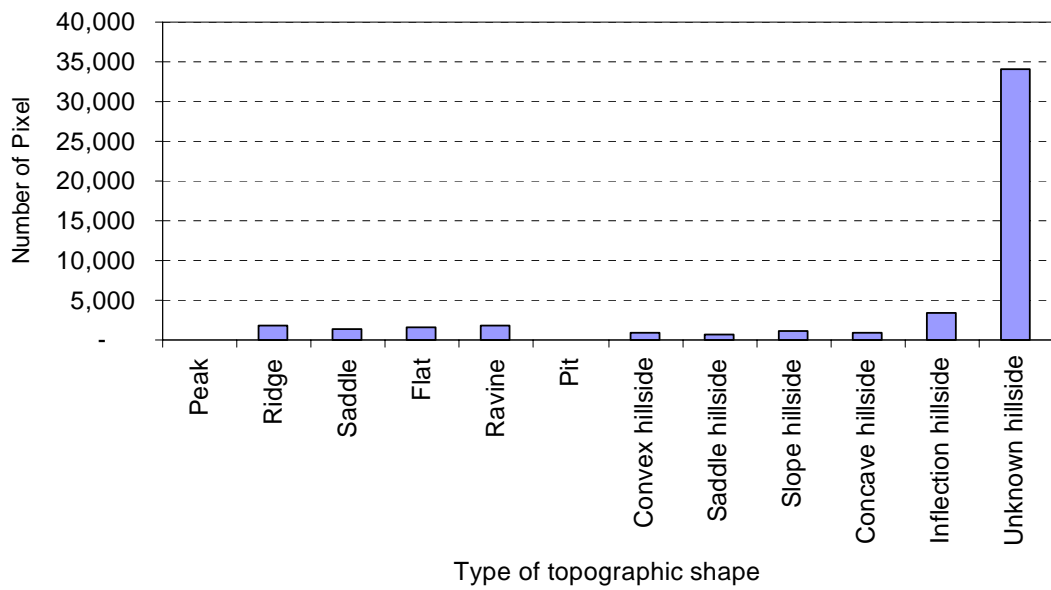
Figure 4-5 Map illustrating b/a ratio as probability of flow-flood susceptibility on landform topography in Nam Ko Yai sub-catchment.

Table 4-3 Relation of flow-flood and landform topography in Nam Ko Yai sub-catchment.

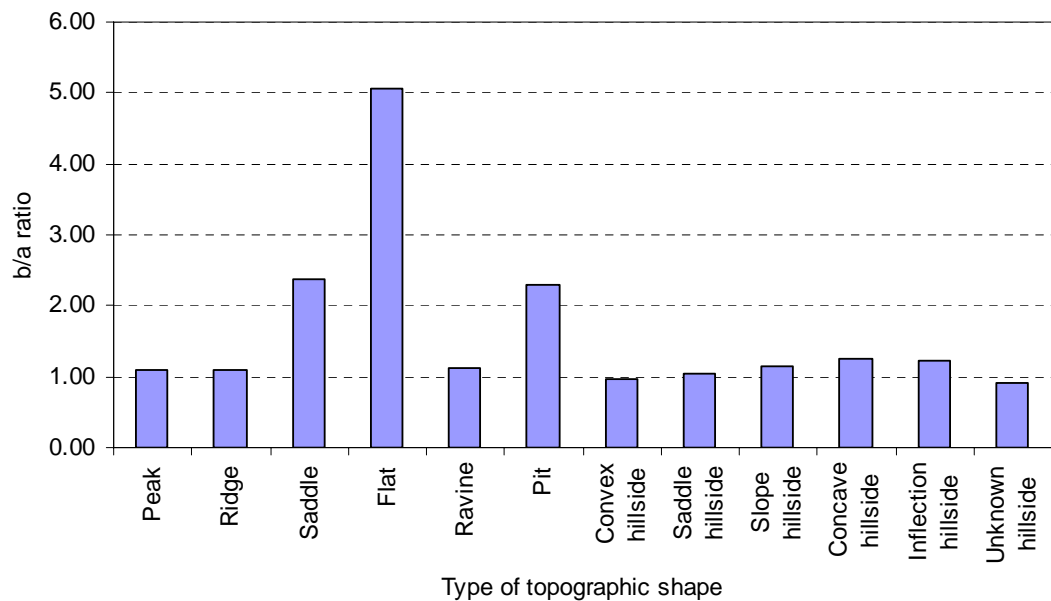
Topography shape	Scar-scouring did not occur		Scar-scouring occur		b/a
	Count	Ratio (%), a	Count	Ratio (%), b	
Peak	767	0.12	63	0.13	1.11
Ridge	23,608	3.67	1,902	3.98	1.08
Saddle	7,126	1.11	1,253	2.62	2.37
Flat	4,500	0.70	1,689	3.54	5.05
Ravine	20,690	3.22	1,731	3.62	1.13
Pit	473	0.07	81	0.17	2.30
Convex hillside	11,581	1.80	826	1.73	0.96
Saddle hillside	8,551	1.33	656	1.37	1.03
Slope hillside	14,091	2.19	1,192	2.50	1.14
Concave hillside	9,236	1.44	867	1.81	1.26
Inflection hillside	37,737	5.87	3,412	7.14	1.22
Unknown hillside	504,375	78.47	34,102	71.38	0.91
Total	642,735	100.00	47,774	100.00	

may be conformed to the attitudes of geological structures (bedding, faults or fracture planes) of potential failure planes. So shear stress in soils or other unattached materials along a potential failure plane in an aspect tends to increase as well.

A moderate probability was observed in east, southeast and south aspect directions that the b/a ratios were 1.82, 1.44 and 1.11, respectively. Whereas a low probability was generally observed in southwest, northeast, north, west and northwest aspect directions that the b/a ratio were 0.84, 0.73, 0.31, 0.30 and 0.22, respectively. So it is concluded that debris flow and debris flood occurrence probability value is lower dependent on the aspect.



a) scar-scoring cell numbers on landform topography



b) b/a ratio on landform topography

Figure 4-6 Histogram distribution of a) scar-scoring number of cells on landform topography, and b) b/a ratio on landform topography in Nam Ko Yai sub-catchment.

It is noted that a very high probability was only observed in flat aspect that the b/a ratio was 4.84. So the flow-flood probability is commonly a high correlation only with the flat area in Nam Ko Yai sub-catchment that especially was in the clear and opened

area along Nam Ko Yai stream channel and its banks as previous mentioned in the relationship between scar-scouring and landform topography. It is also concluded that the aspect is not one of the significant relevant parameters to the flow-flood occurrence and will not be later used to calculate the debris flow-flood susceptibility.

#### 4.2.1.4 Relationship between scar-scouring and geology

Considering the geology of Nam Ko Yai sub-catchment, the frequencies of recent scar-scouring cell number for a given rock unit were analyzed as shown in Figures 4-10, 4-11 and 4-12 and Table 4-5. The probability was noted in the rock units in the sub-catchment from the lower to the upper. For area underlain by Lom Kao Formation (Lk), the b/a ratio was 0.08, indicating a very low probability. For area underlain by Lom Sak Formation (Ls), the b/a ratio was 0.44, indicating a very low probability. For area in Phu Kradung (Pk) the b/a ratio was 2.07, indicating a very high probability. For area in Phra Wihan Formation (Pw), the b/a ratio was 2.77, indicating a very high probability. For area in Phu Phan Formation (Pp), the b/a ratio was 0.17, indicating a very low probability. For area in fluvial deposits (Qa1), the b/a ratio was 2.98, indicating a very high probability.

It was noted in the areas of fluvial deposits (Qa1) consisting of mainly stream deposits, composing of river sands and gravels, silts, clays and gray soils in the middle of the sub-catchment; Phra Wihan Formation (Pw) comprising of gray sandstone, tuffaceous siltstone, and red shale; and Phu Kradung Formation (Pk) composing of red siltstone, conglomeratic sandstone, tuffaceous sandstone and siltstone in western and northern steep-cliff areas, indicating the very high probabilities for the flow-flood occurrence in the most units. The general lithology of low-resistant beds of fluvial deposits (Qa1) and Phu Kradung Formation (Pk), together with other parameters, perhaps play an important role on the flow-flood creation as well.

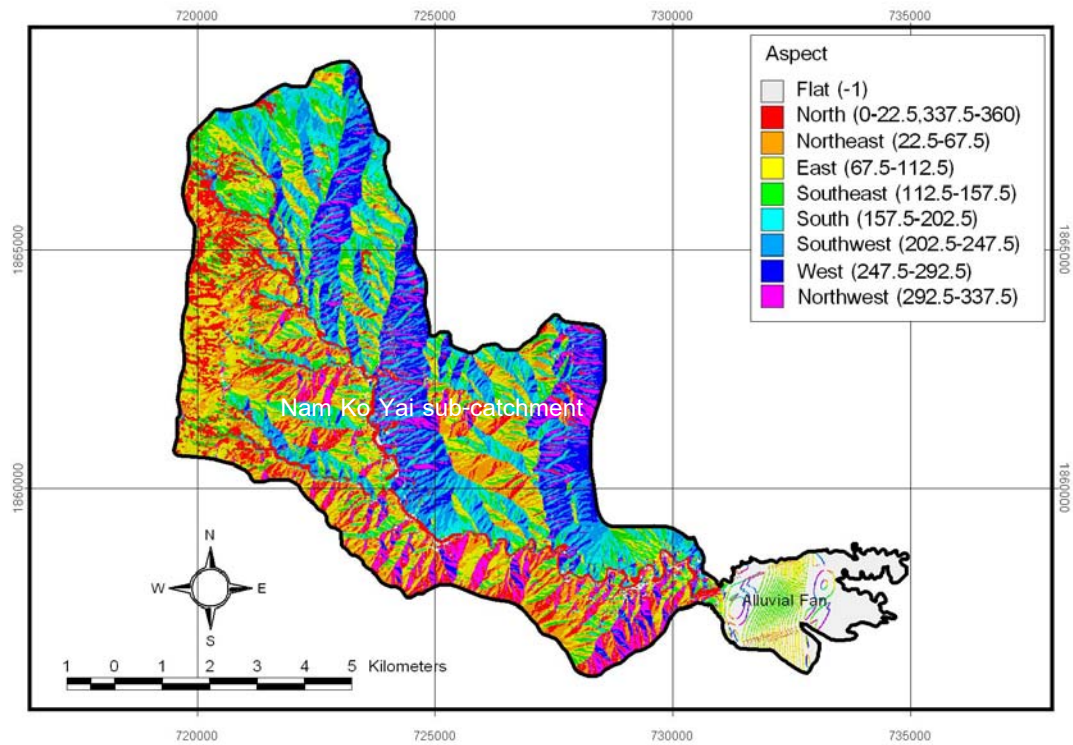


Figure 4-7 Aspect overlay with scar-scouring locations (grouped in red color) in Nam Ko Yai sub-catchment.

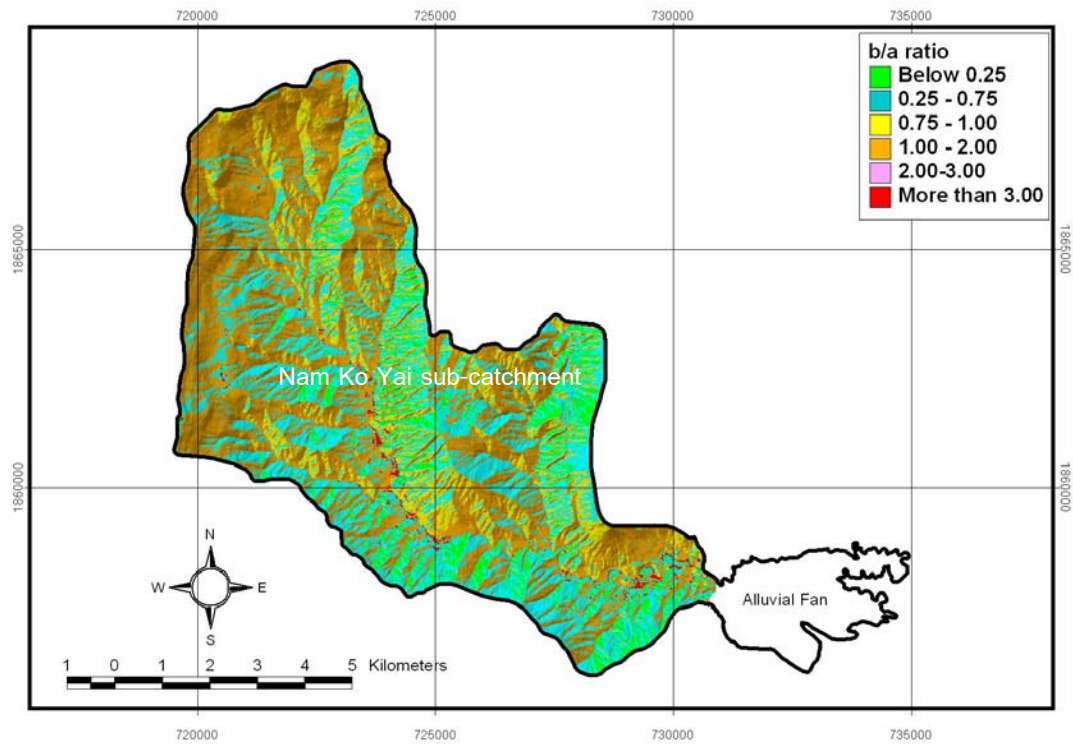
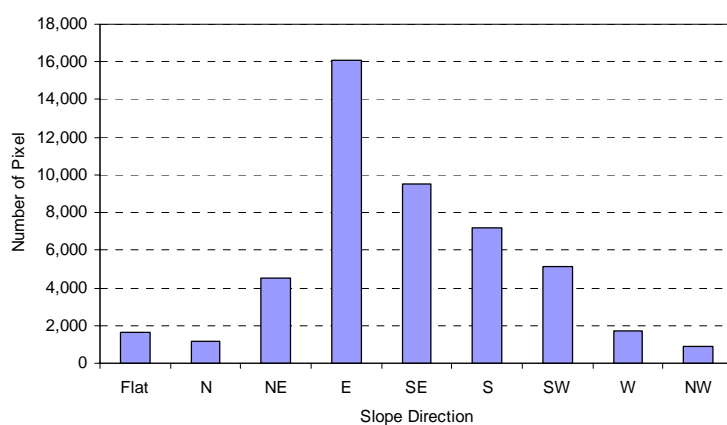


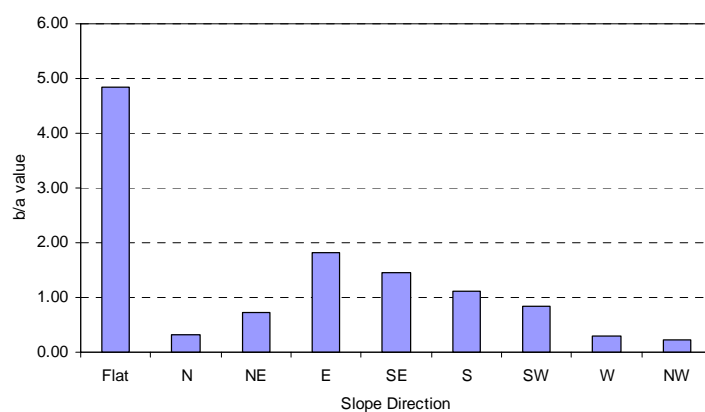
Figure 4-8 Map illustrating b/a ratio as probability of flow-flood susceptibility on aspect in Nam Ko Yai sub-catchment.

Table 4-4 Relation of flow-flood and aspect in Nam Ko Yai sub-catchment.

Aspect direction	Scar-scouring did not occur		Scar-scouring occur		b/a
	Count	Ratio (%) a	Count	Ratio (%) b	
Flat	4,553	0.71	1,639	3.43	4.84
North	51,632	8.03	1,187	2.48	0.31
Northeast	82,971	12.91	4,497	9.41	0.73
East	118,602	18.45	16,073	33.64	1.82
Southeast	88,871	13.83	9,535	19.96	1.44
South	86,917	13.52	7,200	15.07	1.11
Southwest	81,453	12.67	5,103	10.68	0.84
West	74,957	11.66	1,678	3.51	0.30
Northwest	52,779	8.21	862	1.80	0.22
Total	642,735	100.00	47,774	100.00	



a) scar-scoring cell numbers on aspect.



b) b/a ratio on aspect.

Figure 4-9 Histogram distribution of a) scar-scoring number of cells on aspect, and b) b/a ratio on aspect in Nam Ko Yai sub-catchment.

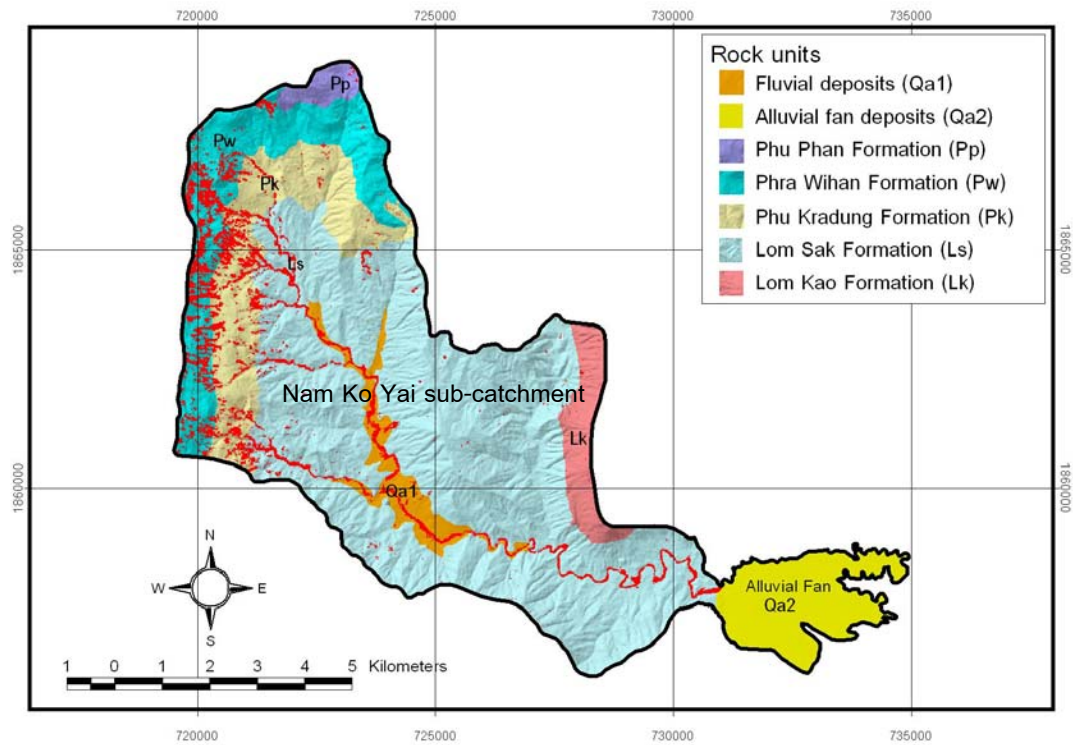


Figure 4-10 Geologic map overlain with scar-scouring locations (grouped in red color) in Nam Ko Yai sub-catchment.

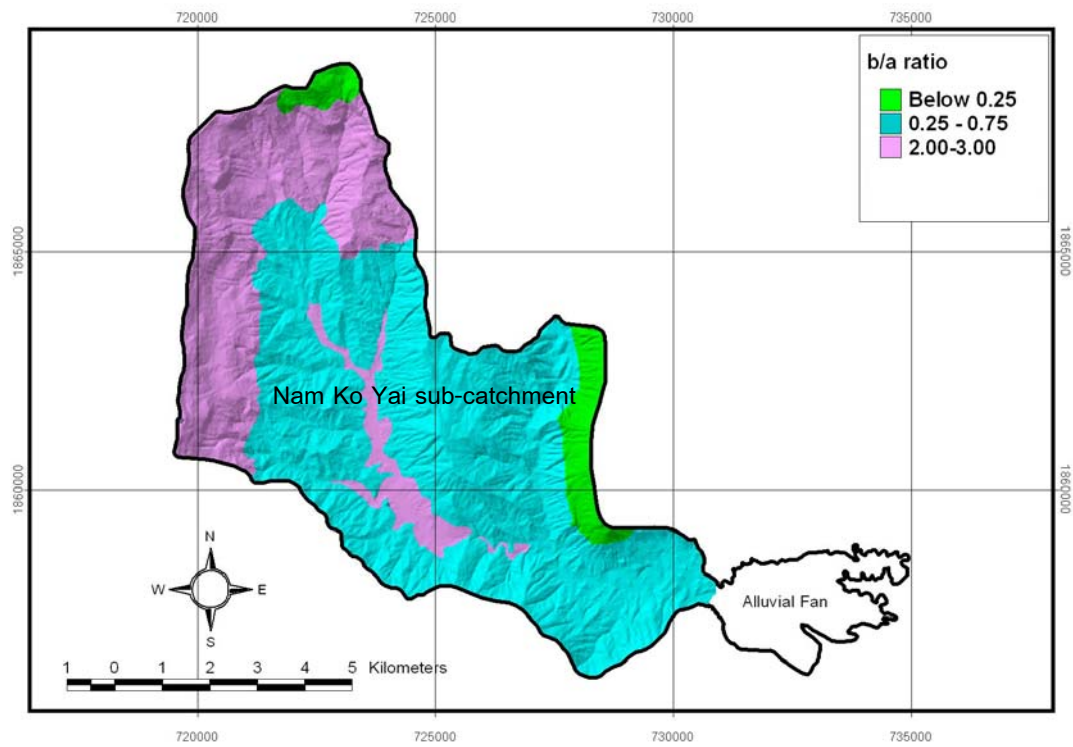


Figure 4-11 Map illustrating b/a ratio as probability of flow-flood susceptibility on geology in Nam Ko Yai sub-catchment.

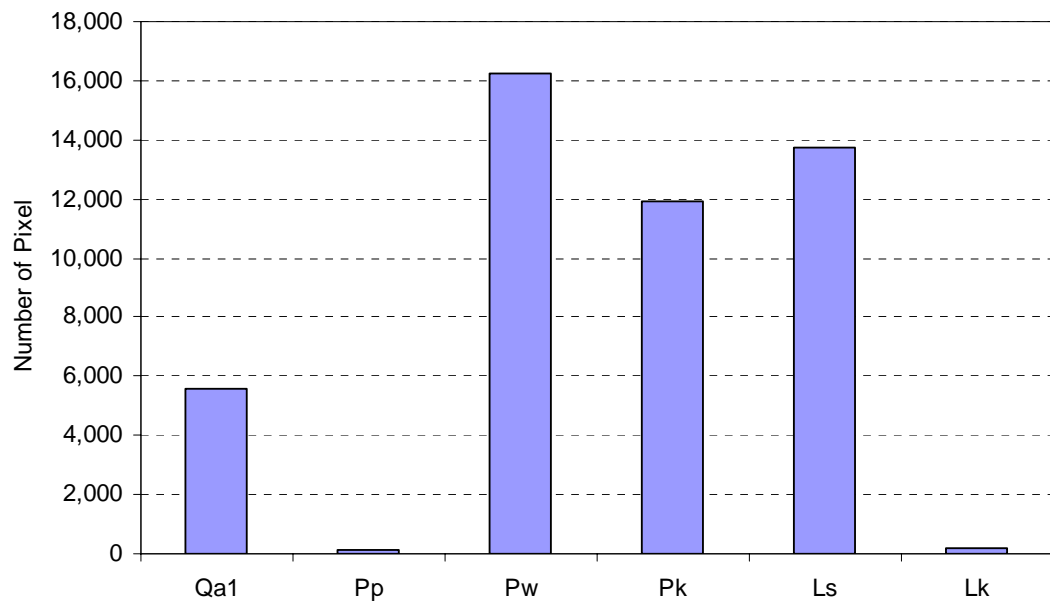
Table 4-5 Relation of flow-flood and geology in Nam Ko Yai sub-catchment.

Rock unit	scar-scouring did not occur		scar-scouring occur		b/a
	Count	Ratio (%) a	Count	Ratio (%) b	
Qa1	25,285	3.93	5,594	11.71	2.98
Pp	10,530	1.64	130	0.27	0.17
Pw	78,827	12.26	16,217	33.95	2.77
Pk	77,320	12.03	11,923	24.96	2.07
Ls	421,652	65.60	13,729	28.74	0.44
Lk	29,121	4.53	181	0.38	0.08
Total	642,735	100.00	47,774	100.00	

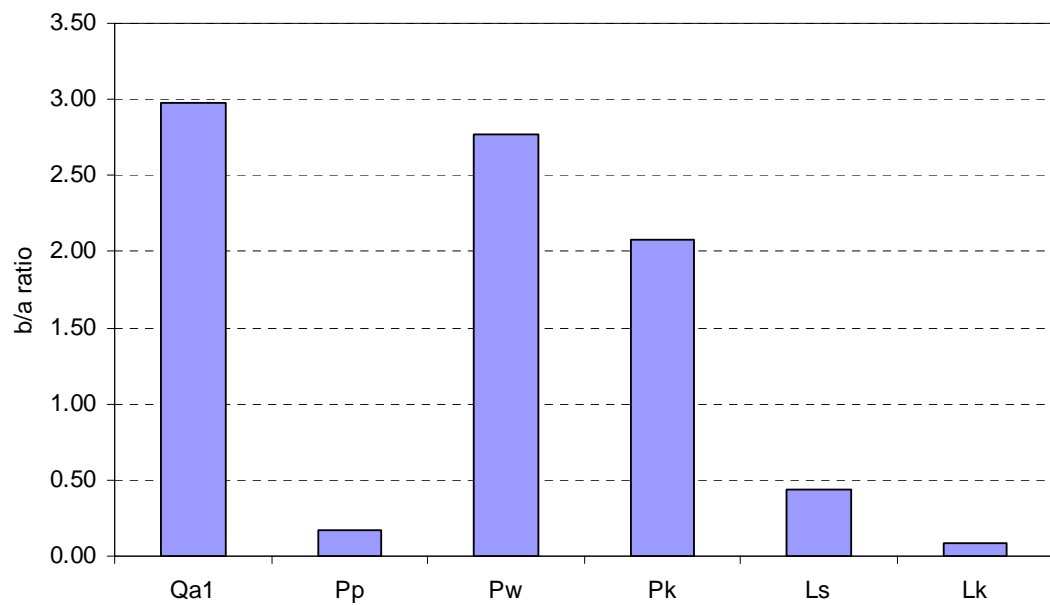
It is noted that the geology is concluded to be ones of the significant relevant parameters in the sub-catchment to the flow-flood occurrence that will be later used to calculate the debris flow-flood susceptibility.

#### 4.2.1.5 Relationship between scar-scouring and soil group unit

In the case of soil group unit in the study area, the frequencies of recent scar-scouring cell number for a given soil group unit were analyzed and presented in Figures 4-13, 4-14 and 4-15 and Table 4-6. For area under soil group unit 29 (that covering a very small area in the sub-catchment), b/a ratio was 3.76, indicating a very high probability. For area under soil group unit 31, b/a ratio was 1.10, indicating a moderate probability. For area under soil group unit 47, ratio was 0.95, indicating a low probability. For area under soil group unit 55, ratio was 1.93, indicating a moderate probability.



a) scar-scoring cell numbers on geology.



b) b/a ratio on geology.

Figure 4-12 Histogram distribution of a) scar-scoring number of cells on geology, and b) b/a ratio on geology in Nam Ko Yai sub-catchment.

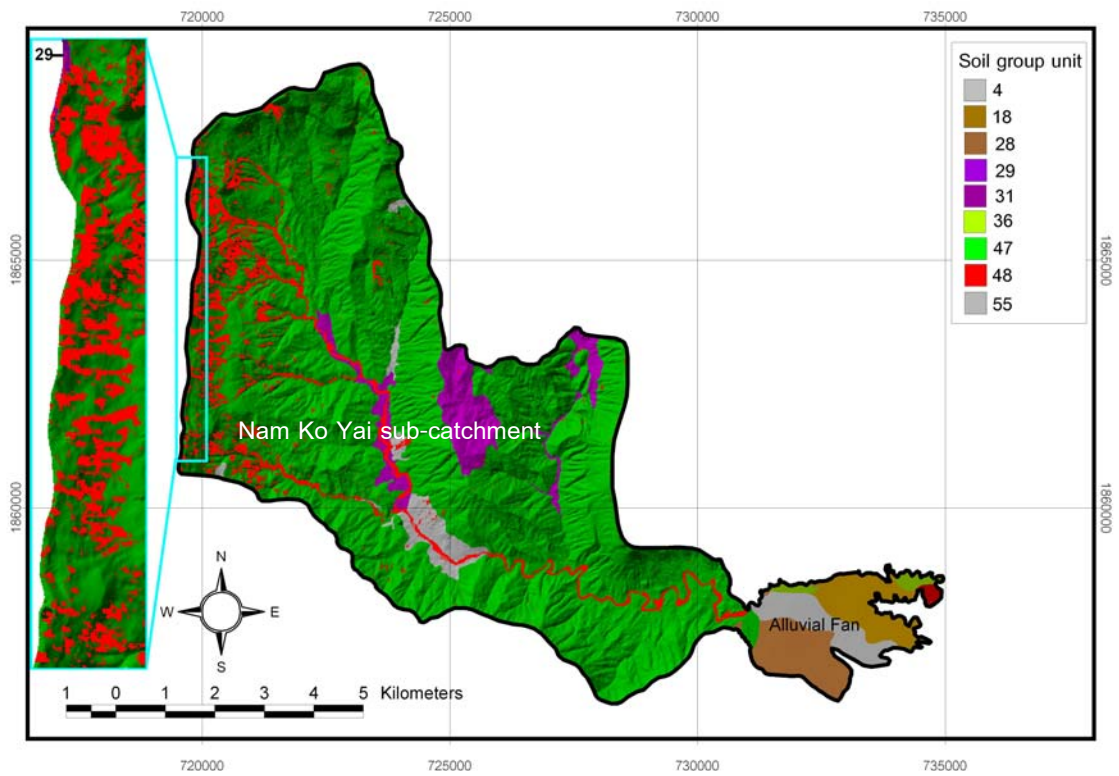


Figure 4-13 Soil group unit map overlain with scar-scouring locations (grouped in red color) in Nam Ko Yai sub-catchment.

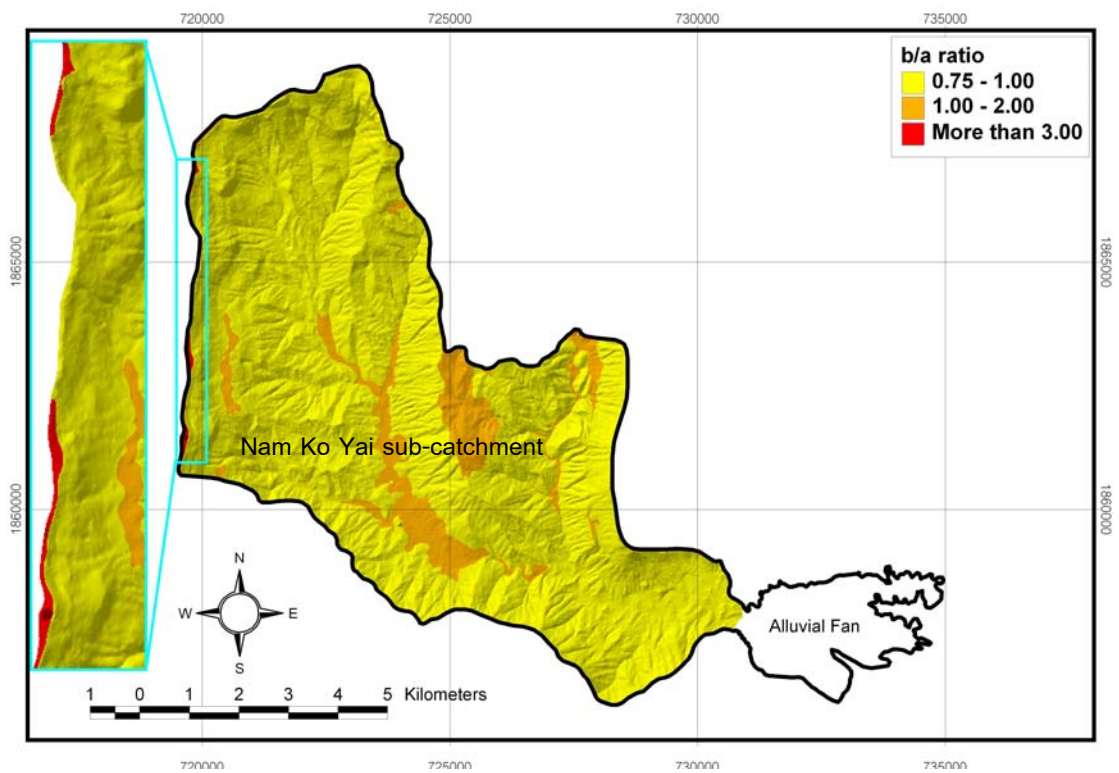
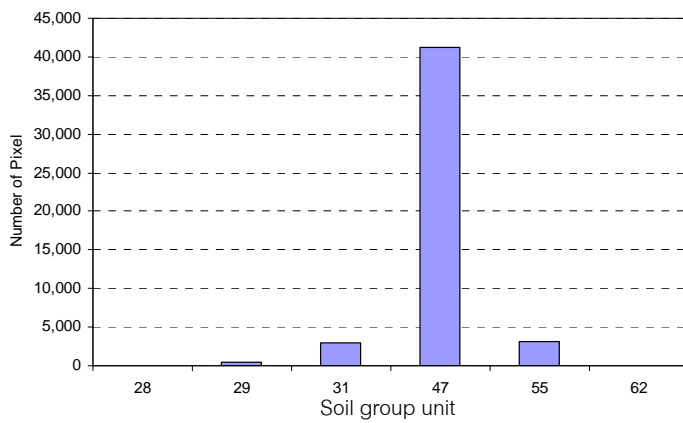


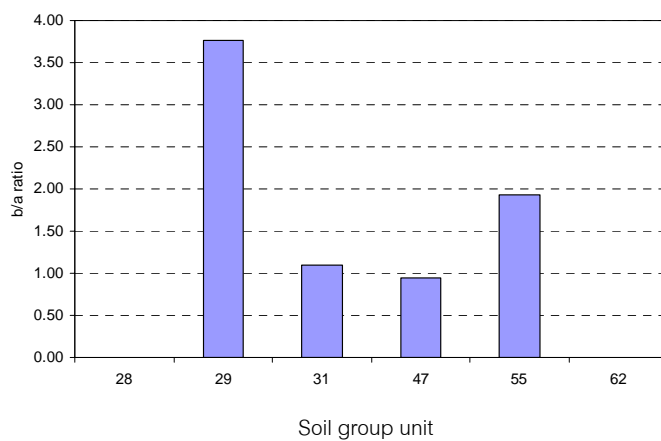
Figure 4-14 Map illustrating b/a ratio as probability of flow-flood susceptibility on soil group unit in Nam Ko Yai sub-catchment.

Table 4-6 Relation of flow-flood and soil group unit in Nam Ko Yai sub-catchment.

Soil major group	scar-scouring did not occur		scar-scouring occur		b/a
	Count	Ratio (%) a	Count	Ratio (%) b	
28	64	0.01	0	0.00	0.00
29	1,857	0.29	519	1.09	3.76
31	35,755	5.56	2,926	6.12	1.10
47	583,306	90.75	41,215	86.27	0.95
55	21,679	3.37	3,114	6.52	1.93
62	74	0.01	0	0.00	0.00
Total	642,735	100.00	47,774	100.00	



a) scar-scoring cell numbers on soil group unit.



b) b/a ratio on soil group unit.

Figure 4-15 Histogram distribution of a) scar-scoring number of cells on soil group unit, and b) b/a ratio on soil group unit in Nam Ko Yai sub-catchment.

It is remarked in the areas of soil group unit 55 and soil group unit 31 in the middle of the sub-catchment, the ratios were 1.93 and 1.10, respectively, generally indicating a moderate probability for the flow-flood occurrence in the most units. So debris flow and debris flood occurrence probability value is lower dependent on the soil group units.

It is remarked that the soil group unit is not one of the significant relevant parameters to the flow-flood occurrence and will not be later used to calculate the debris flow-flood susceptibility.

#### 4.2.1.6 Relationship between scar-scouring and soil thickness

A relationship between the frequencies of scar-scouring cell number and topsoil thickness was attempted with the thickness of less than 50 cm, between 50 and 100 cm, and more than 100 cm (Figures 4-16, 4-17 and 4-18 and Table 4-7). For area which soil thickness was below 50 cm, b/a ratio was 0.95, indicating a low probability. But for the soil thickness between 50-100 cm and more than 100 cm, b/a ratios were 1.93 and 1.23, respectively, indicating a moderate probability. It is found that such relationship is confusing as the frequency was doubtfully high in a small area of 50-100 cm soil-thickness and some further explanation is needed. Perhaps the scar-scouring occurrence was significantly related to the underlying basement rocks or other parameters than just the topsoil thickness alone.

It is also concluded that the soil thickness is not one of the significant relevant parameters to the flow-flood occurrence and will not be later used to calculate the debris flow-flood susceptibility.

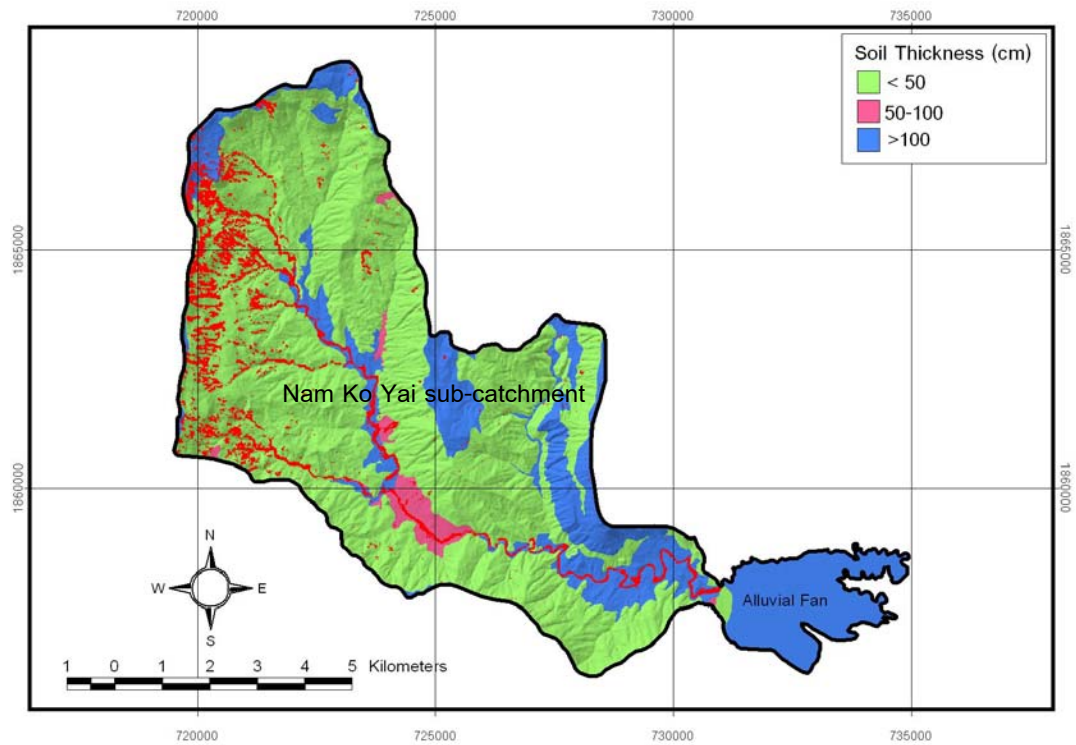


Figure 4-16 Soil thickness map overlain with scar-scouring and depositional locations (grouped in red color) in the study area.

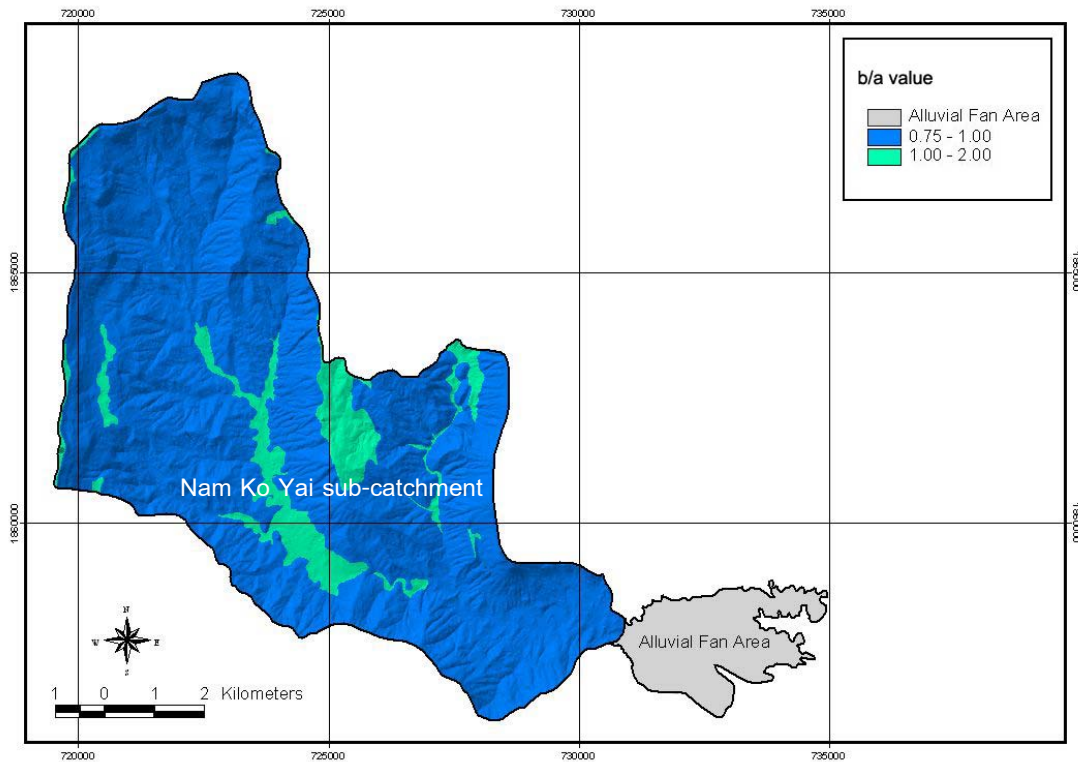
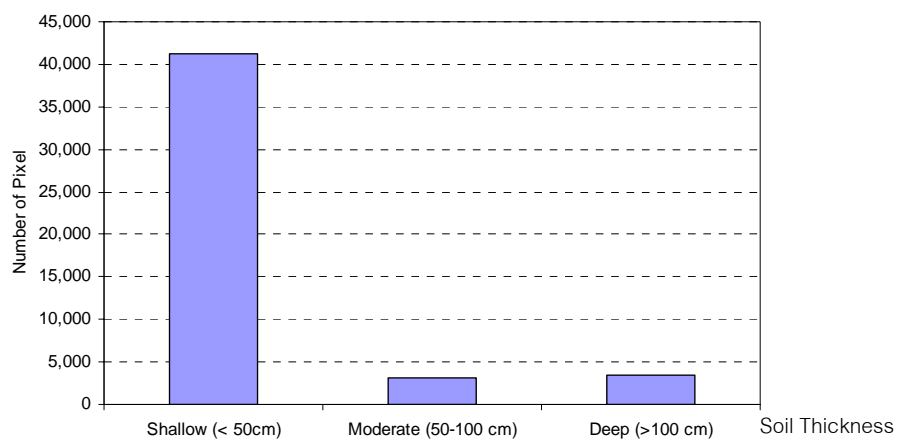


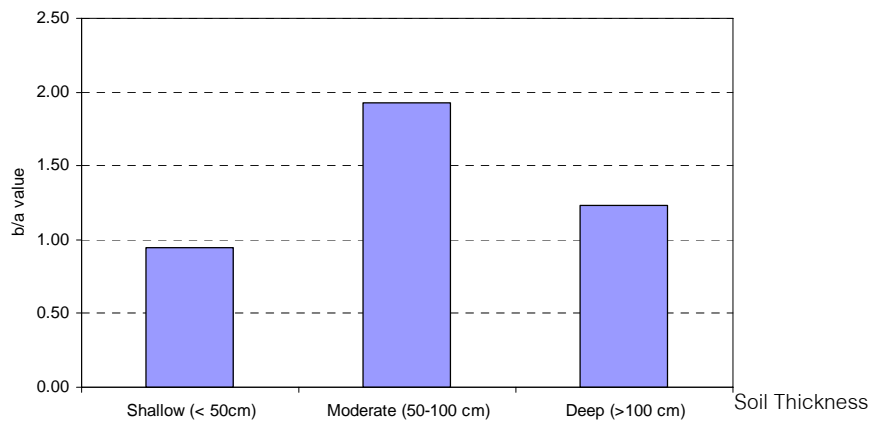
Figure 4-17 Map illustrating  $b/a$  ratio as probability of flow-flood susceptibility on soil thickness in Nam Ko Yai sub-catchment.

Table 4-7 Relation of flow-flood and soil thickness in Nam Ko Yai sub-catchment.

Soil Thickness range	scar-scouring did not occur		scar-scouring occur		b/a
	Count	Ratio (%) a	Count	Ratio (%) b	
Shallow (< 50cm)	583,306	90.76	41,215	86.27	0.95
Moderate (50-100 cm)	21,743	3.38	3,114	6.52	1.93
Deep (>100 cm)	37,612	5.85	3,445	7.21	1.23
Total	642,661	100.00	47,774	100.00	



a) scar-scoring cell numbers on soil thickness.



b) b/a ratio on soil thickness.

Figure 4-18 Histogram distribution of a) scar-scoring number of cells on soil thickness, and b) b/a ratio on soil thickness in Nam Ko Yai sub-catchment.

#### 4.2.1.7 Relationship between scar-scouring and land cover

The frequencies of scar-scouring cell number for a given type of land-cover were also determined (as shown in Figures 4-19, 4-20 and 4-21 and Table 4-8). It was noted that an extremely high probability was observed in the water body area that the b/a ratio was 10.63. A high probability was observed in orchard, paddy field and forest areas that the b/a ratios were 2.69, 2.65 and 1.99, respectively. A moderate probability was generally observed in field crop area that b/a ratio was 1.17. Whereas a very low probability was generally observed in inundated land that b/a ratio was 0.45.

The results in fact reveal an extremely high probability value on the banks just adjacent to the stream course and high in the orchard, paddy field, and forest areas further away, but lower in the cultivate flat areas. This is contrary to a general belief previously mentioned that cultivated lands played a major role in this event. The explanation could be that the flow-flood occurred close to the main stream where there was high energy for erosion and transportation of sediments, and in the orchard, paddy field and forest areas where water could be accumulated and retained to introduce a further more effective process of erosion and transportation.

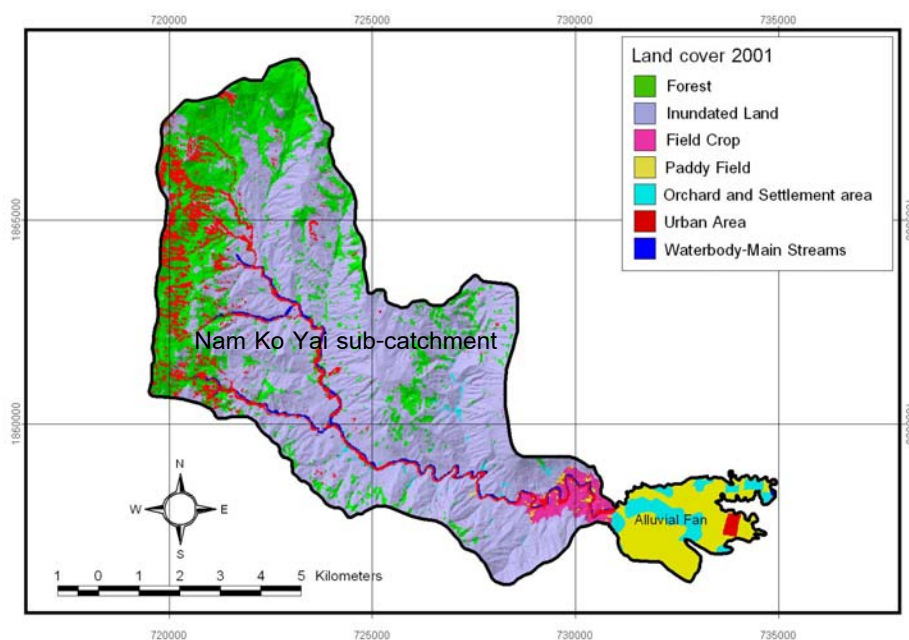


Figure 4-19 Land cover map overlain with scar-scouring locations (grouped in red color) in Nam Ko Yai sub-catchment.

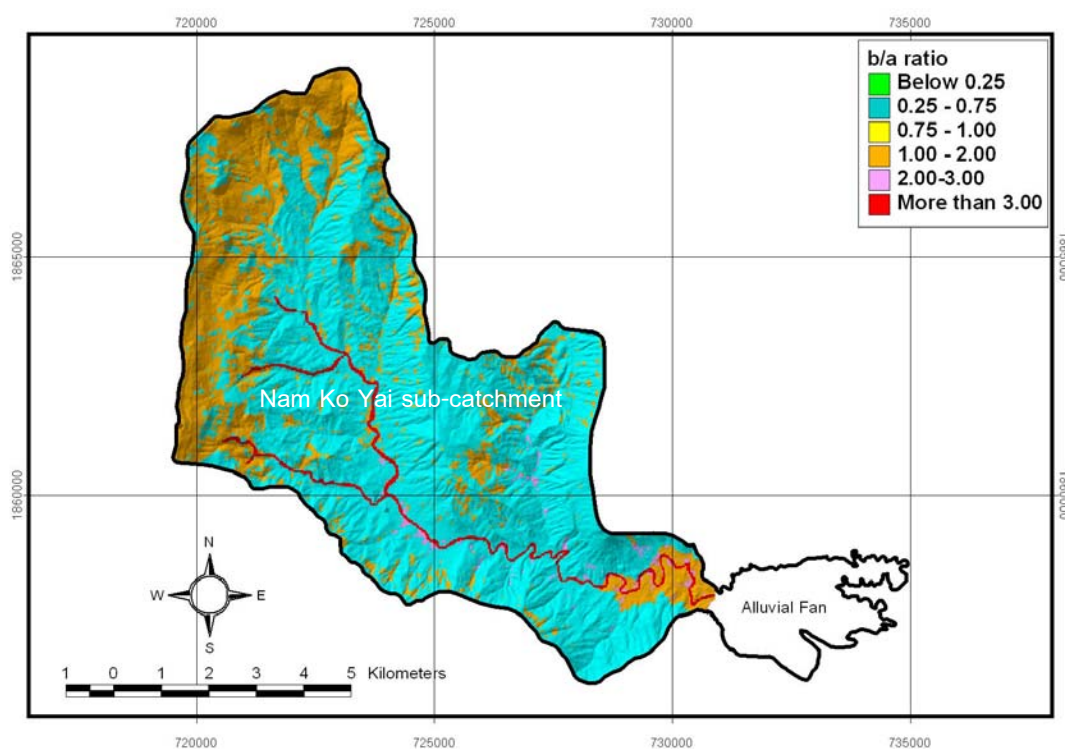
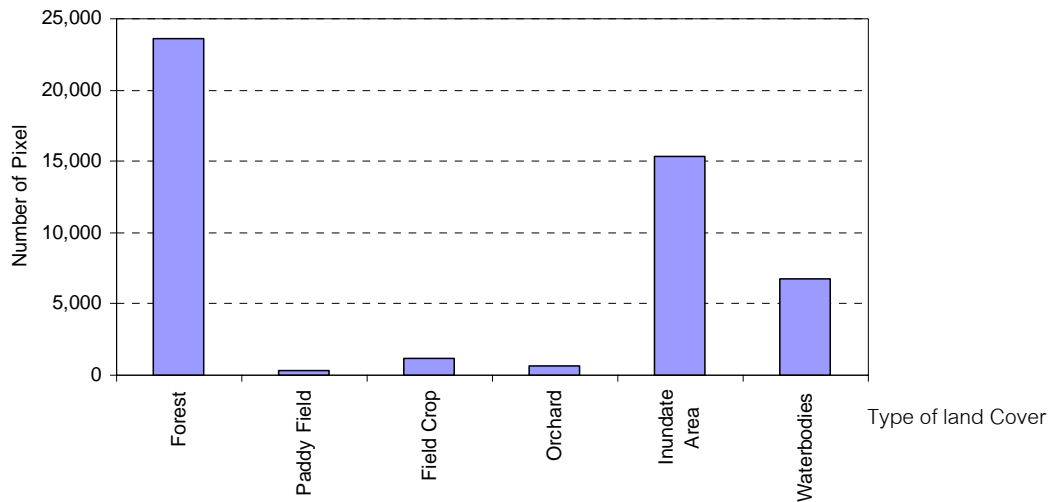


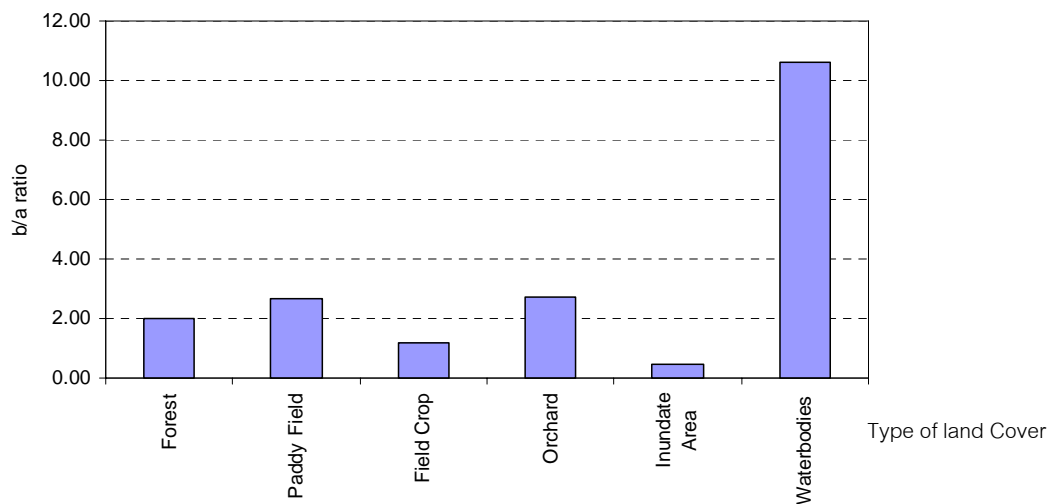
Figure 4-20 Map illustrating b/a ratio as probability of flow-flood susceptibility on land cover in Nam Ko Yai sub-catchment.

Table 4-8 Relation of flow-flood and land cover in Nam Ko Yai sub-catchment.

Land cover type	scar-scouring did not occur		scar-scouring occur		b/a
	Count	Ratio (%), a	Count	Ratio (%), b	
Forest	159,388	24.80	23,572	49.34	1.99
Paddy Field	1,578	0.25	311	0.65	2.65
Field Crop	13,361	2.08	1,165	2.44	1.17
Orchard	3,465	0.54	694	1.45	2.69
Inundated Area	456,432	71.01	15,309	32.04	0.45
Water bodies	8,511	1.32	6,723	14.07	10.63
Total	642,735	100.00	47,774	100.00	



a) scar-scoring cell numbers on land cover.



b) b/a ratio on land cover.

Figure 4-21 Histogram distribution of a) scar-scoring number of cells on land cover, and b) b/a ratio on land cover in Nam Ko Yai sub-catchment.

It is noted that the land cover is concluded to be ones of the significant relevant parameters in the sub-catchment to the flow-flood occurrence that will be later used to calculate the debris flow-flood susceptibility.

#### 4.2.1.8 Relationship between scar-scoring and buffering distance to drainage-line

In the relationship between scar-scoring and buffering distance to drainage-line, the frequencies were determined by counting scar-scoring cell number for the

different range of buffering distance to drainage-line (Figures 4-22, 4-23 and 4-24 and Table 4-9). It is noted that low probabilities were commonly observed in the area which stream proximity was in the ranges of less than 20 m, between 20-30 m, between 30-40 m, between 40-50 m and between 50-60 m, that the b/a ratios were 0.91, 0.89, 0.90, 0.90, and 0.86, respectively. Whereas a moderate probability was generally observed the area which buffering distance to drainage-line was more than 60 m that b/a ratio was 1.18.

The results reveal that flow-flood is generally insignificant relationship with the most of buffering distance to drainage-line range. So stream proximity will not be later used to calculate the debris flow-flood susceptibility.

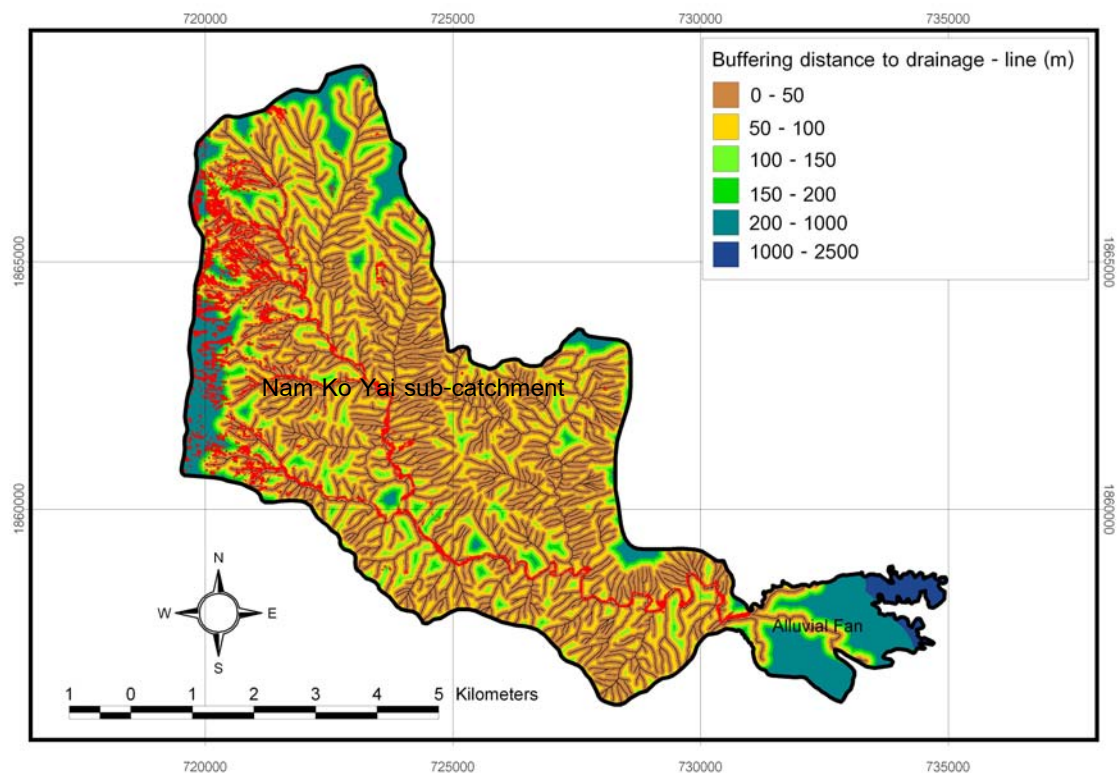


Figure 4-22 Buffering distance to drainage-line map overlain with scar-scouring locations (grouped in red color) in Nam Ko Yai sub-catchment.

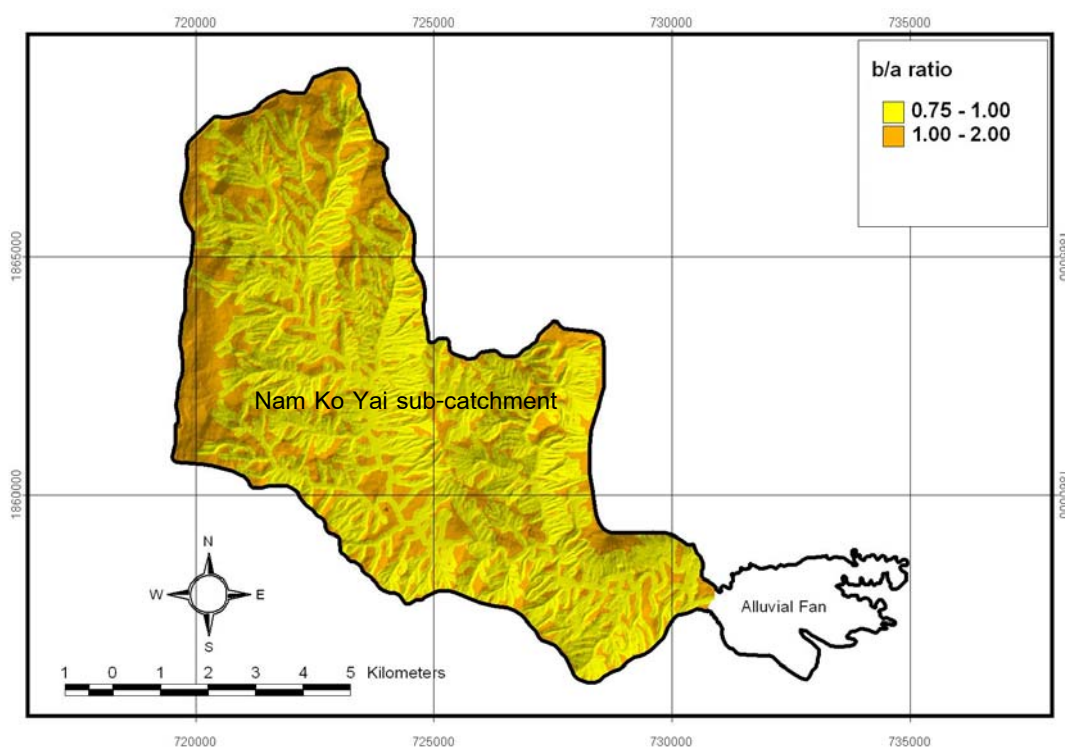
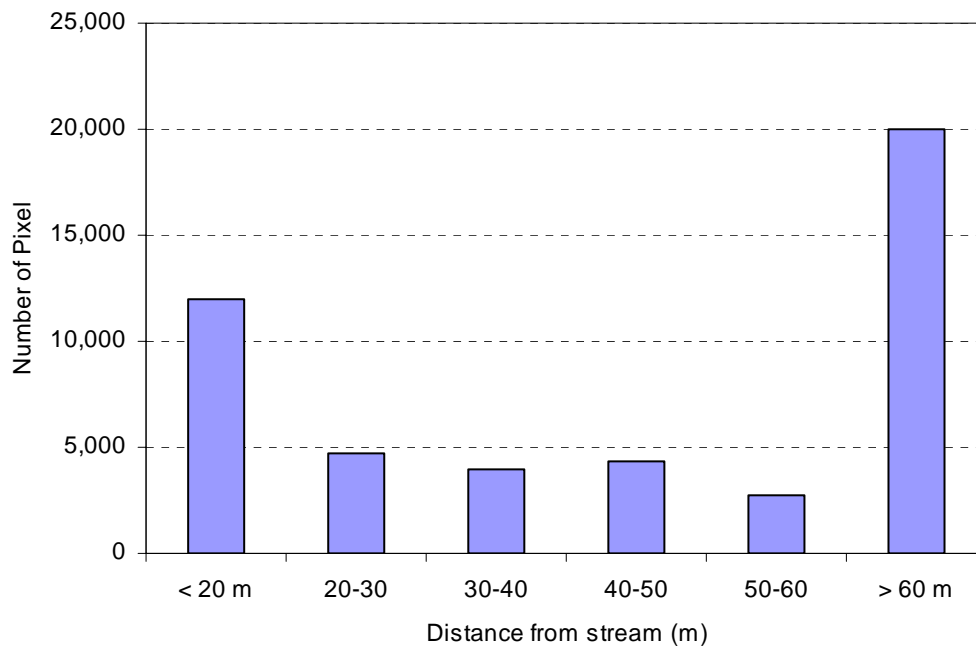


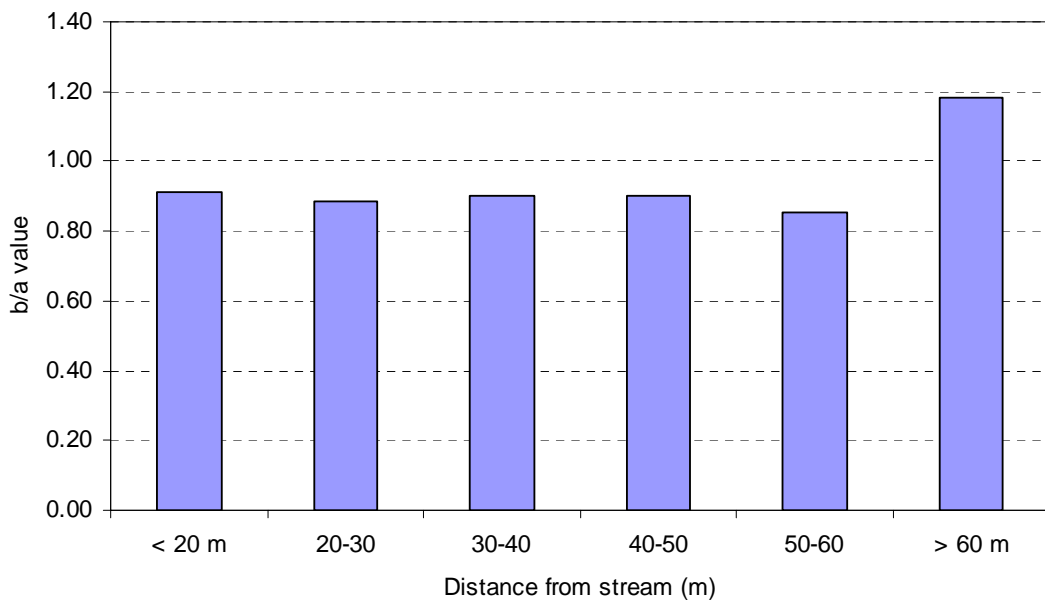
Figure 4-23 Map illustrating b/a ratio as probability of flow-flood susceptibility on buffering distance to drainage-line in Nam Ko Yai sub-catchment.

Table 4-9 Relation of flow-flood and buffering distance to drainage-line in Nam Ko Yai sub-catchment

Stream proximity (m)	scar-scouring did not occur		scar-scouring occur		b/a
	Count	Ratio (%) a	Count	Ratio (%) b	
Less than 20	177,040	27.54	12,024	25.17	0.91
Between 20-30	72,122	11.22	4,749	9.94	0.89
Between 30-40	58,304	9.07	3,918	8.20	0.90
Between 40-50	65,057	10.12	4,347	9.10	0.90
Between 50-60	42,683	6.64	2,713	5.68	0.86
More than 60	227,529	35.40	20,023	41.91	1.18
Total	642,735	100.00	47,774	100.00	



a) scar-scoring cell numbers on buffering distance to drainage-line



b) b/a ratio on buffering distance to drainage-line

Figure 4-24 Histogram distribution of a) scar-scoring number of cells on buffering distance to drainage-line, and b) b/a ratio on buffering distance to drainage-line in Nam Ko Yai sub-catchment.

#### 4.2.2 Calculation of debris flow-flood susceptibility

Using the probability method, the spatial relationships between flow-flood occurrence locations and the significant flow-flood influencing parameters as previously mentioned were derived. It is previously concluded that debris flow and debris flood occurrence probability value is generally much higher dependent on the significant influencing parameters, namely, slope, landform topography, geology, and land cover. Later, these significant influencing parameters were converted to a 10 x 10 m grid for use in the statistical package. In Nam Ko Yai sub-catchment, the total number of cells were 690,509 while the detected scar-scouring number of cells were 47,774. Using GIS software, a grid of 1,292 rows and 1,544 columns, with a point spacing of 10 m was overlain with each geographic coverage for Nam Ko Yai sub-catchment.

The correlation ratios were calculated from relation analysis between the flow-flood and the significant relevant parameters. Therefore the ratio of each parameter's type or range was assigned as the relationship between the flow-flood and each significant parameter's type or range, that is, b/a ratio (ratio between the number of cells where the flow-flood occurred (b) to the number of cells where the flow-flood not occurred (a)) as shown in Tables 4-2, 4-3, 4-5 and 4-8. The flow-flood susceptibility index (FFSI) was calculated by summation of the significant influencing parameter's b/a ratio value weighted to 1 as shown in equation 4-1 below.

$$FFSI = \sum Fr \dots\dots\dots(Equation 4-1)$$

Where: Fr = b/a ratio of each parameter's type or range

The relationship analysis is for the b/a ratio of the area where the flow-flood occurred to the total area. So the value of 1 means an average value. If the value is greater than 1, it means a higher correlation, and lower than 1, lower correlation. The flow-flood susceptibility map was made using the FFSI value index for interpretation, and

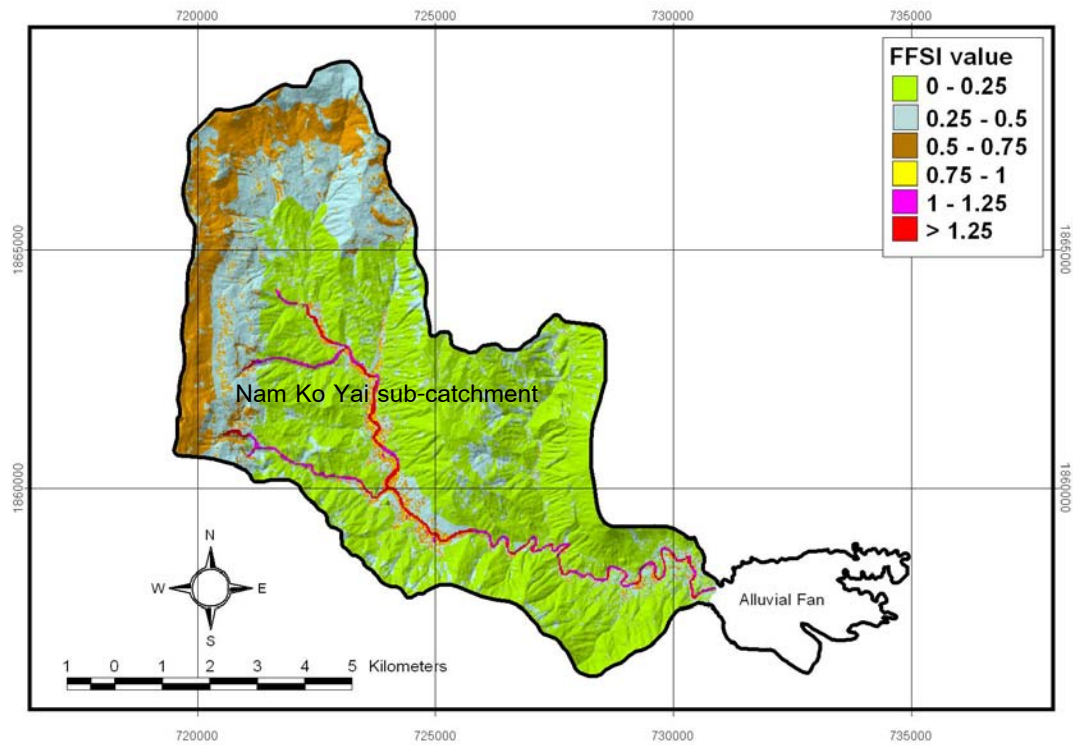


Figure 4-25 Flow-flood susceptibility index (FFSI) of Nam Ko Yai sub-catchment.

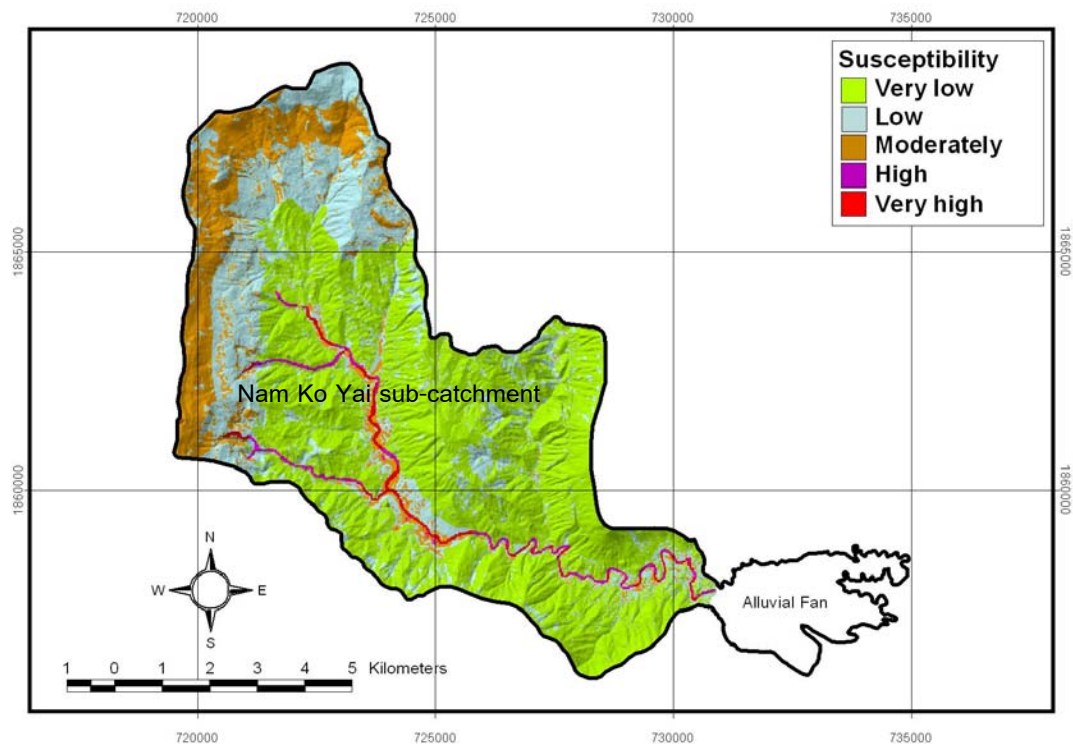


Figure 4-26 Flow-flood susceptibility map illustrating five classes of very high, high, moderate, low, and very low susceptibility in Nam Ko Yai sub-catchment.

was presented in Figure 4-25. The index was further classified by equal areas and grouped into five classes of flow-flood susceptibility map as shown in Figure 4-26. It was remarked that classes of very high-, high-, moderate-, low-, and very low susceptibility, had FFSI value more than 1.25, between 1.00 and 1.25, between 0.50 and 1.00, between 0.25 and 0.50, and less than 0.25, respectively. For Nam Ko Yai sub-catchment of about 69.05 square kilometers, the very high-, low-, moderate-, low-, and very low susceptibility zone cover an area of 0.74, 0.81, 16.73, 18.62 and 32.13 square kilometers, respectively. It is noted that the low- and very low susceptibility zone cover more than 73 % of the total area of Nam Ko Yai sub-catchment.

From the flow-flood susceptibility map of the sub-catchment area as shown in Figure 4-26, it was noted that the very high to very low susceptibility was occurred here. The middle part of Nam Ko Yai stream channel and its adjacent banks had a very high to high flow-flood susceptibility whereas the lower downstream part of the stream had a high flow-flood susceptibility. It was also remarked that the western and northern steep-cliff areas had a low to moderate flow-flood susceptibility whereas the main other parts else of the sub-catchment have in general very low flow-flood susceptibility. The flow-flood susceptibility result was further verified and confirmed by the field investigation of the new evidences and parameters affecting debris flow-flood processes in the following chapter.

## CHAPTER 5

### EVIDENCES AND PARAMETERS AFFECTING DEBRIS FLOW-FLOOD PROCESSES IN NAM KO YAI SUB-CATCHMENT

In this chapter, evidences of geotechnical properties of rocks and soils, as well as evidence of the channel configuration and suspected temporary dam location in Nam Ko Yai sub-catchment are presented.

#### 5.1 Evidences of geotechnical properties of rocks and soils in Nam Ko Yai sub-catchment

For supporting the relationship between the influencing parameters of soil properties and geology, and the flow-flood occurrence in Nam Ko Yai sub-catchment, the detailed field investigation to identify, and collect soil and rock samples for geotechnical analyses had been conducted. The traverse lines of field investigation and sample locations are presented in Figure 5-1. The tabulated data of sample numbers, sample locations, type of samples, rock unit of rock samples, rock grade testing values, and type of laboratory analysis for each sample were summarized in Table 5-1. Some study results and actions are illustrated in Appendix I-III.

The specimens are of two groups, namely, (1) three group-samples of rock units (ten specimens for each group-sample) for a point load testing of the engineering properties (strength), and (2) six soil samples for determining the engineering soil properties. Rock and soil samples were generally collected from the weathered zone of volcanic unit of Lom Sak Formation (Ls). The location photographs were illustrated in Appendix A.

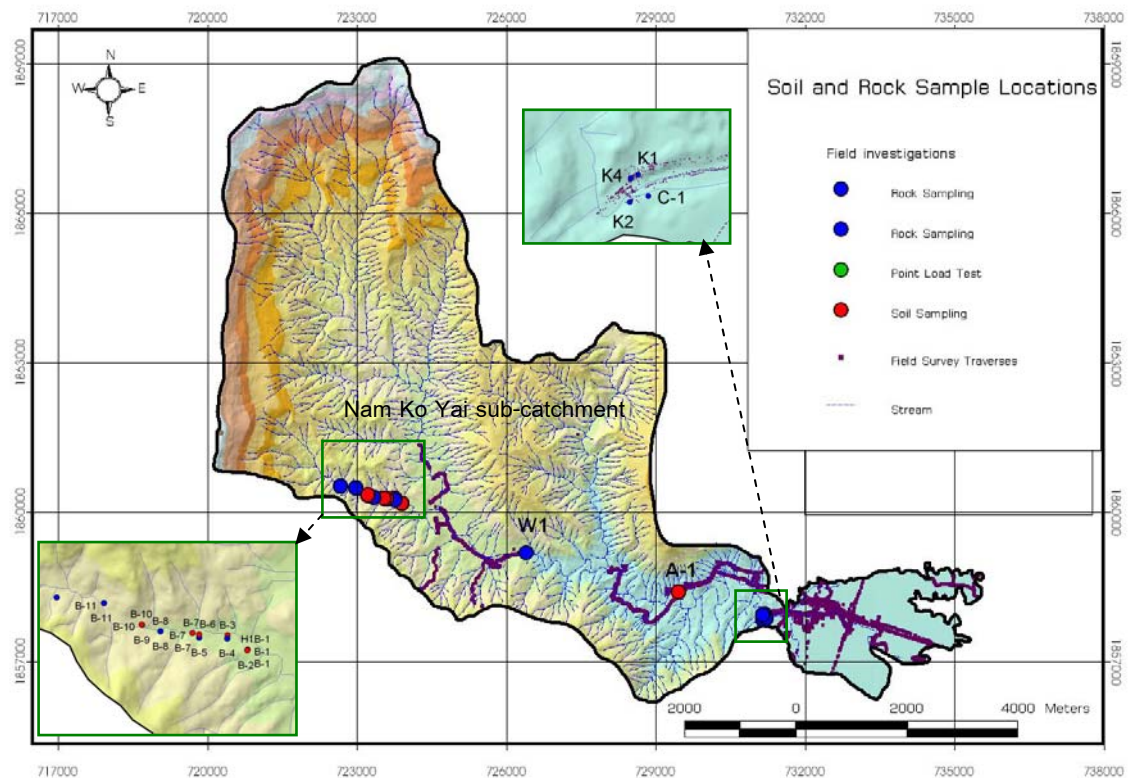


Figure 5-1 Field traverses and sample locations in Nam Ko Yai sub-catchment.

### 5.1.1 Geotechnical study of point load testing

#### 5.1.1.1 Point load testing overview

The point load testing (PLT) is a generally-accepted rock mechanics testing procedure used for verifying a rock strength index in geotechnical practice. The index can be further used to estimate other rock strength parameters. The point load test apparatus and procedure enables an economical testing of core or lump rock samples in a field or laboratory setting. The rock specimens used for the test can be in either geometric regular or irregular shape. This test is to present a data analysis to be used to correlate the point load strength index ( $I_s$ ) with the uniaxial compressive strength ( $\sigma_c$ ). The rock strength determined by the point load testing certainly is an indication of an intact rock strength of the rock samples which of course is not necessarily the strength of the entire rock mass.

Table 5-1 The referenced data of sample numbers, sample locations, type of samples, rock unit of rock samples, rock grade testing values, and type of laboratorial analysis for each sample in the study area.

Specimen number	Location		Sample Type	Rock Unit	Rock Grade Testing Value	Samples Collected for	
						Point Load Test	Soil Test
A-1	Q47 0728840	1858259UTM	Soil	-	-	-	6L
B-1	Q47 0723292	1860034UTM	Rock (Volcanic Complex)	Ls	(H) 5R	(Floated Rock) 10-01Pw	-
						(Floated Rock) 12-01Pk	
						(Floated Rock) 10-01Ls	
B-2	Q47 0723290	1860028UTM	Soil	-	-	-	1L
B-3	Q47 0723164	1860126 UTM	Soil	-	-	-	2L
B-4	Q47 0723160	1860105UTM	Rock (Volcanic Complex)	Ls	4R	-	-
B-5	Q47 0722980	1860110UTM	Rock (Volcanic Complex)	Ls	4R	-	-
B-6	Q47 0722980	1860132UTM	Soil	-	-	-	3L
B-7	Q47 0722937	1860140UTM	Soil	-	-	-	4L
B-8	Q47 0722730	1860152 UTM	Rock (Volcanic Complex)	Ls	3R	-	-
B-9	Q47 0722610	1860192UTM	Rock (Volcanic Complex)	Ls	3R	-	-
B-10	Q47 0722609	1860196UTM	Soil	-	-	-	5L
B-11	Q47 0722364	1860335UTM	Rock (Volcanic Complex)	Ls	3R	-	-
B-12	Q47 0722058	1860371UTM	Rock (c ComplexVolcani)	Ls	5R	-	-
C-1	Q47 0730574	1857811UTM	Rock (Volcanic Complex)	Ls	(L) 5R	-	-
C-2	Q47 0730543	1857709UTM	Rock (Volcanic Complex)	Ls	1R	-	-
C-3	Q47 0730612	1857733UTM	Rock (Volcanic Complex)	Ls	2R	-	-
C-4	Q47 0730547	1857799UTM	Rock (ic ComplexVolcan)	Ls	1R	-	-

Note - All codes are referred to accordingly in the appropriate parts in the text.

The point load tester consists of a hydraulically powered ram and two pointed-platens. One of the platens is stationary while the other is free to move through the application of pressure, delivered via the hydraulically powered ram. The rock specimen to be tested is placed between the two pointed platens and force applied to the rock is increased and eventually caused the rock to fail. The peak pressure applied or the pressure at the rock failure is recorded. This peak applied load is used to calculate the point load strength index ( $I_s$ ), using the equation ASTM D5731-95 and ISRM below.

$$I_s = P/D_e^2 \quad \dots\dots\dots \text{(Equation 5-1)}$$

Where

$P$  = highest force recorded by the instrument to just break the rock

$D_e$  = equivalent diameter (of sample)

The force recorded by the instrument to just break the rock ( $P$ ) is converted to a strength value, equivalent to a 50 mm diameter rock. This produces the so-called  $I_{s(50)}$  value or Size-Corrected Point Load Index. The equation to convert the force reading to  $I_{s(50)}$  value is as follows: (Brook, 1985)

$$I_{s(50)} = FP / (D_e)^2 \quad \dots\dots\dots \text{(Equation 5-2)}$$

Where

$F$  = size correction factor =  $(D_e/50)^{0.45}$

$P$  = applied load (MN)

$D_e = (4A/p)^{0.5}$

$A$  = minimum cross sectional area of the specimen ( $\text{mm}^2$ )

The unit of point load index is MPa. Though the test is considered to cause a tensile failure, this could be converted to compressive strength ( $\sigma_c$ ) by the equation below.

$$(\sigma_c) = 24 I_{s(50)} \dots\dots\dots \text{(Equation 5-3)}$$

### 5.1.1.2 Rock specimen sampling

In this study, the rock specimens were collected from the location B1 (the locations shown in Figure 5.1 and photographs in Appendix I). They were from three rock units below.

- 1) Ten specimens of Phra Wihan sandstone/siltstone (rock unit Pw)
- 2) Twelve specimens of Phu Kradung sandstone (rock unit Pk)
- 3) Ten specimens of Lom Sak volcanic complex (rock unit Ls).

### 5.1.1.3 Point load testing results

The results of point load testing of three groups of rock units are concluded in Table 5-2. Photographs illustrating the rock samples, before and after the test, technique, and results of point load testing in the laboratory were also illustrated in Appendix II.

It was noted that  $I_{s(50)}$  of Pw unit is 1.74 - 3.18 MPa, average 2.66 MPa while  $\sigma_c$  is 41.8 – 76.2 MPa, average 63.9 MPa.  $I_{s(50)}$  of Pk unit is 1.03 – 3.11 MPa, average 2.04 MPa while  $\sigma_c$  is 24.8 – 74.8 MPa, average 49.0 MPa.  $I_{s(50)}$  of Ls unit is 2.76 – 6.65 MPa, average 4.80 MPa while  $\sigma_c$  is 66.3 – 159.6 MPa, average 115.2 MPa. The study results reveal that the volcanic rocks of Ls is the strongest while the Pk sandstone the weakest among the 3 groups. The Pw sandstone has an intermediate  $\sigma_c$  value, though not much higher than that of the Pk specimens.

## 5.1.2 Geotechnical study of soil properties

### 5.1.2.1 Soil sampling preparation

Six soil specimens (number A-1, B-2, B-3, B-6, B-7 and B-10 as shown in Figure 5-2 and Appendix I) were collected from the natural soil layer (1-2 meter thick) that were the weathered products of volcanic rocks (mainly basalt) of Lom Sak Formation (Ls). The

soil samples were collected in a way to avoid the top soils and were of about 0.5 m deep laterally from the outer soil surface to retain the natural moisture content. The collected soil samples were well-packed in plastic bags for further study in the laboratory.

#### 5.1.2.2 Laboratorial study of soil properties

The six soil samples were collected for the laboratorial geotechnical studies which include grain size analysis, determination of Atterberg limits and indices, natural moisture content, and shear strength according to the standard of ASTM (ASTM D 4318-00, D 422-63). Photographs illustrating laboratorial instruments and samples for soil-geotechnical testing are illustrated in Appendix III.

#### 5.1.2.3 Study results of soil geotechnical properties

The analytical results of the soil samples geotechnical properties were summarized in Table 5-3. The soil sample number B-2, B-3, B-6 and B-7 are clay whereas number B-10 and A-1 are clayey sand. Natural water content ( $w_N$ ) in these samples are generally between 21 - 50 %, with plastic limit and liquid limit of soil between 17- 31 and 24 – 55 %, respectively. Plastic index varies from 6 to 26 %.

It was noted that the grain sizes smaller than 0.075 mm (Mesh no.200) were especially of a high content, more than 50 percents of total soil weight. This property is different from the other normal soils that were weathered from the quartz-contained rocks that generally had the grain sizes smaller than 0.075 mm (Mesh no.200) being less than 50 percent of total soil weight. The uniformity coefficient ( $C_u = D_{60}/D_{10}$ ) as  $C_u < 5$  - very uniform,  $C_u = 5$  medium uniform,  $C_u > 5$  – non-uniform, of these six soil samples is higher than 5 indicating a non-uniform characteristic of soil grain size.

It is summarized here that all specimens are non-uniform clay to clayey sand, with natural water content of 21-50 %, and with plastic limit and liquid limit between 17- 31 and 24-55 %, respectively. The clayey soils illustrated a low permeability value of

about  $10^{-2}$  to  $10^{-7}$  m/sec. This indicates that the natural moisture could hardly be drained out of the soils in many cases, which naturally staying close to the liquid limit. If the soils receive more water, their weight increases while the shear strength decreases, thus the soils would be liquefied and easily be liquefied. These soils had varied shear strength values from about 10-100 kPa. Ls Formation soils, however, shear strength values lower than other common soils and thus are highly movable.

Table 5-2 Analytical results of soil engineering properties of the soil samples.

Sample No.	Location	Percent Finer #200 (% clay and silt)	Natural Water Content, % $w_N$	Plastic Limit, % $w_p$	Liquid Limit, % $w_L$	Plastic Index, % $PI = w_L - w_p$	Activity, % $A = PI/\%Clay$	Liquidity Index, % $LI = (w_N - w_p)/PI$	$C_u$	Soil Type			Shear Strength (kPa)
										1*	2*	3*	
B-2	47 Q 0723290/ UTM 1860028	67.6	27.0	20.8	40.5	19.7	0.76	0.31	>5	Clay	CL	A-7-6 (Clayey soils)	40
B-3	47 Q 0723164/ UTM 1860126	87.1	44.9	29.2	54.6	25.4	0.53	0.62	>5	Clay	CH	A-7-6 (Clayey soils)	10
B-6	47 Q 0722980/ UTM 1860132	87.4	33.8	30.6	54.9	24.2	0.53	0.13	>5	Clay	CH	A-7-6 (Clayey soils)	93
B-7	47 Q 0722937/ UTM 1860140	77.3	34.4	25.4	45.6	20.2	0.67	0.44	>5	Clay	CL	A-7-6 (Clayey soils)	22
B-10	47 Q 0722609/ UTM 1860196	62.0	26.7	24.7	38.4	13.7	0.62	0.15	>5	Clay sand	CL	A-6 (Clayey soils)	87
A-1	47 Q 0728840/ UTM 1858259	38.1	21.8	17.4	24.20	6.8	0.31	0.65	>5	Clay sand	ML	A-4 (Silty soil)	9

Note:

1\*. Classification of the Mississippi River Commission

2\*. Classification of Unified Soil Classification System

CL – inorganic clays of low to medium plasticity, gravelly clay, sandy clays, silty clays, lean clays.

CH – inorganic clays of high plasticity, fat clays

ML – inorganic silts and very fine sands, rock flour, silty or clayey fine sands with slight plasticity.

3\*. Classification by AASHTO Soil Classification System

## 5.2 Evidences of a suspected temporary landslide dam location and channel configurations in the central part of Nam Ko Yai sub-catchment

### 5.2.1 Evidences of a temporary landslide dam location

It was always suspiciously how the settlement on the alluvial fan was flooded with muddy water and high quantity of plant debris. One theory was that there could have been a natural landslide dam forming somewhere along the water course, followed by the failure of the dam to have the temporary impound water with debris to flow in a huge amount down below. If this theory was possible, there should be evidences of such dam somewhere upstream from the flooded village.

From the field investigations and orthophotograph interpretation, there was a specific location along the course of Nam Ko Yai stream in the central part of the study area that was looked suspiciously. Here the stream issues from a flat open land behind (upstream) to a very narrow V-shape channel with a sudden change of elevation at Tad Fa waterfall (Figure 5-2). It could be hypothesized that this specific location is suitable for an accumulation of sediments composed of plant debris, soils, and rock boulders to form a natural landslide dam of at least 10 m high (Figures 5-3, 5-4 and 5-5). A field check revealed fallen trees and vegetation traces. This probably indicated that the temporary natural dam was broken, sending the debris and water to flood further downstream, eroding the channel along the way, and finally dropping its loads on the alluvial fan at the canyon mouth.

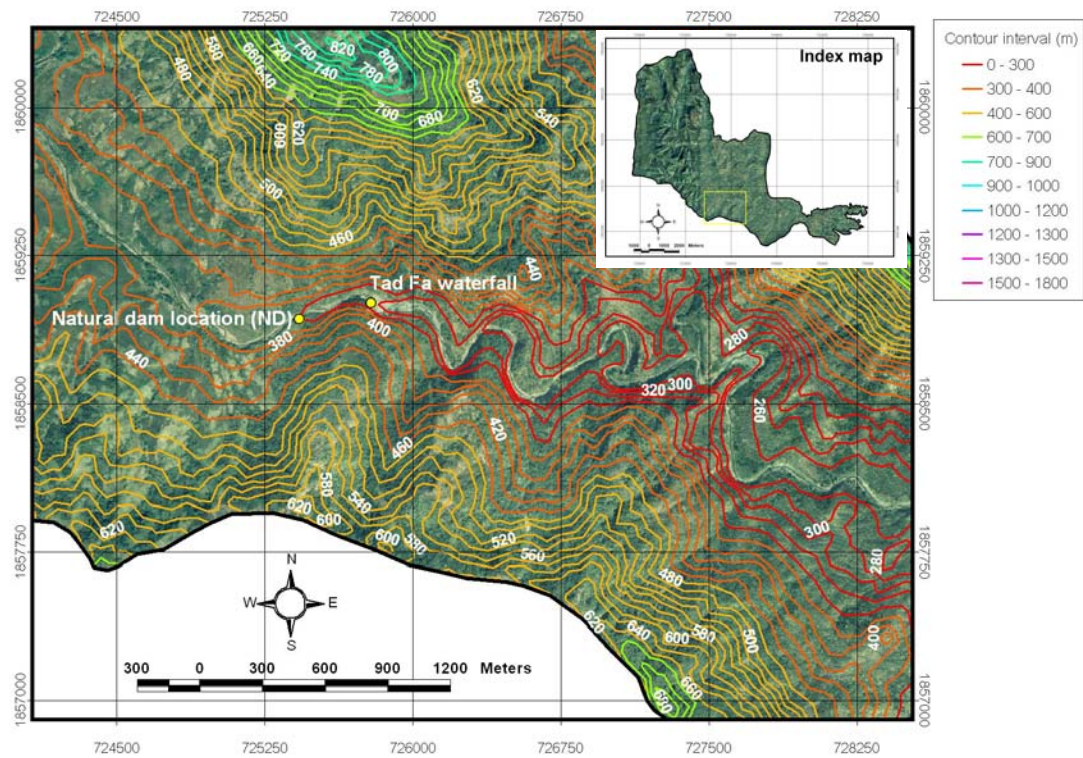


Figure 5-2 Orthophotograph (1:25,000 scale, 9<sup>th</sup> January 2002 after the 8/11 event) illustrating the specific configuration of Nam Ko Yai stream in the central part of the study area.

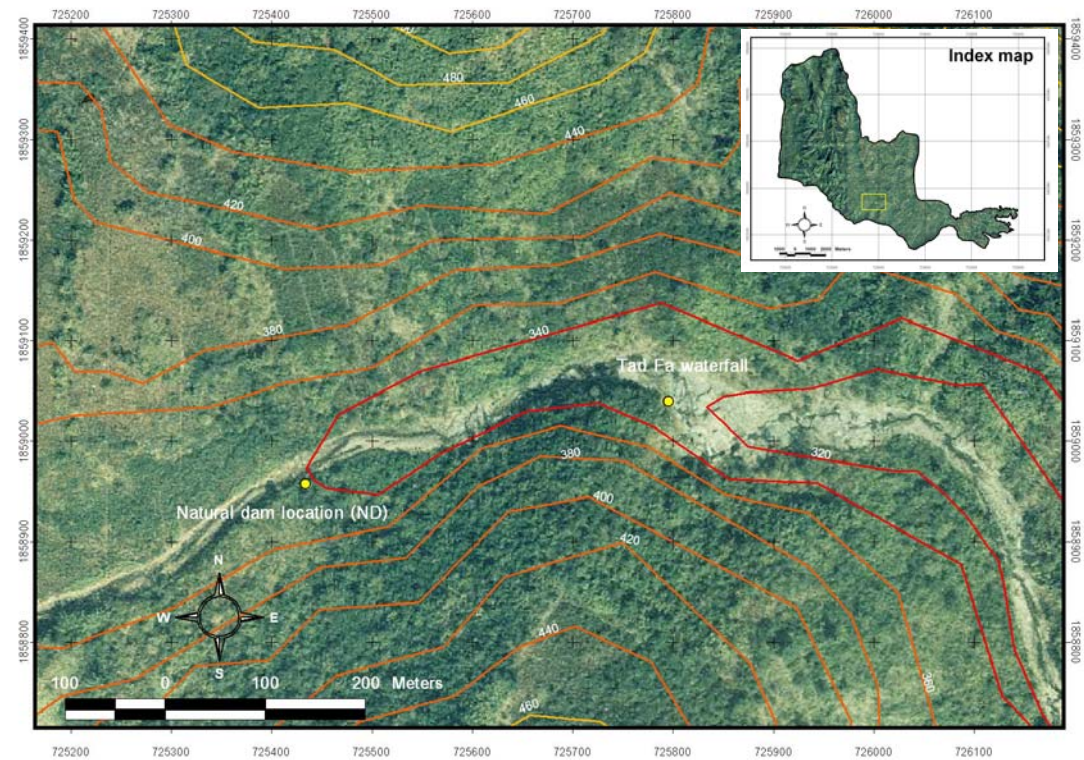


Figure 5-3 Closed-up orthophotograph in Figure 5-2 illustrating the local geography of Nam Ko Yai stream that is suspected to be a natural temporary landslide dam location (ND) in front of the location of Tad Fa waterfall.



Figure 5-4 Photographs (looking eastward direction) illustrating the configuration of Nam Ko Yai stream channel at location ND (referred to Figure 5-3) that is suitable for accumulated sediments for blockage a torrent stream and formed a natural temporary landslide dam. Note: The evidence of transported timbers was still found not only in the channel as a large one but also left as a smaller one at the higher level of the tree-branches (as shown in the inserted photograph that taken at the upstream of Nam Ko Yai stream, 2.5 km. far away from this point).

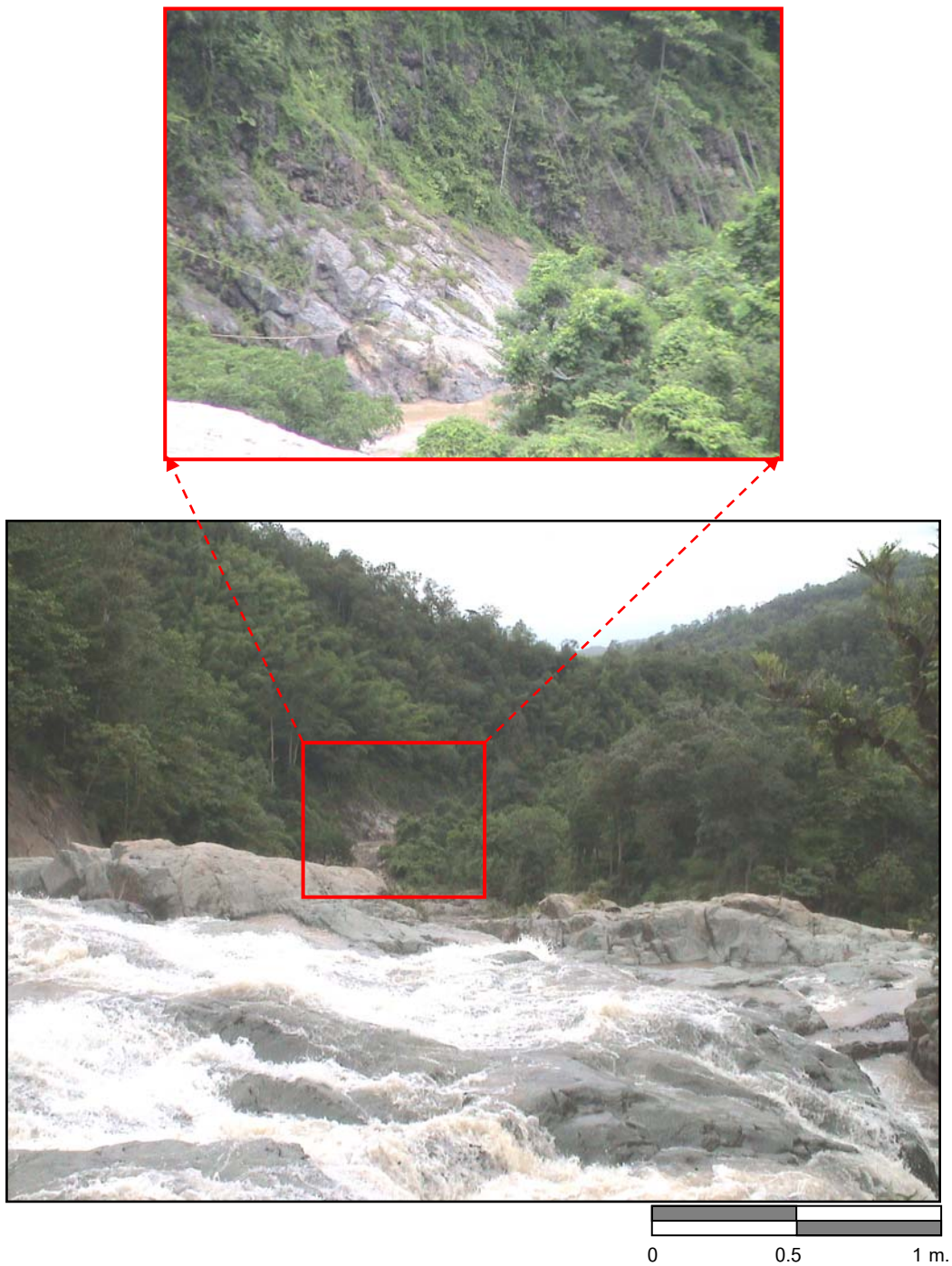


Figure 5-5 Photographs (looking eastward direction) showing the different relief of about 20 m between Tad Fa waterfall (location referred to Figure 5-3) and the downstream V-shape channel that is suitable for increasing water turbulent to form flow-flood occurrence.

### 5.2.2 Evidences of channel configurations

Topographically, the area of Nam Ko Yai sub-catchment immediately upstream from this suspected natural temporary dam location is a flat basinal shape area that can retain the water of about 1,200,000 cubic meters if the dam is 10 m high from the ground surface. This is a flat terrain of very gentle slope, less than 5 degrees (Figure 5-6), surrounded by the steeper slope with abrupt change in elevation (Figs. 5-7 and 5-8). The stream here is of a wide U-shape and was straight for about 2.5 km. The area is suitable for forming a reservoir, a dam was built at the location. Downstream from the waterfall, the stream changes to a narrow V-shape with strong sinuosity for about 8 km to the canyon mouth area (Figure 5-8). This narrow V-shape and strong sinuosity channel is accompanied by increasing energy of torrent stream flow. The observation suggested that this type of destructive mass movement was certainly not caused in the 8/11 occurrence alone. Instead it suggests general repeated strong debris flow-floods in several occasions in the past.

From the base rocks in the upstream from this suspected natural temporary dam location, it is interesting to note that lithology of Lom Sak Formation is mainly composed of non-resistant rocks of volcanic complex as shown in Figure 5-9. So the U-shape upstream of Nam Ko Yai channel is generally controlled by the soft and non-resistant volcanic rocks that are easily eroded as a flat area.

From the channel configuration of Nam Ko Yai stream up- and downstream from the suspected natural dam location (Figure 5-10), the 8/11 flow-flood should follow the pre-existing drainage way. Downstream from the dam, the stream has a V-shape or nearly rectangular cross-section as shown in the cross-section lines of G-H and I-J (Figure 5-11). This narrow V-shape and strong sinuosity channel configuration of Nam Ko Yai stream here also indicates as one of the most influent parameters that allow increasing energy for the torrent stream caused from the broken natural dam to be formed as a severe flow-flood. This destructive form of mass movement strongly eroded and transported sediments (plant debris, soils and rock boulders) along the downstream

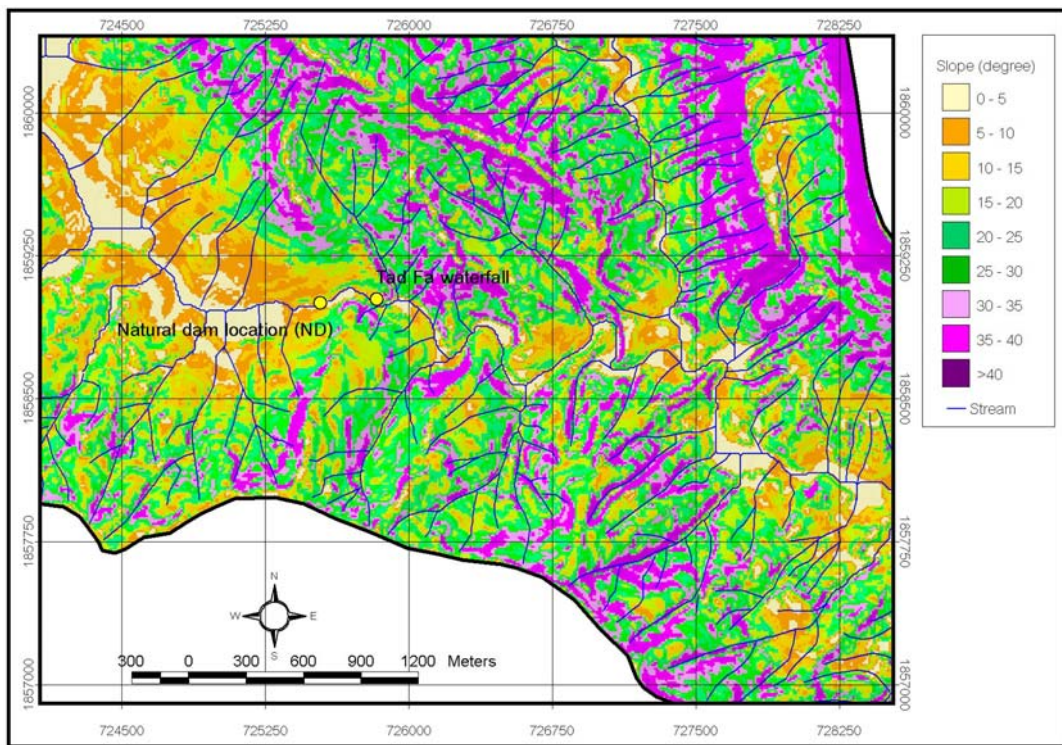


Figure 5-6 Slope map of the upstream and downstream area above and below the suspected natural landslide dam location (ND) in Nam Ko Yai stream channel.

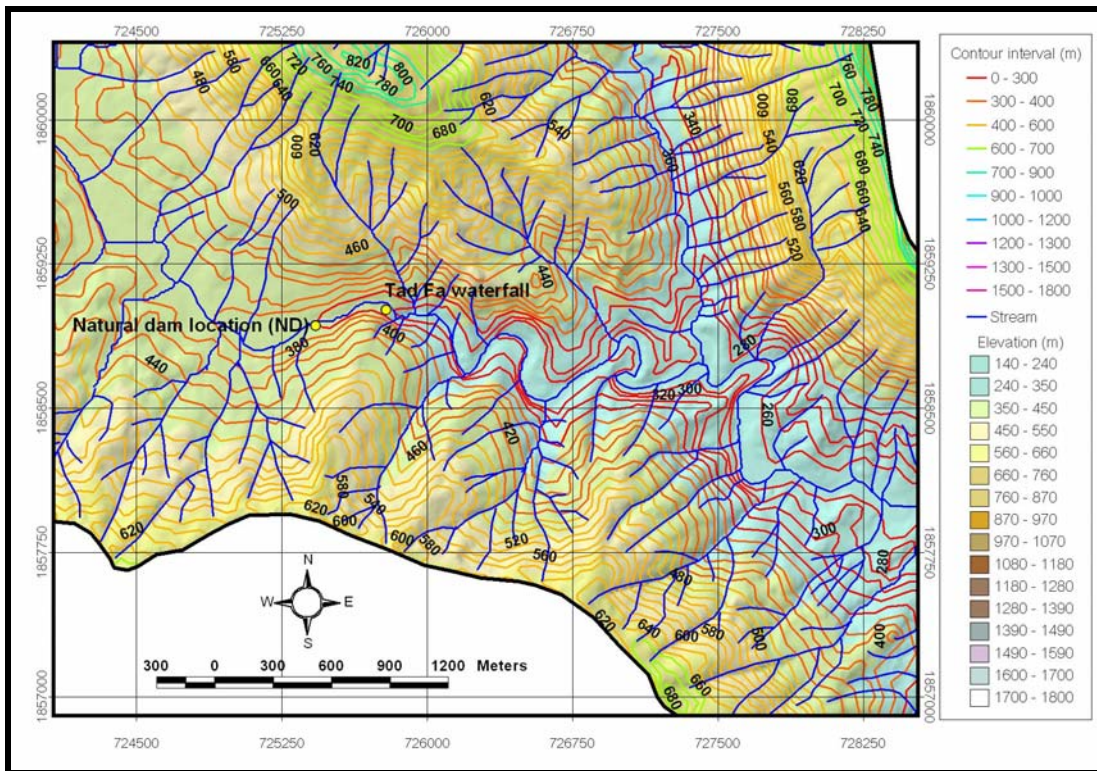


Figure 5-7 Elevation map of the upstream and downstream area above and below the suspected natural landslide dam location (ND) in Nam Ko Yai stream channel.

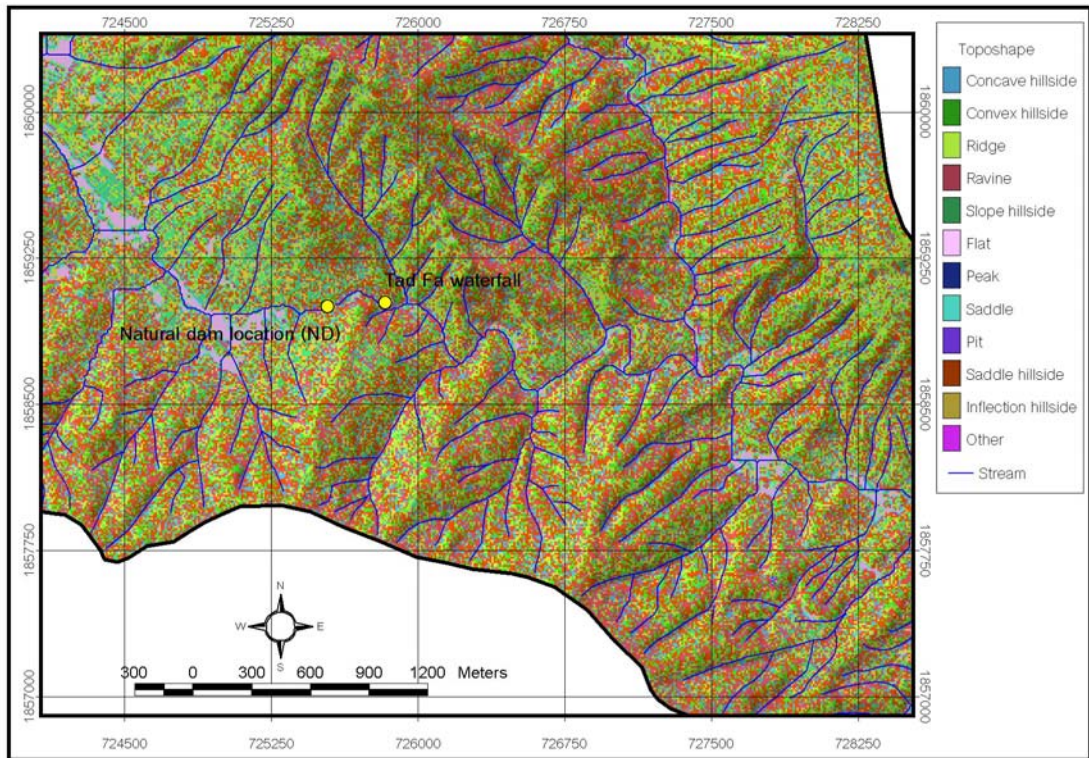


Figure 5-8 Topographic shape of upstream and downstream area away from the suspected natural landslide dam location (ND) in Nam Ko Yai stream channel.



Figure 5-9 Photograph showing the soft and non-resistant volcanic rocks of Lom Sak Formation in the upstream from the suspected natural temporary dam location.

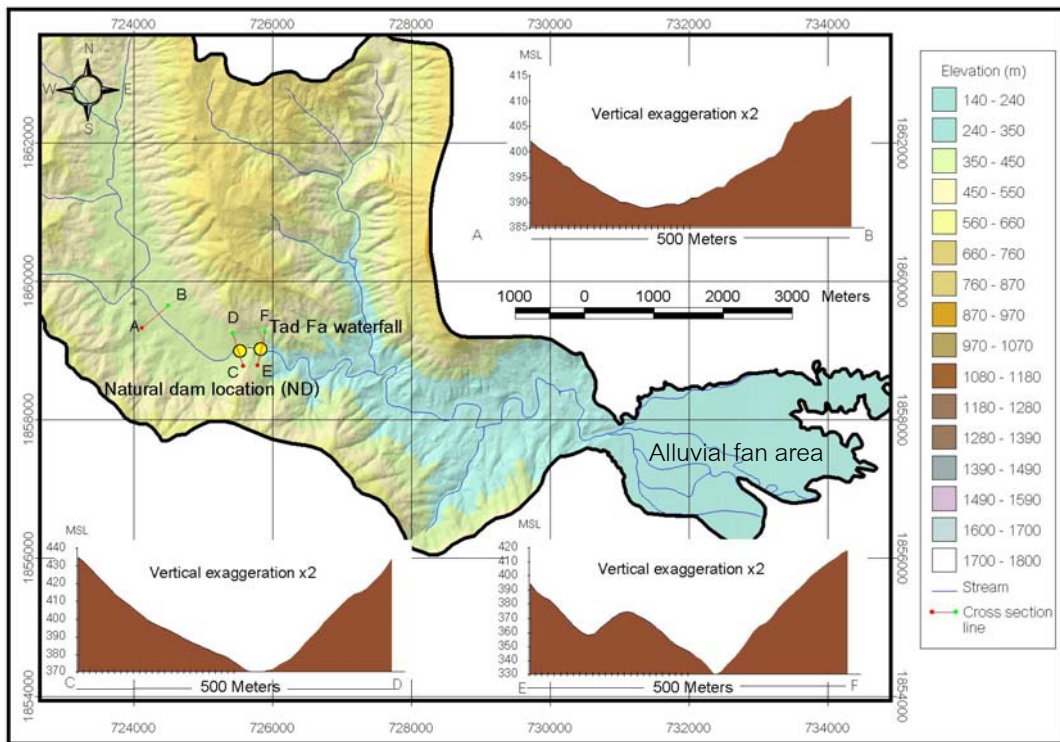


Figure 5-10 Three cross-sections (line A-B, C-D and E-F) across Nam Ko Yai stream channel and its valley at the upstream area, the suspected natural landslide dam location, and Tad Fa waterfall, respectively.

channel, especially in the outer-curvature bank of steep slope and incorporated them into the flow-flood. The evidences of 8/11 event could be observed in the field visit where Nam Ko Yai stream had a steep V-shape cross-section downstream. The traces of the erosional feature in the outer curving-bank were common. Some huge logs or intertwined bamboo clumps were left in the channel or up high on the tree splices as they were not all transported by the torrent stream flows (Figure 5-12).

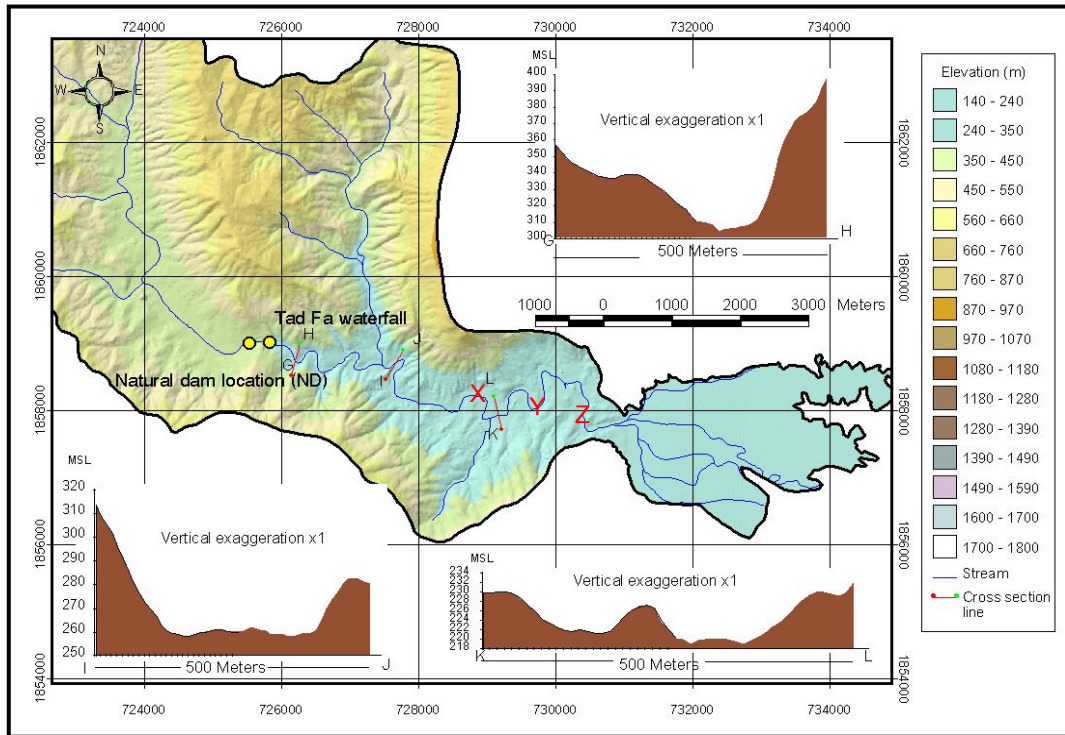


Figure 5-11 Three cross-sections (line G-H, I-J and K-L) across Nam Ko Yai stream channel and its valley at the downstream areas from the suspected natural landslide dam location (ND).

From the base rocks in the downstream from this suspected natural temporary dam location, it is interesting to note that lithology of Lom Sak Formation is mainly composed of high-resistant rocks of volcanic complex as shown in Figure 5-13. So the V-shape downstream with high sinuosity of Nam Ko Yai channel is generally controlled by these high-resistant volcanic rocks with some structural control of fracture lineaments as evidences by mainly channel straight change-directions and the topography.



Figure 5-12 Photographs illustrating a) the traces of erosional feature in the out curving-bank and b) huge logs or intertwined bamboo clumps after the 8/11 flow- flood event in Nam Ko Yai stream channel at location X in Figure 5-11.



Figure 5-13 Photograph showing general characteristics of the high-resistant volcanic rocks of Lom Sak Formation (Ls) in the downstream from the suspected natural temporary dam location.

Besides, newly deposited large boulders were found in the channel lying on the green weeds, where the gradient of stream bed changes from steep to flat (Figure 5-14). Eroded soil banks were also common.

From the field evidences and oblique aerial photograph (Figure 5-15) taken after the 8/11 flow-flood event, mainly the plant debris and soils that had been strongly eroded and transported from the upstream banks of Nam Ko Yai channel with high sinuosity characteristic in flat and hilly valleys were further spread out and deposited in the area of decreased confinement to form an alluvial fan at the toe of mountain front according to their high buoyancy and low viscosity. The descriptions and evidences of previous flow-flood activities in the alluvial fan will be mentioned and discussed in the following chapter.



Figure 5-14 Photographs of the flat valley area with gentle slope in Nam Ko Yai stream channel at location Y in Figure 5-10 illustrating the rock boulder deposits along the bottom channel, as well as the erosional bank that prevailed the previous debris flow deposits with floating texture, unsorted, and unstratified characteristics of about 1.2 m thick.



Figure 5-15 Oblique aerial photographs along Nam Ko Yai stream channel. The photograph, at location Z in Figure 5-11, illustrates the flow-flood track along plant debris and soils had been strongly eroded and transported from its banks before reaching the outlet of the Nam Ko Yai sub-catchment.

(Data source: the photograph was taken on 22<sup>nd</sup> August 2001, 11 days after the 8/11 flow- flood event and provided by Provincial Police of Changwat Phetchabun)

## CHAPTER 6

### EVIDENCES OF DEBRIS FLOW-FLOOD ACTIVITIES IN THE ALLUVIAL FAN

Realizing the parameters and processes that govern flow-flood initiation, transport, and sediment bulking in the area of Nam Ko Yai sub-catchment, the stratigraphic recognition and characteristics of the previous alluvial fan deposits are thus essential for evaluating past flows-floods. A two-step geological evaluation was performed, consisting of an initial delineation of the active depositional area and a subsequent detailed, site-specific analysis of hazards within the active depositional area as suggested by the U.S. National Research Council (1996).

In this chapter, recognition and characterization of the alluvial fan, by defining its activeness as well as the geomorphology and the stratigraphic recognition of the previous alluvial fan deposits were respectively presented as below.

#### 6.1 Recognition and characterization of the alluvial fan

In this part, the activeness of the alluvial fan in the study area was defined as follows.

##### 6.1.1 Defining activeness of the alluvial fan

In this step which was to define an activeness of the alluvial fan, multi-temporal aerial photographs, orthophotographs and Landsat 7 ETM+ imageries were interpreted and integrated with topographic characteristics for preliminary identification of location and morphology. The available multi-temporal low-altitude images of aerial photographs (1:15,000 scale) acquired on 24<sup>th</sup> December 1974 (Figure 6-1), orthophotograph (1:50,000 scale) acquired on 6<sup>th</sup> January 1996 (Figure 6-2), and orthophotograph (1:25,000 scale) acquired on 9<sup>th</sup> January 2002 (Figure 6-3) were used to characterize the Nam Ko Yai canyon mouth and its downstream depositional fan, before and after the 8/11 event. It was obvious that the topographic apex of Nam Ko Yai alluvial fan had only minor

changes between 1974 and 1996. A clear activeness of erosion and deposition was presumed to be caused by the 8/11 flow-flood event (Figure 6-4).

The expanded features of orthophotographs (1:25,000 scale) acquired on 9 January 2002 in Figures 6-4 and 6-5 clearly show the current traces and tracks of debris flood evidenced from the distinctively active alluvial fan deposits. The deposits mainly occurred on the northern bank of the alluvial fan area where the flood severely damaged houses and orchards once existing there as seen in the 1974 aerial photographs and 1996 orthophotographs (Figures 6-2 and 6-3).

Oblique aerial photographs taken after the flood were also the important information sources to characterize the extent of the deposit and validate the analyzed result. The oblique aerial photographs (Figure 6-5) of the severely damaged houses and orchards of Ban Nam Ko Yai perceivably illustrate characteristics and extent of a large volume of the active alluvial fan deposits by the 8/11 flow-flood occurrence. It was noted that the alluvial fan deposit mass on the roads (as seen in Figure 6-5) had been already removed while the debris were still left as in the original manner in the surrounding area. Besides, the fast-moving flow-flood battled and caused damage to houses and other infrastructures during the course of the 8/11 event had also been illustrated as some examples in Figure 6-6.

In the multi-spectral Landsat 7 ETM+ imageries analysis, evidence of the alluvial fan deposit from the 8/11 event were analyzed using NDVI value. NDVI value was also used to detect the depositional locations on the alluvial fan (Figure 6-7). Oblique aerial photographs (in Figure 6-5) of the depositional location in alluvial fan area taken after the event were used to characterize the extent of the deposit and validate analyzed result of NDVI value. It is remarked that the high value of NDVI change (56-107) in Figure 6-7 generally conformed the areas of the most serious damage in Figure 6-5. that covered an area of about 3.49 square kilometers from the total area of about 6.29 square kilometers of the alluvial fan. It is noted that the depositional locations from the 8/11 event cover more than 55 % of the total area of the alluvial fan.

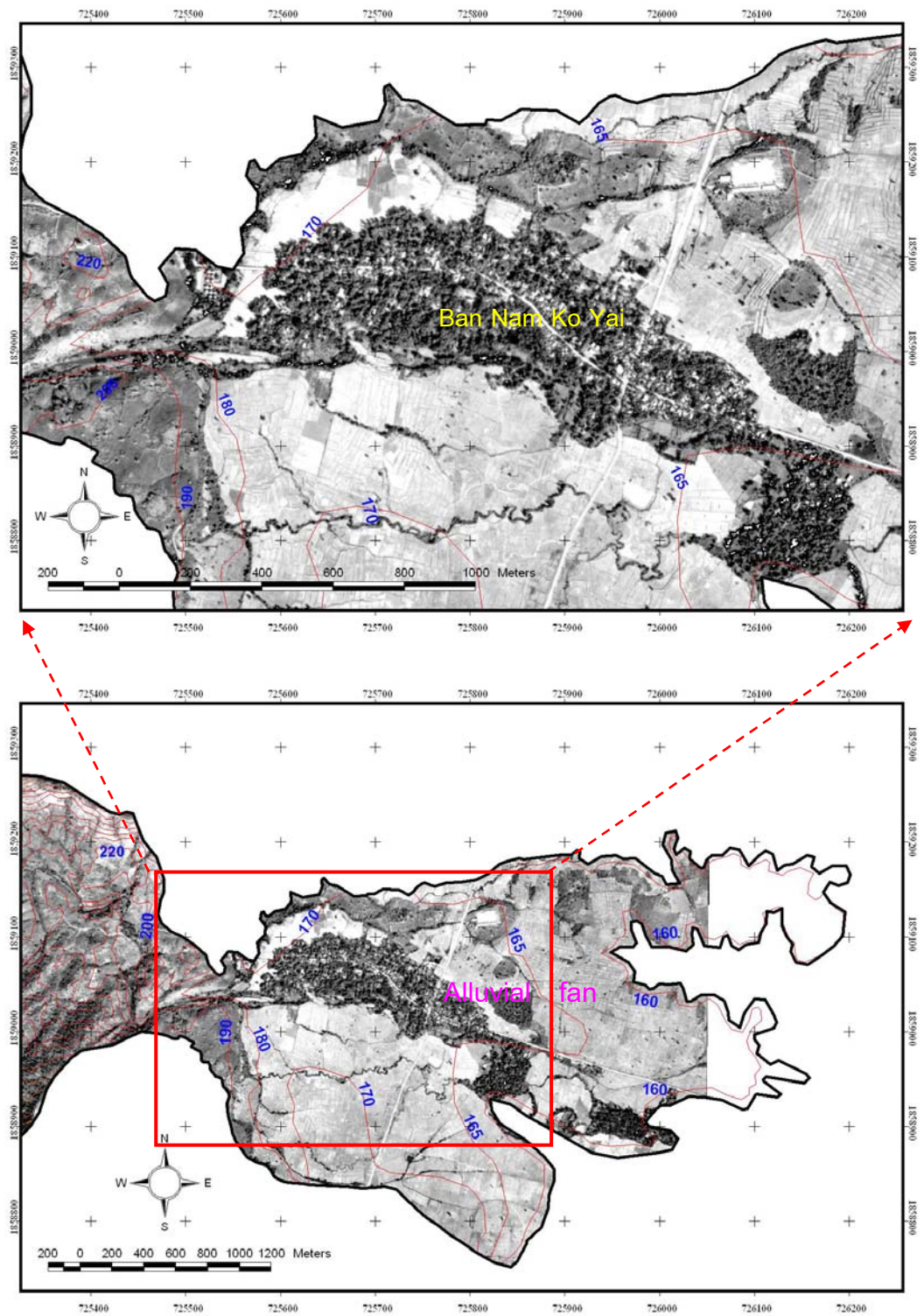


Figure 6-1 Aerial photograph (1:15,000 scale) acquired on 24<sup>th</sup> December 1974 showing characteristics of the alluvial fan at the canyon mouth of Nam Ko Yai stream with contour intervals (in the solid red-line block).

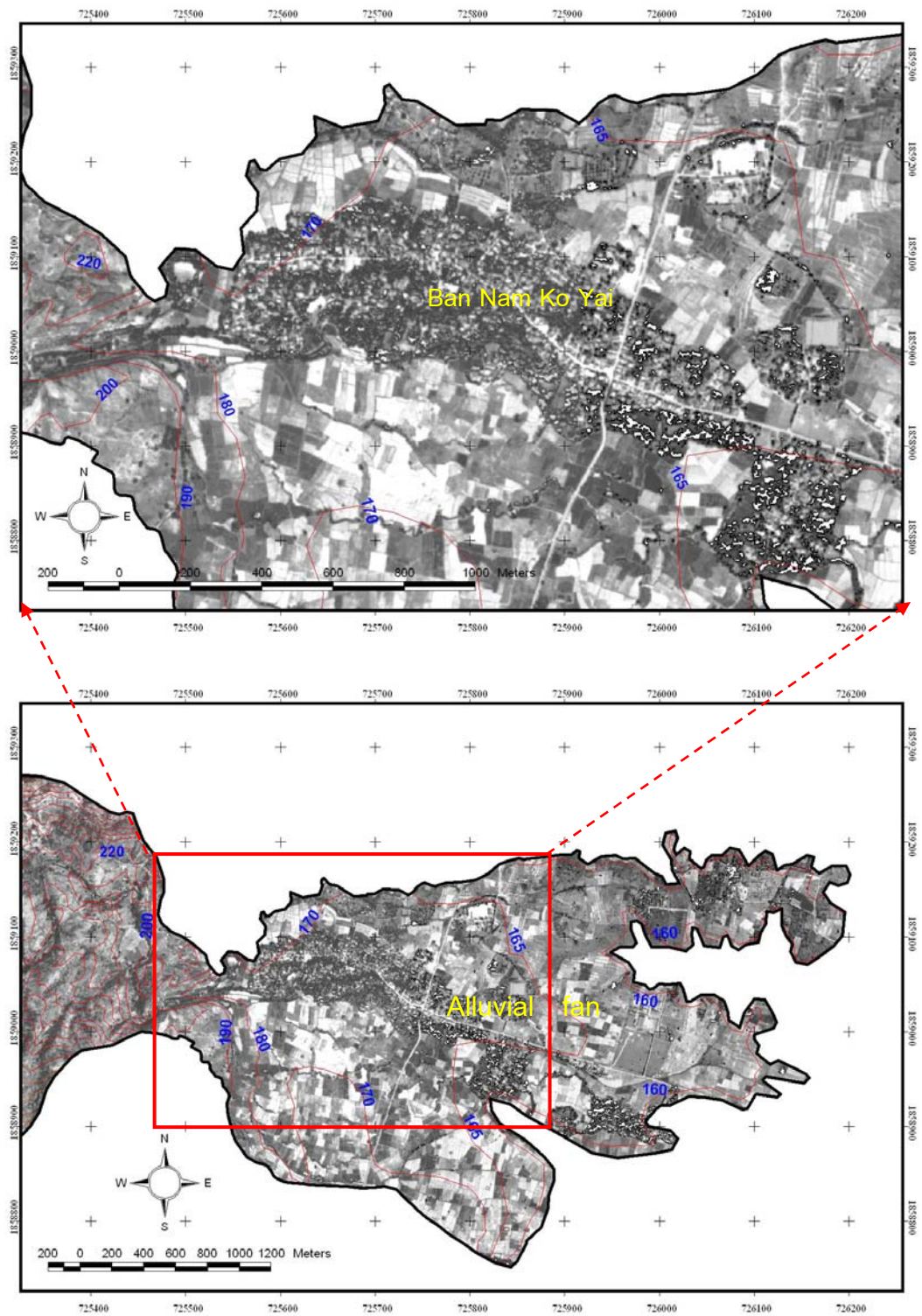


Figure 6-2 Orthophotograph (1:50,000 scale) acquired on 6<sup>th</sup> January 1996 showing characteristics of the alluvial fan at the canyon mouth of Nam Ko Yai stream without significant change in land cover.

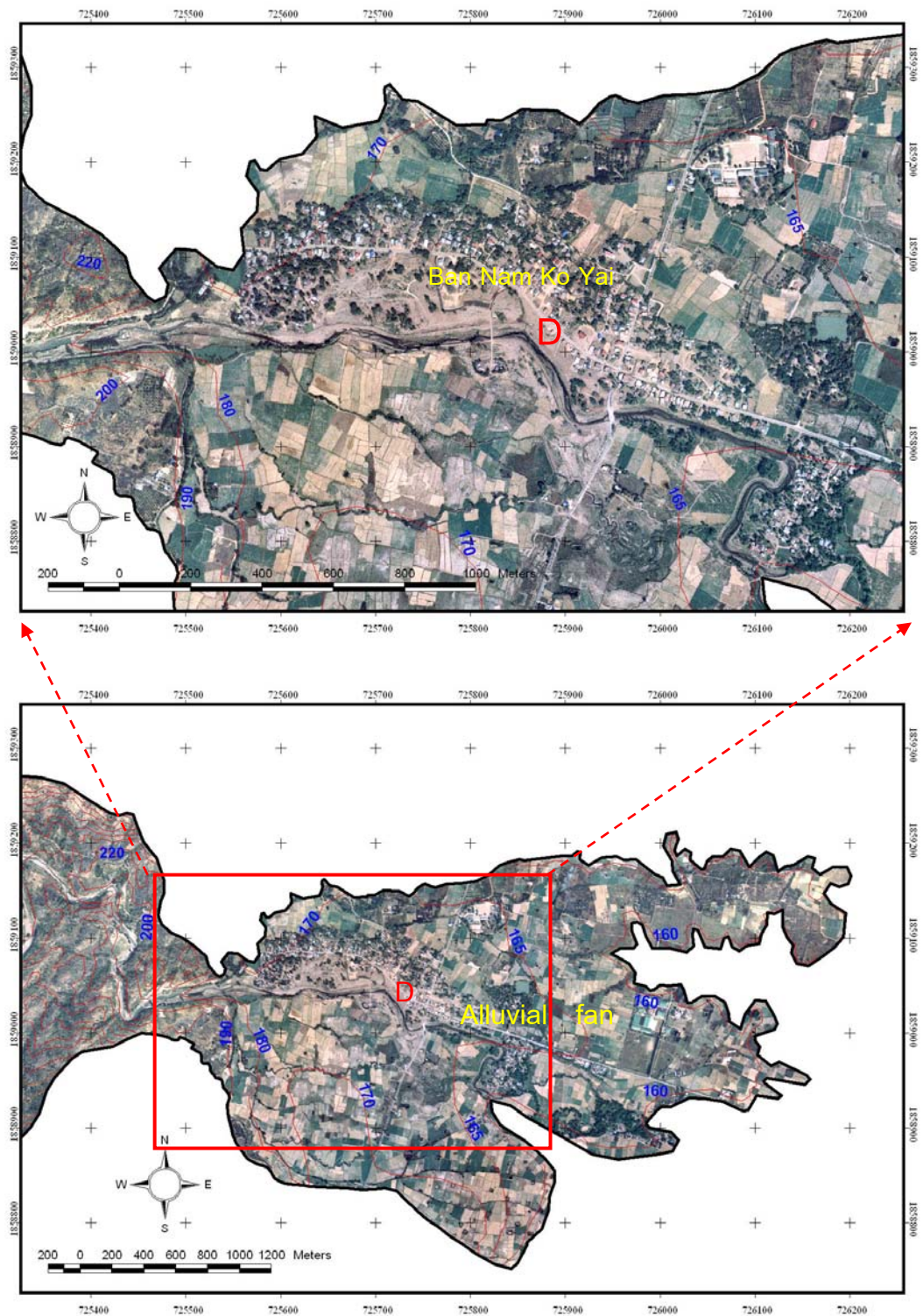


Figure 6-3 Orthophotograph (1:25,000 scale) acquired on 9<sup>th</sup> January 2002 (after the 8/11 flow-flood occurrence) showing the distinctive active alluvial fan deposit. The main area on the northern bank of Nam Ko Yai stream with populated settlement of Ban Nam Ko Yai (brown color zone surrounding the D location) was strongly damaged.

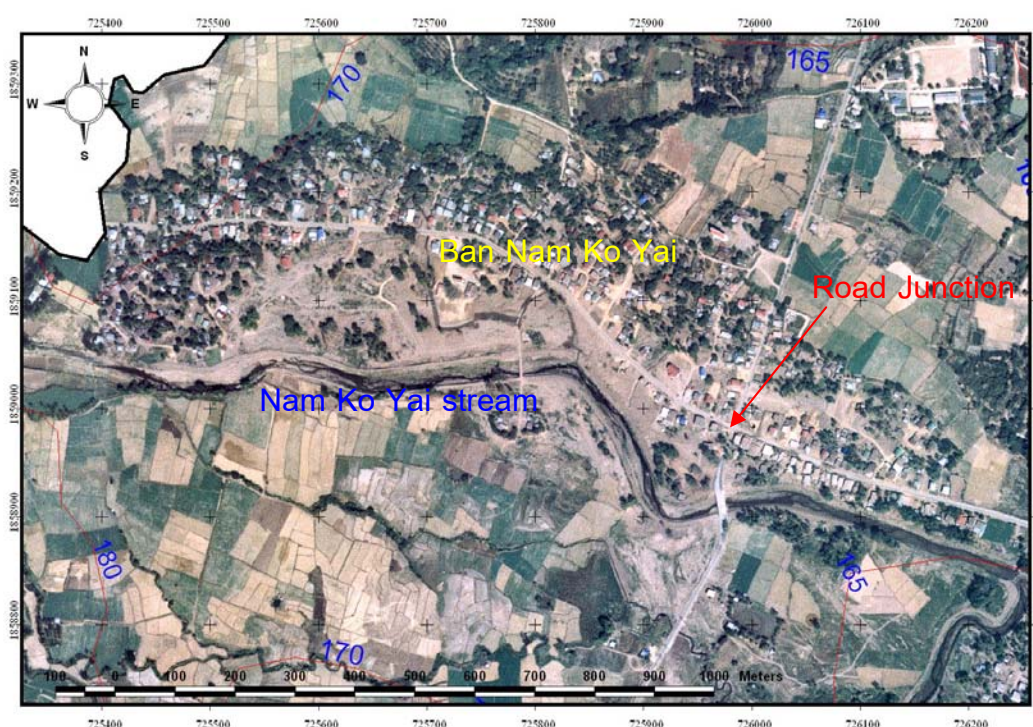


Figure 6-4 Expanded features of orthophotograph (1:25,000 scale) acquired on 9<sup>th</sup> January 2002 (after the 8/11 flow-flood occurrence) showing the clear traces and tracks of flow-flood from the evidences of the distinctively active alluvial fan deposit (in brown color area) that mainly covered and severely damaged houses and orchards in the northern bank of Nam Ko Yai stream. (Note: the road-junction location in this figure will be used to refer to the same location in Figure 6-5)

According to the oblique aerial photographs of the severely damaged settlement area (Figure 6-5), they illustrate characteristics and extent of a large volume of an active alluvial fan deposit. The ground visit was also conducted to investigate and record the flow-flood levels in this area. The flood levels were established from the mud traces on house walls and trees. It was found that the highest level of the flow-flood, 190-200 cm above ground surface, was located in the most severely damaged zone at locations A and B (Figure 6-8). It was also noted that these were the two locations facing the straight course of Nam Ko Yai stream before the channel changed its direction abruptly southerly further downstream. Here, the flood jumped over-bank to destroy houses and orchards and claim lives.



Figure 6-5 Two oblique aerial photographs perceptibly illustrating the characteristics and extension of a large volume of deposited sediments as evidences of 8/11 incidence.



Figure 6-6 Four photographs showing some examples of seriously structural damage of houses and other infrastructures in Ban Nam Ko Yai (in the area between A and B in Figure 6-5) battered and caused by the fast-moving 8/11 flow-flood.

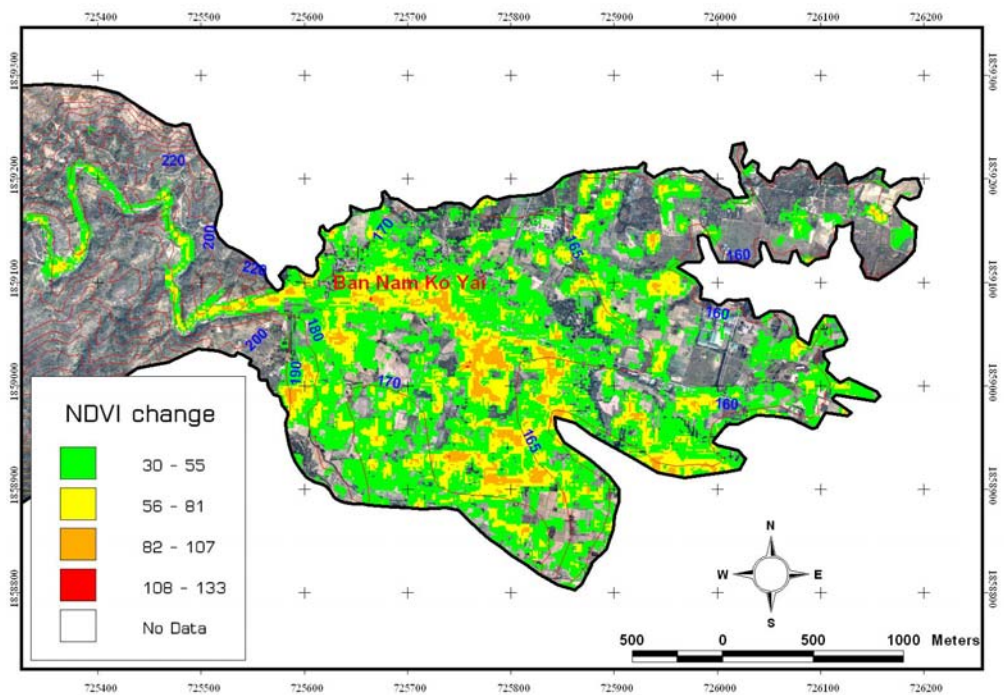


Figure 6-7 Detection change of NDVI value in the depositional location of the alluvial fan (expanded from Figure 3-21) overlain on the orthophotograph (1:25,000 scale) acquired on 9<sup>th</sup> January 2002 (as shown in Figure 6-3).

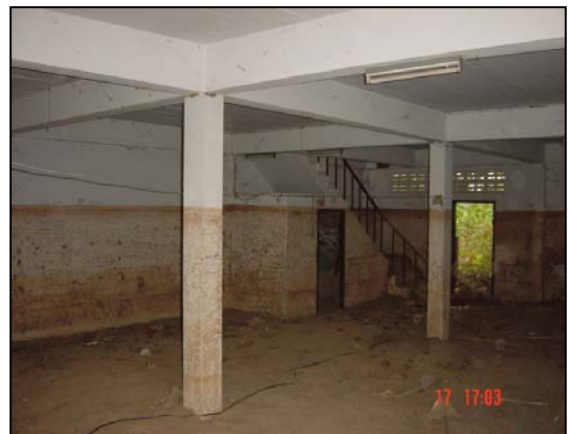
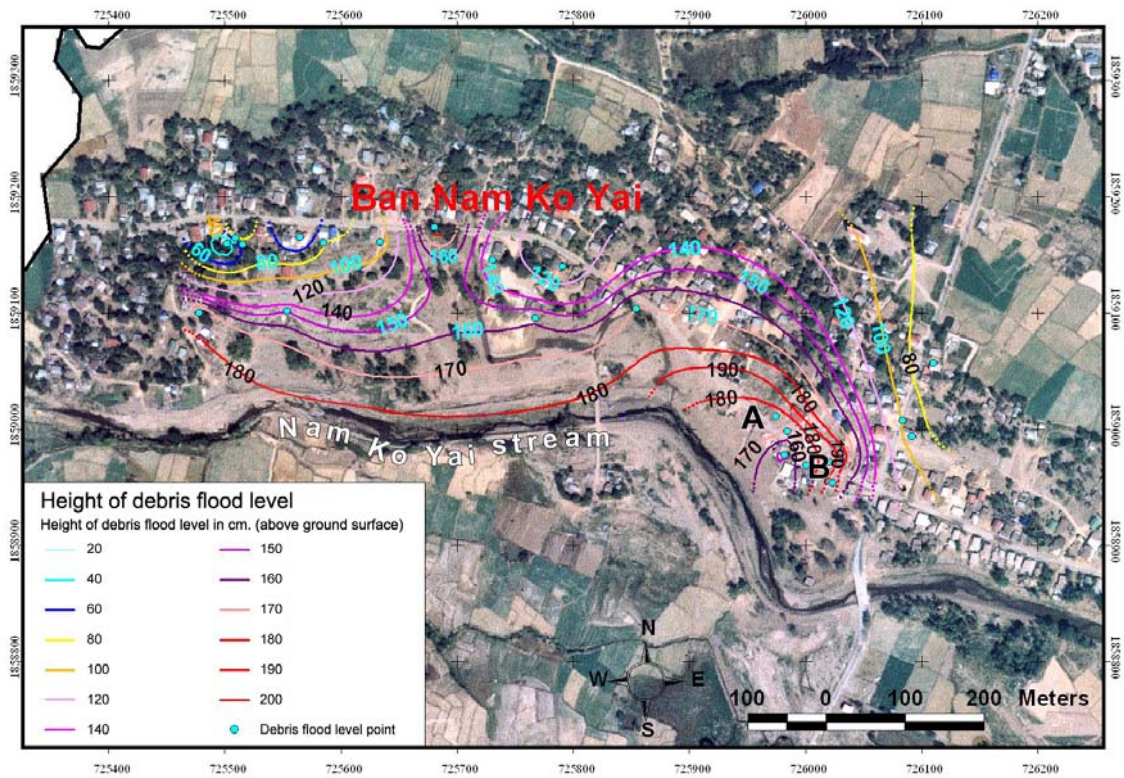


Figure 6-8 Height map of the flow-flood levels detected from the mud traces on the trees and house walls (as illustrating in the attached photographs below the map) in the severely damaged area of Ban Nam Ko Yai after the fast-moving 8/11 flow-flood

### **6.1.2 Defining geomorphology, local subsurface geology, and stratigraphic recognition of the alluvial fan**

In this step, a subsequent detailed and site-specific analysis of the hazard within the active depositional area was characterized. The detailed fan evaluations in this step, namely; geomorphological mapping, resistivity survey and sedimentary sequence study, were used to investigate and describe:

- a) geomorphology of the alluvial fan,
- b) local subsurface geology of the previous alluvial fan deposits, and
- c) stratigraphic recognition of the previous alluvial-fan deposits.

Besides, evidence and relationship between the sedimentary sequences and the flow-flood occurrence in the alluvial fan was presented. The above detailed fan evaluations in this step were respectively presented as below.

#### **6.1.2.1 Geomorphology of the alluvial fan**

As the criteria of an alluvial fan in terms of morphology are that it must have a fan shape, either partially or fully extended, the multi-temporal aerial images (Figures 6-1 to 6-4) and oblique aerial photographs (Figure 6-5) clearly illustrated the typical morphology of an alluvial-fan landform where the village is situated. The landform is a section of stream gradient where long-term channel migration and sediment accumulation became markedly less confined than upstream. Below, gradients of the lower part of the older alluvial fan are gentler than those at the fan apex, as was noted from the wider spacing of contour lines in Figures 6-1 to 6-4, and 6-7. The topographic apex of this active alluvial fan was located at the point where the flow in the stream channel become unconfined and less certain, and thus was coincident with the hydrological apex.

### 6.1.2.2 Local subsurface geology of the previous alluvial fan deposits

According to the resistivity survey in the alluvial fan along the lines NK 01 – NK 05 (as shown in Figure 6-9) to identify the local subsurface geology (thickness and depth of the previous alluvial fan deposits), the results revealed four sedimentary units at a total depth of less than 100 m below ground surface (Figure 6-10). The lowest unit was semi-unconsolidated sediments or weathered rocks of at least 70 m thick to the west with the bed top be noted at a depth of about 30 m below ground surface, and much thinner, less than 10 m to the east, with the bed top be noted at the depth of about 80 m below ground surface.

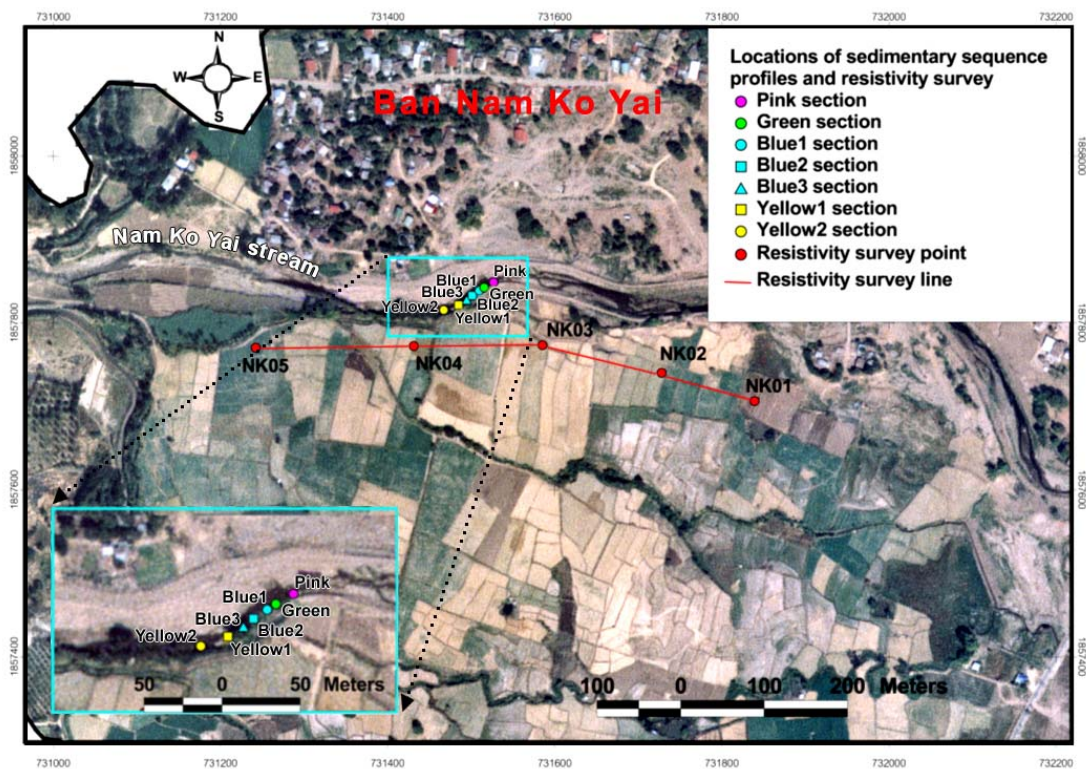


Figure 6-9 Location map of the seven measured stratigraphic profiles and a line of five resistivity survey points used for investigating the stratigraphic recognition and local subsurface geology of the previous alluvial fan deposits.

The overlying second unit was semi-unconsolidated sediments with trapped water in the bed openings. Thickness was 25-70 m and increased to the east. Its shallow horizon was 5 m below ground surface in the west to about 10-20 m to the west. These two lower units are never exposed near the site, but are at surface in the surrounding hills.

The third unit was unconsolidated sediments with trapped water. Thickness was in the range of 5-30 m. The thickest part of this third unit was near the NK 03 line in the central part, where the depth to the top of the unit was from a few meters down to 15 m below ground surface further to the east. The fourth and uppermost unit was of unconsolidated sediments with a thickness of a few meters in the west to 10 m in the east. The fourth unit was commonly exposed on the ground surface along all survey lines, except in the east where it was completely covered by recent topsoils.

#### **6.1.2.3 Stratigraphic recognition of the previous alluvial-fan deposits**

A detailed field study of the previous alluvial fan deposits was conducted along a 5x70 m eroded bank (Figure 6-9) of Nam Ko Yai stream near where the resistivity survey had been performed. According to the information from the local people, this eroded bank of Nam Ko Yai stream was just strongly eroded by the 8/11 flow-flood to allow the previously buried sedimentary deposits of alluvial fan be well exposed. Seven stratigraphic profiles, from east to west; zones Pink, Green, Blue1, Blue2, Blue3, Yellow1, and Yellow2 (marked by the flag colors); were studied to reveal sedimentary sequences in both terms of vertical and lateral stratigraphic correlation. The stratigraphic profiles as mentioned above are actually illustrated in Figure 6-11. The photographs of much closer illustration of the stratigraphic characteristics of their lateral and vertical correlation of the seven stratigraphic profiles are also presented in Figures 6-11 and 6-12.

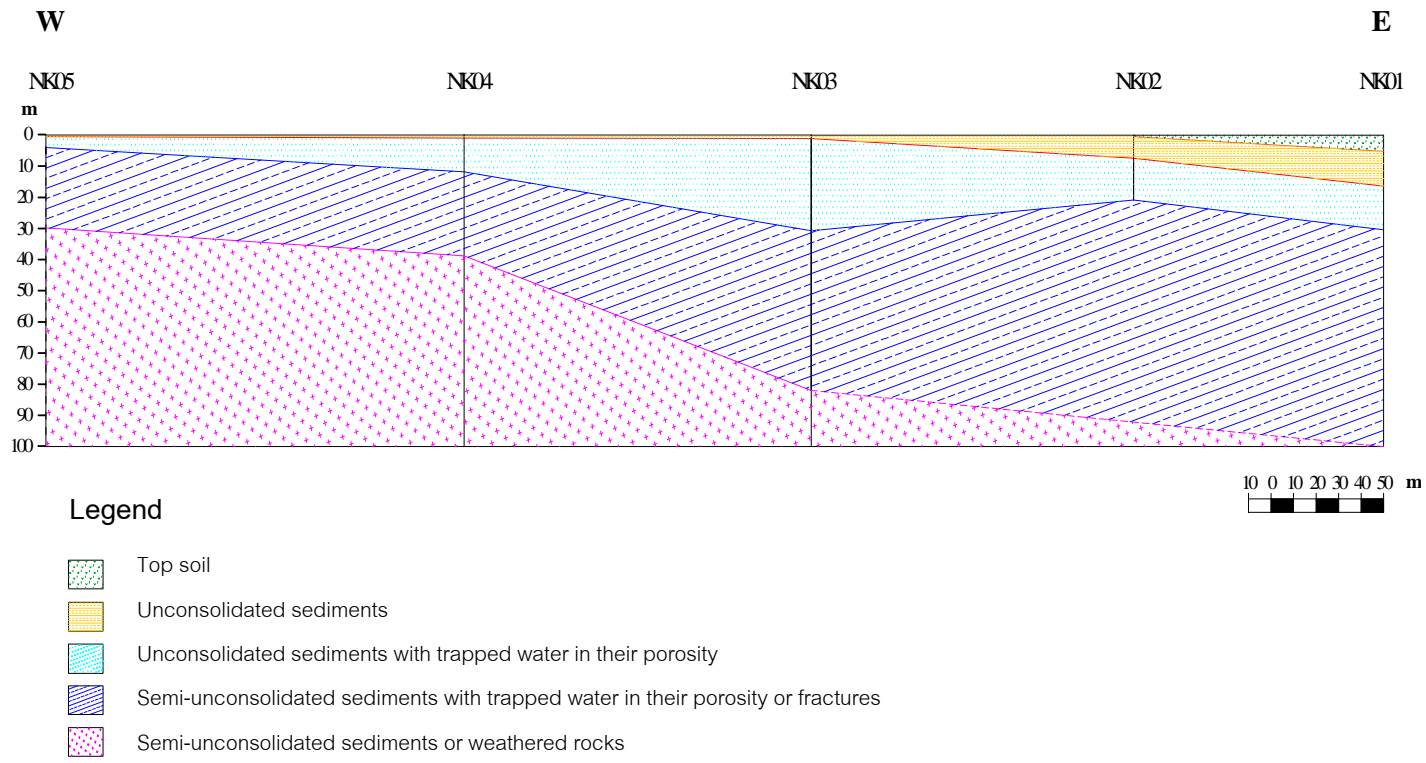


Figure 6-10 Cross-section of the resistivity survey interpreted from the five survey points (NK 01 – NK 05 as shown in Figure 5-9) that revealed four sedimentary units lying less than 100 m below ground surface.

In the observed stream-bank profiles, the lowest sedimentary unit of the previous alluvial fan deposits was a debris flow unit of floating texture, unsorted, and un-stratified material that was exposed in the stream-bed only in the lowest part of the zone Green (Figure 6-13). The coarse-grained fluvial unit of clast-supported texture and fining-upward graded bedding was transitionally deposited on top of the debris flow unit, especially in the middle part of the zone Green, and extended westward (upstream) beyond the zone Yellow2 (Figure 6-14). This coarse-grained fluvial unit was the thickest in the western part and became thinner to the east.

The uppermost part of this eroded-bank profile was a fine-grained fluvial and debris flood unit that was dominantly deposited to form a sharp contact on top of the coarse-grained fluvial unit (as shown in Figures 6-12 to 6-15). The uppermost unit is thicker to the east, especially in the eastern part of the zone Pink. The representative sedimentary and stratigraphic characteristics in completely detailed vertical succession are shown in the zone Green (Figure 6-13) and are from bottom to top the debris flow unit, the coarse-grained fluvial unit, and the fine-grained fluvial and debris flood unit, respectively.

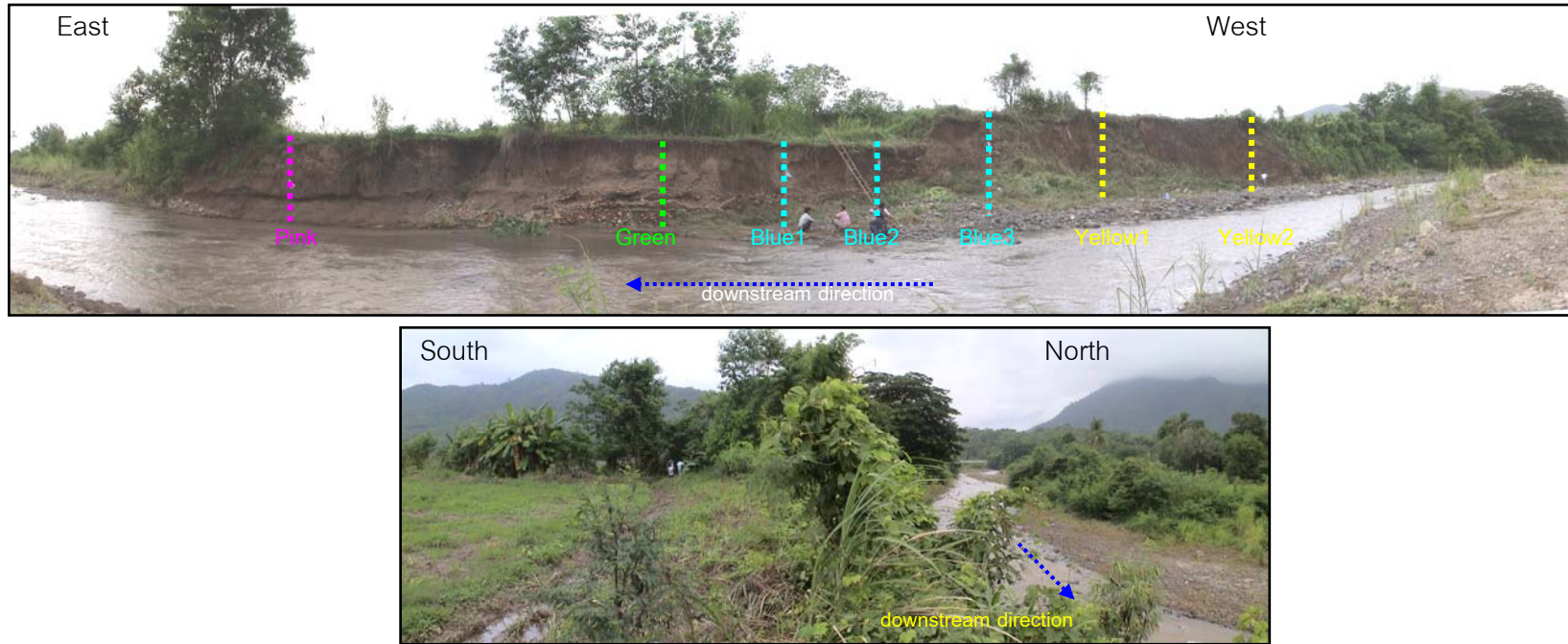


Figure 6-11 Photographs illustrating the actual location of the seven measured stratigraphic profiles (zones Pink, Green, Blue1, Blue2, Blue3, Yellow1 and Yellow2) along the eroded-bank of Nam Ko Yai stream.

(Note: locations of the seven stratigraphic profiles are referred to in Figure 6-9)

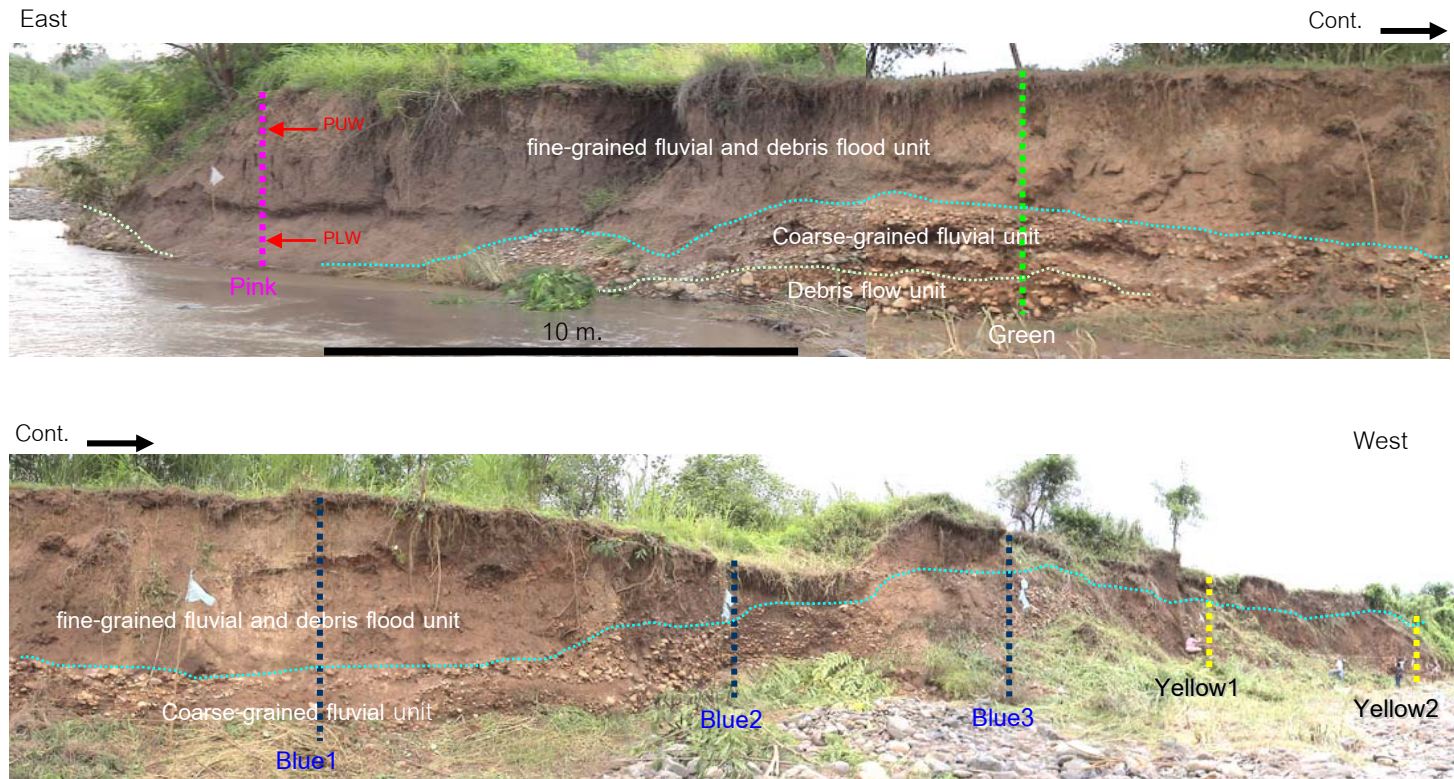


Figure 6-12 Photographs illustrating lateral and vertical stratigraphic characteristics of three sedimentary units (debris flow unit, coarse-grained fluvial unit, and fine-grained fluvial and debris flow unit) of the previous alluvial fan that well exposed along the eroded-bank of Nam Ko Yai stream. (Note: locations of the seven stratigraphic profiles referred to Figures 6-9 and 6-11)



Figure 6-13 Photographs illustrating detailed sedimentary and stratigraphic characteristics in vertical and lateral succession of three sedimentary units (debris flow unit, coarse-grained fluvial unit, and fine-grained fluvial and debris flow unit) of the previous alluvial fan deposits at the zone Green.

(Note: location of the zone Green referred to Figures 6-9 and 6-11)

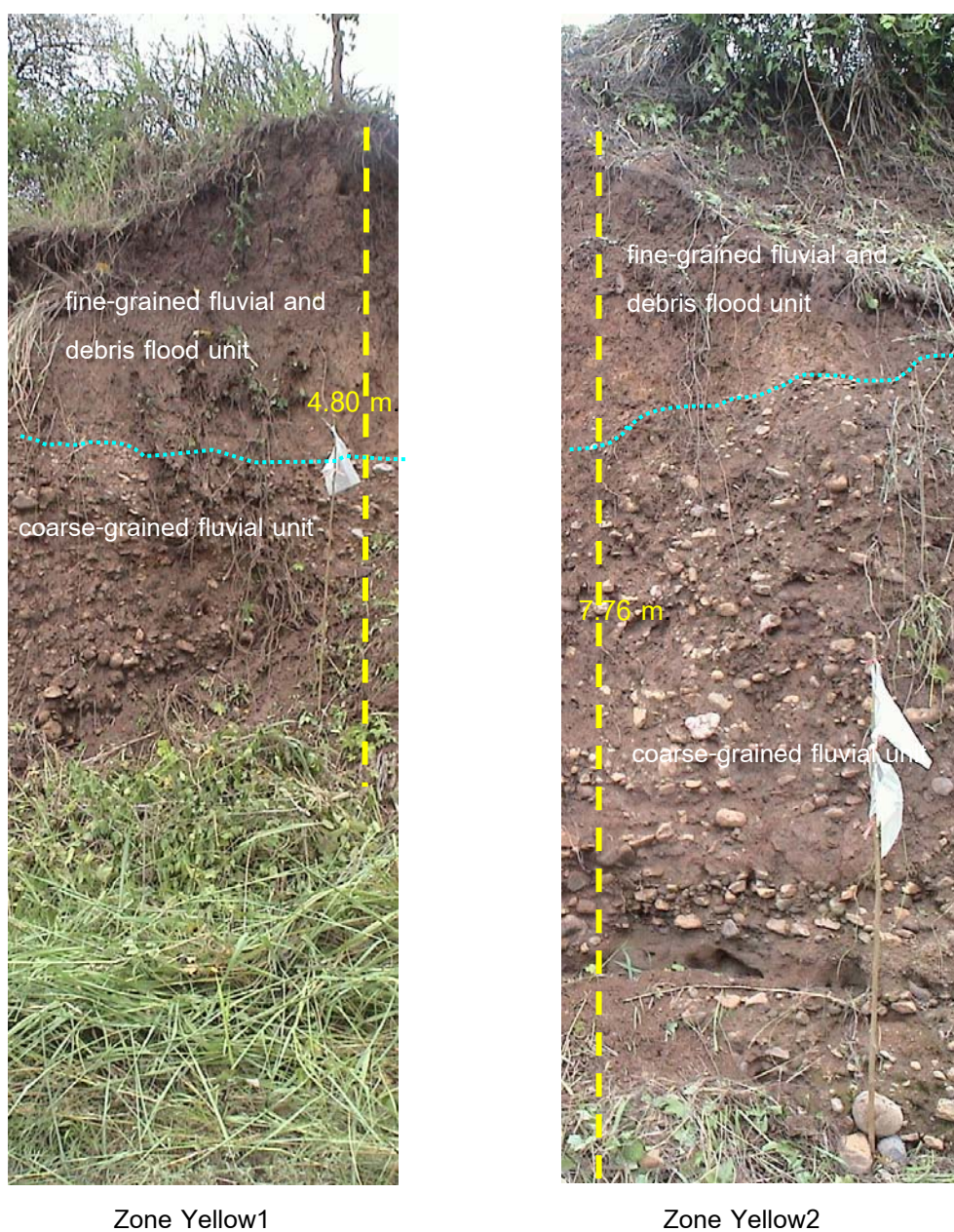


Figure 6-14 Photographs illustrating detailed sedimentary and stratigraphic characteristics in vertical succession of two sedimentary units (coarse-grained fluvial unit, and fine-grained fluvial and debris flow unit) of the previous alluvial fan deposits at the zones Yellow1 and Yellow2.

(Note: location of the zones Yellow1 and Yellow2 referred to Figures 6-9 and 6-11)



Figure 6-15 Photographs illustrating detailed sedimentary and stratigraphic characteristics in vertical succession of the fine-grained fluvial and debris flood unit that overlay with the sharp contact manner on top of the coarse-grained fluvial unit at the zones Blue1, Blue2 and Blue3.

(Note: location of the zones Yellow1 and Yellow2 referred to Figures 6-9 and 6-11)

With respect to the resistivity survey results as previously mentioned, the overall interpreted subsurface characteristics of these survey lines generally conformed to the normal alluvial fan deposits. The third sedimentary sequences unit repeated in the resistivity survey should be the same as the previous alluvial fan deposits in this eroded bank profile as evidenced from the depth and thickness variation from the west to the east. The upper part of the third unit is clearly of the previous fan deposits composing of the coarse-grained fluvial unit, debris flow unit, and fine-grained fluvial and debris flood unit.

Significant evidences of the previous flows-floods found in the uppermost fine-grained fluvial and debris flood unit were two preserved wooden debris fragments, one at the lower part (location PLW) and the other at the upper part (location PUW) of the Pink section (Figures 6-16 and 6-17). It is noted that the PLW sample of the lower location was charcoal characteristic with fibrous texture whereas the sample of the upper location (PUW) was the pale brown wood with rather complete wooden texture (as shown in Figure 6-17). These preserved wooden debris were dated by radiocarbon dating method to have absolute ages of deposition between 2,618 $\pm$  35 before present and post-1950, respectively.

From these radioactive dating results, it is strongly confirmed that this is an active alluvial fan and the debris flow-flood processes had occurred at least twice before the recent 8/11 disastrous event.

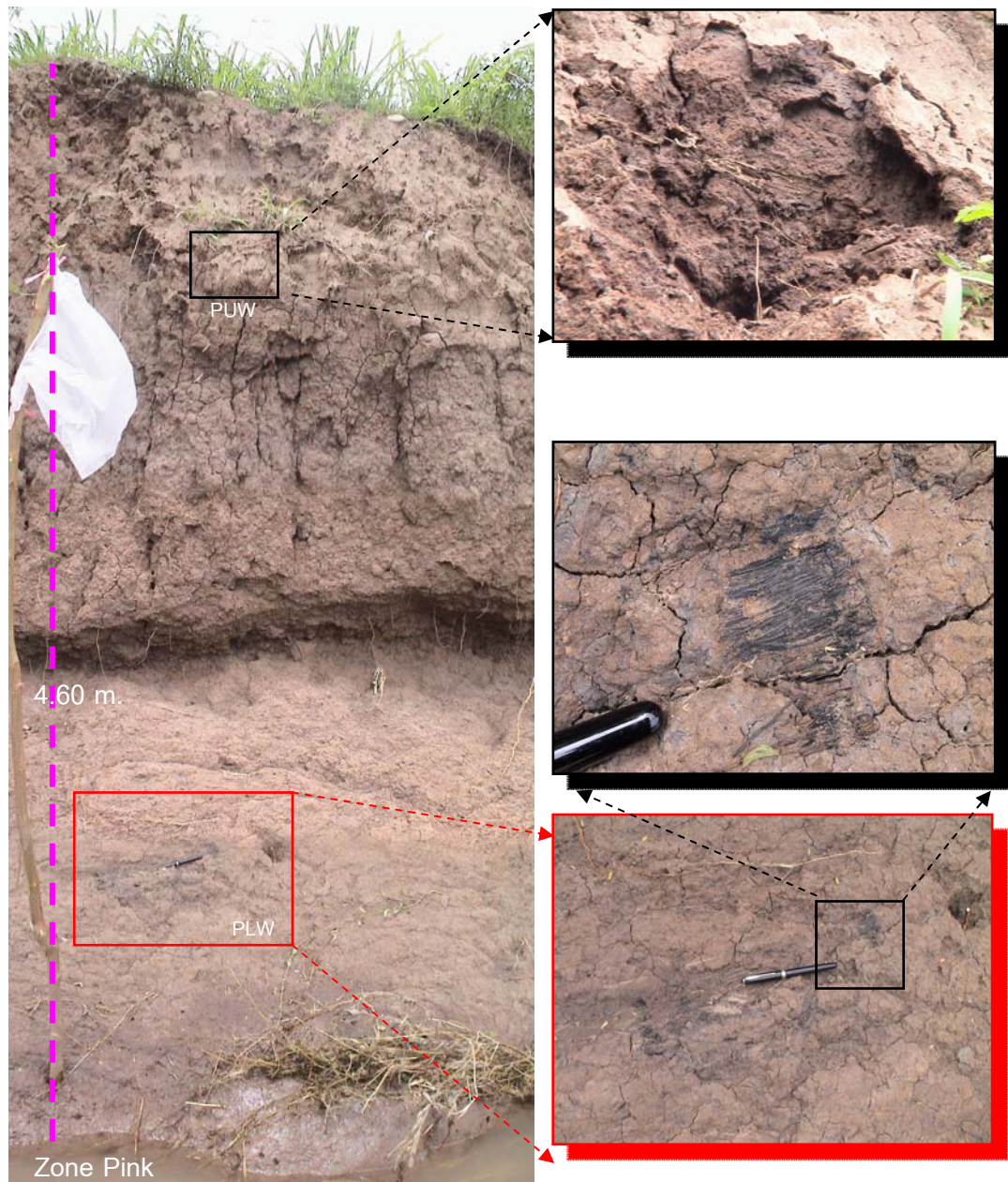


Figure 6-16 Photographs illustrating the general characteristics in the uppermost fine-grained fluvial and debris flood unit at the zone Pink (referred to Figures 6-9 and 6-11) and the preserved large wood debris at the lower part (PLW) and at the upper part (PUW) locations.



Figure 6-17 Closed-up photographs of the collected wood debris samples from the preserved locations at PLW and PUW (as shown in Figure 6-16) illustrating their general characteristics of charcoal characteristic with fibrous texture and pale brown wood with rather complete wooden texture, respectively.

## CHAPTER 7

### DISCUSSION

In this chapter, the results of the study methods as previously mentioned are discussed in three categories. Firstly, the flow-flood susceptibility results are discussed. Secondly, the flow-flood event reconstruction and its potential are proposed and discussed. Finally, the application of FLO-2D simulation results for validation of the suspected natural landslide dam occurrence in the middle of Nam Ko Yai sub-catchment is discussed.

#### 7.1 Debris flow-flood susceptibility results

In this research, a statistical approach to estimating the susceptible flow-flood area using remote sensing technique and the GIS was performed. For the flow-flood susceptibility analysis, the detected scar-scouring locations and the flow-flood related database were constructed for Nam Ko Yai sub-catchment. Using the constructed database, flow-flood susceptibility analysis was done by probability method. It is remarked that the probability method is somewhat simplistic, and the process of input, calculation and output could be understood easily. Moreover, there is no need to convert the database to any other format such as ASCII, as the large amount of data can be processed in the GIS environment quickly and easily.

The relationship of flow-flood and relevant parameters was analyzed for flow-flood susceptibility assessment using the probability method and flow-flood susceptibility map as mentioned above. In Nam Ko Yai sub-catchment, scar-scouring locations detected in multi-temporal aerial photograph and satellite image as well as in field surveys were put into a GIS database. Besides, various maps were constructed from the flow-flood relevant parameters derived from the database as illustrated in Chapter 3. In addition, three-dimensional drape of the interpreted scar-scouring locations through a 1:20,000 base-scale DEM was also illustrated in Figure 7-1 as being

concentrated on the western steep slope, along the stream course, and on the alluvial fan below. These generally included 1:20,000 scale digital topographic map of Land Development Department (LDD), 1:20,000 scale soil property map 1:20,000 scale soil property map of LDD, and 1:50,000 scale geological map of Department of Mineral Resources. The significant influencing parameters involved in the flow-flood susceptibility analysis are slope, landform topography, geology, and land cover.

Using the parameters above, probability method was applied to analyze the flow-flood hazard. The analyzed results were used to reconstruct the GIS database, then to maps. The flow-flood susceptibility map and relevant maps as previously proposed in Chapter 4 might be of great help to planners and engineers for choosing suitable locations to implement developments in Nam Ko Yai sub-catchment. Besides, three-dimensional drape of five classes of susceptibility as very high, high, moderate, low, and very low through 1:20,000 base-scale DEM was also illustrated in Figure 7-2 as the flow-flood susceptibility model in the sub-catchment. It was noted that the very high to very low susceptibility was occurred here. In general, the middle part of Nam Ko Yai stream channel and its adjacent banks had a very high to high flow-flood susceptibility whereas the lower downstream part of the stream had a high flow-flood susceptibility. Whereas the western and northern steep-cliff areas had a low to moderate flow-flood susceptibility whereas the main other parts else of the sub-catchment have in general very low flow-flood susceptibility.

These results can be used as basic data to assist slope management and land use planning. But the method used in this part is valid for generalized planning and assessment purposes only, as it may be less useful at the site-specific scale where local geological and geographic heterogeneities prevail. For the method to be more generally applied, more flow-flood data that are not available in the study area will be needed. Accurate distribution of rainfall that could be combined with a hydrological model of stream flow is one of the most important data needed for an accurate possibility analysis in the sub-catchment.

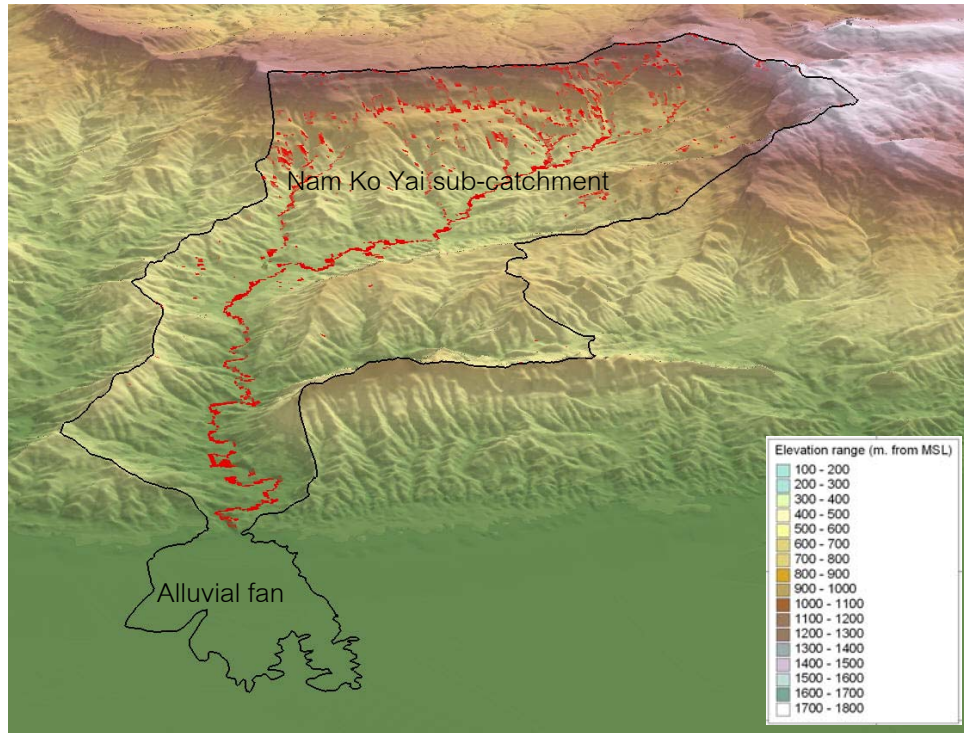


Figure 7-1 Three-dimensional drupe of the interpreted scar-scouring locations (grouped in red color) through a 1:20,000 base-scale DEM in Nam Ko Yai sub-catchment.

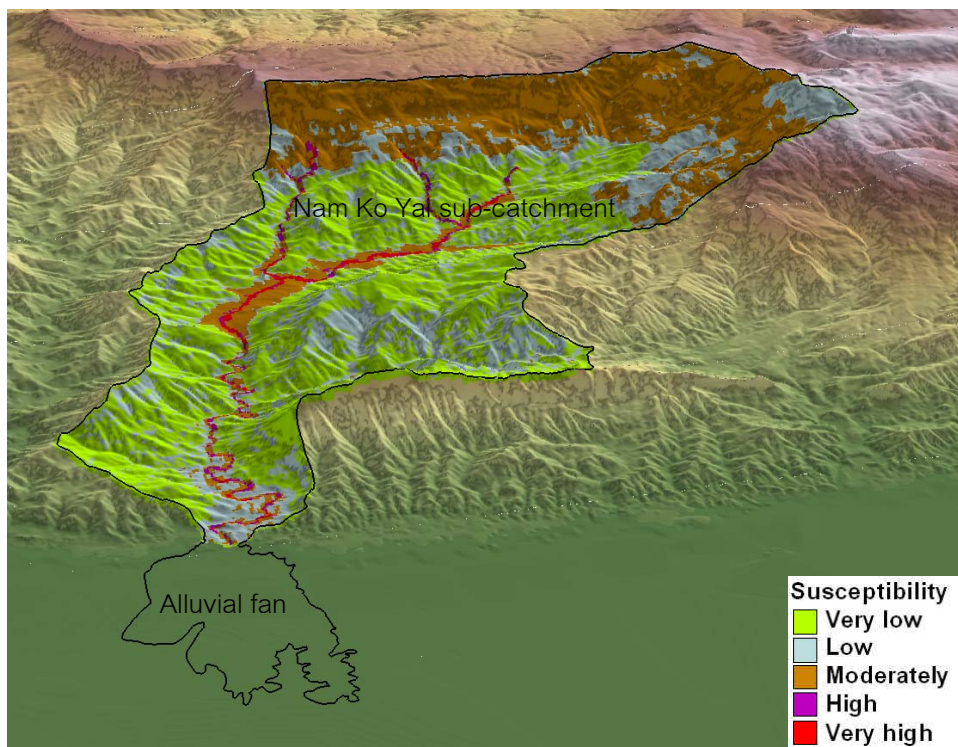


Figure 7-2 Three-dimensional drupe of five classes susceptibility of very high, high, moderate, low, and very low, through a 1:20,000 base-scale DEM in Nam Ko Yai sub-catchment. Very high to very low susceptibility was noted here.

## 7.2 Debris flow-flood event reconstruction and its potential

In this discussed topic, three-dimensional drape of false color composite of Landsat 7 ETM+ (R=5, G=4, B=3) acquired before and after the 8/11 flow-flood occurrence through a 1:20,000 base-scale DEM in Nam Ko Yai sub-catchment and its alluvial fan as modeled in Figure 7-3 and 7-4 are mainly used to illustrate and be referred to with the flow-flood event reconstruction as follow.

The debris flow probably began as shallow circular landslides, on the western and northern steep mountain slopes of Nam Ko Yai sub-catchment after a continuous heavy rainfall period for at least 10 days (before 8/11) that the weakened material with the increasing weight set, thus became highly movable down-slope. The colluvial soil and rock debris of Pw Formation and Pk Formation flow down the forest-covered 30° (or steeper) slopes during the peak of heavy rainfall as previously mentioned in Chapter 4. This could be the potential primary source area for the debris (Figure 7-4).

The debris flow continued further over the central undulated valley area to the main channel of Nam Ko Yai stream. As the sub-catchment plain was extensively deforested during the last decade with only few trees left on its overbank flat land, the large quantity of plant debris observed to be carried further with the water flow must have come from the upslopes with only a small amount from the overbanks. The debris flow was capable of exerting tremendous lateral forces on obstruction in the flow path, as evidenced from the impact of entrained, large boulders in the highest velocity along the main channels of the first order and second order sub-catchments in the steep slope areas.

These high velocity flows severely snapped off a large number of trees from hillsides and over channels, and mixed with re-eroded soils of the detached-landslides at the steep banks down along the main channels to the central area of moderate -to-

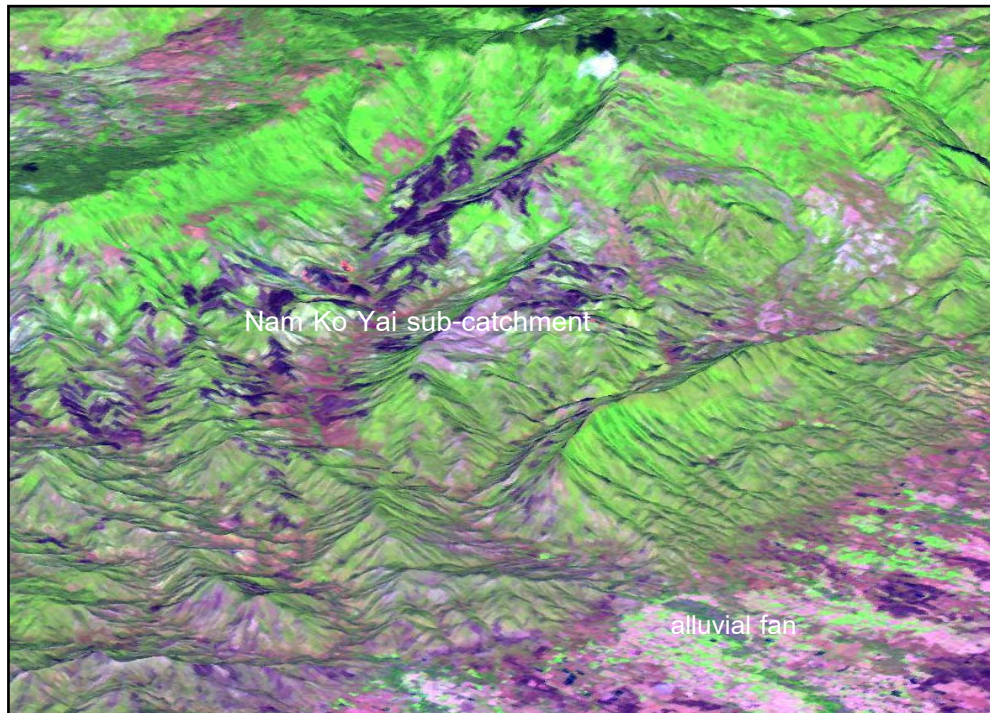


Figure 7-3 Three-dimensional drupe of false color composite of Landsat 7 ETM+ (R=5, G=4, B=3) acquired on 5<sup>th</sup> January 2001 through a 1:20,000 base-scale DEM illustrating the general characteristics before the 8/11 flow-flood occurrence in Nam Ko Yai sub-catchment and its alluvial fan.

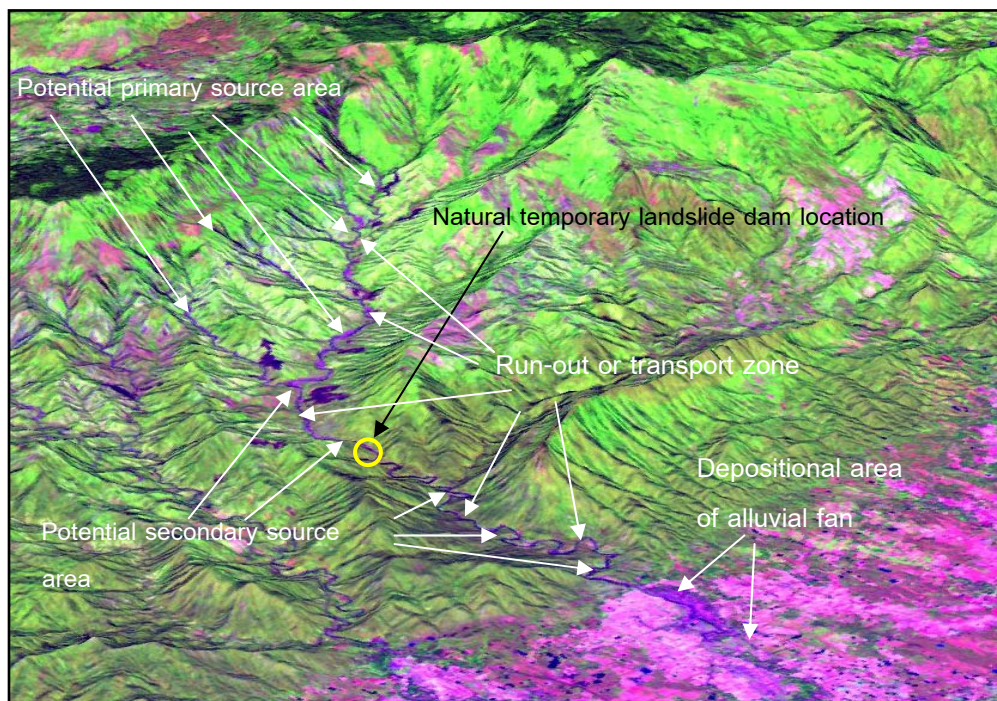


Figure 7-4 Three-dimensional drupe of false color composite of Landsat 7 ETM+ (R=5, G=4, B=3) acquired on 21<sup>st</sup> November 2001 through a 1:20,000 base-scale DEM showing distinguish characteristics after 8/11 flow-flood occurrence in Nam Ko Yai sub-catchment, and the depositional area of alluvial fan.

gentle slope. This could be the potential secondary source area (Figure 7-4) where debris incorporated into the primary debris flows to form a significant volume through the run-out or transport zone as previously mentioned in Chapter 5.

With supporting study results on the soil engineering properties as previously mentioned in Chapter 5, the highly weathered rocks of Ls Formation with its thick residual or colluvial soils appeared to influence the slope failures on the hillsides and debris flows in the channels. These almost undrained clayey soils with increasing load pressure and less internal shear strength would have caused the mass movement beyond the critical load pressure.

Additionally, the previously-mentioned physical nature of the source area and run-out zone to the flow-flood occurrence, the amount and intensity of precipitation falling, steep hill slopes and long-running sinusoidal stream channel were key factors as well. Ten days of continuous rainfall to the cumulative peak on 8/11 triggered the severe flow-flood in these zones of weak materials as mentioned in Chapter 4.

During the flow- flood processes, a temporary natural landslide dam might have built up somewhere in the causeway of this stream, most probably near Tad Fa waterfall. The temporary natural landslide dam could have been formed when debris of plant remains, trees, soils and boulders both from several previous and this 8/11 events were locked at this specific location, forming a reservoir upstream as previously mentioned in Chapter 5. Then another powerful flow-flood might followed to break the dam, perhaps with surges up to 10 m high, to send water and debris flowing further down to destroy the village on the alluvial fan.

After this serious debris flow-flood occurrence in the year 2001 that completely traversed and removed the former sediments along the channels together with almost-entirely wiping out of trees, it should take many more years to let the parameter conditions to build up again. The plant debris and sediments are reduced at present.

This last conclusive remark was noted from a fact that the relative higher amount of rainfall in the following year 2002 in this same area did not resulting a serious flow-flood event except a mild flash flood occurring for only a few hours overbanks.

### **7.3 FLO-2D simulation results for validation of the suspected temporary landslide dam occurrence**

To validate the suspected temporary landslide dam occurrence, some justification must be employed. Here an FLO-2D simulation technique was used.

In general, the FLO-2D is a simple volume conservation model that distributes a flood hydrograph over a system of square grid elements (FLO-2D Users Manual, 2003). It implements the Diffusive Hydrodynamic Model (DHM) created by Hromadka and Yen (1987), which is a simple numerical approach with a finite difference scheme that permits modification of the grid element attributes. FLO-2D software model allows the user to delineate flood hazards and designing flood mitigation. Details can be added to the simulation by turning on or off switch for various components such as street, sediment transport, culverts and many others. Channel flow is one-dimensional, with the channel geometry represented either by natural, rectangular or trapezoidal cross sections, whereas overland flow is modeled two-dimensionally and channel overbank flow is computed when the channel capacity is exceeded. When the flow overtops the channel, it will disperse to other overland grid elements based on topography, roughness and obstructions. Besides, FLO-2D software model also allows to route hyperconcentrated sediment flows as a fluid continuum by predicting viscous and yield stresses as function of sediment concentration is employed and sediment volumes are tracked through the system. As sediment concentration changes for a given grid element, dilution effects, flow cessation and remobilization of deposits are simulated (FLO-2D Users Manual, 2003). It is noted that the later ability of FLO-2D software model cannot firstly be applied in the sub-catchment area because of the lack of sediment-flow data recorded from the 8/11 flow-flood event.

In this discussion, flow-2d simulation was preliminary applied to numerical model of channel flow conditions in terms of water height from the channel floor (hereafter will be conveniently used as *water height*) calculated from the rainfall intensity during 1<sup>st</sup> to 10<sup>th</sup> August 2001 before 8/11 flow-flood event with two scenarios . Firstly, the flow-2d simulation was back analyzed in the condition of the channel topography without a temporary landslide dam (hereafter will be conveniently used as *the condition without dam*). Secondly, the flow-2d simulation was back analyzed in the condition of the channel topography with a temporary landslide dam (hereafter will be conveniently used as *the condition with dam*) that was 10 m high from the channel floor at the location in the central part of the sub-catchment (referred to Figure 7-4). This is conducted to first numerical validating the possibility of the occurrence of a suspected temporary landslide dam in the location as previously mentioned as one of the most important causes of the 8/11 flow-flood event.

There are two important steps to start a simulation with FLO-2D: obtaining the topographic data base and developing the flood hydrograph. For the first step, the 50 m. cell size DTM available for the sub-catchment, that is probably not accurate enough for a highly detailed analysis, but it can be sufficient for a preliminary validation of the suspected landslide dam occurrence. The second step arises from the fact that each flood simulation requires an inflow flood hydrograph on a rainfall data that previously extrapolated in Chapter 3.

Finally, the FLO-2D model created accurate representations of the first- and secondary scenario as shown in Figures 7-5 to 7-9. The details of these two scenarios in the sub-catchment during 9<sup>th</sup> to 11<sup>th</sup> August 2001 (before 8/11 event) are discussed below.

From the simulation with FLO-2D model in the condition of the sub-catchment without dam, it revealed that the water height was apparent at first and increased up to 0.5 - 1.0 m along the stream channels throughout the upper and middle parts of the sub-catchment at 8 p.m. on 9<sup>th</sup> August 2001 (about 31 hours before the 8/11 event) while the rainfall accumulation was more than 100 mm as modeled in Fig 7-5. At 3 a.m. on 10<sup>th</sup>

August 2001 (about 24 hours before the 8/11 event), the water height in the condition without dam was generally increased up to 0.5 - 2.0 m along the stream channels further down in the middle part of sub-catchment while the rainfall accumulation was approximately 120 mm as modeled in Fig 7-6. It is noted that the water height in the further down of middle part along the channels was locally increased to 3.0 – 4.5 m. At 3 a.m. on 11<sup>th</sup> August 2001 (0.5 hour before the 8/11 event) the water height in the condition without dam was generally increased up to 1.0 - 3.0 m along the stream channels in the upper and middle parts, and significantly increased up to 1.0 - 10.0 m in the further down of lower part of sub-catchment while the rainfall accumulation was more than 140 mm as modeled in Figure 7-7.

From the simulation with FLO-2D model in the proposed condition of nearly 10 m height landslide dam occurrence at the location near Tad Fa waterfall (referred to Figure 7-4), it is noted that the water height was generally increased up to 1.0 - 3.0 m along the channels upstream from this location at 3 a.m. on 10<sup>th</sup> August 2001 (about 24 hours before the 8/11 event) while the rainfall accumulation was approximately 110 mm as modeled in Figure 7-8. It is noted that the water height along the channels in the proposed dam location was significant increased up to 5.0 – 12.0 m and less increased further down from this location. At 3 a.m. on 11<sup>th</sup> August 2001 (about 0.5 hour before the 8/11 event) the water height in the condition with dam was generally increased up to 1.0 - 3.0 m along the stream channels in the upper part of sub- catchment, 1.0 - 5.0 m in the middle part upstream from the dam location, 5.0 – 12.0 m in the proposed dam location, and still increased up to 1.0 - 10.0 m in the lower part further down from the proposed dam location while the rainfall accumulation was more than 140 mm as modeled in Figure 7-9.

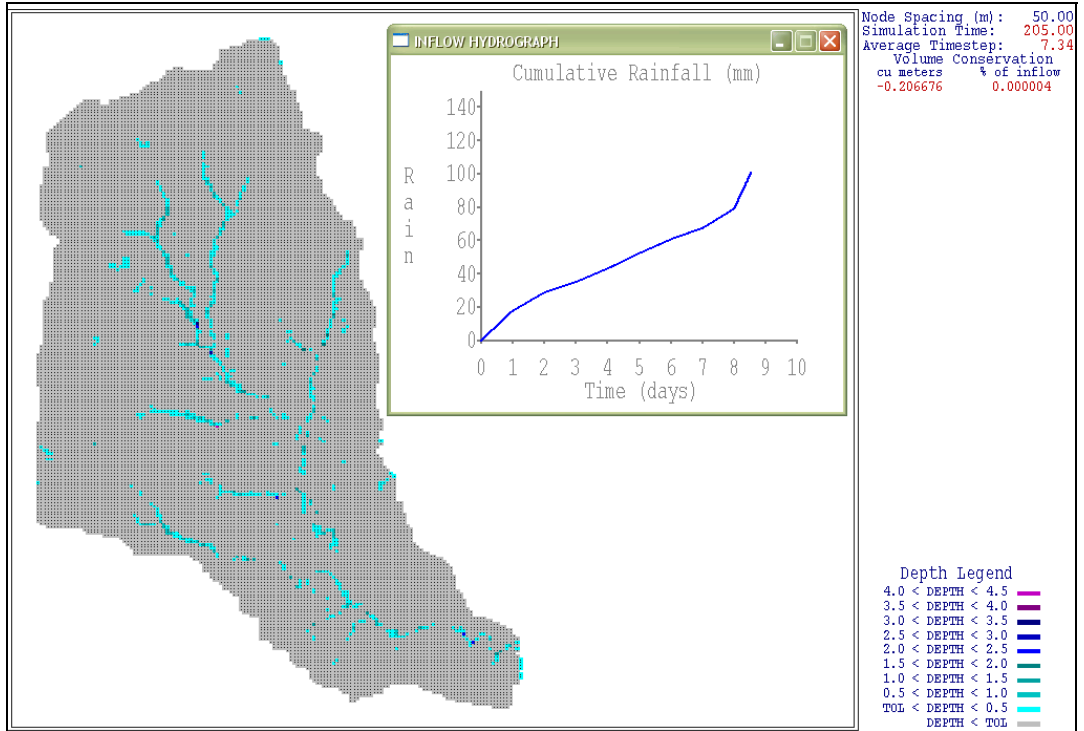


Figure 7-5 FLO-2D simulation results of the channel flow conditions of water height from the condition without dam while the rainfall accumulation was more than 100 mm at 8 p.m. on 9<sup>th</sup> August 2001 (about 31 hours before the 8/11 event).

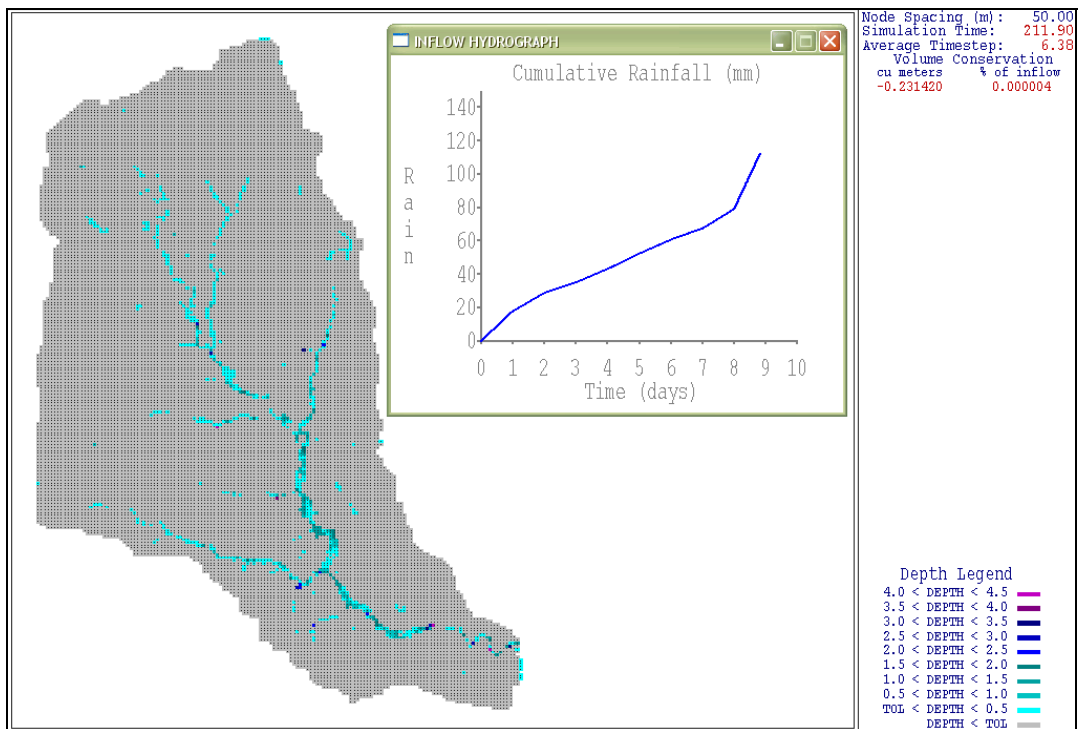


Figure 7-6 FLO-2D simulation results of the channel flow conditions of water height from the condition without dam while the rainfall accumulation was 120 mm at 3 a.m. on 10<sup>th</sup> August 2001 (about 24 hours before the 8/11 event).

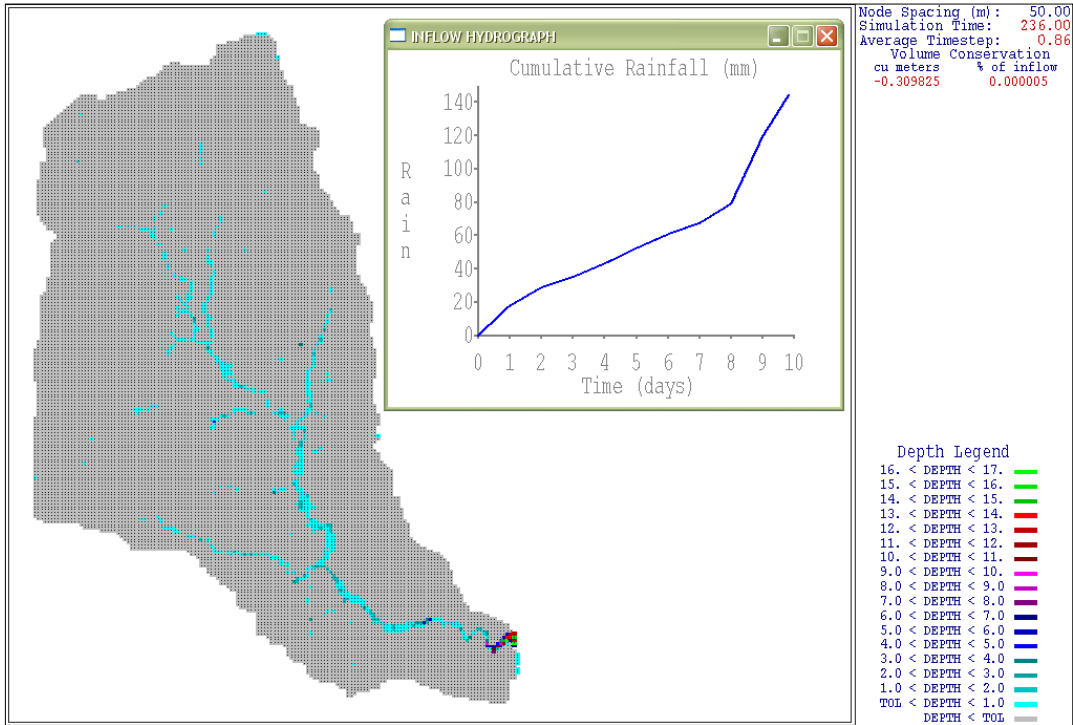


Figure 7-7 FLO-2D simulation results of the channel flow conditions of water height from the condition without dam while the rainfall accumulation was more than 140 mm at 3 a.m. on 11<sup>th</sup> August 2001 (0.5 hour before the 8/11 event).

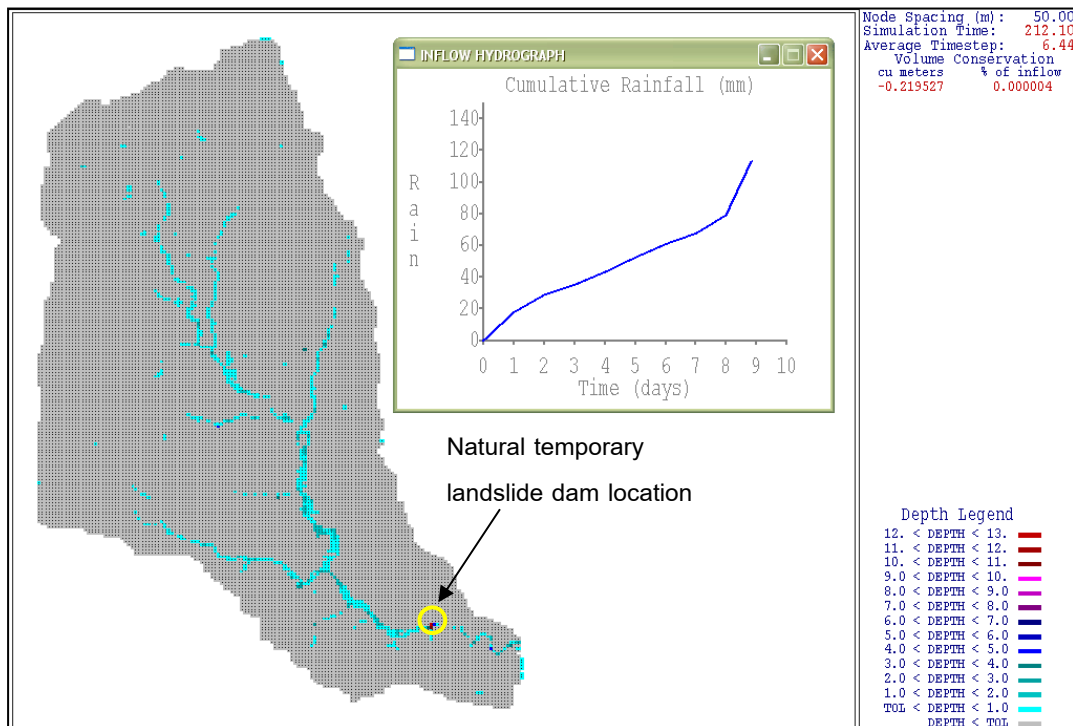


Figure 7-8 FLO-2D simulation results of the channel flow conditions of water height from the condition with dam while the rainfall accumulation was 120 mm at 3 a.m. on 10<sup>th</sup> August 2001 (about 24 hours before the 8/11 event).

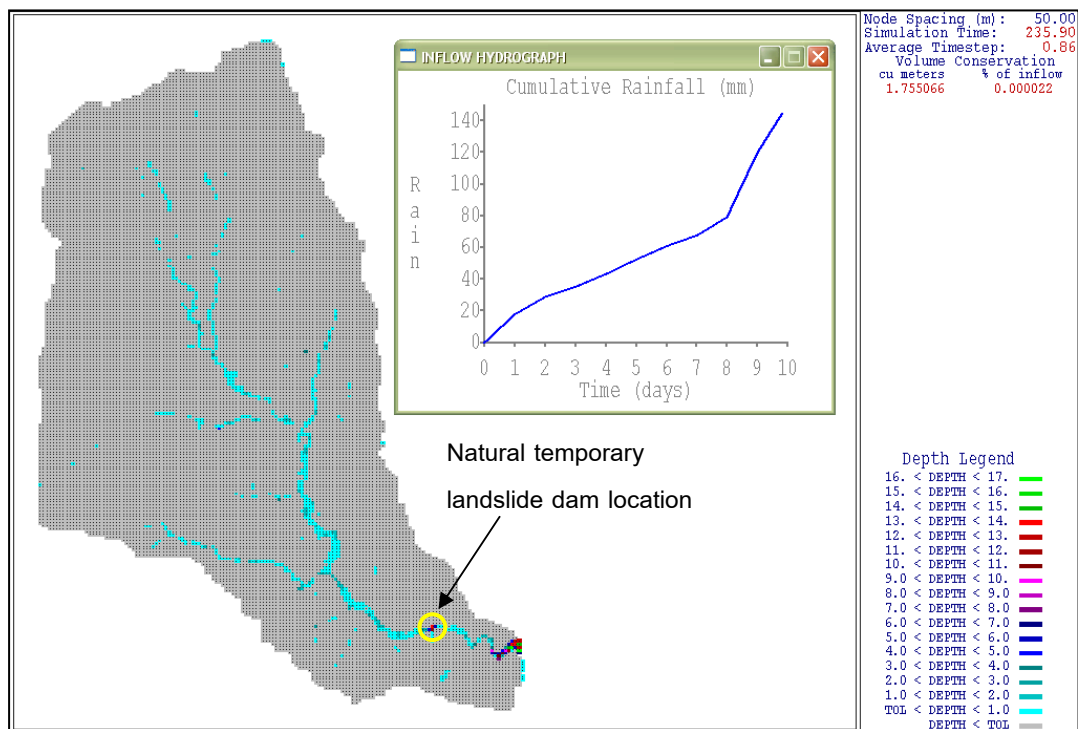


Figure 7-9 FLO-2D simulation results of the channel flow conditions of water height from the condition with dam while the rainfall accumulation was more than 140 mm at 3 a.m. on 11<sup>th</sup> August 2001 (0.5 hour before the 8/11 event).

In conclusion according to the first scenario, the flow-2d simulation was back analyzed in the condition without dam, the channel flow conditions of water height had some significant increasing values in the middle and further lower parts of the sub-catchment during 9<sup>th</sup> to 11<sup>th</sup> August 2001 (before 8/11 event). Whereas, the channel flow conditions in terms of water height had much more increasing values compared to the condition with dam, especially in the middle part of the sub-catchment next to the suspected location of temporary landslide dam.

Although the calculated values from the proposed FLO-2D model above have only some significant to validate the possibility of occurrence of natural landslide dam before the 8/11 flow-flood event, the simulated concept of the landslide dam occurrences can be useful to predict the past and future events in the other locations in the sub-catchment in order to propose the better hazard- and risk mapping in the further studies.

## CHAPTER 8

### CONCLUSION

The evaluation of potential for the 2001 debris flow and debris flood in Nam Ko Yai sub-catchment and its alluvial fan are summarized and concluded with further recommendation below.

#### 8.1. Evaluation of potential for the 2001 debris flow and debris flood

In this research, three data input, which are thematic (GIS and remote sensing) data preparation, field investigation, and laboratory analysis were used to investigate the parameters influencing the debris flow and associated debris flood occurrence on 11<sup>th</sup> August 2001 in Nam Ko area, Changwat Phetchabun, Central Thailand. Furthermore, the purpose is to analyze the potential source area, run-out zone, and depositional area; and to determine the evidences of the potential for hazards in Nam Ko Yai sub-catchment and its active alluvial fan. Finally, the relationship between the sedimentary sequences and the debris flow and debris flood occurrence in the active alluvial fan is also defined.

The input data used for flow-flood hazard assessment consists of several data categories of spatial data from the available resources, digitizing from available maps, and prepared from image interpretation and field investigation data. Thematic maps of the input data produced in this thesis consist of elevation (digital elevation data, Digital Elevation Model-DEM, aspect, slope, landform topography), hydrology (drainage pattern, sub-catchments characteristics), meteorology of rainfall intensity, geology (rock unit), soil properties (soil group unit, soil thickness), flow-flood inventory of scar-scouring and depositional locations, land cover, and infrastructure and human settlement. These input data were further used to analyze the debris flow-flood hazard by the statistic analysis.

To investigate the parameters influencing the debris flow and associated debris flood occurrence, the relationship of debris flow-flood scar-scouring and each relevant parameter was analyzed for debris flow-flood susceptibility assessment using the univariate probability method and landslide susceptibility map. A key assumption using this approach is that the potential (occurrence possibility) of flow-flood processes would be comparable to the actual frequency of flow-flood processes and relationships between each parameter are independent. In Nam Ko Yai sub-catchment, scar-scouring locations detected from orthophotograph interpretation and field surveys were formed into a GIS database. Various maps were constructed from the flow-flood relevant parameters derived from the database. The parameters involved in the debris flow-flood susceptibility analysis are flow-flood inventory of scar-scouring locations, slope, landform topography, geology, soil group unit, soil thickness, land cover, and stream proximity. Using these parameters, probability method was applied to analyze the debris flow-flood hazard. It is concluded that debris flow and debris flood occurrence probability value is generally much higher dependent on the significant influencing parameters, namely, slope, landform topography, geology, and land cover. The analyzed result was used to reconstruct the GIS database, and mapped. Furthermore, calculation of debris flow-flood susceptibility was applied to analyze the debris flow-flood hazard in the sub-catchment. It was concluded from the susceptibility map that the middle part of Nam Ko Yai stream channel and its adjacent banks had a very high to high flow-flood susceptibility whereas the lower downstream part of the stream had a high flow-flood susceptibility. It was also remarked that the western and northern steep-cliff areas had a low to moderate flow-flood susceptibility whereas the main other parts else of the sub-catchment have in general very low flow-flood susceptibility.

For the flow-flood event reconstruction and its potential in Nam Ko Yai sub-catchment, the evidences of geotechnical properties of rocks and soils, as well as evidence of the channel configuration and suspected natural dam location were studied. It was concluded that the disastrous debris flow-flood event was not the work of the unusual high amount of rainfalls alone, as previously theorized. Instead it was the work of combined parameters from the terrain characteristics with specific land cover to the

time-delay for accumulation of debris and sediments. This combination of parameters also cause debris flow-flood accompanied with a high amount of precipitation. The damage could be made greater by a natural temporary landslide dam forming at locations within the stream course, followed by destruction of the dam under the weight of impounded water. After such a disastrous event, it could take time for more plant debris and sediments in the sub-catchment area to accumulate before the next debris flow-flood.

After realizing the parameters and processes that governed flow-flood initiation, transport, and sediment bulking in the area of Nam Ko Yai sub-catchment, the stratigraphic recognition and characteristics of the previous alluvial fan deposits were thus essential to evaluate the past flows-floods here. A geological evaluation was done following a two-step procedure consisting of an initial delineation of the active depositional area, and a subsequent detailed, site-specific analysis of the hazard within the active alluvial fan.

In addition, radiocarbon dating of the preserved wooden debris suggested that the debris flow-flood were recurrent processes at least twice (2,618 $\pm$  35 before present and post-1950, respectively) before this 8/11disastrous event. From the previous stratigraphic sequences of the alluvial fan and these radioactive dating results, it is strongly confirmed that this is an active alluvial fan.

Thus the areas down below, especially where the settlements situate on the distinctive alluvial fan, will always be in danger if no proper caution or preinvestigation is not employed. This kind of tragedy could also happen easily in any other areas if the coincident factors exist.

## **8.2 Recommendation for more accurate evaluation of potential for debris flow and debris flood**

Although the methodology of evaluation is appropriate for this preliminary stage of investigation in the present study area, the derivation using this methodology are based on incomplete or unavailable information in some parameters according to the

limitation of accessibility and rarely records in the past. The evaluation of potential for debris flow and debris flood could be substantially improved if the same methodology is applied systematically and carefully over the entire area. Studies needed for careful evaluation of potential should address the following questions:

- 1) The flow-flood susceptibility analysis using the bivariate probability method to explain the actual frequency of flow-flood processes and relationships between each parameter that are dependent to each other.
- 2) Relations between rainfall, groundwater levels, and debris flow movement. Such relations would permit prediction of timing of debris flows. Real-time prediction and warnings could then be made based on telemetered rainfall, water level, or ground-movement information.
- 3) Detailed site-specific studies including stability analyses of the partly-detached shallow landslides.
- 4) The processes of transformation from shallow landslides to debris flow. Understanding developed through such study could help evaluate the potential for debris flow of the partly-detached shallow landslides.
- 5) Volume analysis of the incorporation of channel sediments or materials scoured from the channels and its banks by debris flow and debris flood.
- 6) The transition from debris flow to debris flood. Understanding of this transition would permit more accurate prediction of the nature of flow from the canyon mouth to the risk area of the active alluvial fan.
- 7) Actual and potential flow paths analysis by using the hydrological flow models (such as FLO-2D model, etc.). Understanding flow directions, flow accumulation and sediment volume in the stream lines and stream order would utilize to delineate the areas of potential debris flow and debris flood hazard.
- 8) Recurrence of debris flow and debris flood at the canyon mouth of alluvial fan area. Systematic field investigation and dating of deposits over the entire alluvial fan would help define the expectable frequency of events from the canyon of Nam Ko Yai sub-catchment.

## REFERENCES

- Alamgir, Md. S., 1997. The application of remote sensing and GIS to the impact assessment and resource management of flood control, drainage and irrigation projects: A case study of Meghna Dhonagoda irrigation project, Bangladesh. Thesis for the degree of Master in Engineering, School of Environment, resources and Development, Asian Institute of Technology, Bangkok, Thailand, 83 pp.
- Anbalagan. D., 1992. Landslide hazard evaluation and zonation mapping in mountainous terrain. Eng. Geol. 32 :267-277.
- Anbalagan. R., and Singh, B., 2001. Landslide hazard and risk mapping in the Himalaya. In: Tianchi , Li , chalise, S.R. and Upreti , B.N. (eds) Landslide Hazard mitigation on the Hindu Kush-Himalayas. International Center for Integrated Mountain Development, Kathmandu, Nepal , pp. 163-188.
- Anderson, M.G., 1988. Modelling geomorphological systems. (n.p.):John Wiley & Sons, 458 pp.
- ASTM D 422-63. Standard Test Method for Particle-Size Analysis of Soils. In Annual Book of ASTM Standards (Vol. 04.08). Philadelphia: American Society for Testing and Materials.
- ASTM D 2487-00. Standard Classification of Soils for Engineering Purposes (Unified Soil Classification System). In Annual Book of ASTM Standards (Vol. 04.08). Philadelphia: American Society for Testing and Materials.
- ASTM D 2488-00. Standard Practice for Description and Identification of Soils (Visual-Manual Procedure). In Annual Book of ASTM Standards (Vol. 04.08). Philadelphia: American Society for Testing and Materials.
- ASTM D 4318-00. Test Method for Liquid Limit, Plastic Limit, and Plasticity Index of Soils. In Annual Book of ASTM Standards (Vol. 04.08). Philadelphia: American Society for Testing and Materials.

- ASTM D5731-95. Standard test method for determination of the point load strength index of rock. Annual Book of ASTM Standards, 04.08. Philadelphia: American Society for Testing and Materials.
- Brown, E.T. (eds.) 1981. Rock Characterization Testing and Monitoring: ISRM Suggested Methods. International Society for Rock Mechanics: Pergamon Press.
- Aung, Z., 1991. The study of landslide susceptibility using the GIS approach, West of Amphoe Phi Pun, Nakhon Sri Thammarat Province. Master's Thesis, Asian Institute of Technology. Bangkok, Thailand, 84 pp.
- Bell, F.G., 1999. Geological hazards : Their assessment, avoidance and mitigation. E & FN Spon, an imprint of Routledge, pp. 1-12, 114-163, 245-281, 390-439.
- Beverage, J.P., and Culbertson, J.K., 1964. Hyperconcentrations of suspended sediment: American Society of Civil Engineers, Journal of the Hydraulics Division 90, HY6:117-126.
- Blair, T.C., and McPherson, J.G., 1994. Alluvial fan processes and forms, in Abrahams, A.D., and Parsons A.J., editors, Geomorphology of desert environments: London, Chapman and Hall, pp. 355-402.
- Bonham-Carter, G.F., 1996. Geographic information systems for geoscientists, modelling with GIS. Canada Pergamon Press, 398 pp.
- Brabb, E.E., 1984. Innovative approaches to landslide hazard and risk mapping. International Symposium on Landslides, Toronto, Canada 1 (September):307-323.
- Brand, E.W., 1984. Landslide in Southeast Asia: a state –of-the-art report. Proceeding of the 4<sup>th</sup> International Symposium on Landslides 1:17-59.
- Breunig, M., 1996. Integration of spatial information for geo-information systems. Lecture notes in earth sciences, Springer-Verlag Berlin Heidelberg, 171 pp.
- Burrough, P.A., 1986. Principals of geographical information systems and land resources assessment. Clerandon Press, Oxford, England, 194 pp.

- Cannon, S. H., 1997. Evaluation of the potential for debris and hyperconcentrated flows in Capulin Canyon as a result of the 1996 Dome Fire, Bandelier National Monument, New Mexico: U.S. Geological Survey, Open File Report 97-136.
- Carrara, A., 1983, Multivariate models for landslide hazard evaluation. Mathematical Geology 15, 3:403-427
- Carrara, A., Cardinali, M., Detti, R., Guzzetti, F., Pasqui, V., and Reichebach, P., 1991. GIS techniques and statistical models in evaluating landslide hazard. Earth Surf Proc Landforms 16:427-445.
- Carrara, A., Cardinali, M., Detti, R., Guzzetti, F., and Reichebach, P., 1995. GIS-based techniques for mapping landslide hazard. In: Carrara A, Guzzetti F (eds) Geographical information systems in assessing natural hazards. Kluwer, Dordrecht, pp. 135-176.
- Chandler J.H. and Brunsden D., 1995, Steady state behaviour of the Black Ven Mudslide: the application of archival analytical photogrammetry to studies of landform change. Earth Surface Processes and Landforms, 20:255-275.
- Chandler J.H. and Moore, R., 1989, Analytical photogrammetry: A method for monitoring slope instability. Quarterly Journal of Engineering Geology, 22:97-110.
- Chi, K., Lee, K, and Park, N., 2002. Landslide stability analysis and prediction modeling with landslide occurrences on KOMPSAT EOC imagery. Korean Journal of Remote Sensing 18, 1:1-12.
- Corominas, J., Remondo, J., Farias, P., Estevao, M., Zezera, J., Teran, J. D., Dikau, R., Schrott, R. D. L., Moya, J., and Gonzalez, A., 1996. Debris flow. In Report No. 1 of the European Commission Environment Programme Contract No. EV5V-CT94-0454: landslide recognition (Dikau, R., Brunsden, D., Schrott, L., and Ibsen, M., eds.), John Wiley & Sons, 251 pp.
- Costa, J. E., and Jarrett, R.D., 1981. Debris flow in small mountain channels of Colorado and their hydrologic implication. Bulletin of the Association of Engineering Geologists, XVIII, 3:309-322.

- Costa, J. E., 1984. Physical geomorphology of debris flows. In Developments and Applications of Geomorphology (Eds J. E. Costa and P. L. Fleisher), Springer-Verlag, pp. 268-317.
- Costa J. E., 1988. Rheologic, morphologic, and sedimentologic differentiation of water floods, hyperconcentrated flows, and debris flows. In Baker, V.E., Kochel, C.R., and Pat-ton, P.C., editors, Flood geomorphology: New York, John Wiley and Sons, pp. 113-122.
- Crozier, M. J., 1973. Techniques for the morphometric analysis of landslips. Zeitschrift für Geomorphologie N.F. 17, 1:78-101.
- Crozier, M. J., 1986. Landslides: causes, consequences & environment. Croom Helm, London, 252 pp.
- Cruden, D.M., 1991. A simple definition of a landslide, Bulletin of International Association of Engineering Geology 43:27-29.
- Dai, F. C., Lee C. F., Li, J, and Xu, Z. W., 2001. Assessment of landslide susceptibility on the natural terrain of Lantau Island, Hong Kong. Environmental Geology 40 (3) January 001, Springer-Verlag, pp. 381-391.
- DeGraf, J.V., 1991. Increased debris flow activity due to vegetation change. Proceeding of the 6<sup>th</sup> International Symposium on Landslides:Chrischurch, New Zealand, pp. 1365-1373.
- Dikau, R., Brunsten, D., Schrott, L., and Ibsen, M., 1996. Landslide recognition. Report No. 1 of the European Commission Environment Programme Contract No. EV5V-CT94-0454. John Wiley & Sons, 251 pp.
- Environmental Geology Division, 2003. Project of landslide hazard mapping in Thailand. Department of Mineral Resources (www.dmr.go.th), Ministry of Natural Resources and Environments, Bangkok, Thailand. (in Thai)
- ESCAP, 1989. Catastrophic landslides and sheet flooding in an intermontane tropical basin, southern Thailand, 20 pp.

- ESCAP, 1997. Guidelines and manual on land-use planning and practices in watershed management and disaster reduction, United Nations, June, 1997, 127 pp.
- Einstein, H. H., 1988. Landslide risk assessment procedure. In: Bonnard C (ed) Proceedings of the Fifth International Symposium on Landslides 2:1075- 1090
- Fernandez, C.I., Castillo, T.F.D., Handouni, R.E., and Montero, J.C., 1999. Verification of landslide susceptibility mapping: a case study. Earth Surf Proc Landforms 24:537-544.
- FLO-2D Users Manual, 2003. Version 2003.06, Nutrioso, Arizona, USA.
- Fookes, P.G., Dale, S.G., Land, J.M., 1991. Some observations on a comparative aerial photography interpretation of a landslipped area. Quarterly Journal of Engineering Geology 24:249-265.
- Gagon, H., 1975. Remote sensing of landslide hazards on quick clays of Eastern Canada. Proceedings 10th International ERIM, Ann Arbor, Michigan, pp. 803-810.
- Giraud, R. E., 2002. Guidelines for the geological evaluation of debris-flow hazards on alluvial fan. Rocky Mountain - 54th Annual Meeting (May 7–9, 2002): Cedar City, Utah.
- Giraud, R. E., 2005. Guidelines for the geological evaluation of debris-flow hazards on alluvial fan in Utah. Miscellaneous publication 05-6, Utah Geological Survey, Department of Natural Resources, 20 pp.
- Goodchild, M.F., Steyaert, L.T., Parks, B.O., Johnston, C., Maidment, D., Crane, M., and Glendinning, S., 1996. GIS and environmental modeling: progress and research issues. GIS World, Inc., 486 pp.
- Gupta, R.P., and Joshi, B.C., 1989. Landslide hazard zoning using the GIS approach – a case study from the Ramganga catchment, Himalayas. Eng Geol 28:119-131.
- Gupta, A. K. Saha R. P., and Arora, M. H., 2002. GIS-based landslide hazard zonation in the Bhagirathi (Ganga) valley, Himalayas. INT. J. Remote Sensing 23, 2:357-369.

- Hansen, A., 1984. Landslide hazard analysis. Slope instability: edited by D. Brunsten and D. B. Prior. (n.p.):John Wiley& Sons, pp. 523-601.
- Harper, S .1996 . Debris flow triggered by the November 1988 rainstorm in Phipun district, Nakhon Si Thammarat province, southern Thailand .Docteral dissertation, Department of Geography, Graduate school, University of Geogia.
- Hartlen, J. and Viberg, L., 1988. General report: evaluation of landslide hazard. In Proc., Fifth International Symposium in Landslides (C.Bonnard ed), Lausanne, A.A. Balkema, Rotterdam, Netherlands, Vol.1: 3-35.
- Henry, J.K., and Heinke,G. W., 1996. Environmental science and engineering, second edition. (n.p.):Printice-Hall International Inc., pp. 85-110.
- Hromadka, T.V., and Yen, C.C., 1987. Diffusive hydrodynamic model. US Geological Survey, Water Resources Investigations Report 87-4137, Denver Federal Center, Colorado.
- Huang, S.L. and Chen, B.K., 1991. Intergration of Landsat and terrain information for landslide study. Proceedings 8th Thematic (ERIM), Denver, Colorado, Vol 2: 743-754.
- Hutchinson, J. N., 1988. Morphological and geotechnical parameters of landslides in relation to geology and hydrology. In Landslides, Proc. 5th. Int. Symp. on Landslides (Ed. C. Bonnard), Vol. 1:3-35.
- International Association of Engineering Geology (IAEG), 1976. Engineering geological maps: A guide to their preparation, UNESCO Press, Paris, 79 pp.
- Ikeya, H., 1974. Introduction for Sabo Works. Tokyo:Bunkyou-ku.
- Innes, J., 1985. Lichenometric dating of debris flow deposits on alpine colluvial fans in southwest Norway. Earth Surface Processes and Landforms 10:519-524.
- Iverson, R.M., 2003. The debris-flow rheology myth, in Rickenmann, D., and Chen, C.L., editors, Proceedings of the Third International Conference on Debris-Flow Hazards Mitigation - Mechanics, Prediction, and Assessment, September 10-12, 2003, Davos, Switzerland: Rotterdam, Millpress, pp. 303-314.

- Jishan, W., and Tianchi, L., 2001. Behavior and characteristics of debris flows. In Landslide Hazard Mitigation in the Hindu Kush-Himalayas, International Center for Integrated Mountain Development, Kathmandu, Nepal, pp. 203-214.
- Jworchan, I .L .1995 .Initiation of November 1988 debris flows in Khao Luang, southern Thailand .Disertation Proposal, Asian Institute of Technology, Bangkok, Thailand, 94 pp.
- Khantaprab, C. 1993. Disaster: A case study of southern Thailand. Chulalongkorn University, Bangkok, Thailand (In Thai).
- Lee, S., and Min, K., 2001. Statistical analysis of landslide susceptibility at Yongin, Korea. Environmental Geology 40:1095-1113.
- Lee, S., Chang, B.,Choi W., and Shin, E., 2001. Regional susceptibility, possibility and risk analyses of landslides in Ulsan Metropolis City, Korea.
- Local Government Office, 2002. Information of risk areas in Changwat Phetchabun. Special Activity Section, Local Government Office of Changwat Phetchabun, Ministry of Interior, Thailand. (in Thai)
- Lynn M. Highland, Stephenson D. Ellen, Sarah B. Christian, and William M. Brown, 1997. Debris-Flow Hazards in the United States, U.S. Geological Survey Fact Sheet 176-97.
- Maireang, V., Chotikkai, J., and Duangduan, P., 1982. Soil mechanics. Department of Civil Engineering, Kasetsart University. (in Thai)
- Marzo, M., and Puigdefabregas, C., 1993. Alluvial sedimentation. Special Publication Number 17 of the International Association of Sedimentologists, Blackwell Scientific Publications, 586 pp.
- McGregor, D.F.M, and Thompson, D.A., 1995. Geomorphology and land management in a changing environment. John Wiley & Sons, 339 pp.
- Mc Donalds and Grubbs (1975); Meijerink, A. M. L., de Brouwer, H. A. M., Mannaerts, C. M., and Valenzuela, C., 1994. Introduction to the use of Geographic Information Systems for practical hydrology. International Institute for Aerospace Survey and

- Earth Sciences (ITC) Publication Number 23, Enschede, The Netherlands, 242 pp.
- Miall, A.D., 1996. The geology of fluvial deposits. Springer-Verlag Heidelberg, 582 pp.
- Miyajima, S., 2001. Debris flow studies in Japan. In: Tianchi , Li , chalise, S.R. and Upreti, B.N. (eds) Landslide Hazard Mitigation in the Hindu Kush-Himalayas, International Center for Integrated Mountain Development, Kathmandu, Nepal, pp. 215-228.
- Morgan, B.A., Wieczorek, G.F., Campbell, R.H., and Gori, P.L., 1997. Debris-flow hazards in areas affected by the June 27, 1995 storm in Madison County, Virginia: U.S. Geological Survey, Open File Report 97-438.
- Morgan, R.P.C., 1986. Soil erosion and conservation. Longman Scientific & Technical, 298 pp.
- Nagarajan, R., Mukherjee, A., Roy, A. and Khire, M.V., 1998. Temporal remote sensing data and GIS application in landslide hazard zonation of part of Western Ghat, India. INT. J. Remote Sensing 19, 4:573-585.
- Naranjo, J.L., Van Westen, C.J., and Soeters, R., 1994. Evaluation the use of training areas in bivariate statistical landslide hazard analysis: a case study in Colombia. Int. Inst. Aerospace Surv. Earth Sci. J 3:292-300.
- National Economic and Social Development Board (NESDB), 1997. Natural hazard management in southern region of Thailand. Natural Resources Faculty, Prince of Songkla University and UNDP: 461 pp. (in Thai)
- Natural Resources Canada, 2002. Quantitative prediction models for landslide hazard mapping. Available from:  
[http://www.nrcan.gc.ca/gsc/mrd/sdalweb/sdi\\_cd/intro.html](http://www.nrcan.gc.ca/gsc/mrd/sdalweb/sdi_cd/intro.html)
- Niemann, K.O., and Howes, D.E., 1991. Applicability of digital terrain models for slope stability assessment. Int. Inst. Aerospace Surv. Earth Sci. J. 1991-3:127-137.

- Nilaweera, N.S., 1994. Effects of tree roots on slope stability: The case study of Khao Luang mountain area, southern Thailand. Asian Institute of Technology, Bangkok, Thailand.
- NOAA-USGS Flow Task Force, 2005. NOAA-USGS debris-flow warning system-Final report. U.S. Geological Survey Circular 1283, 47 pp.
- Nutalaya, P., 1991. Catastrophic landslides and sheet flooding in an intermontane tropical basin, southern Thailand. Asian Institute of Technology, Bangkok, Thailand.
- Office of the United Nations Disaster Relief Co-ordinator (UNDRO), 1980. Natural disasters and vulnerability analysis. Report of Expert Group Meeting (9-12 July 1979), Geneva, 49 pp.
- Osterkamp, W.R., and Hupp, C.R., 1987. Dating and interpretation of debris flows by geologic and botanical methods at Whitney Creek Gorge, Mouth Shasts, California. Geol. Am. Rev. Eng. Geol. VII:157-163.
- Owen, L.A., Sharma, M.C., and Bigwood, R., 1995. Mass movement hazard in the Garhwal Himalaya: the effects of the 20 October 1991 Garhwal earthquake and the July-August 1992 monsoon season. In: McGregor, D.F.M., and Thompson, D.A. (eds) geomorphology and land management in a changing environment. (n.p.): John Wiley & Sons, pp.69-88.
- Pachauri, A.K., and Pant, M., 1992. Landslide hazard mapping base geological attributes. Eng Geol 32:100-81.
- Pantanahiran, W. 1994. The use of Landsat imagery and digital terrain models to assess and predict landslide activity in tropical area. Doctoral Dissertation, University of Rhode Island, U.S.A.
- Pattanakanok, B., 2001. Landslide risk assessment from 3 dimension of Landsat (Abstract). Conference of Mapping and Geo-informatics, 17-18 December 2001, Bangkok, Thailand. (in Thai)
- Petak, W.J., and Atkisson, A.A., 1982. Natural hazard risk assessment and public policy.

Springer-Verlag New York Inc. 489 pp.

Petchprayoon, P., 2002. The prediction of flash floods caused by dam failure and overflow through a spillway case study at the Tha Dan Dam, Changwat Nakhon Nayok. Master Science Thesis, Graduate School, Mahidol University, Thailand, 166 pp. (in Thai)

Phien-wej, N., Zhibin, T., and Aung, Z. 1991. Unprecedented landslides in granitic mountain of southern Thailand. Glissements De Terrain 2:1387-1393.

Pierson, T.C., and Costa, J.E., 1987. A rheologic classification of subaerial sediment-water flows, in Costa, J.E., and Wiezorek, G.F., editors, Debris flows/avalanches: Geological Society of America, Reviews in Engineering Geology VII:1-12.

Popescu, M.E., 1992. A suggested method for reporting landslide causes. The international Geotechnical Societies' UNESCO Working Party on World Landslide Inventory, Civil Engineering Institute, Department of Soil Mechanics and Foundation Engineering, Bucharest, Romania, 12 pp.

Price, M.F., and Heywood, I.D. 1994. Mountain environment and geographic information System. (n.p.):Briston, PA: Taylor & Francis, 375 pp.

Pye, K., 1994. Sediment transport and depositional processes. Blackwell Scientific Publications, 397 pp.

Rengers et al. (1992). Rengers, N., Soeters, R., and Westen, C. J. V., 1993. Remote sensing and GIS applied to mountain hazard mapping. Episodes 15, 1: 4:27-4:36.

Research and Development Center of Soil Engineering and Foundation, 2002. Developing proposal report of a study on sustainable solution for slope stabilization. Department of Civil Engineer, Faculty of Engineer, Kasetsart University, 22 p. (In Thai)

Royal Academic Engineering, 1995. Landslides hazard mitigation: with Particular

- Reference to Developing Countries. Proceeding of a Conference held on Friday November 12, 1997 at the Royal Society, 6 Carlton House Terrace, London. The Royal Academic Engineering, 124 pp.
- Ruenkraitersa, T., and Chinpongsonond, P., 1980. Geological seismological aspects of landslides in northern Thailand. Report No. 51. Bangkok: Material and Research Division, Department of Highway.
- Ruangsak, P., 2002. Rainfall and Tear at Nam Ko. Forth edition. Thammarak Printing, 200 pp. (in Thai)
- Sabin, F.F., 1997. Remote Sensing, Principles and Interpretation, Third Edition. W.H. Freeman and Company, New York.
- Saha, A. K., and Arora, M. K., 2002. GIS-based landslide hazard zonation in the Bhagirathi (Ganga) valley, Himalayas. INT. J. Remote Sensing 23, 2:257-369.
- Sauchyn, D.J. and Trench, N.R., 1978, Landsat applied to landslide mapping. Photogrammetric Engineering and Remote Sensing 44, 6:735-741.
- Secretariat Office of Government, 2002. (Draft) Technical report. Conducted by the technical committees for mitigation of flash flood and debris flow at Ban Nam Ko and Ban Nam Chun, Amphoe Lom Sak, Changwat Phetchabun, 13 pp. (in Thai)
- Senneset, K., 1996. Landslides, Volume 1; Proceedings of the seventh international symposium on landslides , 17 – 21 June, 1996 / Trondheim, A.A. Balkema / Rotterdam / Brookfield, 370 pp.
- Sgzen, M. L., 2002. Data driven landslide hazard assessment using geographic information systems and remote sensing. A thesis submitted to the Graduate School of Natural and Applied Sciences of the Middle East Technical University for the degree of doctor of philosophy in the department of geological engineer, 196 pp.
- Sharpe, C.F.S., 1938. Landslides and related features – a study of mass movements of soils and rocks. New York, Columbia University Press, 137 pp.

- Singhroy, V., Mattar, K., and Gray, A.L., 1998. Landslide characterization in Canada using interferometric SAR and combined SAR and TM images. Advances in Space Research 21, 3:465-476.
- Singhroy, V., and Mattar, K., 2000. SAR images techniques for mapping areas of landslide. Canada Centre for Remote Sensing, Ottawa, Canada.
- Singhroy, V., 2000. Landslide risk assessment with high spatial resolution remote sensing satellite data. Canada Centre for Remote Sensing, Ottawa, Canada.
- Slosson, J.E., and Havens, G.W., Shuirman, G., and Slosson, T.L., 1991. Harrison Canyon debris flows of 1980. Environ Geol Water Sci 18, 1:27-38.
- Spiker, E.C., and Gori, P.L., 2000. National landslide hazards mitigation strategy: A framework for loss reduction. Open-file report 00-450, Department of Interior–U.S. Geological Survey, 49 pp.
- Soeters, R., and Van Westen, J.V., 1996. Slope instability recognition, analysis, and zonation. In Turner, A.K., and Schuster, R.L. (eds) landslides investigation and mitigation. Transport Research Board special Report 247, National Research Council, National Academic Press, Washington, D.C., pp. 129-177.
- Stephens, P.R., 1988. Use of satellite data to map landslides. Proceedings 9th Asian Conference on Remote Sensing, Bangkok, pp. 1-7.
- Strandberg, C.A., 1967. Aerial Discovery manual. Wiley and Sons, New York, 249 pp.
- Takeji, A., 1980. Landslides, collapses and debris flows (in Japanese). Tokyo: Kajima Syuppan.
- Tangjaitrong, S., 1994. Modeling landslide hazard using imaged-based GIS. A thesis submitted for the degree of Doctor of Philosophy , The Australian National University, 545 pp.
- Tantiwanit, 1992. A study of landslide disaster in the Kathun area, southern Thailand. Geological Survey Division, Department of Mineral Resources, Bangkok, Thailand. (in Thai)

- Taylor, S.B., 1999. Comparative geomorphic analysis of surficial deposits at three central Appalachian watersheds: implications for controls on sediment-transport efficiency. Dissertation submitted for the degree of Doctor of Philosophy in Geology, the College of Arts and Sciences at West Virginia University, 308 pp.
- Terlien, M.T.J., 1996. Modelling spatial and temporal variations in rainfall-triggered landslides. International Institute for Aerospace Survey and Earth Sciences (ITC), Publication Number 32, 254 p.
- Terlien, M.T.J., Van Asch, T.W.J., and Van Westen, C.J., 1995. Deterministic modelling in GIS-based landslide hazard assessment. In: Carara A., Guzzetti F. (eds) geographical information systems in assessing natural hazards. Kluwer, Dordrecht, pp. 57-77.
- Thassanapak, H., 2001. Potential landslide assessment of Changwat Phuket. Master Thesis, Department of Geology, Graduate School, Chulalongkorn University, 320 pp.
- Thinaphong, K., 1987. A hydro-cartographic information system approach to watershed response simulation using integrated spatio-temporal variabilities from Landsat and ancillary sources. Dissertation for the degree of Doctor of Engineering, Asian Institute of Technology, Bangkok, Thailand, 255 pp.
- Tianchi, Li, chalise, S.R. and Upreti , B.N. ,2001. Landslide Hazard mitigation on the Hindu Kush-Himalayas. International Center for Integrated Mountain Development, Kathmandu, Nepal, 312 pp.
- Tingsanchali, 1989. Debris flow caused by heavy rainfall and landslides. Technical Journal of AIT 2:22-31.
- Tomblin, J.,1994. Main activities of the IDNDR and UNDHA in disaster mitigation. Proceedings of the International Seminar on Erosion and Sediment Control (ISESC), STC, Yogyakarta, Indonesia, January 11-14,1994, pp.1-12.

- Turner, A.K., and Schuster, R.L., 1996. Landslides investigation and mitigation. Transport Research Board special Report 247, National Research Council, National Academic Press, Washington, D.C. 230 pp.
- U.S. Geological Survey, 1982. Goals and tasks of the landslide part of a ground-failure hazards reduction program. Geological Survey Circular 880. United States Department of the Interior, 48 pp.
- U.S. National Research Council, 1982. Selecting a methodology for delineating mudslide hazard areas for the National Flood Insurance Program. National Academic Press, Washington, D.C., 35 pp.
- U.S. National Research Council, 1996. Alluvial Fan Flooding. Committee on Alluvial Fan Flooding, Water Science and Technology Board, Commission on Geosciences, Environment, and Resources. National Academy Press, Washington, D.C., 167 pp.
- Van Westen, J.V., 1993. Application of geographic information systems to landslide hazard zonation. Int. Inst. Aerospace Surv. Earth Sci. Publ. No. 15, Enschede.
- Van Westen, J.V., I. Van Duren, I.H.M.G. Kruse, and M.T.J. Terlien, 1993. GIZZIS: training package for Geographic Information Systems in Slope Instability Zonation. International Institute for Aerospace Survey and Earth Sciences (ITC) Publication Number 15, Enschede, The Netherlands, ITC. Volume 1, Theory, 245 pp., Volume 2, Exercises, 359 pp. Box of 10 diskettes.
- Van Westen, J.V., 1994. GIS in landslide hazard zonation : a review, with examples from the Andes of Columbia. In Mountain Environments and Geographic Information Systems. (n.p.):Taylor & Francis, pp. 165-136.
- Varnes, D.J.,1958. Landslide types and processes. In Special Report 29: Landslides and Engineering Practice (E.B. Eckel, ed.), HRB, National Research Council, Washington, D. C., pp. 20-47.
- Varnes, D.J.,1978. Slope movement types and processes. In Special Report 176: Landslides: Analysis and Control (R.L. Schuster and R.J. Krizek, eds.), Transport

- Research Board (TRB), National Research Council, Washington, D. C., pp. 11-33.
- Varnes, D.J., 1984. Landslide hazard zonation: A review of principles and practice natural hazards 3: UNESCO, France, 63 pp.
- Wadge, G., Wislocki, A.P., and Pearson, E.J., 1998. Spatial analysis in GIS for natural hazard assessment: environmental modeling with GIS, pp. 332-338.
- Wannakao, L., Achwichai, L., Buapan, C., and Muangnoicharoen, N., 1985. The study of rock slope stability at Km. 18-24 along Lom Sak-Chum Phrae highway. Department of Geotechnology, Khonkaen University, Thailand.
- Wieczorek, G.F., Ellen, S., Lips, E.W., Cannon, S.H., and Short, D.N., 1983. Potential for debris flow and debris flood along the Wasatch Front between Salt Lake City and Willard, Utah, and measures for their mitigation. U.S. Geological Survey, Open file report 83-635, 46 pp.
- Wieczorek, G.F., Larsen, M.C., Eaton, L.S., Morgan, B.A. and Blair, J. L., 2001. Debris-flow and flooding hazards associated with the December 1999 storm in coastal Venezuela and strategies for mitigation: U.S. Geological Survey, Open File Report 01-0144, 20 pp.
- Wieczorek, G.F., Gori, P.L., Campbell, R.H., and Morgan, B.A., 1995. Landslide and Debris-Flow Hazards caused by the June 27, 1995, Storm in Madison County, Virginia: U.S. Geological Survey, Open file report 95-822, 14 pp.
- Wieczorek, G.F., Morgan, B.A., Campbell, R.H., Orndorff, R.C., Burton, W.C., Southworth, C.S., and Smith, J.A., 1996. Preliminary Inventory of Debris-Flow and Flooding Effects of the June 27, 1995, Storm in Madison County, Virginia, Showing Time Sequence of Positions of Storm Cell Center: U.S. Geological Survey, Open File report, 96-13, 8 pp.
- Wroth, C. P., 1979. Correlation of some engineering properties of soils. Proc. 2nd BOSS Conference, London, pp. 121-312.

- Wroth, C. P. and Wood, D. M., 1978. The correlation of index properties with some basic engineering properties of soils. Canadian Geotechnical Journal 14, 2:137-145.
- Yhinaphong, K., 1987. Hydro-cartographic information system approach to watershed response simulation using integrated spatio-temporal variabilities from landsat and ancillary sources. A dissertation submitted in partial fulfillment of the requirements for the degree of Doctor of Engineering, Asian Institute of Technology, Thailand, 255 pp.
- Yooyen, W., 1985. Geology of Amphoe Lom Kao. Geological investigation report No. 0031, Geological Survey Division, Department of Mineral Resources, Bangkok, Thailand, 21 pp. (in Thai)
- Zinck, J. A., Lopez, J., Metternicht, G., Shrestha, D. P., and Vazquez-Selem, 2001. Mapping and modelling mass movements and gullies in mountainous areas using remote sensing and GIS techniques. International Journal of Applied Earth Observation and Geoinformation (JAC) 3, 1: 43-53.
- Zhibin, T., 1991. A study of landslides in weathered granitic slopes in Amphoe Phi Pun, Nakhon Si Thammarat, Thailand. Thesis for the degree of Master of Science, Asian Institute of Technology, Bangkok, Thailand, 51 pp.

## APPENDICES

## APPENDIX A

Photographs illustrating seventeen locations of the rock and soil samples collected for geotechnical study (sample locations referred to Figure 5-1)

Appendix A-1 Location A-1



Appendix A-2 Location B-1



Appendix A-3 Location B-2



Appendix A-4 Location B-3



Appendix A-5 Location B-4



Appendix A-6 Location B-5



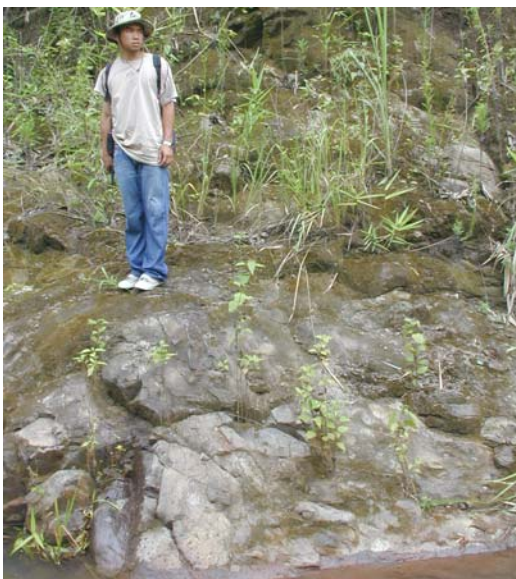
Appendix A-7 Location B-6



Appendix A-8 Location B-7



Appendix A-9 Location B-8



Appendix A-10 Location B-9



Appendix A-11 Location B-10



Appendix A-12 Location B-11



Appendix A-13 Location B-12



Appendix A-14 Location C-1



Appendix A-15 Location C-2



Appendix A-16 Location C-3



Appendix A-17 Location C-4



Appendix A-18 Location C-4



## APPENDIX B

Photographs illustrating the locations of collected rock samples for geotechnical laboratorial studies and technique of point load testing in the Rock Mechanics Laboratory, Geological Engineering, Suranaree University of Technology

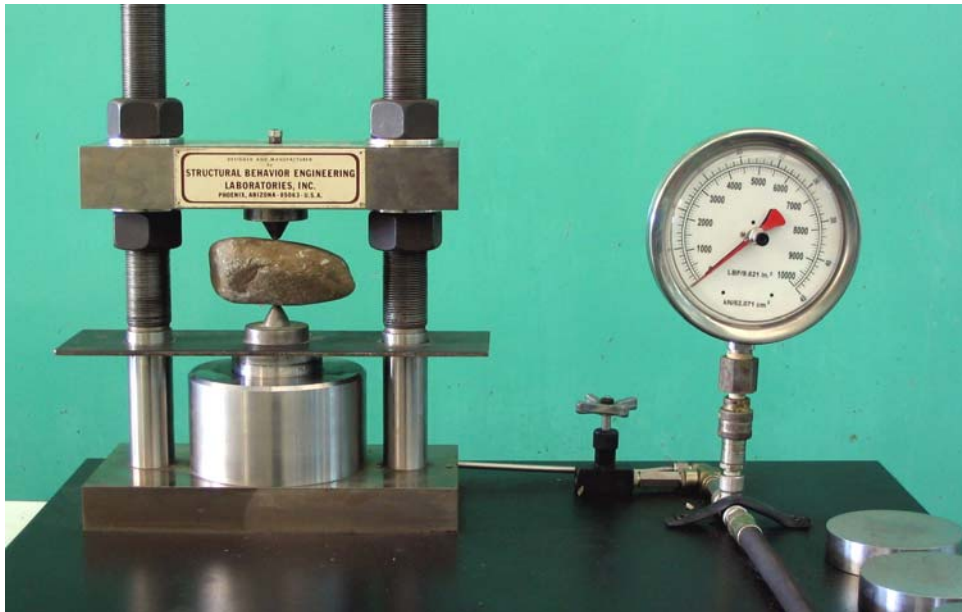
Appendix B-1 Field location along a stream (location B-2 as shown in Figure 5-1) from where rock specimens were collected for point load testing



Appendix B-2 The representative three rock-sample types of Phra Wihan sandstone/siltstone (lithologic unit Pw), Phu Kradung sandstone (lithologic unit Pk), and Lom Sak volcanic complex (lithologic unit Ls) respectively, that used in the point load testing



Appendix B-3 The point load apparatus (SBEL PLT-75) that has the highest force up to 75,000 pounds



Appendix B-4 Demonstration of a rock specimen forced by head-press until it is broken



Appendix B-5 Characteristics of ten rock specimens of Phra Wihan sandstone/siltstone (lithologic unit Pw) before point load testing



Appendix B-6 Characteristics of ten rock specimens of Phra Wihan sandstone/siltstone (lithologic unit Pw) after point load testing



Appendix B-7 Characteristics of twelve rock specimens of Phu Kradung sandstone/siltstone (lithologic unit Pk) before point load testing



Appendix B-8 Characteristics of twelve rock specimens of Phu Kradung sandstone/siltstone (lithologic unit Pk) after point load testing



Appendix B-9 Characteristics of ten rock specimens of Lom Sak volcanic complex (lithologic unit Ls) before point load testing



Appendix B-10 Characteristics of ten rock specimens of Lom Sak volcanic complex (lithologic unit Ls) after point load testing



Appendix B-11 Results of point load index strength test of rock specimens of Phra Wihan sandstone (Pw)

Number of Specimens : 10									
Rock Type : Pra Wihan Sandstone (Pw)									
Specimen No.	W	D	P	$D_e^2 = \frac{4WD}{\pi}$	$D_e$	$I_s = \frac{P}{D_e^2}$	$F = \frac{(D_e/50)^{0.4}}{5}$	$I_{s(50)}$	$\sigma_c = 24 I_{s(50)}$
	(mm)	(mm)	(kN)	(mm <sup>2</sup> )	(mm)	(MPa)		(MPa)	(MPa)
Pw - 1	49.1	117.3	18.0	7337	85.7	2.45	1.27	3.13	75.0
Pw - 2	40.9	94.0	12.5	4898	70.0	2.55	1.16	2.97	71.3
Pw - 3	54.0	127.1	11.5	8743	93.5	1.32	1.33	1.74	41.8
Pw - 4	82.0	50.2	12.0	5244	72.4	2.29	1.18	2.70	64.9
Pw - 5	72.8	42.0	8.7	3895	62.4	2.23	1.10	2.47	59.2
Pw - 6	78.5	47.4	9.4	4740	68.8	1.98	1.15	2.29	55.0
Pw - 7	54.8	36.8	7.8	2569	50.7	3.04	1.01	3.05	73.3
Pw - 8	71.6	30.6	6.5	2791	52.8	2.33	1.03	2.39	57.3
Pw - 9	61.1	27.3	7.0	2125	46.1	3.29	0.96	3.18	76.2
Pw - 10	37.5	32.4	4.7	1548	39.3	3.04	0.90	2.73	65.4
							MAX	3.18	76.2
							MIN	1.74	41.8
							MEAN	2.66	63.9
							S.D.	0.45	10.8

Appendix B-12 Results of point load index strength test of rock specimens of Phu Kradung sandstone (Pk)

Number of Specimens : 12									
Rock Type : Phu Kradung Sandstone (PK)									
Specimen No.	W	D	P	$D_e^2 = \frac{4WD}{\pi}$	$D_e$	$I_s = \frac{P}{D_e^2}$	$F = \frac{(D_e/50)^{0.4}}{5}$	$I_{s(50)}$	$\sigma_c = 24 I_{s(50)}$
	(mm)	(mm)	(kN)	(mm <sup>2</sup> )	(mm)	(MPa)		(MPa)	(MPa)
Pk - 1	112.0	51.3	7.8	7319	85.6	1.07	1.27	1.36	32.6
Pk - 2	106.4	48.9	5.5	6628	81.4	0.83	1.25	1.03	24.8
Pk - 3	112.5	59.8	8.1	8570	92.6	0.95	1.32	1.25	29.9
Pk - 4	108.2	52.0	9.9	7167	84.7	1.38	1.27	1.75	42.0
Pk - 5	89.8	45.4	11.2	5194	72.1	2.16	1.18	2.54	61.0
Pk - 6	112.8	63.5	14.0	9125	95.5	1.53	1.34	2.05	49.3
Pk - 7	103.9	43.1	11.6	5705	75.5	2.03	1.20	2.45	58.8
Pk - 8	62.0	55.3	12.0	4368	66.1	2.75	1.13	3.11	74.8
Pk - 9	89.7	41.8	12.0	4776	69.1	2.51	1.16	2.91	69.8
Pk - 10	102.5	50.0	9.0	6529	80.8	1.38	1.24	1.71	41.1
Pk - 11	97.8	51.3	8.5	6391	79.9	1.33	1.24	1.64	39.4
Pk - 12	65.0	48.5	9.8	4016	63.4	2.44	1.11	2.71	65.2
							MAX	3.11	74.8
							MIN	1.03	24.8
							MEAN	2.04	49.0
							S.D.	0.69	16.6

Appendix B-13 Results of point load index strength test of rock specimens of Lom Sak  
Volcanic Complex (Ls)

Number of Specimens : 10									
Rock Type : Lom Sak Volcanic Complex (Ls)									
Specimen No.	W	D	P	$D_e^2 =$ $4WD/\pi$	$D_e$	$I_s =$ $P/D_e^2$	$F =$ $(D_e/50)^{0.4}$ 5	$I_{s(50)}$	$\sigma_c = 24I_{s(50)}$
	(mm)	(mm)	(kN)	(mm <sup>2</sup> )	(mm)	(MPa)		(MPa)	(MPa)
Ls - 1	96.5	51.9	26.0	6380	79.9	4.08	1.23	5.03	120.8
Ls - 2	125.5	52.2	38.8	8345	91.4	4.65	1.31	6.10	146.3
Ls - 3	117.8	54.3	25.5	8148	90.3	3.13	1.30	4.08	98.0
Ls - 4	105.3	37.7	28.7	5057	71.1	5.68	1.17	6.65	159.6
Ls - 5	141.1	45.9	37.6	8250	90.8	4.56	1.31	5.96	143.1
Ls - 6	115.1	56.6	17.5	8299	91.1	2.11	1.31	2.76	66.3
Ls - 7	103.8	52.9	18.0	6995	83.6	2.57	1.26	3.24	77.8
Ls - 8	140.2	35.3	22.2	6305	79.4	3.52	1.23	4.34	104.1
Ls - 9	117.1	30.2	19.2	4505	67.1	4.26	1.14	4.87	116.8
Ls - 10	93.3	25.2	14.4	2995	54.7	4.81	1.04	5.01	120.2
							MAX	6.65	159.6
							MIN	2.76	66.3
							MEAN	4.80	115.3
							S.D.	1.24	29.8

Appendix B-14 Analytical results of point load testing by the method of ISRM of Brown (1981) and ASTM D5731-95.

Rock Unit	Description	No. of Samples	$I_{s(50)}$ (MPa)	Approx. UCS (MPa)	Grade	
Pw	Gray sandstone /siltstone	10	2.66	63.9	R4	Strong rock
Pk	Red siltstone	12	2.04	45.0	R3	Medium strong rock
Ls	Volcanic complex	10	4.80	115.2	R5	Very strong rock

Note:  $I_{s(50)}$  – Point load strength index

UCS – Uniaxial compressive strength,  $(\sigma_c) = 24 I_{s(50)}$

## APPENDIX C

Photographs illustrating laboratorial instruments and technique in soil-geotechnical testing in the Rock Mechanics Laboratory, Geological Engineering, Suranaree University of Technology

Appendix C-1 Sieve Analysis used for grain size distribution



Appendix C-2 Retained soils from each sieve class



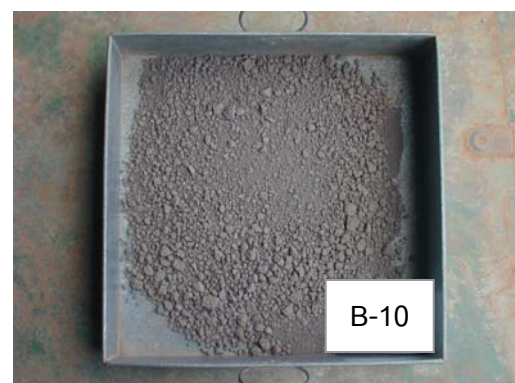
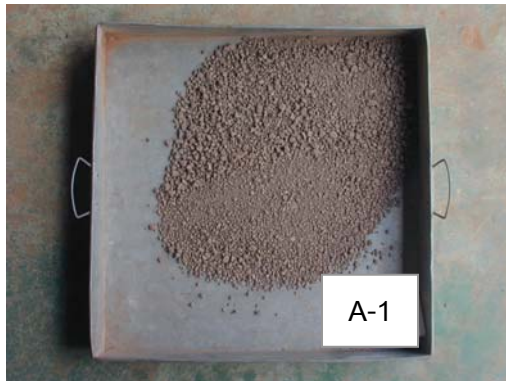
Appendix C-3 Grain size distribution of soils from sedimentation by Hydrometer Test



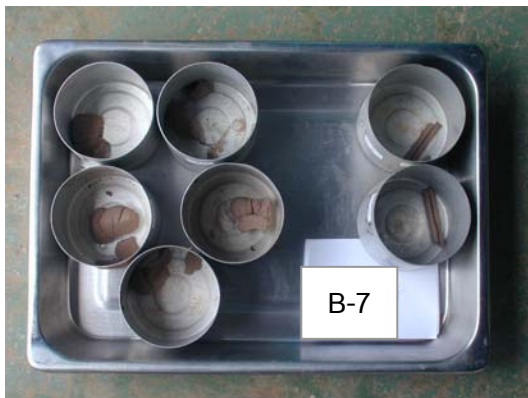
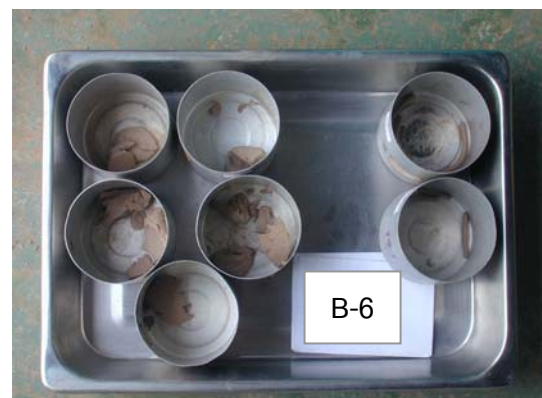
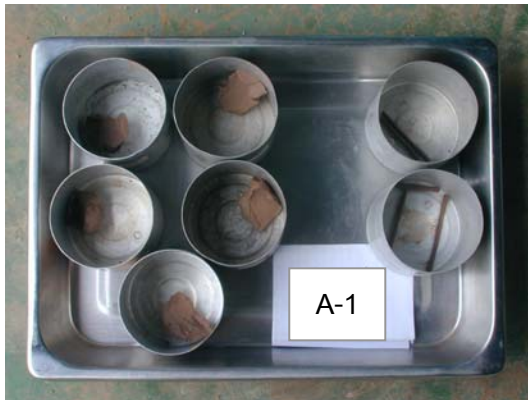
Appendix C-4 Copper bowl apparatus for liquid limit of soil samples



Appendix C-5 Dried and crushed soil samples (number A-1, B-2, B-3, B-6, B-7 and B-10) used for soil-geotechnical testing



Appendix C-6 Oven-dried soil samples (number A-1, B-2, B-3, B-6, B-7 and B-10) used for Plastic Limit ( $w_p$ ) and Liquid Limit ( $w_L$ ) testing



## APPENDIX D

Letter from Dr. Philip E. LaMoreaux, Edition-in-Chief of Environmental Geology, and the manuscript title "2001 debris flow and debris flood in Nam Ko area, Phetchabun province, central Thailand" for publication in *Environmental Geology of USA*.



March 22, 2006

**Editor-in-Chief**  
Dr. Philip E. LaMoreaux

**Assistant Editor**  
Ann McCarley

**Street Address:**  
1009 23rd Avenue  
Tuscaloosa, AL 35401

**Post Office Address:**  
P.O. Box 2310  
Tuscaloosa, AL 35403  
USA  
Tel. (01)-(205)-391-3535  
Fax (01)-(205)-752-4043  
email pel@dbtech.net

**Editor for Europe**  
Dr. Gunter Dörhöfer

**Assistant Editor for Europe**  
Ms. Sigrid Dörhöfer

Niedersächsisches Landesamt  
Für Bodenforschung  
P.O. Box 510 153  
D-30631, Hannover, Germany  
Tel. (49)-(511)-643-2494  
Fax (49)-(511)-643-2304/3687  
email environmental.geology@nlfb.de  
envgeo@freenet.de

Dr. Nopadon Muanoicharoen/Sombat Yumuang  
Department of Geology, Faculty of Science  
Chulalongkorn University, Phyathai Road  
Bangkok 10330, THAILAND

Dear Nopadon and Sombat:

I have reviewed the manuscript, "2001 debris flow and debris flood in Nam Ko area, Phetchabun province, central Thailand".

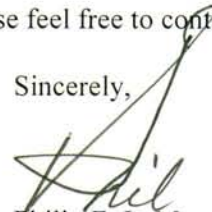
The manuscript is very interesting and good; however, it needs a few revisions before publication in *Environmental Geology*. Enclosed for your review is a copy of your edited manuscript and a few reviewer comments. You must incorporate the suggested revisions and **resubmit to this office two hardcopies of the revised manuscript** for publication in *Environmental Geology*.

You must also submit your manuscript, tables, and figures on diskette(s) or CD-ROM, according to the enclosed instructions. Please fill out the bottom of the form and return it with the diskette.

Springer Publishing Company has begun publication of the journal in electronic form as well as in the present form of a printed journal, therefore, enclosed is a transfer of copyright form that must be signed before your manuscript can be published. Please complete the form and return it with your revised manuscript.

If you have any questions, please feel free to contact me.

Sincerely,

  
Philip E. LaMoreaux  
Editor-in-Chief

Enclosures: Edited manuscript, copyright form, colored publication form letter, diskette submission instructions, formatting instruction sheet

## **2001 debris flow and debris flood in Nam Ko area, Phetchabun province, central Thailand**

S. YUMUANG

**Abstract** The factors of the debris flow and debris flood (debris flow-flood) occurrence on 11 August 2001 on the active Nam Ko alluvial fan in Phetchabun province, central Thailand were studied. Evidences of past activity registered in the alluvial fan, and the debris flow-flood event were reconstructed. The disastrous debris flow-flood event was not the work of the unusual high amount of rainfalls alone, as previously theorized, but is a work of combined factors from the terrain characteristics with specific land covers to the time-delay for accumulation of debris and sediments. This combination of factors could lead to a debris flow-flood after a high amount of precipitation. The process could also be worse if a landslide formed a natural dam, then the dam was destroyed under the weight of impounded water. After such a disastrous event, it would take time for more plant debris and sediments in the sub-catchment area to accumulate before the next debris flow-flood.

*S. Yumuang*

*Department of Geology, Faculty of Science, Chulalongkorn University,*

*Phyathai Road, Patumwan District, Bangkok 10330, Thailand*

E-mail: sombat@gisthai.org

Tel: +66-2-2185442

Fax: +66-2-2185464

**Keywords** *Debris flow and debris flood - GIS and remote sensing - Nam Ko - Phetchabun - Thailand*

## Introduction

On 11 August 2001 (8/11) at 3:30 a.m., a disastrous debris flow and associated debris flood (debris flow-flood) severely damaged Nam Ko Yai village on the alluvial fan just below the canyon mouth of the Nam Ko Yai stream (Fig. 1), a major tributary of Pa Sak river in Lom Sak district, Phetchabun province, central Thailand. The flood water, full of debris and fallen trees, destroyed several houses on the stream banks and claimed 136 lives with over 5 million US dollars in property damage. This is one of many severe tragedies caused by the debris flow-flood in Thailand in the past few decades.

### Figure 1

A complete understanding of the processes and the factors that influenced this incident in Nam Ko Yai sub-catchment and the alluvial fan below in terms of action, source areas and run-out zones, as well as the identification of the potentials for hazards has never been accomplished. Expected frequency of such a debris flow-flood in this area is yet to be evaluated. However, a case study analysis of this event will provide essential basic information to mitigate future debris flow-floods under similar geographical conditions.

This study identifies the relationship of influencing factors of the debris flow-flood occurrence, defines the evidences of past activity registered in the alluvial fan, and determines the potential for future disastrous events in this area. The results will provide planners and decision-makers with adequate and understandable information for more effective planning with the appropriate strategies to reduce and mitigate debris-flow hazards and related phenomena in a long term risk analysis that could occur in areas of similar geographical conditions, and particularly, along the western flank of Phitsanulok-Phetchabun mountain range.

## General concepts

Debris flows and related sediment flows are fast-moving flow-type landslides composed of slurry of rock, mud, organic matter, and water that move down drainage-basin channels onto alluvial fans. Debris flows are generally initiated by one of two processes, by land sliding or by sediment bulking of surface water flows from intense rainfall or rapid snowmelt on steep slopes or in channels. When flows reach an alluvial fan and lose channel confinement, they spread laterally. In addition to being debris-flow-deposition sites, alluvial fans are also often favored sites for settlement. Debris flows pose a hazard different from other types of landslides and floods due to their rapid movement and destructive power. In addition to threatening lives, debris flows can damage buildings and infrastructure by sediment burial, erosion, direct impact, and associated flooding.

Beverage and Culbertson (1964), Pierson and Costa (1987), and Costa (1988) describe the following flow types that build alluvial fans based on generalized sediment-water concentrations and resulting flow behavior: stream flow (less than 20% sediment by volume), hyperconcentrated flow (20 to 60% sediment by volume), and debris flow (greater than 60% sediment by volume). All three flow types can occur during a single event. The U.S. National Research Council (1996) also considers stream, hyperconcentrated, and debris-flow types in alluvial-fan flooding. The term debris flood has been used to describe hyperconcentrated flow (Wieczorek et al. 1983), waterfloods with large sediment load (Costa and Jarrett 1981), sediment flow (Miyajima 2001) and mud flood (National Research Council 1982).

Understanding the processes that govern a debris flow-flood initiation, debris- and water-transport action in the drainage basin, sediment bulking and deposition on the alluvial fan is vital to hazard evaluation. The guidelines for such geologic evaluation are necessary for safe and appropriate land use to prevent loss of life and property damage. The general technique used address debris flow-flood hazards is to evaluate past flows on the alluvial fan and the drainage basin, as well as channel sediment-supply conditions (Cannon 1997; National Research Council 1996; Giraud 2002).

## Investigation methods

Three data inputs were used: thematic data preprocessed from geographic information system (GIS) and remote sensing techniques, field observation, and mechanical testing of soil and rock samples. Scar-scouring locations in Nam Ko Yai sub-catchment and deposition locations in the alluvial fan were detected and interpreted from multi-temporal satellite images, aerial photographs, rectified orthophotographs. Field visits were performed to determine the nature of some debris. The univariate probability analysis method of Dai et al. (2001) was used to present the spatial relationships between the detected scar-scouring locations and major debris flow-flood factors. To define the evidence of past debris flow-flood activity recorded in the alluvial fan, the geologic evaluation and age determination were used in a two-step procedure. This procedure (National Research Council 1996) consists of an initial delineation of the active depositional area and a subsequent detailed site-specific analysis of the hazard within the active depositional area.

The digitally based inventory of important input data themes in the study area was also preprocessed and compiled from secondary data, field investigation and interpretation of the multi-temporal rectified orthophotographs (1:25,000 and 1:50,000 scales), as well as satellite images of medium resolution (Landsat TM) and of high resolution (IKONOS). These important input data themes were provided a basis for detailed analysis of initial terrain and damage sites using GIS and remote sensing techniques of Varnes (1984) and Westen (1994). These input data themes (Table 1) were primarily used for defining the evidence of past debris flow-flood activities, analyzing the factors affecting flow-flood processes, and identifying the potential for flow-flood hazards.

<h3>Table 1</h3>
------------------

### Description of the study area

The study area (Fig. 2) is in the northwestern corner of the main upper Pa Sak catchment at the feet of Khao Ko and Phu Hin Rong Kla Mountains in the

Phitsanulok-Phetchabun range. Nam Ko Yai village is situated on the alluvial fan. The sub-catchment area is 14 km long and 5 km across. The upstream rims are bounded by the steep slopes to a maximum altitude of 1,746 m in the northwestern part, down to the gentler slopes, then flat rolling sub-catchment terrain and the alluvial fan is at an altitude of 160 m.

## Figure 2

Various rock units ranging from the uppermost Paleozoic and Mesozoic sedimentary and volcanic rocks to younger unconsolidated sediments occur in the study area. Stratigraphically, the lowest rock unit generally exposed in the eastern part of the study area is Permian Lom Kao (Lk) Formation. It consists of folded limestone, massive shale and slaty shale. Unconformably above is the Triassic Lom Sak (Ls) Formation that is a volcanic complex, plus siltstone, shale and slate. Ls Formation covers most of the study area, especially adjacent to the central stream channel. Ls Formation is subsequently angular-unconformably overlaid by the gently westerly-dipping Khorat Group that is mainly exposed on the steepest and highest western and northern rims, near the tops of a flat highland away from the study area. This Khorat Group consists of Phu Kradung (Pk) Formation (red siltstone, conglomeratic sandstone, tuffaceous sandstone and siltstone) and Phra Wihan (Pw) Formation (gray sandstone, tuffaceous siltstone, and red shale), both Jurassic in age, and Phu Phan (Pp) Formation (pebbly sandstone) of Cretaceous period. The younger unconsolidated sediments (Qa) of Quaternary age are mainly stream deposits, composed of river sands and gravels, silts, clays and gray soils along the drainage system. The Qa sediments also include those that form the alluvial fan from the canyon mouth to the southeastern limit of the area.

The Nam Ko Yai sub-catchment is covered by dense forests on the western and northern high steep-slopes. Within the undulating valley floor along Nam Ko Yai stream in the central part of the sub-catchment, deforestation preceded agricultural usage. Erosion includes: sheet and rill, mass movement, gullies and badlands, that are widespread across the sub-catchment area. In the eastern

extreme of the sub-catchment and on the alluvial fan, there are irrigated orchards and densely populated settlements.

In this upper Pa Sak region, the average annual rainfall normally exceeds 1,000 mm. The climate is tropical, occasionally with tropical storms in the early and middle periods of rainy season (June-October). The tropical storm “Usa-ngi” that passed through during the first two weeks of August 2001 was blamed for the 8/11 tragedy.

### **Evidence and factors affecting debris flow-flood processes in Nam Ko Yai sub-catchment**

Factors affecting the 8/11 event included: landforms, slope gradient, underlying materials, land cover and unusual amount of rainfall. Evidence of the 8/11 occurrence were scar-scouring and depositional locations from the flow/flood. A key assumption is that the potential (occurrence possibility) of the debris flow-flood processes is the same as the actual frequency of those processes.

Landsat 7 ETM+ imageries data and geomorphometric data (e.g. slope, terrain aspect, topographic shape, etc.) were derived from a Digital Elevation Model (DEM) and combined to determine and classify newly formed distinctive scar-scouring and depositional locations in the sub-catchment and alluvial fan areas. These characteristics were detected in the Landsat imageries, aerial photographs and rectified orthophotographs. Brief field traverses were carried out locally. The ground-truth information was used to verify and adjust the accuracy of Landsat imagery classification, as well as aerial photograph and rectified orthophotograph interpretation.

Two sets of multi-spectral Landsat imageries of different periods, one on 5 January 2001 (before 8/11) and the other on 21 November 2001 (after 8/11), were classified (Fig. 3). Preprocessing of the six spectral bands of these Landsat imageries involve an atmospheric correction based on the standard atmospheric-model approach. Orthorectification was accomplished using GIS vectors of road- and stream data, as well as a DEM interpolated from contour vectors (1:25,000

scale). Slope and terrain aspect were calculated from the DEM. A Normalized Different Vegetation Index (NDVI) was created from the red and infrared spectral bands. NDVI was used to establish a threshold of vegetated and unvegetated pixels in the images for change detection at the scar-scouring and depositional locations (Fig. 4).

### Figure 3

### Figure 4

The classification scheme used to detect the scar-scouring and depositional locations utilized a user-specified hierarchical structure to eliminate non-relevant image objects. The first level was a division between the vegetated and unvegetated objects based on their NDVI value. The choice of 150.00 NDVI value (ratio) was empirically based on an inspection of the objects from the ground-truth information. Those objects with NDVI value below 150.00 were considered as unvegetated objects, and those above 150.00 as vegetated ones.

The scar-scouring and depositional locations were identified and validated. Classification accuracy was determined by comparing a sample of classified pixels with ground-truth information derived from the rectified orthophotographs and field observation (Fig. 5). The validity of the classified results was tested through the identified ground-truth information of the scar-scouring and depositional locations.

### Figure 5

The univariant probability analysis was used to present the spatial relationship between the detected scar-scouring locations and each of the flow-flood related factors. Factors were the rock units (lithology), geomorphology (elevation, slope and topographic shape), soil thickness, land cover, and hydrological data (catchment characteristics and rainfall intensity). The spatial data revealed the correlation between the scar-scouring locations and those influent factors. For

this, the spatial data were converted to a 10 x 10 m grid or cell (ARC/INFO GRID type) then further converted to ASCII data for a use with a general statistical program. In the study area, the total number of cells was 753,423 while the detected scar-scouring number of cells was 50,935. The correlation ratings were performed on the relationship between the detected scar-scouring locations and each factor's range, i.e., the ratio of the number of cells where scar-scouring was not detected to the number of cells where scar-scouring was detected. The relationship analysis is based on the ratio of the area of detected scar-scouring to the total area. A value of 1 defines an average value. The value greater than 1 means a high correlation, and less than 1 a low correlation. A high correlation indicates a high probability of the scar-scouring occurrence.

For slope configuration (Fig. 6), it was concluded that the steeper the slope, the greater the landslide probability was. For the slope inclination of 35-40° and more than 40°, the ratios were 1.57 and 1.70, respectively, indicating a slightly high probability for the scar-scouring occurrence in both cases.

## Figure 6

For elevation above mean sea level (Fig. 7), the higher elevation, the greater the scar-scouring probability. For elevations between 1,000-1,100; 1,100-1,200; 1,200-1,300; and 1,300-1,400 m, the ratios were 3.16, 3.41, 3.99, and 2.54, respectively, indicating a very high probability for scar-scouring. Similar elevation ranges were observed in the steep-cliff areas.

## Figure 7

The different topographic units, peak, ridge, saddle, flat, ravine, pit, convex hillside, concave hillside, slope hillside, inflection hillside, saddle hillside, seemed to be less significant. The frequencies of scar-scouring locations for any specific topographic shape were varied.

The frequencies of scar-scouring as related to the lithologic groups (Fig. 8) were determined for the different stratigraphic units. In the alluvial deposits (Qa1), Phra Wihan (Pw), Phu Kradung (Pk) and Lom Sak (Ls) Formations, the ratios were 3.188, 3.079, 2.302, and 2.713, respectively, indicating very high probabilities for scar-scouring occurrence in all units.

## Figure 8

A relationship between the frequencies of scar-scouring and topsoil thickness was also attempted. Ranges of less than 50 cm, between 50 and 100 cm, and more than 100 cm were defined. Topsoil thickness was insignificant. Perhaps the scar-scouring occurrence was more directly related to the underlying basement rocks than to topsoil thickness.

Lom Sak (Ls) Formation is the most wide-spread rock unit in the study area and supplied the most debris of all sizes for deposition along the channel-bank of the stream system. The debris were further transported downstream toward the alluvial fan, and perhaps formed a significant temporary landslide dam along the way. Special interest was paid to engineering properties of the weathered products of this rock formation. Six weathered samples from this rock unit were collected along a tributary from the main Nam Ko Yai stream channel to the toe of the steep slope just below the exposures of Khorat Group. Geotechnical studies performed included grain size analysis, determination of Atterberg limits and indices, natural moisture content, and shear strength (Table 2). All specimens were non-uniform clay to clayey sand, with natural water content of 21-50 %, with the plastic limit and liquid limit between 17-31 and 24-55 %, respectively. The clayey soils also illustrate a low permeability value of about  $10^{-2}$  to  $10^{-7}$  m/sec. This indicates that the natural moisture could hardly be drained out of the soils, which staying close to the liquid limit. If the soils receive more water, their weight increases while the shear strength decreases, thus the soils would easily flow. These soils had varied shear strength values from about 10-100 kPa. Ls Formation soils, however, had shear strength values lower than other common soils thus were highly movable.

## Table 2

The relationship between the scar-scouring and different types of land cover (Fig. 9) was also determined. The study revealed a high probability value on the banks close to the stream course and in forest areas further away, but lower in the cultivated flat areas. This is contrary to a general belief that cultivated lands played a major role in this event. The explanation could be that the debris flow-flood occurred close to the main stream where there was high energy for erosion and transportation of sediments, and in the forested areas where water could be accumulated and retained to introduce more effective transport when the catastrophic event occurred.

## Figure 9

The rainfall records during 1-10 August 2001, a period of 10 days before the 8/11 occurrence, were collected from seven surrounding rain-gauge stations (Fig. 10). The frequency of scar-scouring was determined by counting the scar-scouring locations in each isohyet range of rainfall accumulation. The results revealed a high probability value of scars-scouring locations in the western areas where the rainfall accumulation was over 150 mm during this period (Fig 11).

## Figure 10

## Figure 11

In addition, the rainfall data and the inflow hydrograph from rainfall data of 1-10 August 2001 (pre-8/11 period) in related to the configuration of sub-catchment and channel characteristics were analyzed. The result was used as one of the most critical factors to identify the potential for the debris flow-flood. The graph of rainfall measurements in August 2001 from seven surrounding locations (Fig. 10) is presented in Figure 12. The average 24-hour rainfall value of pre-8/11 period was 12.98 mm. The two highest values of about 60 and 100 mm recorded on 10

August 2001 at the Ban Lao Ya station (southwest of the study area) and Ban Hin Hao station (northeast of the study area), respectively. The pattern of rainfall during 1-11 August 2001 recorded in most stations was the same as that of continuous rainfall during 2 - 14 August 2002.

## **Figure 12**

The debris flow-flood may have begun before 11 August 2001 when the storm was in progress. Soils may have reached critical saturation at an earlier point, especially in the mountainous areas in the western and northern parts of the sub-catchment where the strongest intensity of rainfall was noted.

### **Evidence of the channel configuration and proposed natural dam location in the central part of Nam Ko Yai sub-catchment**

From field investigations and rectified orthophotograph interpretation at a point along the course of Nam Ko Yai stream in the middle of the study area, the stream here issues from a flat open land to a very narrow V-shape channel with a sudden change of elevation at Tad Fa waterfall (Fig. 13). It could be hypothesized that this specific location is suitable for an accumulation of sediments composed of plant debris, soils, and rock boulders to form a natural dam. A field check revealed fallen trees and vegetation traces. This probably indicated that the temporary natural dam was broken, sending the debris and water to flood further downstream, eroding the channel along the way, and finally dropping its load on the alluvial fan at the canyon mouth. The evidences of 8/11 event could be observed where Nam Ko Yai stream had a steep V-shape cross-section. The traces of the erosional feature in the outer curving-bank were common. Some huge logs or intertwined bamboo clumps were left in the channel. Newly deposited large boulders were found in the channel where the gradient of stream bed changes from steep to flat. Eroded soil banks were also common.

## Figure 13

Topographically, the area of Nam Ko Yai sub-catchment immediately upstream from this proposed natural dam location is a basin shape of about 100,000 square meters. This flat terrain is of a very gentle slope, less than  $5^\circ$ , surrounded by sloping walls with abrupt change in elevation. The stream here was of a wide U-shape and was straight for about 2,500 m. The area is suitable for forming a reservoir if a dam was built at the location. Downstream from the waterfall, the stream changes to a narrow V-shape with strong sinuosity for about 8,000 m to the canyon mouth area. This narrow V-shape and strong sinuosity channel is accompanied by increasing energy of torrent stream flow. This destructive form of mass movement was certainly not caused by the 8/11 alone, but indicates repeated strong debris flow-flood in the past.

From the field evidences and the oblique aerial photographs taken immediately after the 8/11 occurrence, the plant debris and soils transported from the sinusoidal stream banks (Fig. 14) were spread out onto the alluvial fan at the toe of the mountain front. This fan was concluded to have been formed by several similar debris flow-flood activities in the past.

## Figure 14

### **Evidence of past debris flow-flood activity in the alluvial fan**

The stratigraphic characteristics of the alluvial fan deposits are essential for evaluating past flows. A two-step geological evaluation was performed, consisting of an initial delineation of the active depositional area and a subsequent detailed, site-specific analysis of hazards within the active depositional area as suggested by the National Research Council (1996).

In step 1, which was to define an activeness, multi-temporal aerial photographs, rectified orthophotographs and Landsat 7 ETM+ imageries were interpreted and

integrated with topographic characteristics for preliminary identification of location and morphology. Detailed investigation of past representative sedimentary sequences and resistivity investigation were also conducted to determine the criteria for alluvial fan activeness.

The available multi-temporal low-altitude images of aerial photographs (1:15,000 scale) taken on 24 December 1974, rectified orthophotograph (1:50,000 scale) taken on 6 January 1996, and rectified orthophotograph (1:25,000 scale) taken on 9 January 2002 (Fig. 15) were used to characterize the Nam Ko Yai canyon mouth and its downstream depositional fan before and after the 8/11 event. The topographic apex of Nam Ko Yai alluvial fan had only minor changes between 1974 and 1996. A clear activeness of erosion and deposition was presumed to be from the 8/11 flow-flood event.

## **Figure 15**

The expanded features of rectified orthophotographs (1:25,000 scale) taken on 9 January 2002 in Figures 15 and 16 clearly show current traces and tracks of debris flood evidenced from the distinct and active alluvial fan deposit. The deposits mainly occurred on the northern bank of the alluvial fan area where the flood severely damaged houses and orchards dominantly seen in the 1974 aerial photograph and 1996 rectified orthophotograph.

In the multi-spectral Landsat 7 ETM+ imageries analysis, evidences of the alluvial fan deposit from the 8/11 event were analyzed using NDVI value. NDVI value was also used to detect the depositional locations on the alluvial fan (Fig. 16). Oblique aerial photographs taken after the flood were used to characterize the extent of the deposit and validate analyzed result. The high value of NDVI change (56-107) in Figure 16 generally conformed the areas of the most serious damage in Figure 17.

## **Figure 16**

## Figure 17

The oblique aerial photographs of the severely damaged settlement areas (Fig. 1) illustrate characteristics and extent of a large volume of an active alluvial fan deposit. The flood levels were established from mud traces on house walls and trees. The highest level of the debris flood, 190-200 cm above the ground level, was located in the most severely damaged zone at locations A and B (Fig.17). The two locations faced the straight course of Nam Ko Yai stream before the channel changed direction abruptly further downstream. Here, the flood jumped over-bank to destroy houses and orchards and claim lives.

In step 2, a subsequent detailed and site-specific analysis of the hazard within the active depositional area was characterized. The multi-temporal aerial images and oblique aerial photographs clearly illustrate the typical morphology of an alluvial-fan landform where the village is situated. The landform is a section of stream gradient where long-term channel migration and sediment accumulation became markedly less confined than upstream. Below, gradients of the lower part of the older alluvial fan are gentler than those at the fan apex, as was noted from the wider spacing of contour lines in Figures 15 and 16. The topographic apex of this active alluvial fan was located at the point where the flow in the stream channel become unconfined and less certain, and thus is coincident with the hydrological apex.

The results of the resistivity survey investigated along the lines NK 01 – NK 05 (Fig. 18) to identify the local three-dimensional geology (thickness and depth of the older alluvial deposits), revealed four sedimentary units at a total depth of less than 100 m below the ground surface. The lowest unit was semi-unconsolidated sediments or weathered rocks of at least 70 m thick to the west with the bed top at a depth of about 30 m below ground surface (Fig. 18), and much thinner, less than 10 m to the east, with the bed top be noted at a depth of about 80 m below the ground surface. The overlying second unit was semi-unconsolidated sediments with trapped water in the bed openings. Thickness was 25-70 m and increased to the east. Its shallow horizon was 5 m below ground surface in the

west to about 10-20 m to the east. These two lower units are never exposed near the site, but are at surface in the surrounding hills. The third unit was unconsolidated sediments with trapped water. Thickness was in the range of 5-30 m. The thickest part of this third unit was near the NK 03 line in the central part, where the depth to the top of the unit was from a few meters down to 15 m below the ground surface further to the east. The fourth and uppermost unit was of unconsolidated sediments with a thickness of a few meters in the west to 10 m in the east. The fourth unit was commonly exposed on the ground surface along all survey lines, except in the east where it was completely covered by recent topsoils.

## **Figure 18**

A detailed field study of the previous alluvial fan deposits in the fourth unit was conducted along a 5x70 m eroded bank of Nam Ko Yai stream near where the resistivity survey had been performed. Seven stratigraphic profiles were studied to reveal sedimentary sequences in both terms of vertical and lateral stratigraphic correlation. The location map of the measured stratigraphic columns and the line of resistivity survey points are shown in Figure 19 and the actual profiles in Figure 20.

## **Figure 19**

## **Figure 20**

In the observed sections, the lowest sedimentary unit of the older alluvial fan deposits was a debris flow unit of floating texture, unsorted, and un-stratified material that was exposed in the stream-bed only in the eastern part. The coarse-grained fluvial unit of clast-supported texture and fining-upward graded bedding was transitionally deposited on top of the debris flow unit, especially in the middle part, and extended westward (upstream). This coarse-grained fluvial unit was the thickest in the western part and became thinner to the east. The uppermost part of this eroded-bank profile was a fine-grained fluvial and debris

flood unit that was dominantly deposited to form a sharp contact on top of the coarse-grained fluvial unit. The uppermost unit is thicker to the east, especially in the eastern part. The representative and complete detailed sedimentary and stratigraphic characteristics in vertical succession are shown in Figure 21, from bottom to top, the debris flow unit, the coarse-grained fluvial unit, and the fine-grained fluvial and debris flood unit, respectively.

## Figure 21

The overall interpreted subsurface characteristics of resistivity survey lines generally conformed to the normal alluvial fan deposits. The third sedimentary sequences unit repeated in the resistivity survey should be the same as the older alluvial fan deposits in this eroded bank profile as evidenced from the depth and thickness variation from the west to the east. The upper part of the third unit is clearly of the older fan deposits composing of the coarse-grained fluvial unit, debris flow unit, and fine-grained fluvial and debris flood unit.

Significant evidences of the previous debris floods found in the eastern part of uppermost fine-grained fluvial and debris flood unit were two preserved wooden debris fragments, one at the lower part (location PLW) and the other at the upper part (location PUW) as shown in Figure 22. These preserved wooden debris were dated by radiocarbon dating method to have the absolute ages of deposition between 2,618 +/-35 years before present and post-1950, respectively. From these radioactive dating results, it is strongly confirmed that this is an active alluvial fan and that debris flow-flood process had occurred at least twice before the 8/11 disastrous event.

## Figure 22

### Debris flow-flood event reconstruction

The results of the study methods were used to reconstruct the 8/11 event as follows.

The debris flow probably began as a shallow circular landslide on the western and northern steep mountain slopes of Nam Ko Yai sub-catchment after a continuous heavy rainfall period for at least 10 days (before 8/11) that weakened the material with the increasing weight. It thus became highly movable down-slope. The colluvial soils and rock debris of Pw Formation and Pk Formation flow down the forest-covered 30° (or steeper) slopes from a high elevation (800-1,500 m) during the peak of heavy rainfall. This could be the primary source area for the debris (Fig. 23). The debris flow continued further over the central undulated valley area to the main channel of Nam Ko Yai stream. As Nam Ko Yai sub-catchment plain was extensively deforested during the last decade with only few trees left over its overbank flat land, the large quantity of plant debris observed must have come from the upslopes. The debris flow was capable of exerting tremendous lateral forces on obstruction in the flow path, as evidenced from the impact of entrained, large boulders in the highest velocity along the main channels of the first order and second order sub-catchments in the steep slope areas.

These high velocity flows severely snapped off a large number of trees, removed trunks from hillsides and over channels, and mixed with re-eroded soils of the detached-landslides at the steep banks down along the main channels to the central area of moderate-to-gentle slope. This could be the potential secondary source area (Fig. 23) where debris incorporated into the primary debris flows to form a significant volume through the run-out zone or transport zone of the sub-catchment.

## **Figure 23**

With supporting study results on the soil engineering properties, the highly weathered rocks of Ls Formation with its thick residual or colluvial soils appeared to influence the slope failures on the hillsides and debris flows in the channels. These almost undrained clayey soils with increasing load pressure and

less internal shear strength would have caused the mass movement beyond the critical load pressure.

Additionally, the previously-mentioned physical nature of the source areas and run-out zones to the flow-flood occurrence, the amount and intensity of precipitation falling, steep hill slopes and long-running sinusoidal stream channel were key factors as well. Ten days of continuous rainfall to the cumulative peak on 8/11 triggered the landslides and flow-flood in these zones of weak materials.

During these landslides and the flow- flood processes, a temporary natural dam might have built up somewhere in the causeway of this stream, most probably near Tad Fa waterfall. The temporary natural dam could have been formed when debris of plant remains, trees, soils and boulders both from several previous and the 8/11 events were locked at this specific location, forming a reservoir upstream. Then another powerful debris flow-flood followed to break this dam, perhaps with surges up to 10 m high to send water and debris flowing further down to destroy the village on the alluvial fan.

After this serious debris flow-flood occurrence in the year 2001 that completely traversed and removed the former sediments along the channels, it should take many more years to let the factor conditions to build up again. The plant debris and sediments are reduced at present. The relatively higher amount of rainfall in the following year 2002 in the same area did not result in a serious flow-flood event except a mild flash flood.

## **Figure 24**

### **Conclusion**

The disastrous 8/11 debris flow-flood event was not the work of the unusual high amount of rainfall alone, as previously theorized. Instead it was the work of combined factors from the steep terrain characteristics underlain by specific soils with natural moisture close to the liquid limit that could not be drained, and with

specific land cover with time-delay for accumulation of debris and sediments. This combination of factors could also cause debris flow-flood accompanied with a high amount of precipitation. The damage could be made greater by a temporary natural landslide dam forming at locations within the stream course, followed by destruction of the dam under the weight of impounded water. The areas down below, especially the settlements on the distinctive alluvial fan, will always be in danger if no proper caution or preinvestigation is employed.

## Acknowledgements

The Graduate School of Chulalongkorn University and the Ministry of Interior provided a partial funding for this study. Dr. Nopadon Muangnoicharoen of Chulalongkorn University and Dr. Kittitep Fuangkhajorn of Suranaree University of Technology critically reviewed the concepts of this research. The technical supports were provided by the staff of Geo-Informatics Center for Thailand (GISTHAI) of Chulalongkorn University and the staff of Geo-mechanical Research Unit, Suranaree University of Technology.

## References

- Beverage JP, Culbertson JK (1964) Hyperconcentrations of suspended sediment: American Society of Civil Engineers, Journal of the Hydraulics Division, 90 (HY6):117-126
- Cannon SH (1997) Evaluation of the potential for debris and hyperconcentrated flows in Capulin Canyon as a result of the 1996 Dome Fire, Bandelier National Monument, New Mexico. U S Geological Survey Open File Report 97-136
- Costa JE (1988) Rheologic, morphologic, and sedimentologic differentiation of water floods, hyperconcentrated flows, and debris flows. In: Baker VE, Kochel CR, Patton PC, (eds) Flood geomorphology. New York, John Wiley and Sons:113-122

- Costa JE, Jarrett RD (1981) Debris flow in small mountain channels of Colorado and their hydrologic implication. *Bulletin of the Association of Engineering Geologists XVIII* (3):309-322
- Dai FC, Lee CF, Li J, Xu ZW (2001) Assessment of landslide susceptibility on the natural terrain of Lantau Island, Hong Kong. *Environmental Geology* 40 (3):381-391
- Giraud RE (2002) Guidelines for the geological evaluation of debris-flow hazards on alluvial fan. Rocky Mountain Geological Society 54th Annual Meeting May 7–9, 2002 Cedar City, Utah
- Miyajima S (2001) Debris flow studies in Japan. In: Tianchi L , Chalise SR, Upreti BN (eds) *Landslide Hazard Mitigation in the Hindu Kush-Himalayas*, International Center for Integrated Mountain Development, Kathmandu, Nepal:215-228
- National Research Council (1982) *Selecting a methodology for delineating mudslide hazard areas for the National Flood Insurance Program*. National Academy Press, Washington, D.C.
- National Research Council (1996) *Alluvial fan flooding: Washington, D.C.*, National Academy Press, Committee on Alluvial Fan Flooding 172
- Pierson TC, Costa JE (1987) A rheologic classification of subaerial sediment-water flows. In: Costa JE, Wieczorek GF (eds) *Debris flows/avalanches*. Geological Society of America, *Reviews in Engineering Geology VII*:1-12
- Van Westen, JV. (1994) GIS in landslide hazard zonation: a review, with examples from the Andes of Columbia. In *Mountain Environments and Geographic Information Systems*. Taylor & Francis Ltd.:165-136
- Varnes DJ (1984) *Landslide hazard zonation: A review of principles and practice natural hazards UNESCO, France Vol.3*
- Wieczorek GF, Ellen S, Lips EW, Cannon SH, Short DN (1983) Potential for debris flow and debris flood along the Wasatch Front between Salt Lake City and Willard, Utah, and measures for their mitigation. U.S. Geological Survey Open file report 83-635



Fig. 1 1a) Two oblique aerial photographs perceptibly illustrating the characteristics and extension of a large volume of deposited sediments; and 1b) four closed-up photographs illustrating the seriously battered structural damage of houses, orchard trees and other infrastructures in Nam Ko Yai village caused by the fast-moving debris flow-flood occurrence on 11 August 2001 (8/11)

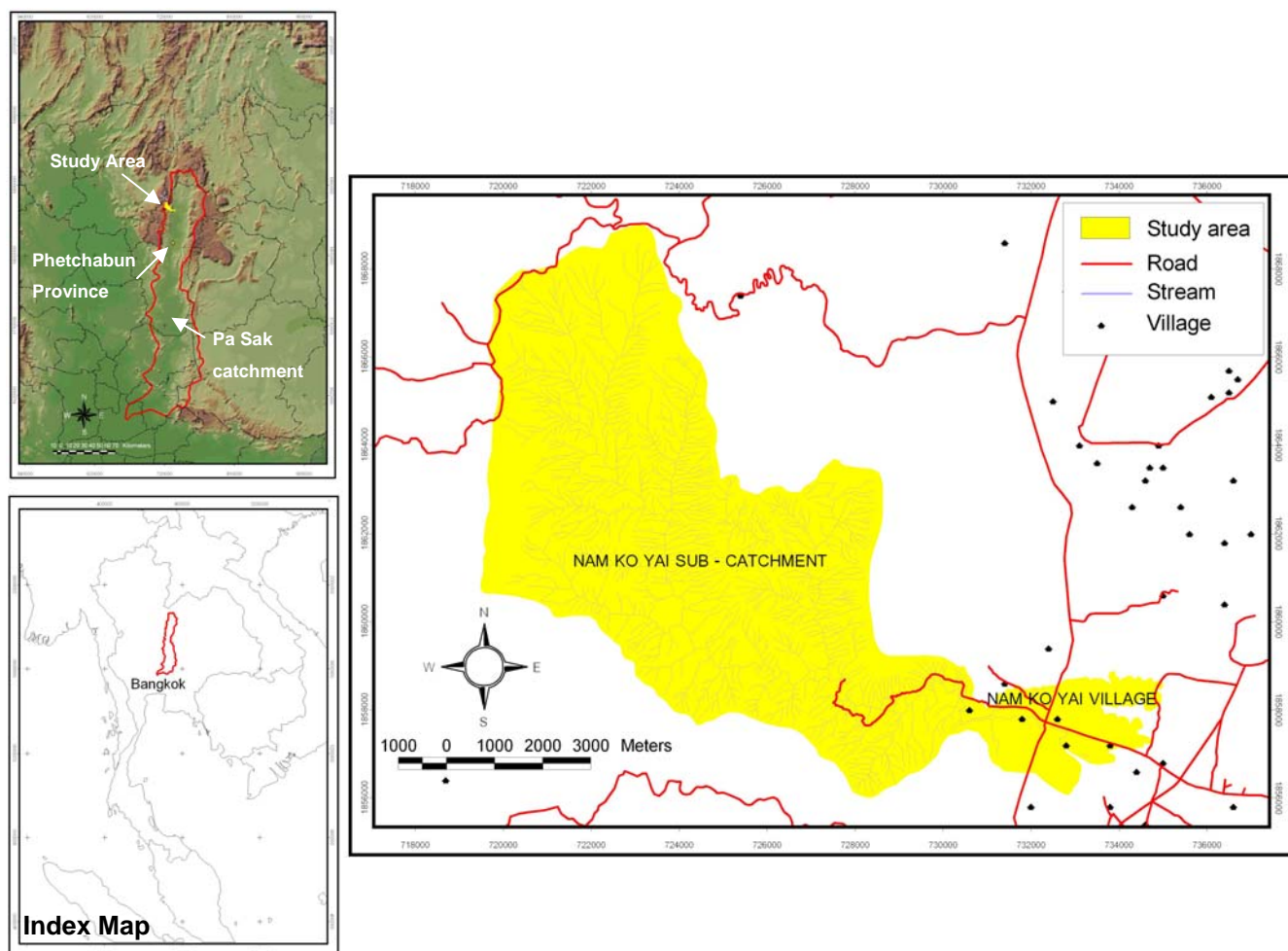


Fig. 2 Geographical location map of the study area in Pa Sak catchment, central Thailand. The coordinates are according to the Universal Transverse Mercator projection with 47 North Zone in Indian 1975 ellipsoid

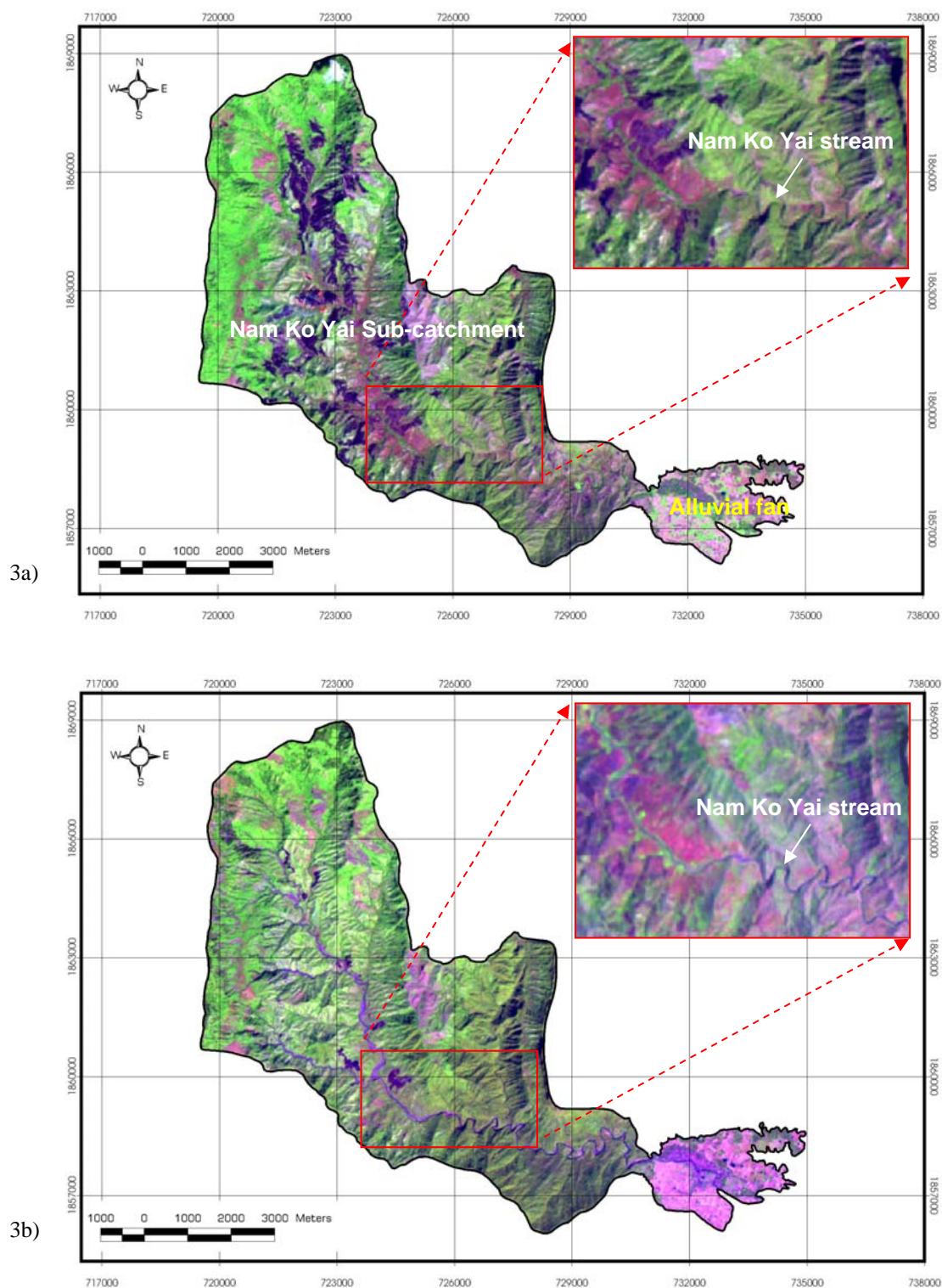


Fig. 3 3a) False color composite of Landsat 7 ETM+ (R=5, G=4, B=3) of the study area acquired on 5 January 2001 (before the debris flow and debris flood occurrence); and 3b) false color composite of Landsat 7 ETM+ (R=5, G=4, B=3) of the study area acquired on 21 November 2001 (after the occurrence) that show the distinctively changed features, especially in the main channels of Nam Ko Yai stream and its alluvial fan just below the canyon mouth

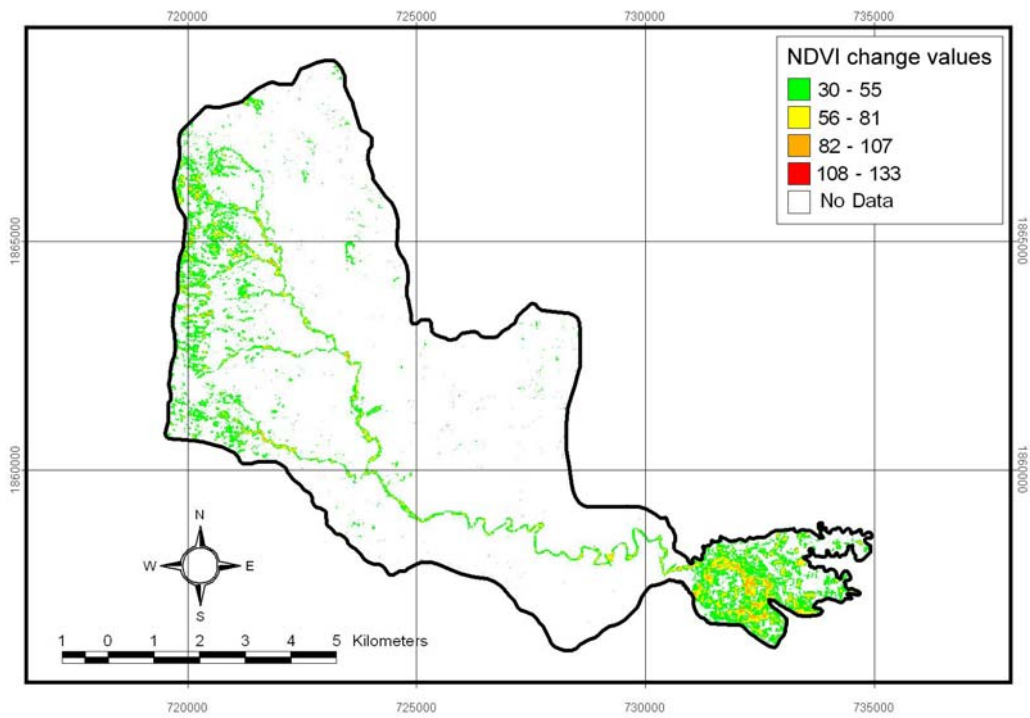


Fig. 4 The resulted significant change detection of NDVI showing scar-scouring and depositional locations in Nam Ko Yai sub-catchment and its alluvial fan that are caused from the 8/11 debris flow-flood occurrence

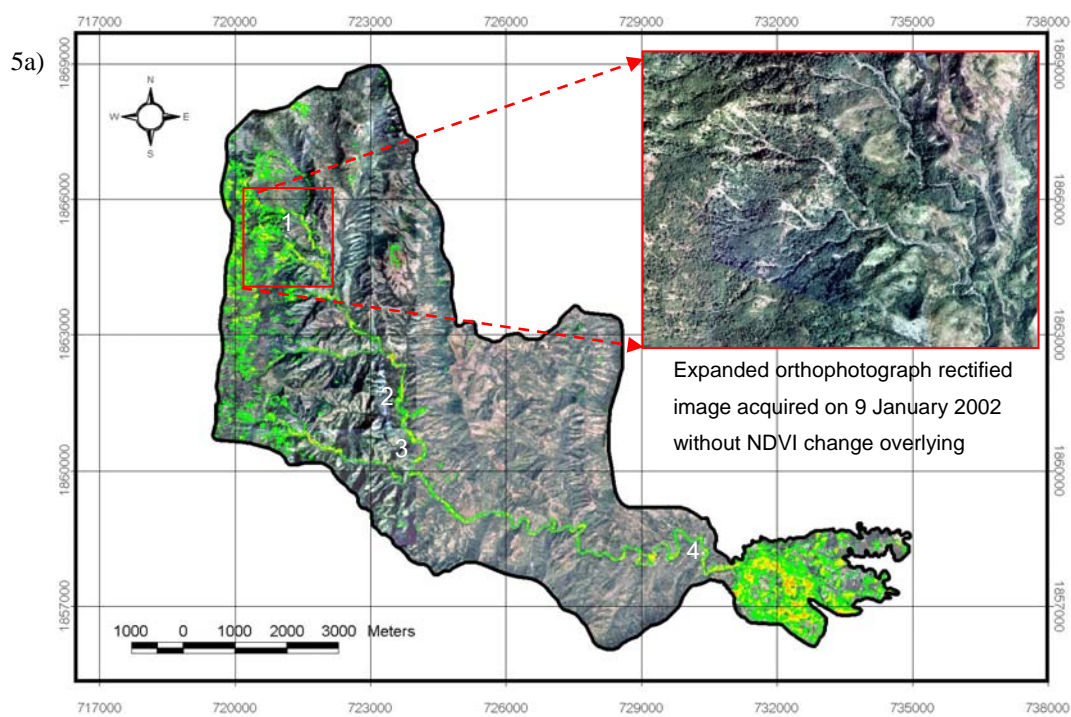


Fig. 5 5a) The significant change of NDVI (from Fig. 4) overlain on the orthophotograph rectified image acquired on 9 January 2002 (after the debris flow-flood occurrence); and 5b) the photographs of four locations (number referred to the location in the map) taken a few days in Nam Ko Yai sub-catchment after the 8/11 event showing the ground truth evidences

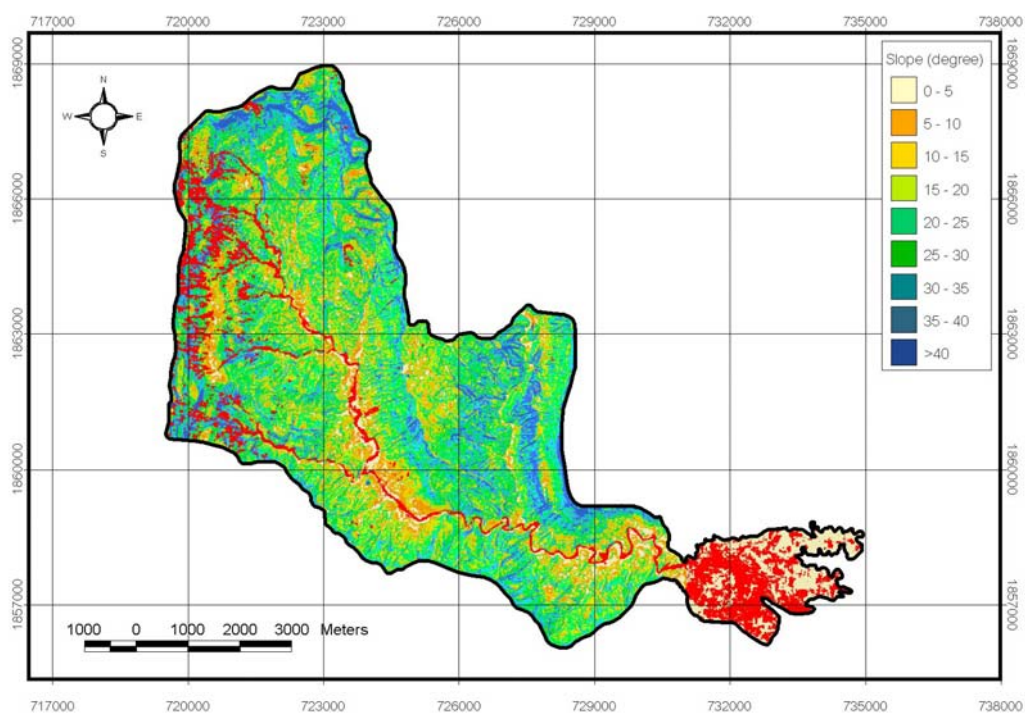


Fig. 6 Slope map overlain with scars-scouring and depositional locations (in red) in the study area

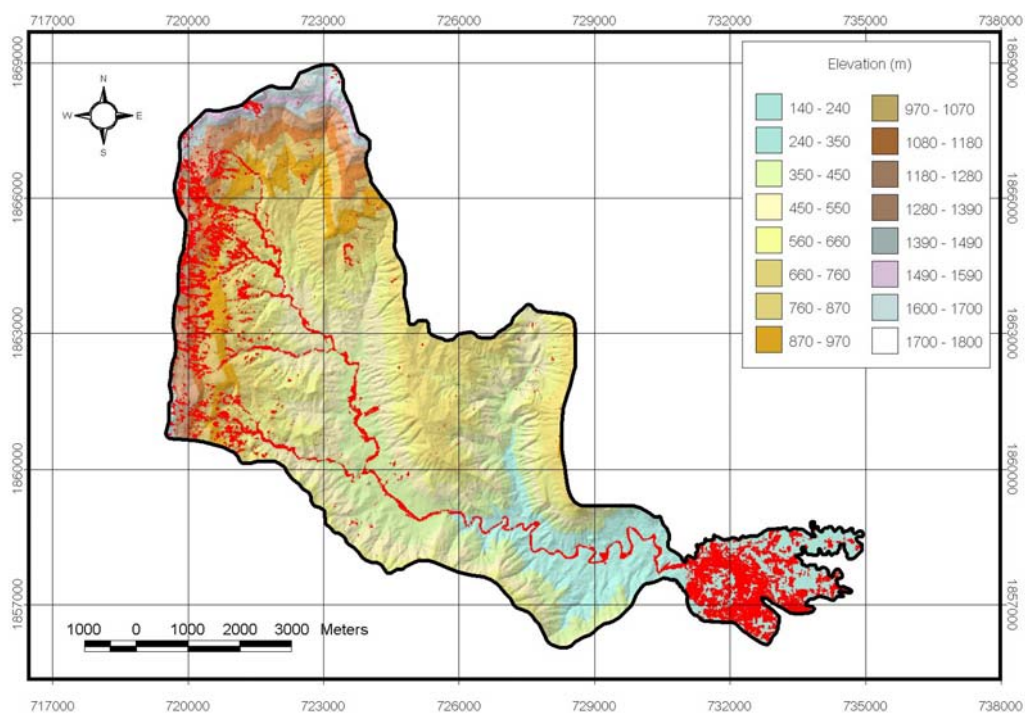


Fig. 7 Elevation map overlain with scar-scouring and depositional locations (in red) in the study area

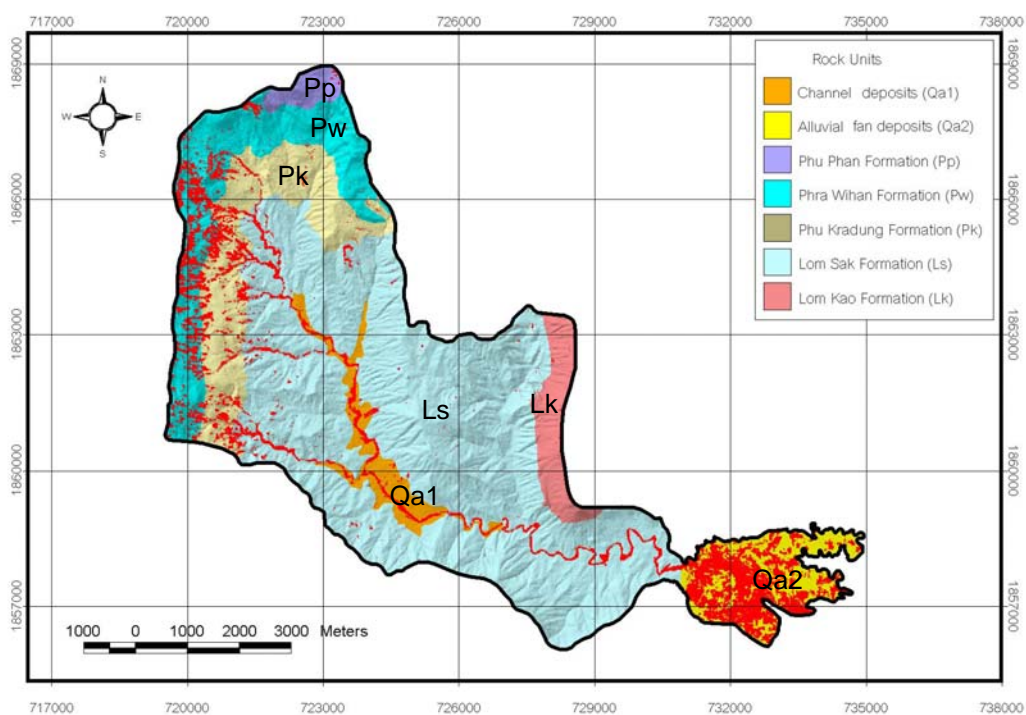


Fig. 8 Rock unit map overlain with scar-scouring and depositional locations (in red) in the study area

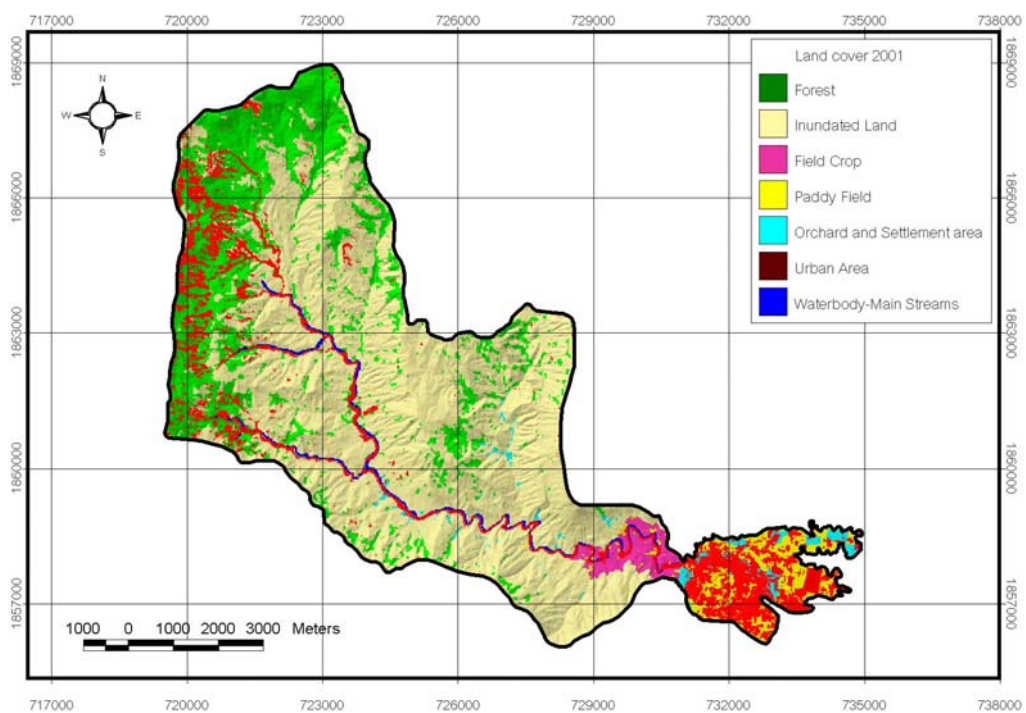


Fig. 9 Land cover map overlain with scar-scouring and depositional locations (in red) in the study area

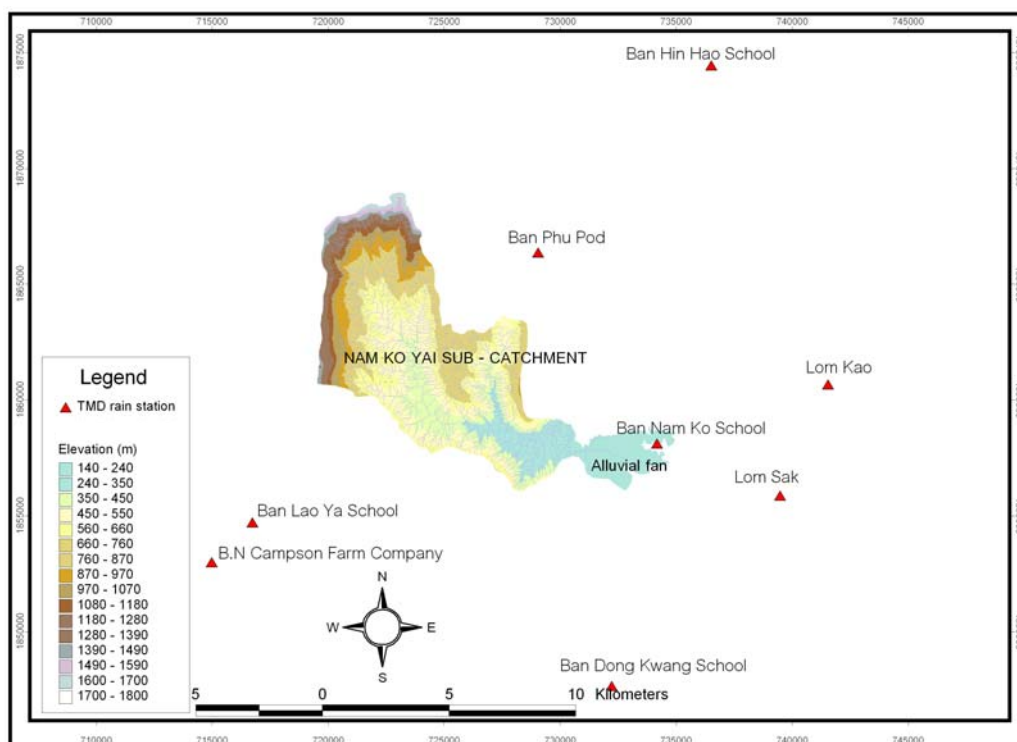


Fig. 10 Location of seven TMD (Thai Meteorological Department) rainfall measurement stations (red triangles) near the study area

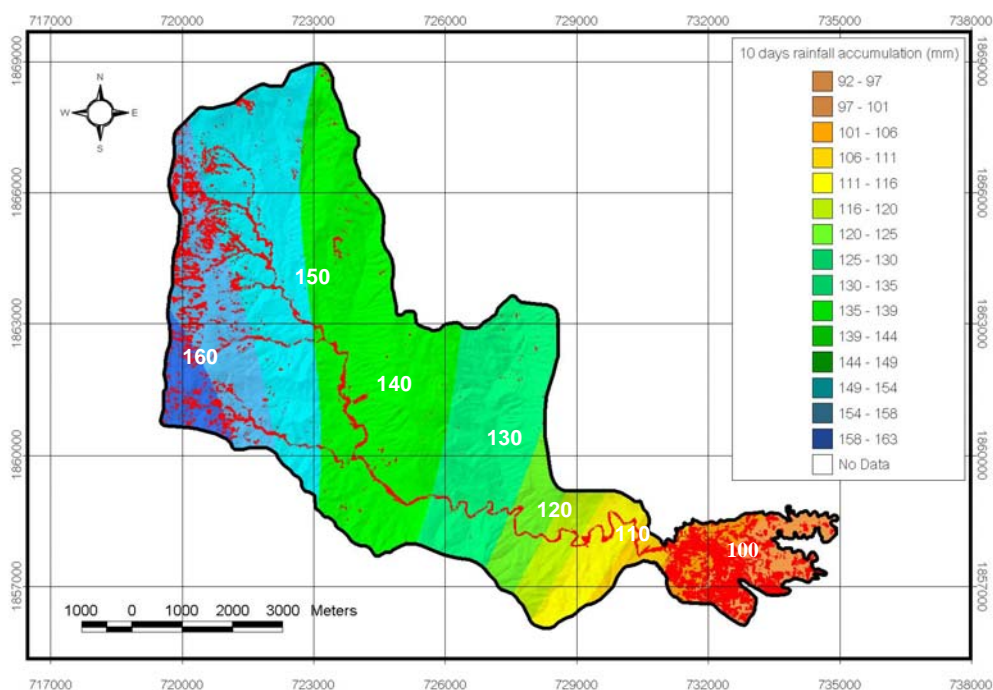


Fig. 11 Rainfall accumulation in the period of 1-10 August 2001 (before the 8/11 debris flow and debris flood occurrence) overlain with scar-scouring and depositional locations (in red) in the study area

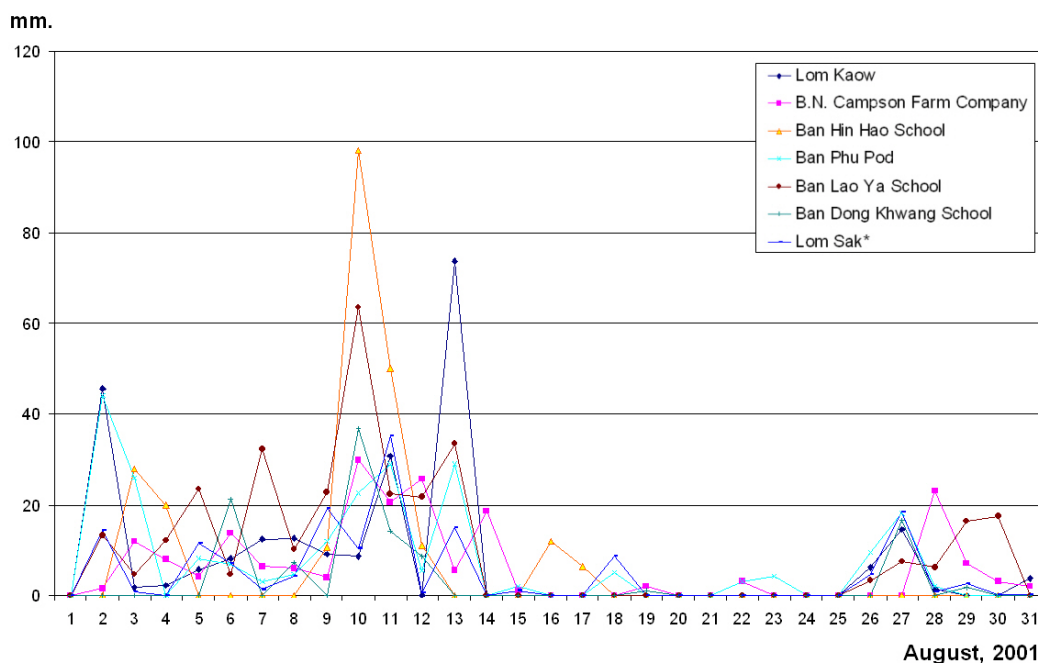


Fig. 12 The graph showing the pattern distribution of rainfall measurements in August 2001 recorded from the seven locations (Fig. 10) near the study area

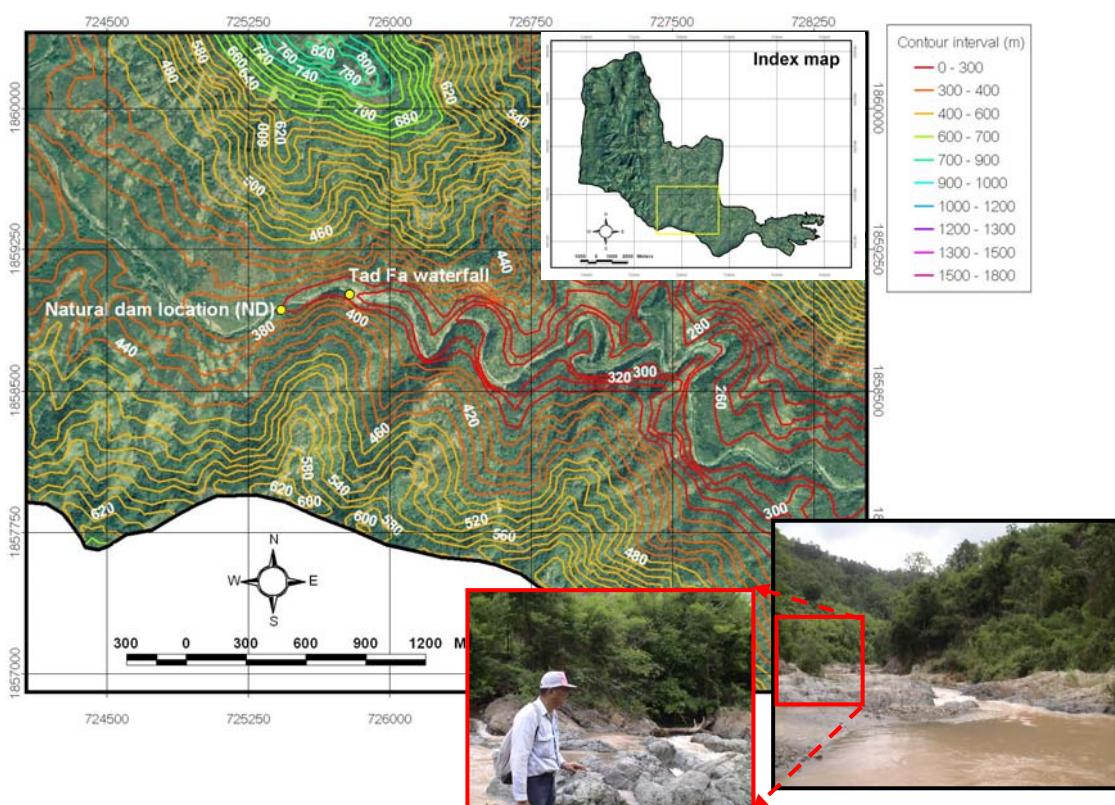


Fig. 13 The orthophotograph rectified image (1:25,000 scale, January 9, 2002 after the 8/11 event) overlain with the contour intervals (20 m) showing the specific configuration of Nam Ko Yai stream located in the lower central part of the study area proposed to be the natural dam location (ND) in front of the location of Tad Fa waterfall



Fig. 14 The oblique aerial photograph (taken on 22 August 2001, 11 days after the event) along the channel of Nam Ko Yai stream with the high sinuosity characteristic illustrating the debris flow-flood track along plant debris and soils had been strongly eroded and transported from its banks before reaching the canyon mouth outlet of the stream

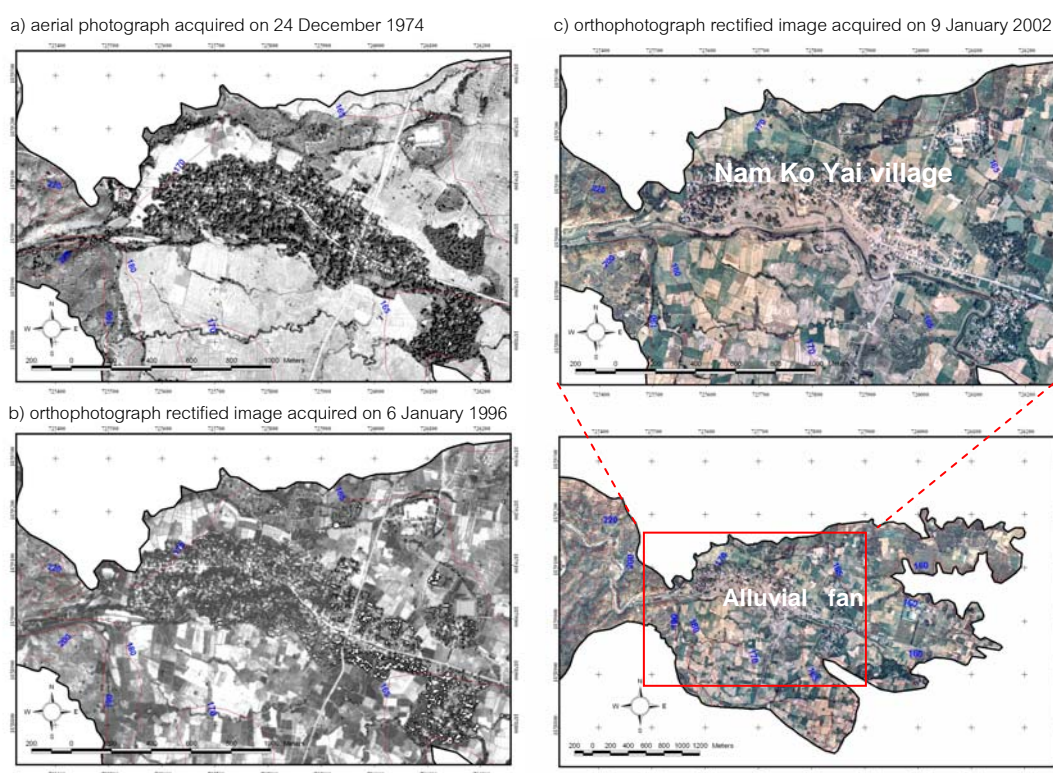


Fig. 15 The multi-temporal low-altitude images of aerial photograph and orthophotograph (with contour intervals in red line) acquired on three different periods: a) 24 December 1974, b) 6 January 1996, and c) 9 January 2002 showing the distinct identification of the topographic apex of Nam Ko Yai stream in the alluvial fan that was slightly modified from 1974 until 1996. Pronounced and still active changes are evident following the 8/11 debris flow-flood

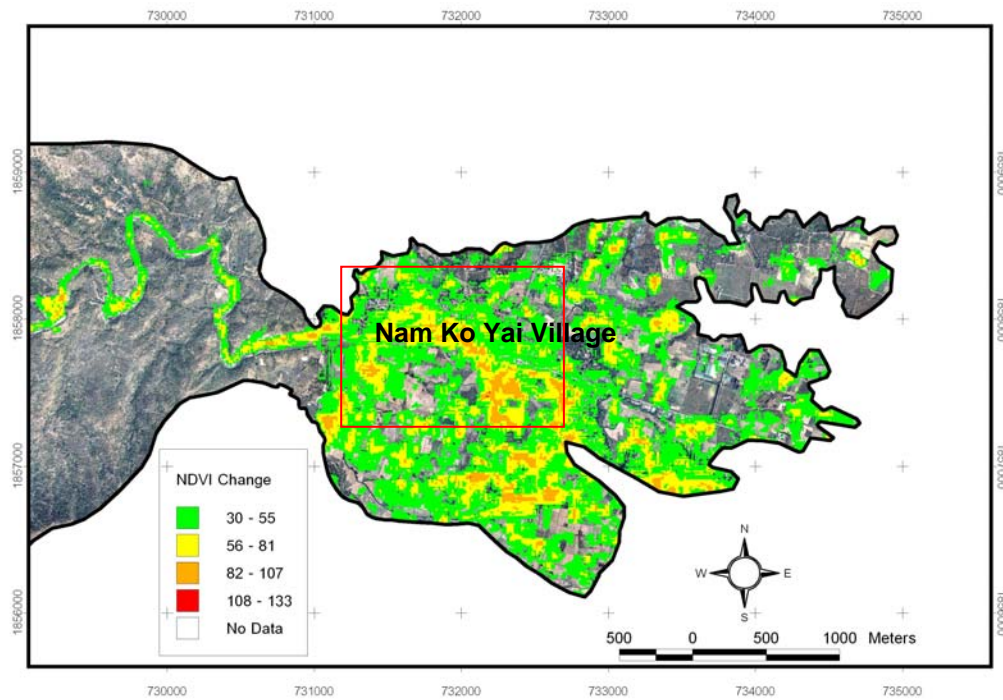


Fig. 16 The detection change of NDVI in the depositional location of the alluvial fan (expanded from Fig. 4) overlain on the orthophotograph rectified image (1:25,000 scale) acquired on 9 January 2002. The brown-colored zones are new traces of fan deposit after 1996

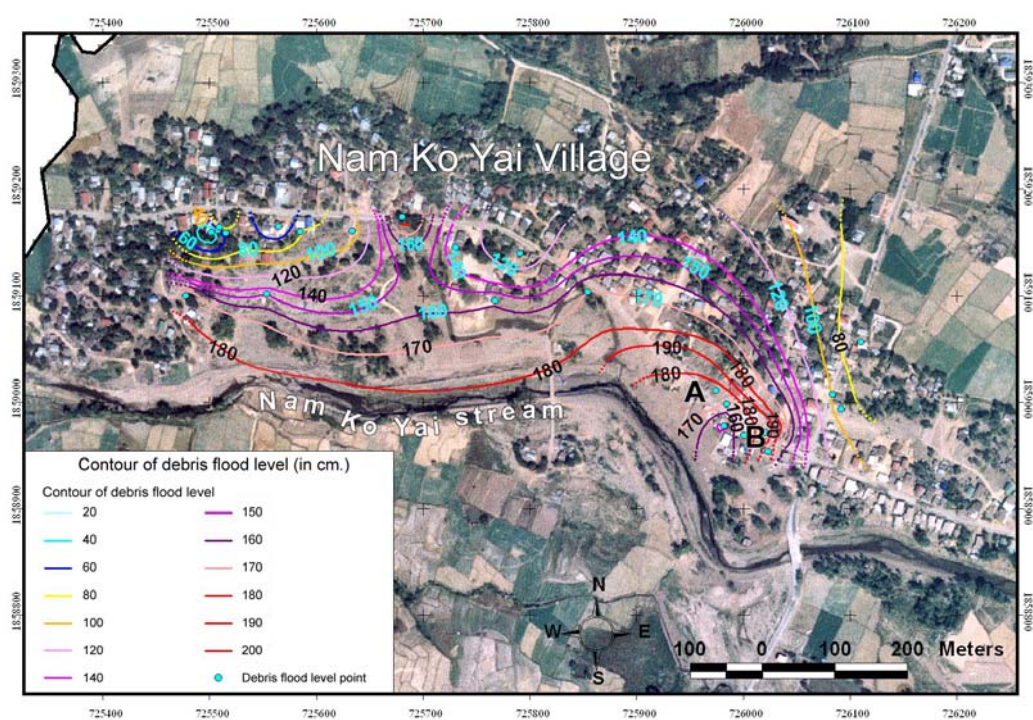


Fig. 17 The expanded orthophotograph rectified image (1:25,000 scale) acquired on 9 January 2002 (red outline in Fig. 16) showing the contours of debris flood levels (in cm) above the ground surface (detected from the thin brown film left at house-walls and trees) in the strongly damaged area of Nam Ko Yai village caused by the 8/11 debris flow-flood

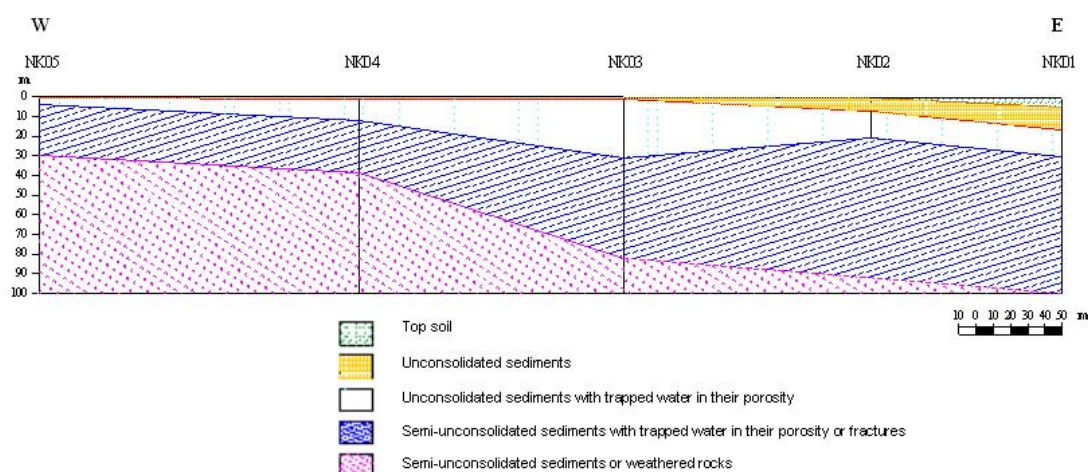


Fig. 18 The cross-section of the resistivity survey interpreted from the five survey points (NK 01 – NK 05) as shown in Fig. 19) that revealed four sedimentary units lying less than 100 m below ground surface

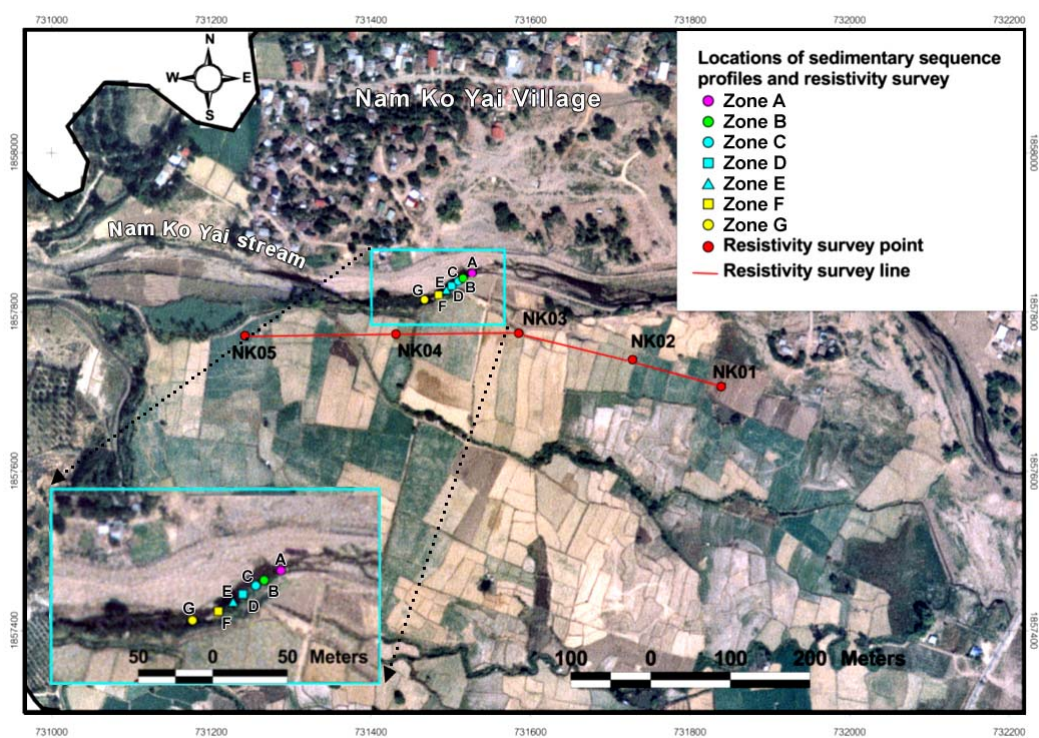


Fig. 19 The location map of seven measured stratigraphic profiles (A, B, C, D, E, F, G) along the eroded bank of Nam Ko Yai stream, and a line of five resistivity survey points (NK01 – NK05) used for investigating the stratigraphy, sedimentology and subsurface geology of the older alluvial fan deposits

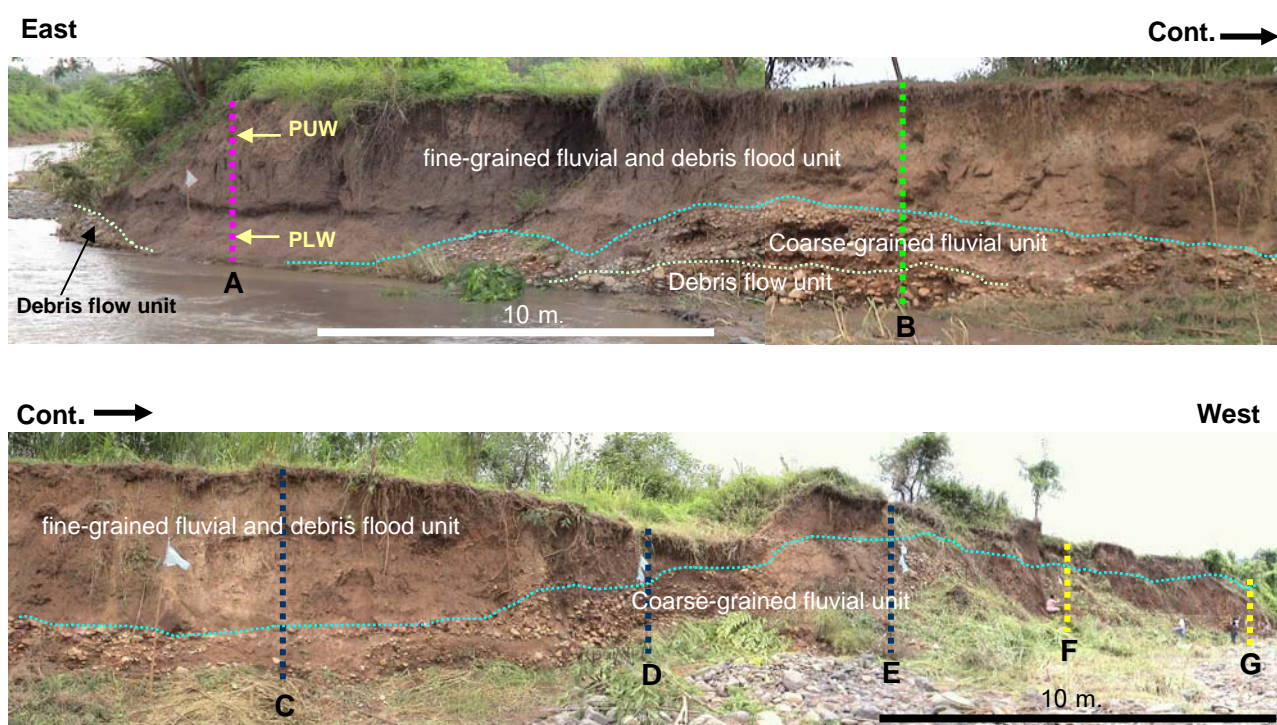


Fig. 20 The lateral and vertical stratigraphic characteristics of debris flow and debris flood deposits of older alluvial fan along the eroded-bank of Nam Ko Yai stream with the locations of those seven measured stratigraphic profiles (A, B, C, D, E, F, G)

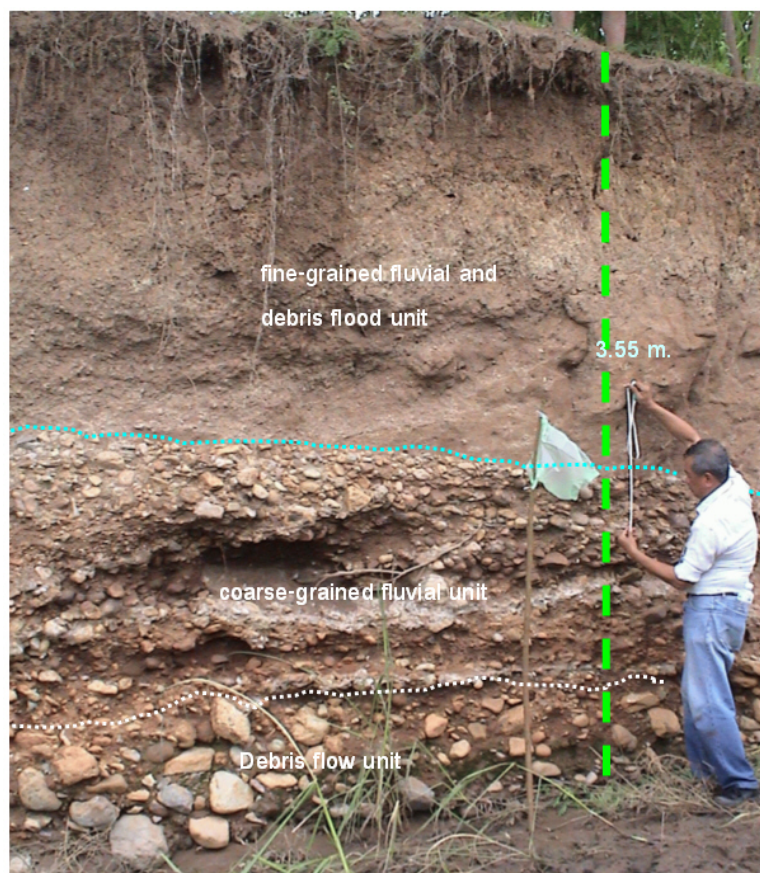


Fig. 21 The measured stratigraphic profile B showing the debris flow unit underlain by the coarse-grained fluvial unit with the transitional contact, and the uppermost fine-grained fluvial and debris flood unit overlying on top of the coarse-grained fluvial unit with a sharp contact

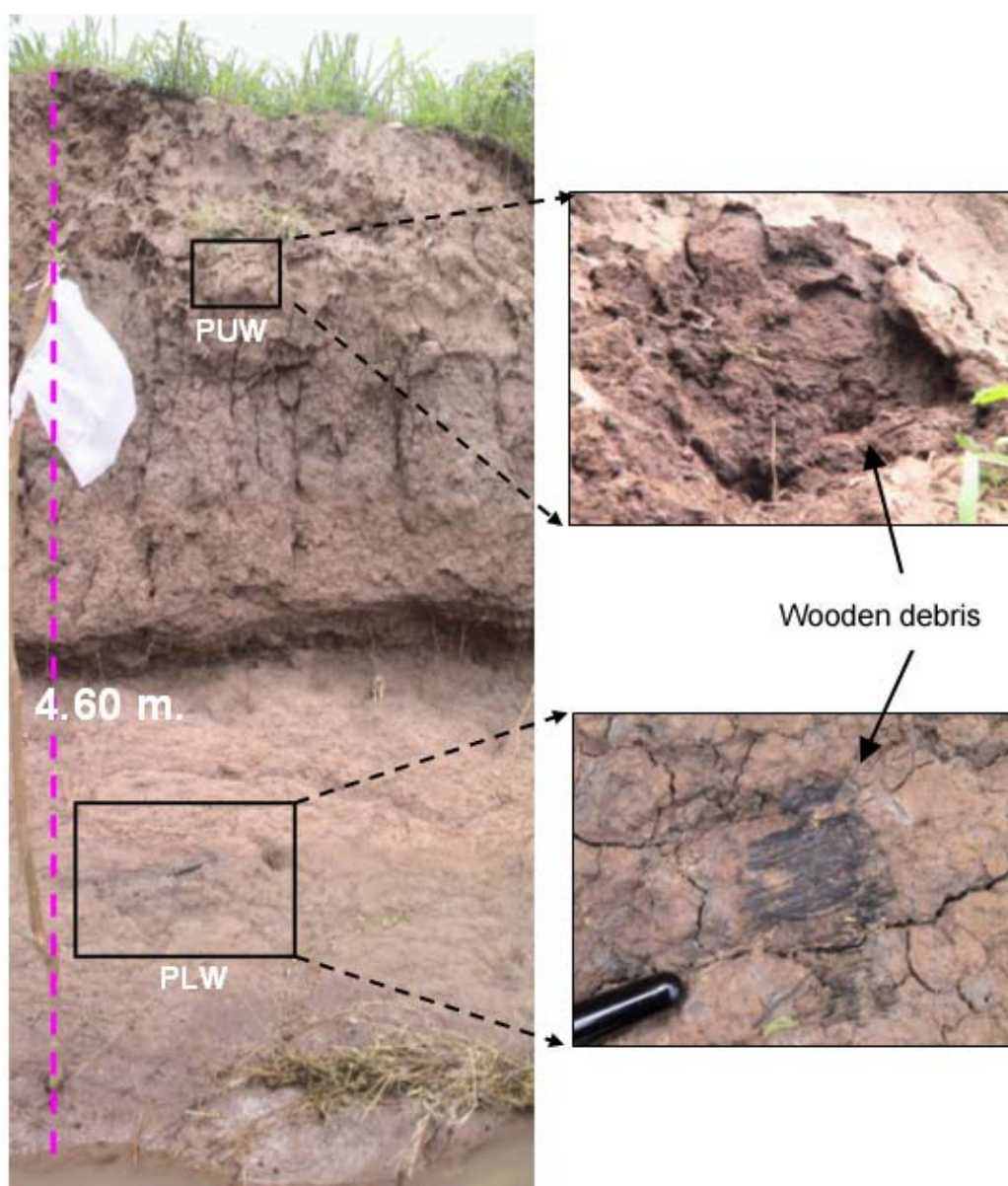


Fig. 22 The measured stratigraphic profile of the uppermost fine-grained fluvial and debris flood unit illustrating its general characteristics and two locations of preserved wooden debris at the lower part (location PLW) and upper part (location PUW)

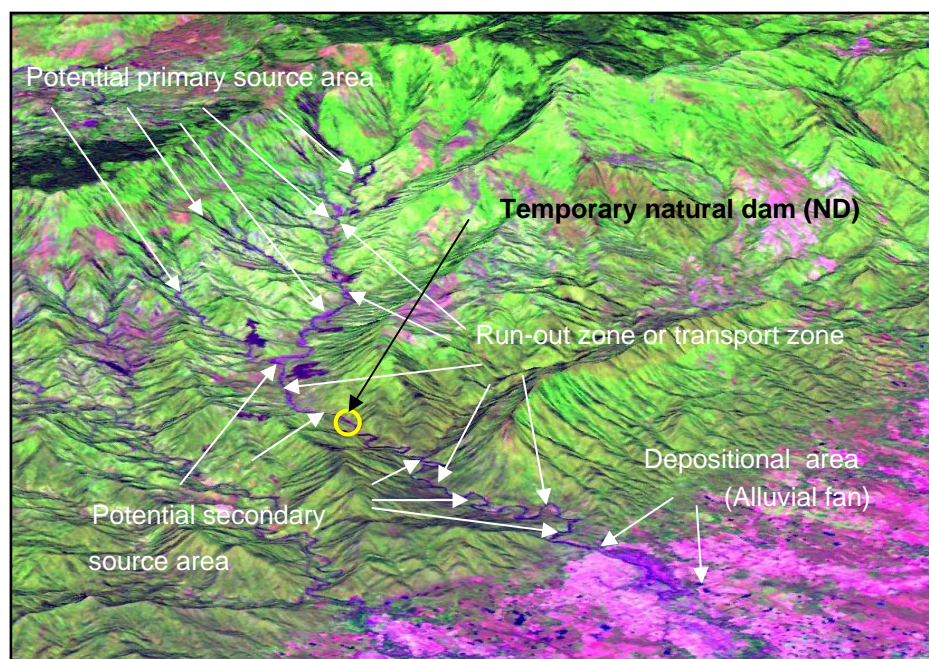


Fig. 23 Three-dimensional view of Nam Ko Yai sub-catchment and its alluvial fan modeled by overlaying the false color composite of Landsat 7 ETM+ (R=5, G=4, B=3) acquired on 21 November 2001 through the base-scale DEM showing the main features after the debris-flood occurrence with identified potential hazard zones of the potential primary and secondary source areas, the run-out zone or transport area, the proposed location of a temporary natural dam, and the depositional area

Table 1 Overview of the important input data themes discussed

Main theme	Sub theme	Made through
A. Debris flow and debris flood inventory map	A1. Scar-scouring & depositional locations	Multi-temporal image interpretation, Multi-temporal image classification, Field investigation
B. Geomorphological map	B1. Digital Elevation Model (DEM)	Topographic map, Existing photogrammetric-elevation data
	B2. Slope	With GIS from a DEM
	B4. Topographic shape	With GIS from a DEM ,Image interpretation, Field investigation
D. Geological map	D1. Rock unit	Existing geological map, Image interpretation, Field investigation
E. Soil map	E1. Soil unit	Existing soil properties map, Field investigation
	E2. Soil thickness	Existing soil properties map, Field investigation
F Land cover map	F1. Land cover	Multi-temporal image interpretation, Multi-temporal image classification, Field investigation
G. Hydrological map	G1. Sub-catchment characteristics	Topographic maps, DEM extraction, Field mapping
	G2. Drainage network	Topographic maps, DEM extraction
	G4. Rainfall intensity	Existing information, Inflow hydrograph analysis
H. Elements at risk map	H1. Settlement area	Image interpretation, Field investigation

Table 2 The analytical results of some important soil engineering properties of the six soil samples collected from the weathered natural zone of volcanic complex of Lom Sak Formation (Ls) in the study area

Sample No.	Location	Percent Finer #200 (% clay and silt)	Natural Water Content, $w_N$	Plastic Limit, $w_P$	Liquid Limit, $w_L$	Plastic Index, $PI = w_L - w_P$	Activity, $A = PI/\%Clay$	Liquidity Index, $LI = (w_N - w_P)/PI$	$C_u$	Soil Type			Shear Strength (kPa)
										1*	2*	3*	
2-B	47 Q 0723290/ UTM 1860028	67.6	27.0	20.8	40.5	19.7	0.76	0.31	>5	Clay	CL	A-7-6 (Clayey soils)	40
3-B	47 Q 0723164/ UTM 1860126	87.1	44.9	29.2	54.6	25.4	0.53	0.62	>5	Clay	CH	A-7-6 (Clayey soils)	10
6-B	47 Q 0722980/ UTM 1860132	87.4	33.8	30.6	54.9	24.2	0.53	0.13	>5	Clay	CH	A-7-6 (Clayey soils)	93
7-B	47 Q 0722937/ UTM 1860140	77.3	34.4	25.4	45.6	20.2	0.67	0.44	>5	Clay	CL	A-7-6 (Clayey soils)	22
10-B	47 Q 0722609/ UTM 1860196	62.0	26.7	24.7	38.4	13.7	0.62	0.15	>5	Clay sand	CL	A-6 (Clayey soils)	87
1-A	47 Q 0728840/ UTM 1858259	38.1	21.8	17.4	24.20	6.8	0.31	0.65	>5	Clay sand	ML	A-4 (Silty soil)	9

Note:

1. Classification of The Mississippi River Commission

2. Classification of of Unified Soil Classification System

CL – inorganic clays of low to medium plasticity, gravelly clay, sandy clays, silty clays, lean clays.

CH – inorganic clays of high plasticity, fat clays

ML – inorganic silts and very fine sands, rock flour, silty or clayey fine sands with slight plasticity.

3. AASHTO Soil Classification System

## Curriculum Vitae

Name : Sombat Yumuang  
Place of birth: Prachinburi  
Year of birth: 1957  
Office address: Department of Geology, Faculty of Science, and  
Head of Geo - Informatics Center for Thailand (GISThai)  
Chulalongkorn University, Bangkok 10330, Thailand  
Tel/Fax : 662-2140610, 662-2185442  
E-mail : sombat@gisthai.org Website: www.gisthai.org

### Education and Degree:

1983	Chulalongkorn University	Bangkok, Thailand
	M.Sc. (Geology), Department of geology, Faculty of Science	
1980	Chulalongkorn University	Bangkok, Thailand
	B.Sc. (Geology), Department of geology, Faculty of Science	

### Professional working experiences:

1992 - Present	Assistant Professor, Department of geology, Faculty of Science, Chulalongkorn University
1997-1999	Deputy Director, Chula Unisearch, Chulalongkorn University
1999 - 2001	Deputy Director, Environmental Research Institute, Chulalongkorn University
2000 - Present	Head, Geo - Informatics Center for Thailand (GISThai)

### On going research and publications:

Application of GIS and remote sensing on geohazards, earth sciences, environments, and socio-economics (more detail in [www.gisthai.org](http://www.gisthai.org)).